Influence of Anthropogenic Climate Change on the Ecophysiology of the Cold-Water Coral *Lophelia pertusa*

Einfluss des anthropogenen Klimawandels auf die Ökophysiologie der Kaltwasserkoralle *Lophelia pertusa*

D i s s e r t a t i o n

zur Erlangung des Doktorgrades
an der Mathematisch-Naturwissenschaftlichen Fakultät
der Christian-Albrechts-Universität zu Kiel

vorgelegt von

Armin U. Form

Kiel, im März 2011

Referent: Prof. Dr. Ulf Riebesell

Korreferent: Prof. Dr. Dieter Piepenburg

Tag der mündlichen Prüfung: 26.04.2011

Zum Druck genehmigt: 26.04.2011

gez. Prof. Dr. Lutz Kipp

(Der Dekan)

"It is not the strongest of the species that survives, nor the most intelligent; it is the one that is most adaptable to change." attributed to Charles Darwin (1809 - 1882)

Index

Index of Figures

Index of Tables

List of Symbols and Abbreviations

ASH	Aragonite Saturation Horizon
ASS	Aragonite Saturation State
ASW	Artificial Seawater
BWT	Buoyancy Weight Technique
CA	Carbonic Anhydrase
CRS	Closed Recirculating System
CWC	Cold-Water Coral
CWC-MS	Cold-Water Coral Maintenance System
DBL	Diffusive Boundary Layer
DIC	Dissolved Inorganic Carbon
DIN	Dissolved Inorganic Nitrogen
DIP	Dissolved Inorganic Phosphorus
DO	Dissolved Oxygen
DOM	Dissolved Organic Matter
GMT	Generic Mapping Tools
GUI	Graphical User Interface
HCB	Hermetically Closed Bioreactor
Ind	Individuals
LTE	Long-Term Experiment
LTE-S	Long-Term Experimental System
M	Molar concentration, mol L^{-1}
MO_2	Oxygen Consumption
NSW	Natural Seawater
POC	Particulate Organic Carbon
POM	Particulate Organic Matter
ROV	Remote Operating Vehicle
SCB	Semi-Closed Bioreactor
SMS	Seafloor Masssive Sulphide
STE	Short-Term Experiment
TA	Total Alkalinity
TAAT	Total Alkalinity Anomaly Technique
TSRE	Temperature Stress Response Experiment
Ω_{Ar}	Aragonite Saturation

Summary

The scleractinian coral *Lophelia pertusa* (Caryophylliidae) is the most common framework-forming cold-water coral with a global distribution. *L. pertusa* bioherms are hot-spots of biodiversity because their three-dimensional framework provides niches and nursery grounds for a variety of species, including commercially important fish species. In contrast to shallow-water corals from the tropics, very little is known about the ecophysiology of cold-water corals such as *L. pertusa* and their sensitivity towards climate change. The present study intends to start filling this knowledge gap by examining a variety of *L. pertusa*'s ecophysiological responses (e.g. food uptake, respiration, growth, fitness, behaviour) under present-day (in the following referred as "ambient") and experimentally manipulated environmental conditions.

Living specimens of *L. pertusa* from two Norwegian cold-water coral locations (Oslofjord and Sula Reef Complex) were collected during two research cruises with the aid of the manned submersible JAGO and transferred into a newly established closed recirculating system at IFM-GEOMAR. Long-term analyses (>3 years) of dissolved inorganic nutrients revealed the high tolerance of *L. pertusa* to rising concentrations of nitrate and phosphate. However, for the main toxic compound - ammonium - it could be demonstrated that the corals' polyp behaviour alters if concentrations are increased to > 17 µmol L^{-1}.

Food availability is thought to be one of the most important factors determining cold-water coral distribution and growth. This study provides feeding rates for three live food organisms encompassing different sizes and qualities. It also describes the food uptake mechanism for mesozooplankton based on the first video documentation of the whole feeding process.

The effect of rising temperatures (ocean warming) on the oxygen consumption, fitness, and behaviour was investigated through a combination of short-term and long-term aquarium experiments. This study shows that at ambient conditions of 7.5 °C *L. pertusa* exhibits low respiration rates of ~ 0.3 µmol O_2 g^{-1} h^{-1} which may increase up to 58 % after a relatively small temperature change (+ 3.5 °C). High Q_{10} values of 3.7 ± 0.7 in these corals and significantly depressed RNA/DNA ratios in coral polyps maintained for 2 weeks under elevated temperatures (11°C) revealed that *L. pertusa* is sensitive to small temperature changes even though analyses of their behaviour may suggest some acclimatisation.

L. pertusa exhibits relatively low bulk calcification rates that vary over time and applied measurement methods. On average calcification amounts to 8.7 x 10^{-3} % d^{-1} which is intermediate in the broad range of reported *L. pertusa* growth rates. Interestingly, corals fed under nearby *ad libitum* conditions showed no relationship between food quality/quantity and growth. This indicates a degree of regulation in the feeding mechanism and may suggest that calcification is rather dependent on a basic metabolic rate than on specific food supply.

The impact of increasing concentrations of CO_2 (ocean acidification) on *L. pertusa* growth rates and fitness was examined in a short-term (one week) and a long-term (8 months) experiment. This study shows for the first time that - when kept under long-term exposure to elevated CO_2 levels - *L. pertusa* is capable to compensate for adverse effects as experienced during short-term incubations. Net growth is sustained even in waters undersaturated with respect to aragonite ($\Omega_{Ar} < 1$). These results suggest that cold-water coral reefs, the majority of which will be exposed to undersaturated waters before the end of this century, may not suffer immediate wide-spread extinction as previously projected. However, the fact that even a temperature increase of about 3 °C seems to be of higher relevance in respect to fitness than a doubling of the pCO_2 emphasises the problem of synergistic impacts between ocean warming and ocean acidification and the need for further long-term incubation experiments.

Kurzfassung

Die Steinkoralle *Lophelia pertusa* (Caryophylliidae) ist die häufigste riffbildende und weltweit verbreiteste Kaltwasserkorallenart. Die von ihr gebildeten Lebensräume sind „hot-spots“ der Artenvielfalt da ihre dreidimensionalen Gerüstbauten marinen Lebewesen, darunter fischereiwirtschaftlich relevante Fischarten, Rückzugsort und Brutstätte bieten. Im Gegensatz zu den im Flachwasser beheimateten tropischen Korallen ist über die Ökophysiologie der Kaltwasserkorallen, insbesondere hinsichtlich ihrer Empfindlichkeit gegenüber dem Klimawandel, bisher sehr wenig bekannt. Die vorliegende Arbeit beabsichtigte daher damit zu beginnen, diese Wissenslücke zu schließen. *L. pertusa* wurde in Experimenten unter natürlichen und manipulierten Bedingungen bezüglich ihrer Reaktionen auf ein breites Spektrum an ökophysiologischen Parametern (Nahrungsaufnahme, Atmung, Wachstum, Fitness und Verhalten) untersucht.

Während zwei Forschungsfahrten wurden mit dem bemannten Tauchboot JAGO lebende Korallenstöcke von *L. pertusa* an zwei norwegischen Kaltwasserkorallenriffen (Oslofjord und Sula Riffkomplex) entnommen und in eine eigens am IFM-GEOMAR errichtete geschlossene Kreislaufanlage überführt. Die Auswertung von Wasserproben inorganisch gelöster Nährstoffe - die regelmäßig über drei Jahre hinweg analysiert wurden - zeigten, daß *L. pertusa* eine hohe Toleranz gegenüber Nitrat und Phosphaten aufweist. In einem Kurzzeitversuch konnte allerdings auch gezeigt werden, daß sich das Korallenpolypenverhalten sichtbar verändert, wenn das als toxisch bekannte Ammonium Konzentrationen > 17 µmol L^{-1} übersteigt.

Nahrungsverfügbarkeit wird als einer der wichtigsten Wachstums- und Verbreitungsfaktoren von Kaltwasserkorallen betrachtet. Diese Arbeit liefert Fraßraten von drei verschiedenen Lebendfutterorganismen und beschreibt die Art und Weise der Nahrungsaufnahme für Mesozooplankton anhand der ersten Videodokumentation des gesamten Nahrungsaufnahme-prozesses.

Der Effekt des Temperaturanstiegs (Ozeanerwärmung) auf den Sauerstoffverbrauch, die Fitness und das Verhalten von *L. pertusa* wurde durch eine Kombination aus Kurz- und Langzeitexperimenten erforscht. Die Studie zeigte, daß bei einer natürlichen Temperatur von 7,5 °C *L. pertusa* eine niedrige Respirationsrate von ca. 0,3 µmol O_2 g^{-1} h^{-1} aufweist. Allerdings ist bereits eine relativ geringe Temperaturerhöhung (+ 3,5 °C) ausreichend, um die

Respirationsrate um bis zu 58 % zu erhöhen. Ein hoher Q_{10}-Wert von 3,7 ± 0,7 dieser Korallen und signifikant erniedrigte RNA/DNA-Verhältnisse in Korallenpolypen welche für zwei Wochen unter erhöhten Temperaturen (11 °C) gehältert wurden, lassen erkennen, daß *L. pertusa* empfindlich gegenüber geringen Temperaturveränderungen ist, selbst wenn Verhaltensanalysen eine gewisse Akklimatisierung nahelegen.

Die Kalzifizierungsrate gesamter *L. pertusa*-Stöcke war relativ gering, lag mit durchschnittlich 8,7 x 10^{-3} % d^{-1} allerdings innerhalb der für diese Art beschriebenen großen Bandbreite und variierte außerdem je nach angewandter Messmethode und Zeit. Interessanterweise zeigten Korallen welche *ad libitum* gefüttert wurden keine Abhängigkeit zwischen der Futterqualität/-quantität und dem Wachstum. Dies deutet auf eine gewisse Regulationsfähigkeit des Fraßmechanismus hin und könnte außerdem bedeuten, daß Kalzifizierung eher von einem metabolischen Grundumsatz als vom spezifischen Nahrungsangebot abhängt.

Der Einfluss steigendender CO_2-Konzentrationen (Ozeanversauerung) auf die Wachstumsraten und Fitness von *L. pertusa* wurde in einem Kurz- und Langzeit-Experiment erfolgreich untersucht. Die Studie zeigte zum ersten Mal, daß *L. pertusa* unter Langzeiteinfluss erhöhter CO_2-Konzentrationen in der Lage ist, ihre Wachstumsraten aufrechtzuhalten, während diese unter Kurzzeiteinfluss signifikant abnahmen. Selbst in für Aragonit untersättigtem Seewasser ($\Omega_{Ar} < 1$) konnte Nettowachstum erhalten werden. Diese Ergebnisse legen daher nahe, daß Kaltwasserkorallenriffe, welche bereits gegen Ende des Jahrhunderts mehrheitlich in untersättigtem Seewasser liegen werden, eventuell weniger vom Aussterben bedroht sind, als bisher vermutet. Die Tatsache, daß allerdings bereits eine Temperaturerhöhung von 3 °C für die Fitness von *L. pertusa* von höherer Relevanz scheint als eine Verdopplung des pCO_2 verweist auf das Problem synergistischer Einflüsse zwischen Ozeanerwärmung und Ozeanversauerung und betont die Wichtigkeit zukünftiger Langzeit-Experimente.

1. Introduction

Norwegian fishermen have known of cold-water corals for hundreds of years (Fosså *et al.* 2002). In 1755 the Bishop of Bergen, Erich Pontoppidan described in his book "*The Natural History of Norway*" fishermen selling coral bushes to the local apothecaries for medicinal purposes (Wilson 2001). Three years later, this "entirely white" coral was described scientifically by Carl von Linné in his magnum opus "*Systema Naturae*" as *Madrepora pertusa* (= *Lophelia pertusa*) (Fig. 1). In the nineteenth century pioneering deep-sea dredging surveys like the HMS Challenger Expedition (1872-6) revealed a global distribution of cold-water corals. But it took until the late 60s of the twentieth century before the first human observed living cold-water corals in the spotlight of a manned research submersible (Milliman *et al.* 1967); for a historical review see Roberts *et al.* (2009). Improvements in deep-sea technology like multibeam echosounders and remotely operated vehicles (ROV) drastically expanded our knowledge of cold-water corals within the last twenty years: like their warm-water relatives some cold-water coral species also form large and extensive reefs and today there is growing evidence, that on a global scale, cold-water coral reefs may exceed the coverage of all shallow-water tropical coral reefs (Freiwald *et al.* 2004).

Fig. 1 The cold-water coral *Lophelia pertusa* (as *Madrepora pertusa*) by Johann Ernst Gunnerus, 1768 (from Moen (2006)).

1.1. The cold-water coral *Lophelia pertusa*

1.1.1. Taxonomy and morphology

Taxonomically the monospecific genus *Lophelia* belongs to the family Caryophyllidae within the order of Scleractinia (Tab. 1). Amongst the 1,486 known scleractinian species, 706 are azooxanthellate (without symbiotic algae in their tissue) of which 615 may be considered as

deep-water (> 50 m) corals (Cairns 2007). Azooxanthellates are typically solitary in habit and only about 25 % are colonial. To date there are 17 known species of deep, cold-water, framework-forming scleractinians of which only six species are widespread, with *L. pertusa* being the most common one (Roberts *et al.* 2009). *L. pertusa* is a pseudocolonial species characterised by a dendroid branched (arborescent) calcareous skeleton consisting of either long thin or dense short corallites (CSA International Inc. 2007). The corallites contain the individual coral polyps and like all Hexacorallia, the septa and tentacles of *L. pertusa* are organised radially-aligned in multiples of six. New polyps are formed by intratentacular budding sensu Vaughan & Wells (1943) from the corallite edge adjacent to primary septa with an indirect mesenterial linkage between the new and the mother polyp (Mortensen 2001). If corallites of adjacent branches grow denser they sometimes fuse together (anastomose) which stabilises the further development of the three-dimensional framework. *L. pertusa* exhibits a remarkable intraspecific morphological variation (Zibrowius 1984). Based on branching patterns and corallite characteristics like height and shape, wall thickness and budding rate, several distinct morphotypes are described (Newton *et al.* 1987; Freiwald *et al.* 1997). Additionally, besides the predominantly white (transparent) appearance, *L. pertusa* occurs also in yellow, orange, and red colour varieties (Freiwald *et al.* 2004). To date it is unknown, if these variations are genetically or environmentally controlled.

Tab. 1 Systematic overview of *L. pertusa*.

Taxon	Name
Phylum	Cnidaria
Class	Anthozoa
Subclass	Hexacorallia (= Zoantharia)
Order	Scleractinia (= Madreporaria)
Suborder	Caryohyllina
Superfamily	Caryophyllioidea
Family	Caryophylliideae *Dana, 1846*
Genus	*Lophelia*
Species	*Lophelia pertusa* *Linnaeus, 1758*

1.1.2. Coral growth and biomineralisation

L. pertusa is - like other deep-sea organisms - a relatively slow growing and long-lived animal (Rogers 1999). Reported growth rates are between 2 - 26 mm yr^{-1} (Mikkelsen *et al.* 1982; Bell & Smith 1999; Mortensen 2001; Roberts 2002; Orejas *et al.* 2008) and some of their reef structures have been growing for hundreds or thousands of years (e.g. the Sula Reef Complex with > 8,000 years; see 2.1.1) making cold-water coral reefs the oldest known bioherms of the

deep-sea. However, apart from a few exceptions almost all of our knowledge about the physiological processes controlling growth and biocalcification in scleractinian corals is based on studies conducted on shallow-water zooxanthellate corals. Today several hypothesis are proposed and vividly debated (Gattuso *et al.* 1999a; Cohen & McConnaughey 2003; Allemand *et al.* 2004; Erez *et al.* In press). The coral skeleton is extracellular beneath the polyps tissue. The polyp itself can simplistically be regarded as a "bag" enclosing a coelenteric cavity that can be opened to the seawater by a mouth. The body walls of the polyp consist of two epithelial layers - the ectoderm (outer layer) and the endoderm (inner layer). These are separated by an extracellular matrix of collagen, the mesogloea. Ecto- and endoderm occur both as oral and aboral layers with specific characteristics each. The two layers facing the skeleton are the aboral endoderm and ectoderm while the two layers facing the seawater are oral endoderm and ectoderm. Calcification takes place in the extracellular calcifying fluid or medium (ECF/ECM) located in the small space between the aboral ectoderm (calicoblastic epithelium = calicodermis) and the dead skeleton and is separated from the seawater by four layers of cells (Fig. 2). Thus the calcification or skeletogenesis occurs in a "biologically-controlled medium" (Allemand *et al.* 2004).

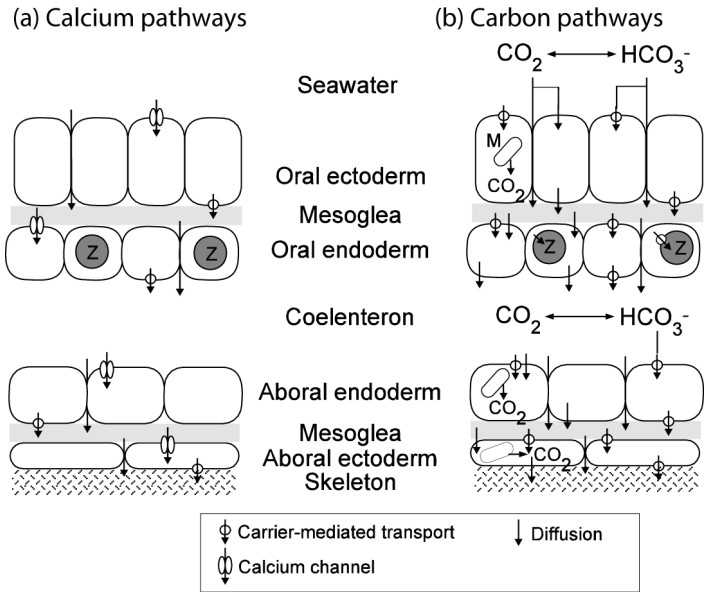

Fig. 2 Possible calcium (**a**) and carbon (**b**) pathways involved in calcification and photosynthesis in scleractinian corals. M = mitochondria; Z = zooxanthellae. Modified from Gattuso *et al.* (1999a).

The skeleton of scleractinian corals consists of calcium carbonate ($CaCO_3$) crystallised in aragonite (orthorhombic system) and a small fraction of organic compounds (0.1 - 1%) consisting of acidic sulphated polysaccharides, sugars and proteins (Cuif & Dauphin 2005; Puverel *et al.* 2005; Dauphin *et al.* 2008). For the calcification process the calicodermis has to supply calcium and dissolved inorganic carbon to the ECF/ECM:

$$Ca^{2+} + HCO_3^- \rightarrow CaCO_3 + H^+ \quad \textbf{Eq. 1}$$

Generally there are two possible mechanisms for the transport of the molecules through the epithelial layers: (1) a paracellular pathway, between cells, or (2) a transcellular pathway through the calicoblastic cells (Berrridge & Oschman 1972). While the first one is driven by an electrochemical gradient - meaning its transport is diffusional and passive, the latter one is active (against a gradient) with specific membrane transporters such as carriers and pumps.

While there is some evidence for carrier mediated (e.g. Ca^{2+}/H^+ ATPase, L-type Ca^{2+} channels) calcium transport across the calicoblastic epithelium in warm-water corals (Tambutte *et al.* 1996; Zoccola *et al.* 2004), the pathways for DIC are largely unknown. However, inhibitor studies point to the involvement of anion exchangers (e.g. HCO_3^-/Cl^- exchangers) in these epithelia (Tambutte *et al.* 1996). A significant part of the inorganic carbon incorporated by coral calcification probably stems from metabolically produced CO_2 (Lucas & Knapp 1997; Furla *et al.* 2000). In an isotopic approach - examining stable carbon and oxygen ratios in coral skeletons - Adkins *et al.* (2003) found incorporated respired carbon in the skeletons of the two cold-water corals *Desmophyllum cristagalli* and *Lophelia pertusa*. Carbonic anhydrase (CA) might be a key component of the calcification machinery; inhibition of this enzyme was reported to reduce coral calcification rates drastically (Tambutte *et al.* 1996; Furla *et al.* 2000; Al-Horani *et al.* 2003a, b; Marshall & Clode 2003; Tambutte *et al.* 2007). Within calicoblastic cells it catalyses the interconversion of metabolically produced CO_2 to HCO_3^- destined for the ECF/ECM (Tambutte *et al.* 1996). CA was also found in the organic matrix (OM) secreted by the calicodermis. The complex biochemical and structural composition of the OM indicates its mediative character in the nucleation process of new $CaCO_3$ (Fukuda *et al.* 2003; Watanabe *et al.* 2003; Cuif & Dauphin 2005; Puverel *et al.* 2005).

1.1.3. Distribution and habitat characteristics

L. pertusa is a comopolitan cold-water coral with highest abundances found on the continental margins in the North Atlantic (Zibrowius 1980; Freiwald *et al.* 2004). A dense band of *L. pertusa* bioherms stretches along the eastern Atlantic continental margin from the Barents Sea down to West Africa and records from the western margin of the Atlantic indicate that there might be a similar band from Nova Scotia down to the Florida Straits and into the Gulf of Mexico (Freiwald *et al.* 2004). *L. pertusa* is also known in parts of the Mediterranean Sea, the Gulf of Mexico, the Caribean Sea and in the Indian and Pacific Oceans (Zibrowius 1973; Cairns 1984). The currently known places of occurrence (Fig. 3, red dots) reflect more the intensity of the research and mapping activities in some countries than the real global distribution which is probably more reliably indicated by ecoenvironmental prediction models (Fig. 3, yellow areas).

The northernmost record of *L. pertusa* is from the Hjelmsøybank at 71°21'N, 24°00'E in the south-western Barents Sea (Fosså *et al.* 2000), while the southernmost location is on the sub-Antarctic Macquarie Ridge at 51°00'S, 162°01'E off New Zealand (Cairns & Stanley 1982). The shallowest occurrence of live *L. pertusa* is at 39 m depth in Trondheimsfjord, Norway (Rapp & Sneli 1999) and the deepest extend down to 3,383 m in the New England Seamount chain in the North Atlantic (Zibrowius 1980). Despite this large bathymetric range, most *L. pertusa* coral reefs have been recorded between 200 and 1,000 m (Zibrowius 1980; Freiwald & Wilson 1998).

As a coral colony grows the complexity of the framework increases and a cold-water reef developes. Thus cold-water corals like *L. pertusa* are also referred as bioengineers (Jones *et al.* 1994). The largest known *L. pertusa* reef is the Røst Reef stretching 35 - 40 km along the continental shelf break southwest of the Lofoten Island off northern Norway and encompassing an area of approximately 100 km^2 (Rogers 1999; Freiwald *et al.* 2004; Fosså *et al.* 2005).

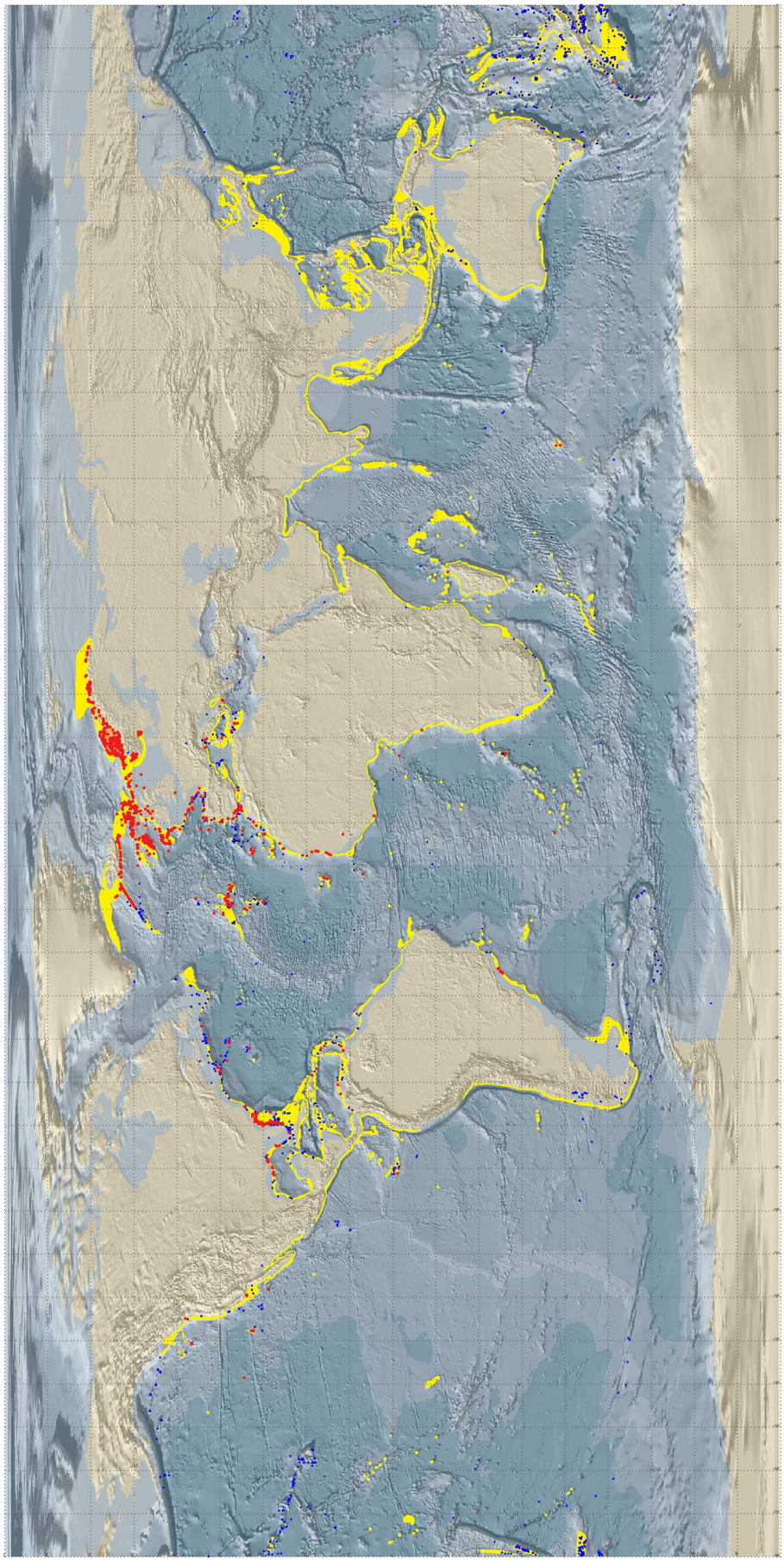

Fig. 3 Global distribution of recorded *Lophelia pertusa* occurences (red), predictive distribution (yellow), and distribution of general known cold-water coral reefs (blue). Source: World Conservation Monitoring Centre of the United Nations Environment Programme (UNEP-WCMC 2009).

Cold-water coral reefs provide structural habitat for a diverse assemblage of other organisms including commercially important fish species (Fosså *et al.* 2002; Costello *et al.* 2005). In contrast to tropical corals, a cold-water reef is typically segmented into three major subhabitats (macrohabitats):

(1) the zone of living corals - hosting only a few species like the mutualistic symbiont *Eunice norvegicus* (Polychaeta) or the parasite *Hyrrokkin sarcophaga* (Foraminifera),
(2) an intermediate dead coral framework zone - consisting of live and dead *L. pertusa* and a highly diverse species assemblage of many taxonomic groups, and
(3) the coral rubble zone - representing the most degraded state of the reef which hosts mainly encrusting sponges and echiurid worms (Rogers 1999; Freiwald *et al.* 2004).

On a smaller scale four corresponding microhabitats were distinguished: (1) surface of living corals, (2) detritus covered surface of dead corals, (3) skeletal cavities created by boring sponges and (4) inter-branch free space (Mortensen *et al.* 1995).

1.1.4. Environmental drivers of distribution

For the initial settlement of its larvae *L. pertusa* needs a solid hard substratum and prefers typically bathymetric features like mound structures, oceanic ridges, or the summits and flanks of seamounts. This areas typically coincide with strong water currents and high productivity (Genin *et al.* 1986; Frederiksen *et al.* 1992; Thiem *et al.* 2006). Although *L. pertusa* can tolerate salinities ranging from 32 in Scandinavian fjords to > 38 in the Ionian Sea (Strømgren 1971; Taviani *et al.* 2005) they are most commonly associated with oceanic water masses exhibiting a salinity of 35 - 37 (Roberts *et al.* 2003; Freiwald *et al.* 2004). The thermal tolerance of *L. pertusa* ranges between 4 and 13.8 °C (Freiwald *et al.* 2004; Taviani *et al.* 2005).

Dissolved oxygen concentration (DO) at sites inhabited by *L. pertusa* in the north-east Atlantic was most commonly between 3 and 5 mL L^{-1} (referred as “local oxygen minimum zones”) (Freiwald 2002). In the Gulf of Mexico, relatively low DO of 2.6 - 3.2 mL L^{-1} have been reported by Schroeder (2002). In the framework of an “environmental niche factor analysis” (ENFA), Davies *et al.* (2008) calculated a global DO range of 4.3 - 7.2 mL L^{-1}. This corresponds well to other examinations of the respiratory metabolism of *L. pertusa* revealing that this coral regulates its oxygen consumption over a wide range of oxygen concentrations

but that it is unable to maintain normal aerobic activity below approximately 3 mL L^{-1} (Dodds *et al.* 2007).

In their study on hydrographic parameters and their relation to living cold-water coral reef occurances, Dullo *et al.* (2008) confirmed that cold-water corals in the North Atlantic tolerate a wide range of environmental conditions but that the distribution follows a seawater density envelope of sigma-theta (σ_θ) = 27.35 - 27.65 kg m^{-3}. They conclude that density is a basic prerequisite for coral development, growth and distribution which may be linked to lateral transport processes of coral larvae at this specific density envelope (Dullo *et al.* 2008).

The enhanced water currents surrounding cold-water coral reefs (see above) are thought to support and concentrate the food supply ("current accerleration hypothesis") (Mortensen 2001; Kiriakoulakis *et al.* 2005; Thiem *et al.* 2006). Little is known about the food sources of *L. pertusa* but *in situ* and aquarium observations suggest that *L. pertusa* feeds on calanoid copepods and other mesozooplankton (Heinrich & Freiwald 1997; Mortensen 2001; Roberts & Anderson 2002). The occurrence of a few cold-water coral reefs close to light hydrocarbon seepage has led to the hypothesis, that corals are in part depending on a food chain supported by chemosynthetic bacteria ("hydraulic theory") (Hovland *et al.* 1998; Hovland & Risk 2003). While this theory is still controversely discussed (Hovland 2008; Roberts *et al.* 2009), stable carbon isotope examinations have not found any evidence for a link between seepages and cold-water coral nutrition (Noé *et al.* 2006). Additionaly, $\delta^{15}N$ signatures (Duineveld *et al.* 2004; Duineveld *et al.* 2007) and fatty acid compositions (trophic markers) within *L. pertusa* tissues (Dodds *et al.* 2009) as well as spatial meta-analysis (Guinotte *et al.* 2006; Davies *et al.* 2008) strongly imply that cold-water corals are predominantely supported by surface production rather than a chemosynthetic food chain.

There is increasing concern that the seawater carbonate chemistry and respectively the aragonite saturation horizon (ASH) are also important drivers in the horizontal (global) and vertical distribution of *L. pertusa*. Since this is the main topic of this thesis, this aspect is adressed separately in the next chapter concerning anthropogenic impacts and threats to cold-water corals.

1.2. Anthropogenic impacts and threats to cold-water corals

1.2.1. Seabed activities

Fisheries

To date the most severe and acute threat to cold-water coral reefs is physical damage from bottom trawling (Freiwald *et al.* 2004; Roberts *et al.* 2009). In former times fishermen avoided fishing within the reef structures in order to prevent losing or destroying their nets. With the technological advance, nets were strengthened, kept open by heavy otter boards (trawl doors), and equipped with "rockhopper" gear allowing them to ride across even rough grounds such as coral reefs. Thus bottom trawling along the shelves and continental margins increased drastically in the late 1980s (Gordon 2001; Fosså *et al.* 2002) and with it the collateral damages to cold-water coral ecosystems (Fig. 4 B). Only about a decade later, 30 - 50 % of the known *L. pertusa* reefs on the Norwegian shelf were estimated to be either impacted or damaged by trawling (Fig. 4 A) (Fosså *et al.* 2002). Massively damaged *L. pertusa* habitats have also been documented on the European continental margin, on seamounts off Tasmania, and from the east and west coasts of North America (Koslow *et al.* 2001; Hall-Spencer *et al.* 2002; Mortensen 2005). As a secondary effect of the trawling muddy deep-see sediments were resuspended, resulting in long-term sedimentation rates which may in turn smother corals living nearby (Rogers 1999). Although not examined on cold-water corals, a negative relation between sedimentation and growth rates was well documented on tropical shallow-water corals (Dodge *et al.* 1974; Hudson *et al.* 1982; Dodge & Szmant-Froelich 1985). Other fishing gears and methods like dredges, bottom-set gillnets and long-lines are - to a lower extent - also documented threats to cold-water corals (Witherell & Coon 2001; Fosså *et al.* 2002; Husebo *et al.* 2002).

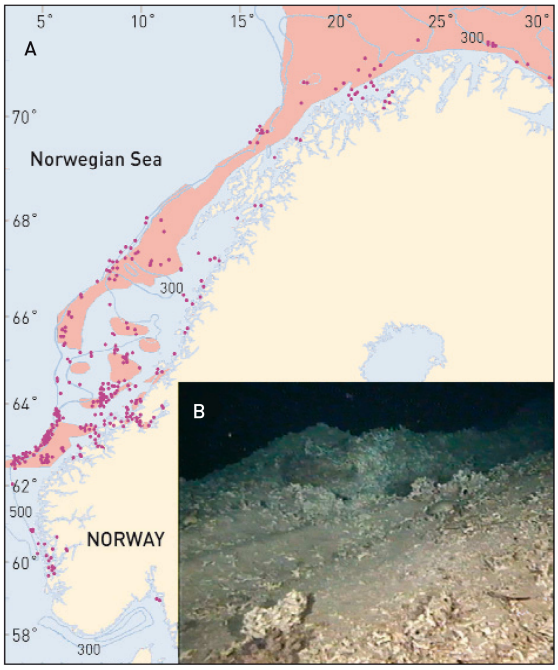

Fig. 4 A) Areas of bottom trawl activities (pink) on the Norwegian shelf in relation to *L. pertusa* occurrences (dots). **B**) Destroyed reef at 190 m depth (Source: Freiwald *et al.* (2004)).

Today there is fortunately a raising scepticism about the sustainability of bottom fishing within cold-water coral reefs and Norwegian authorities have closed the Sula Ridge and several other areas to bottom fishing. However, many cold-water coral reefs are located beyond the exclusive economic zone of individual nations on the High Seas with no clear ownership or jurisdiction making them potentially vulnerable to over-exploitation and unregulated activities (Davies *et al.* 2007).

Hydrocarbon exploitation, pipelines and cables

The still increasing demand on oil and gas and the diminishing production from shelf seas have moved hydrocarbon companies into increasingly deeper areas (Kemp & Stephen 2005). Although it has to be noted that relatively large and healthy looking *L. pertusa* colonies were found on oil rigs in the North Sea (Bell & Smith 1999; Roberts 2002; Gass & Roberts 2006) the indirect impact due to discharges (e.g. rock cuttings, drilling fluids, produced waters) or catastrophes like the "Deepwater Horizon" explosion and oil spill in the Gulf of Mexico in April 2010 suggest a profound intrusion on deep-sea ecosystems.

The anchoring of oil and gas platforms and the emplacement of pipelines and cables for telecommunication and electricity can physically damage *L. pertusa* reef structures (Freiwald *et al.* 2004). Furthermore in order to avoid stresses with fishing activities - the cables (especially transatlantic communication cables) were buried in the seabed with special undersea ploughs which will in turn resuspend sediment with the implications mentioned above.

Future threats

For a long time deep-sea and extra-terrestrial mining was the stuff of science-fiction novels and Hollywood movie productions. While the latter remains - for now - fantasy, the former will become a commercial reality within the next years. Companies currently acquire mining rights for deep-water exploitation of "seafloor massive sulphide" (SMS) deposits found in close proximity to active sulphide-forming hydrothermal vent systems. The SMS are highly enriched in precious metals such as gold, copper, zinc, and silver (Halfar & Fujita 2007). Drilling in the world's first SMS resource, located in 1,600 m water depth in the Bismarck Sea (north of Papua New Guinea), commenced in October 2010 and productive full-scale excavation is planned for early 2013 (Solwara 1 Project, see Nautilus Minerals Inc. (2011)). These and other upcoming projects (e.g. mining of manganese nodules and crusts) bear

potential environmental risks including benthic disturbances, sediment plumes and toxic effects on the water column (Ahnert & Borowski 2000; Glasby 2000; Halfar & Fujita 2007) with unknown implications in terms of lost biological resources (Roberts *et al.* 2009).

The sequestration of CO_2 into the deep-sea was proposed as an approach to mitigate rising atmospheric CO_2 levels caused from the burning of fossil fuels (see next chapter). However, direct injection of liquefied CO_2 into great depths has proven to cause adverse effects to diversity and survivorship of the deep-sea benthic meiofauna (Barry *et al.* 2004; Thistle *et al.* 2005; Ricketts *et al.* 2009). Maybe other methods like the sequestration of CO_2 into deep-sea basalt formations would have a lesser impact but the dimension of such an approach is so monumental[1] that without a sound scientific basis and consensus it is not responsible to risk endangering one of our last great wildernesses.

1.2.2. Climate change

Deforestation, land-use change and most importantly the combustion of fossil hydrocarbon fuels are increasing the atmospheric concentrations of greenhouse gases. In the last 100 years, rising CO_2 concentrations have increased the global surface temperature by 0.56 to 0.92 °C. Another 1.1 to 6.4 °C is projected for the end of the 21st century (IPCC 2007)[2]. For the second half of the 20th century it was calculated that the oceans adsorbed approximately 84 % of the heat added to the Earths' climate system (Levitus *et al.* 2005).

The sensitivity of shallow-water zooxanthellate corals to increasing temperatures has been documented extensively (see Hoegh-Guldberg (1999) for a comprehensive review). The endosymbiotic dinoflagellates (Protozoa: *Symbiodinium* spp.) capture solar energy and nutrients. Through a complex host-symbiont interaction they provide their host with > 95 % of its metabolic requirement. As a consequence of this symbiosis and an environmental adaptation, the thermal tolerance of most scleractinians from the tropics is limited to a relatively narrow range of ± 1 - 2 °C. Within their natural temperature range, growth rates typically increase with temperature, but drop above the optimum temperature (Coles & Jokiel 1978; Edmunds 2005; Rodolfo-Metalpa *et al.* 2006). Under various stress conditions (e.g., prolonged temperature increase/decrease, increased solar radiation, changes in water

[1] For resulting in a measurable decline in the atmospheric CO_2 concentration.
[2] The relatively large range in the projected temperatures depends on the applied emission scenario (rapid introduction of clean and efficient technologies vs. fossile fuel-intensive) rather than uncertainties in the understanding of the Earths' climate system (oceans, atmosphere, continents, and cryosphere).

chemistry, starvation, etc.) the corals expel their obligatory zooxanthellae which results in a bleaching of the coral. Like a "domino effect", the bleaching very often continues even after the initial stress factor is obsolete. If a coral colony survives bleaching - and respectively the causing stress factor - it may recover its dinoflagellates but typically shows reduced growth, calcification, and fecundity afterwards (Hoegh-Guldberg 1999). In the last decades, mass coral bleaching has increased worldwide in intensity and frequency (Hoegh-Guldberg 1999; Donner *et al.* 2005; Hoegh-Guldberg *et al.* 2005).

For a long time it was thought that the deep-sea is buffered against the effects of surface-driven cycles and impacts (Menzies 1965). Now there is growing evidence that ocean warming has penetrated depths between 700 and 3,000 m (Barnett *et al.* 2005). The physiological thermal tolerance of the cold-water coral *L. pertusa* is still unknown. To date, only one study examined the effects of short-term temperature shifts on the metabolic activity of this species. When exposed to elevated temperatures but within their ecoenvironmental range in the field (6.5 - 11 °C), the oxygen consumption increased three-fold from the colder to warmer treatments (Dodds *et al.* 2007). Corresponding van't Hoff Q_{10} values ranged between 5.4 to 8.3 and exceeded the van't Hoff Q_{10} rule of 2 - 3 for biochemical and physiological processes, suggesting a strong sensitivity of *L. pertusa* to abrupt temperature changes. However, compared to shallow-water corals, *L. pertusa* inhabits a relatively wide temperature range (see above) and in the study of Dodds *et al.* (2007) it was also demonstrated that - in the given temperature range - *L. pertusa* was able to maintain its rate of oxygen consumption independent over a wide range of pO_2 values. In summary, the high Q_{10} values imply an increase in metabolic rate, which in turn would affect the energy budget of the coral and may influence survival if the increased energy requirements could not be compensated from food supply (Dodds *et al.* 2007).

As outlined above, the nutrition of *L. pertusa* was suggested to be dependent on surface production (see 1.1.4). For the North East Atlantic it was estimated that 2 - 4 % of the spring-bloom surface production was transferred in form of biogenic particles (POM, mainly phytodetritus) to the seafloor (Gooday & Hughes 2002). Phyto- and zooplankton productivity has been shown to be affected by climatic fluctuations (Edwards *et al.* 2001; Hawkins *et al.* 2003; Schippers *et al.* 2004; Pitois & Fox 2006). Thus changes in surface environmental variables may also have indirect implications for *L. pertusa* and associated deep-sea organisms.

Ocean acidification – the chemical background

Perhaps the most fundamental change to our oceans within the last million years is also linked to rising atmospheric CO_2 concentrations. Since the beginning of the Industrial Revolution in the mid of the 18th century, atmospheric CO_2 concentrations increased from approximately 280 to 387 parts per million (ppm) (Solomon *et al.* 2007). The rate of this nearly 40 % increase is at least one order of magnitude faster than what our planet has experienced for millions of years (Doney & Schimel 2007). The current atmospheric CO_2 concentration is higher than it has been for more than 800,000 years (Lüthi *et al.* 2008). Like all gases, atmospheric CO_2 (g) stands in a thermodynamic equilibrium with the CO_2(aq) dissolved in the oceans (Henry's Law):

$$CO_2(g) \rightleftharpoons CO_2(aq) \qquad \textbf{Eq. 2}$$

The air-sea gas exchange is relatively fast on a timescale of several months. It has been estimated that over the past 250 years the oceans have absorbed about 30 % of the anthropogenic carbon emission related to 525 billion tons of CO_2 (Sabine & Feely 2007). When CO_2 dissolves in seawater, it reacts with the water to form carbonic acid (H_2CO_3) which dissociates in subsequent acid-base reactions to bicarbonate (HCO_3^-) and carbonate (CO_3^{2-}) ions. Since it is difficult to analytically distinguish between the two unionised species CO_2 and H_2CO_3, they usually are combined to the hypothetical aqueous species CO_2* (Dickson *et al.* 2007). Thus the solution chemistry of carbon dioxide can be described by the following two equations:

$$CO_2^*(aq) + H_2O(l) \rightleftharpoons H^+(aq) + HCO_3^-(aq) \qquad \textbf{Eq. 3}$$

$$HCO_3^-(aq) \rightleftharpoons H^+(aq) + CO_3^{2-}(aq) \qquad \textbf{Eq. 4}$$

The corresponding equilibrium concentrations are given by stoichiometric constants which are a function of ionic strength, temperature, and pressure (see review by Millero (2007)):

$$K_0 = [CO_2^*] / f_{CO_2} \qquad \textbf{Eq. 5}$$

$$K_1 = [H^+][HCO_3^-] / [CO_2^*] \qquad \textbf{Eq. 6}$$

$$K_2 = [H^+][CO_3^{2-}] / [HCO_3^-] \qquad \textbf{Eq. 7}$$

The bracketed values [i] are the total concentrations of species i and f_{CO_2} stands for the fugacity of carbon dioxide in the gas phase (see Dickson (2007)).

The sum of the three carbon species is termed total dissolved inorganic carbon (DIC[1]):

$$DIC \equiv \sum CO_2 = [CO_2] + [HCO_3^-] + [CO_3^{2-}] \quad \textbf{Eq. 8}$$

For surface seawater conditions, approximately 90 % of the inorganic carbon is bicarbonate ion, 9% is carbonate ion and only 1 % is dissolved CO_2. However, increased dissolution of CO_2 into seawater results in more bicarbonate ions and protons (Eq. 3, left to right). The protons react with the more alkaline carbonate ions to another bicarbonate ion (Eq. 4, right to left). Thus the net effect of the dissolution of CO_2 in seawater is an increase in protons and bicarbonate ions, whereas the carbonate ion concentration decreases (Fig. 5).

As the acidity of a solution is defined as

$$pH = - \log_{10}[H^+] \quad \textbf{Eq. 9}$$

increasing H^+ concentrations in the seawater means a lowering (acidification) of the corresponding pH level. Over the past 250 years, the average ocean surface water pH has decreased by approximately 0.1 units from 8.21 to 8.10 (Caldeira & Wickett 2003; Orr *et al.* 2005). Until the end of this century, atmospheric CO_2 concentration are expected to exceed 800 ppm leading to a further decrease of 0.3 - 0.4 pH units (Orr *et al.* 2005; Solomon *et al.* 2007).

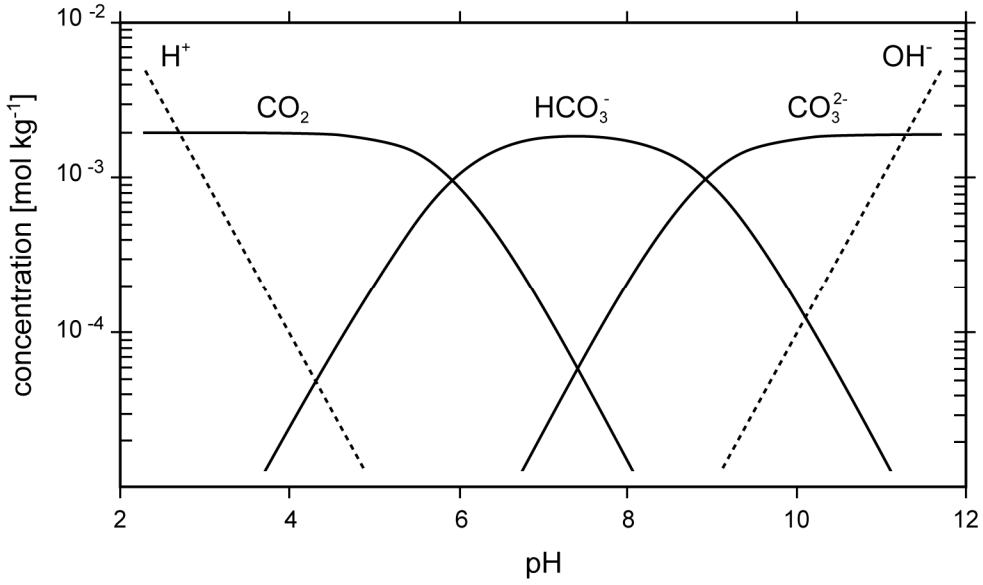

Fig. 5 Concentrations of dissolved carbonate species, H^+, and OH^- in seawater as a function of pH (Bjerrum plot). Figure modified after Wolf-Gladrow *et al.* (2007).

[1] also referred to as TCO_2 or C_T

The buffering capacity of seawater towards additional protons can be expressed by the alkalinity. More precisely, the total alkalinity is defined as the concentration of all anions in the seawater that can accept protons (for details see Zeebe & Wolf-Gladrow (2001)):

$$TA = [HCO_3^-] + 2\,[CO_3^{2-}] + [B(OH)_4^-] + [OH^-] - [H^+] + \text{minor components} \quad \textbf{Eq. 10}$$

The dissolution of marine calcium carbonates ($CaCO_3$) facilitates the uptake of anthropogenic CO_2 by increasing the TA:

$$CaCO_3 + CO_2 + H_2O \rightleftharpoons 2HCO_3^- + Ca^{2+} \quad \textbf{Eq. 11}$$

However, projected anthropogenic CO_2 inputs will occur within just about 300 years which is much too fast for dissolution of calcareous sediments to neutralise anthropogenic CO_2 with the consequence of continuous and rapidly decreasing saturation states.

The saturation state of seawater with respect to $CaCO_3$ is defined as the ion product of calcium and carbonate ion concentrations:

$$\Omega = \frac{[Ca^{2+}][CO_3^{2-}]}{K_{sp}^*} \quad \textbf{Eq. 12}$$

where K^*_{sp} is the solubility product which depends on temperature, salinity, pressure and the particular mineral phase, aragonite, calcite or high-Mg calcite (Mucci 1983). While $[Ca^{2+}]$ is a major constituent of seawater, the saturation state primarily depends on the carbonate concentration.

Below $\Omega = 1.0$, the seawater is undersaturated with respect to carbonate and $CaCO_3$ begins to dissolve. In the oceans, the depth of the boundary between saturation and undersaturation is referred to as saturation horizon (lysokline). Aragonite is approximately 1.5 times more soluble than calcite. Thus the aragonite saturation horizon (ASH) is shallower than the calcite saturation horizon (CSH). Because of a longer deep-water circulation which allows the accumulation of more DIC from respired CO_2, the ASH and CSH in the Indian and Pacific Oceans are shallower than in the Atlantic Ocean (Broecker 2003).

In summary, the decrease of carbonate concentration and the respective saturation state due to increasing anthropogenic CO_2 leads to a shoaling of the saturation horizon and thus favours the dissolution of marine carbonates.

Ocean acidification – the biological implications

The vast majority of marine carbonate production is biologically mediated. Biocalcification is a fundamental physiological process forming protective shells or skeleton structures in planktonic (e.g. coccolithophores, foraminiferans, pteropods) as well as benthic (e.g. calcareous algae, corals, echinoderms, molluscs) organisms.

Calcifying plankton

Because of their important role in marine food webs and their contribution to the marine carbon cycle, most laboratory and mesocosm plankton studies were conducted on bloom-forming coccolithophorids such as *Emiliania huxleyi* and *Gephyrocapsa oceanica*. While most of the studies reported reduced calcification rates of 25 - 66 % and malformations of the calcitic coccoliths when pCO_2 was increased to 560 - 840 ppm (Riebesell *et al.* 2000; Zondervan *et al.* 2001; Zondervan *et al.* 2002; Sciandra *et al.* 2003; Delille *et al.* 2005; Engel *et al.* 2005) converse responses reported by Iglesias-Rodríguez *et al.* (2008) suggesting a misinterpretation of the data (Riebesell *et al.* 2008) or the potential for considerable variability between different coccolithophore species and strains (Turley *et al.* 2010). Ocean acidification affects not only phytoplanktonic calcification. On the community level of a natural plankton assemblage maintained in mesocosm enclosures, Riebesell *et al.* (2007) reported a 27 % and 39 % enhanced DIC uptake at elevated pCO_2 concentrations of 700 and 1,050 ppm, respectively, compared to present levels. While nutrient uptake in the same treatments remained unaffected, the C:N ratio shifted toward higher levels, indicating an excess CO_2 sequestration potential by the biological pump with possible implications for marine biogeochemical cycling and marine ecosystem dynamics (Riebesell *et al.* 2007). Another prominent group of marine phytoplankton are nitrogen-fixing cyanobacteria. At elevated pCO_2 concentrations, increased N_2- and CO_2-fixation rates, growth rates and N:P ratios were measured, suggesting also a negative feedback to atmospheric CO_2 increase (Barcelos e Ramos *et al.* 2007; Hutchins *et al.* 2007).

Dissolution of their aragonitic shells was shown for the cosmopolitan euthesomatous pteropod *Clio pyramidata* when exposed to undersaturated seawater with respect to aragonite ($\Omega_{Ar} < 1$) (Orr *et al.* 2005). Moreover, examinations on paleoceanographic records have shown that the calcitic shell weight of planktonic foraminiferans decreased by 4 - 8 % and 6 - 14 % - when grown under decreased carbonate ion concentrations equivalent to 560 and 740 ppm CO_2,

respectively - compared to the pre-industrial level of 280 ppm (Spero *et al.* 1997; Bijma *et al.* 1999; Barker & Elderfield 2002).

Calcifying benthos

Detrimental effects due to ocean acidification was also demonstrated in a variety of benthic calcifiers. Apart from corals, decreased calcification rates or shell growth under climate-relevant CO_2 increase were reported for coralline algae (Jokiel *et al.* 2008; Kuffner *et al.* 2008; Martin & Gattuso 2009), bivalves (Gazeau *et al.* 2007), gastropods and sea urchins (Shirayama & Thornton 2005). In some species however, enhanced calcification in response to elevated pCO_2 was observed (Wood *et al.* 2008; Gooding *et al.* 2009; Ries *et al.* 2009). For the brittlestar *Amphiura filiformis* increased calcification under high pCO_2 was accompanied by increased metabolic rates and a loss of arm muscle mass (Wood *et al.* 2008). Hence it was emphasised that the physiological costs incurred by this compensatory process may reduce survival and fitness (Wood *et al.* 2008).

Shallow-water corals and coral reefs

While it was known for a long time that coral calcification changes alkalinity (Smith & Pesret 1974; Smith & Key 1975), the converse that calcium carbonate saturation influences the calcification was first realised by Gattuso *et al.* (1998). Since then numerous studies have revealed a negative trend in calcification rates with increasing pCO_2 concentrations (Gattuso *et al.* 1999b; Marubini & Atkinson 1999; Langdon *et al.* 2000; Marubini *et al.* 2001; Leclercq *et al.* 2002; Langdon *et al.* 2003; Marubini *et al.* 2003; Ohde & Hossain 2004; Langdon & Atkinson 2005; Schneider & Erez 2006; Marubini *et al.* 2008; Andersson *et al.* 2009; Cohen *et al.* 2009). The responses vary between and also within species but on average, a doubling of the pre-industrial pCO_2 concentrations results in a 20 % decrease in the calcification rate (see reviews by Erez *et al.* (In press) and Kleypas & Yates (2009)). The effect might be more dramatical on the early life stages as Albright *et al.* (2008) recently demonstrated. At projected pCO_2 scenarios for the years 2065 (560 ppm) and 2100 (720 ppm) growth rates of coral juveniles decreased by 50 and 78 %, respectively, compared to present day level.

Deviating from this consistent negative trend are results on two zooxanthellate temperate coral species from the Mediterranean which were recently found to be unaffected by pCO_2 concentrations projected for the coming decades (Ries *et al.* 2009; Rodolfo-Metalpa *et al.* 2010).

As mentioned above, ocean acidification affects the balance of the carbonate species and thus the seawater pH. In a systematic approach to find out which of these parameters is in particular controlling the calcification rate in corals, Schneider and Erez *et al.* (2006) manipulated the carbonate system by (1) varying pH, without changing DIC, (2) varying DIC, keeping pH constant, and (3) varying DIC, keeping pCO_2 constant. Calcification rates in all experiments were positively correlated with $[CO_3^{2-}]$ - indicating that this factor predominantly controls the rate of calcification rather than pH or DIC (Schneider & Erez 2006). This supports previous findings from the Biosphere 2 experiment which have shown that coral/algal community calcification rates correlated best with Ω_{Ar} (Langdon *et al.* 2000; Langdon *et al.* 2003). It is also in accordance with geochemical findings, linking the precipitation of inorganic carbonates to a function of Ω_{Ar} (Burton & Walter 1987).

However, for the coral *Madracis auretenra* it was shown that calcification rates strongly responded to variations in bicarbonate concentration rather than carbonate concentration, aragonite saturation state or pH (Jury *et al.* 2009). This may suggest that CO_3^{2-} (or Ω_{Ar}) is not always the controlling parameter and that coral responses to ocean acidification are more diverse than currently thought (McConnaughey *et al.* 2000; Jury *et al.* 2009; Ries *et al.* 2009). Moreover, in their natural environment, shallow-water corals sometimes experience large diurnal shifts in pH (e.g. 7.9 - 8.1; (Bates *et al.* 2001; Suzuki & Kawahata 2003)) indicating that shallow-water corals - to a certain degree - are already adapted to small variations in external pH (Erez *et al.* In press).

Whatever the controlling factor may be, both ocean acidification and seawater warming will influence the corals' life and their ecosystem simultaneously. To date the great majority of ocean acidification related studies was conducted in laboratory tanks or mesocosms whereas field studies were focused on ocean warming research. However, two ecosystem studies examined the combined effect of temperature and Ω_{Ar} on coral reef communities from the Gulf of Aqaba and West Pacific. Both studies show consistently that net carbonate production (production minus bioerosion) decreased significantly with decreasing saturation state and temperature (Ohde & van Woesik 1999; Silverman *et al.* 2007). Based on their dataset Silverman *et al.* (2009) estimated that on a global scale almost all shallow-water coral reefs will cease to grow and start to dissolve once atmospheric CO_2 concentration reaches 560 ppm, a level projected for the mid of the century (Solomon *et al.* 2007).

Analyses of cores from the Great Barrier Reef revealed a relatively good correlation of calcification rates with temperature and showed no signs of a decline within a record of the past 400 years. During the last two decades, however, calcification rates decreased up to 21 %. This was thought to reflect synergistic effects between temperature increases and ocean acidification (Lough & Barnes 2000; Cooper *et al.* 2008; De'Ath *et al.* 2009). On a geological timescale, life on Earth has experienced five great mass extinction events. In all cases, coral reefs disappeared for several million years ("reef gaps") from the paleo record (Stanley & Fautin 2001; Stanley 2003). While the causes are complex and manifold, they are all primarily linked to the carbon cycle and atmospheric carbon dioxide levels (Zachos *et al.* 2005; Veron 2008). The paleo record also tells us that the dramatic speed of projected future changes in the seawater chemistry and its environmental pressure on marine calcifiers is unprecedented in the past 65 million years (Ridgwell & Schmidt 2010). Although Fine and Tchernov (2007) have demonstrated the potential of a scleractinian coral to survive undersaturated seawater conditions ($\Omega_{Ar} < 1$) by becoming a sea anemone-like animal the slow reef recovery after extinction events suggests the evolution of new species rather than recolonisation by survivors (Veron 2008).

Cold-water corals

In contrast to their shallow-water relatives, virtually nothing is known about the effects of climate change on cold-water corals such as *L. pertusa*. To date only one study reported results from acidification experiments on cored and dredged coral samples, carried out during two research cruises. However, despite the methodological limitations of this short-term study, it was clearly shown, that *L. pertusa* exhibits drastically reduced calcification rates of 30 and 56 % when ambient seawater pH was reduced by 0.15 and 0.3 units, respectively (Maier *et al.* 2009).

The fact that over 95 % of all presently known cold-water coral reefs are located in waters supersaturated with respect to aragonite strongly suggests that the aragonite saturation state is an essential driver for their distribution (Guinotte *et al.* 2006; Davies *et al.* 2008; Tittensor *et al.* 2009). In the North Atlantic the ASH is very deep (> 2,000 m) and carbonate dissolution rates are low compared to the North Pacific, where the ASH is shallow (50 - 600) (see above and Feely *et al.* (2004)). Although scleractinian cold-water corals can be found in both ocean basins, large and complex reef structures like the *L. pertusa* bioherms are only present in the North Atlantic. The North Pacific is dominated by octocorals (soft corals, stoloniferans, sea

fans, sea pens, gorgonians) and stylasterids, which both mainly use calcite - the most stable polymorph of $CaCO_3$ - to build their spicules and skeletons (Cairns & Macintyre 1992).

As ocean acidification continues, the depth of the aragonite saturation horizon will rise closer to the sea surface. In the North Atlantic observations show that the saturation horizon has shoaled 80 - 400 m since pre-industrial times (Feely *et al.* 2004; Tanhua *et al.* 2007) and might shoal another 2,000 m until the end of this century as suggested by models (Orr *et al.* 2005). Based on these projections, Guinotte *et al.* (2006) have overlaid locations of 410 known cold-water coral bioherm locations (Freiwald *et al.* 2004) and found that 70 % of these locations will be in corrosive (undersaturated) waters by the end of the century (Fig. 6).

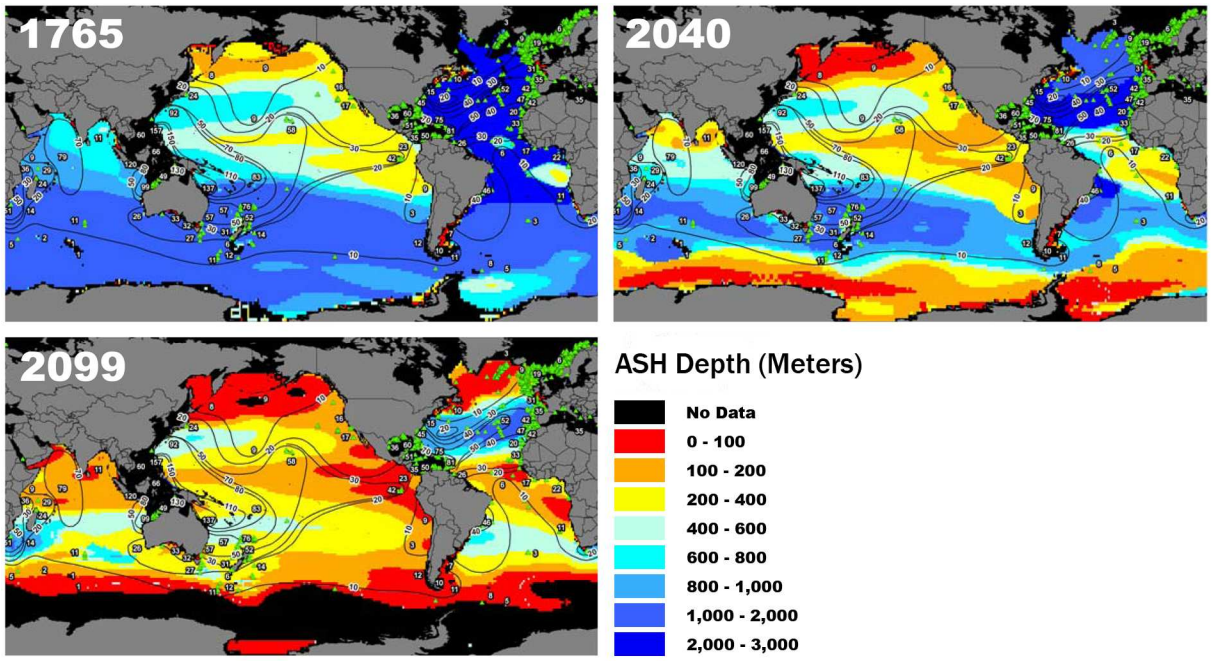

Fig. 6 Projected depth of the aragonite saturation horizon (ASH) for the years 1765 (pre-industrial), 2040, and 2099, locations of the six main bioherm-forming cold-water coral species (green triangles), and diversity contours for 706 species of azooxanthellate corals. Black areas appearing in the Southern Ocean and North Pacific in the year 2099 indicate areas where ASH depth has reached the surface. From Guinotte *et al.* (2006) (modified).

Moreover, if cold-water corals are as sensitive as their shallow-water relatives where relative small reductions in the aragonite saturation state cause a substantial decrease in calcification, then their calcification rates may decline well before seawater becomes corrosive (Turley *et al.* 2007). These detrimental impact may be amplified if other effects of climate change (ocean warming, changes in current patterns, salinity or food availability) will act in concert.

In view of this, cold-water coral reefs are suspected to be amongst the most vulnerable marine ecosystems and due to the apparent lack of knowledge numerous reports and policy documents have highlighted the urgent need for representative studies examining the effects of climate change on cold-water corals (Freiwald *et al.* 2004; Raven *et al.* 2005; Guinotte *et al.* 2006; Kleypas *et al.* 2006).

1.3. Thesis outline

Thesis aims & objectives

The aim of the present research was to start filling this actual lack of knowledge (see above) by manipulative experimentation on live cold-water corals of the main bioherm-forming species *Lophelia pertusa*.

At the beginning of this work (2006) our knowledge of the biology of *L. pertusa* was very scarce. Only a few studies reported results from *in situ* or aquarium observations (Rogers 1999; Mortensen 2001). Nothing was published about principal ecophysiological parameters such as feeding rates, respiration rates, calcification rates or tolerances towards water properties (salinity, temperature, dissolved inorganic nutrients). Consequently there was also no information available for methodological issues with respect to cultivation (let alone within closed recirculating systems) and experimentation. Therefore the following main objectives were specified:

(1) Development of two aquarium systems. One for general cold-water coral husbandry which mimics natural conditions and one for experimental purposes allowing manipulations on climate-change related water properties.

(2) Maintaining of corals' health and condition by monitoring water properties suspected to be critical for health and by optimising feeding regimes under close examination of their nutrition (food sources, prey capture, food quality and food uptake rates).

(3) Development or adaptation (from shallow-water coral research) of methods for measurements on important ecophysiological parameters (calcification rate, behaviour, respiration rate, performance) and characterising *L. pertusa* with respect to these parameters.

(4) Examining the impacts of anthropogenic environmental change on the ecophysiology of *L. pertusa* in short- and long-term experiments by applying (1) - (3).

Thesis structure

The structure of the thesis represents mainly a monographic work with its classical segmentation into Introduction, Material & Methods, etc. This design was chosen in order to allow going deeper into technical details and to avoid redundancies in the more experimental parts. However, this layout was sometimes voided like - for example - in chapter 2 (Material & Methods) which provides information about the experiments as well as their motivation. Finally the whole work is cross-linked (with hyperlinks in its electronic version).

Work strategy

Live cold-water corals were sampled during two research cruises. The first subsection of 2.1 describes the sampling site characteristics, sampling procedures and the maintenance of the animals on board (2.1.1). The next subsection (2.1.2) addresses the first objective: the establishment of a large closed recirculating system (CRS) for the husbandry of the collected live corals and the development of a set of four smaller CRS for experimental purposes.

Objective 2: The water quality of both aquatic systems was monitored regularly during all incubation phases with respect to physicochemical parameters and dissolved organic nutrients. A small experiment (2.1.3.3) assesses the effects of increasing ammonium concentrations on the behaviour of *L. pertusa*. Feeding experiments with different prey qualities and quantities were carried out in order to optimise feeding regimes (objective 2) but also to characterise *L. pertusa* with respect to an important physiological parameter (food uptake; objective 3). Additionally the prey-capture behaviour was video-documented for the first time.

The next five subsections of 2.2 address techniques and experiments for the determination of parameters relevant for the cold-water corals' ecophysiology (objective 3). Coral growth rates during long-term incubation periods - whether under manipulated conditions or not - were determined non-destructively by repeated underwater weighings of the corals (2.2.1.1). In short-term experiments of several days, the weight increment was too small for a standard balance and therefore calcification was determined analytically from changes in total alkalinity (2.2.1.2). Data normalisation and length-weight relationship was performed for comparing results (2.2.1.3). For short-term experimentation two types of bioreactors were developed. While the first one was a hermetically sealed system (2.2.2.1), the second was semiclosed (2.2.2.2). It needs to be mentioned that the closed system was early replaced

through a semiclosed version and therefore no results could be presented in the thesis. However, the closed system also has the potential for good experimentation (especially when acidification through HCl is the only option available) and was therefore left in the Material & Methods section. A multi-channel digital video recording system was developed (PoBeMon) and applied for studies on the coral polyp extension behaviour (2.2.3). Recorded video material was analysed semiautonomously by an innovative image recognition algorithm. Respiration rates of the *L. pertusa* holobiont (coral polyp with associated bacteria and cryptofauna) were examined at ambient and elevated temperatures (objective 4) with the aid of closed respiration chambers equipped with advanced optode technology (2.2.4). As a bioenergetic indicator for fitness and stress, RNA/DNA ratio measurements were applied on a variety of marine animals including tropical shallow-water corals. This method was adapted to *L. pertusa* (2.2.5) and applied in the framework of the climate-change related experiments.

Three main experiments were carried out to investigate the impact of rising seawater temperatures and CO_2 concentrations on the ecophysiology of *L. pertusa* (objective 4). In a temperature stress experiment (2.3.1) the corals were exposed to three different temperatures and their responses were examined with respect to oxygen consumption (optodes), behaviour (PoBeMon), and fitness (RNA/DNA ratios). The effects of ocean acidification were first investigated in a short-term experiment, conducted with the semiclosed bioreactors and four different pCO_2 concentrations (2.3.2.1). The corals' response was characterised with respect to growth rates (TA changes) and fitness (RNA/DNA ratios). Finally, to test the long-term effect of increased CO_2 concentrations - a second acidification experiment was conducted in which the corals were exposed to three pCO_2 levels for several months. The long-term experiment took place in the four experimental CRS and as an ecophysiological response, the growth rates were determined in distinct intervals (buoyant weight changes).

Chapter 3 (Results) attempts to bring together the results and findings from all the measurements and experiments mentioned above. Chapter 4 (Discussion) relates the results to current knowledge (where possible) and chapter 5 (Significance & Outlook) provides a final overview about the contribution of this thesis to our knowledge of the ecophysiology of *L. pertusa* in general and with respect to climate change.

2. Material and Methods

2.1. General cold-water coral cultivation

2.1.1. Locations and sampling

The cold-water coral specimens used within the framework of this study were sampled during two scientific cruises in Norwegian waters: the RV ALKOR cruise AL275 in March 2006 and the RV ALKOR cruise AL316 in March 2008 (Fig. 7).

Fig. 7 Overview of Southern Norway and the coral sampling sites during RV ALKOR cruise 275 in 2006 and RV ALKOR cruise 316 in 2008 (red markers). Map generated with Google Maps and GMT.

RV ALKOR cruise 275 - Oslofjord, 2006

The sampling area of this cruise included the southern Oslofjord inlets east and west of the Søster Islands. The collection of viable coral samples and associated reef fauna was realised during eight dives with the manned submersible JAGO between 26th and 29th March 2006.

Sampling site characteristics

The Western and Eastern Oslofjord Inlets (WOI and EOI) are about 7 nm-long and pass the Søster Islands on both sides (Fig. 8). They are connected to the main Oslofjord Trough in the north and the eastward continuation of the Norwegian Channel in the south. The two inlets are characterised by steep inclined rock outcrops, sediment- and mud-rich troughs and drumlins which shape the complex seabed topography (Rüggeberg & Form 2007). The EOI consists of several 140 to 200 m deep troughs separated by narrow thresholds which are generally less than 120 m deep and teeming with ridges covered by corals (*Lophelia pertusa*) and other epibenthic organisms. These reef structures are estimated to be approximately 8,700 to 7,800 years old (Mikkelsen *et al.* 1982). The WOI also features narrow thresholds but exhibits comparatively deeper troughs ranging up to 320 m.

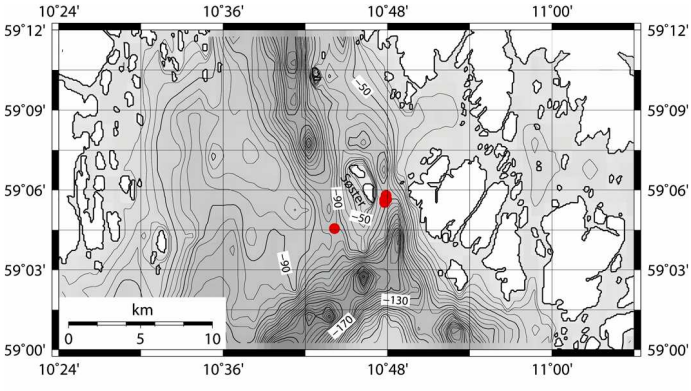

Fig. 8 Overview of the coral sampling sites with the Western and Eastern Oslofjord Inlets around Søster Islands. Red dods represent sampling site coordinates during JAGO dives. Image generated with GMT and bathymetric data from GEBCO_08 (2009).

Sampling

During the dives, selected viable branches of cold-water coral *Lophelia pertusa* and associated reef fauna (crabs, sponges, molluscs, brachiopods, gastropods, and bryozoans) were carefully garnered with JAGOS's hydraulic manipulation arm and stored in a sampling basket attached to the front of the submersible. Simultaneously, water samples were taken with Niskin bottles attached to the submersible. In addition, the upper water masses were sampled with a CTD rosette (Multi Water Sampler, Hydry-Bios) for particulate organic carbon and nitrogen (POC/PON), inorganic nutrients (nitrate, nitrite, silicate and phosphate), total alkalinity (TA), dissolved inorganic carbon (DIC) and photosynthetic pigments analyses. Altogether, seven JAGO dives were performed on two mounds of the inner EOI, where corals are abundant and collection could be performed at the reef base with the lowest impact on the ecosystem ("surgical sampling"). Dive number eight was performed on a small mound of the central channel SW of the southern Søster Island. The exact sampling positions are listed in Appendix B. For further analyses of the investigated reef structures, video and photo documentation were performed during the dives. After each return of the submersible JAGO

to RV ALKOR, all samples were set directly into large buckets filled with fresh, clean seawater.

Maintenance on board

Due to the stress induced mucus production of the corals an acclimatisation period of approximately 30 to 40 minutes was necessary until the reaction abated enough so that the collected organisms could be transferred from the buckets into the prepared transportation tanks (750 L PVC) stored in the wet laboratory of RV ALKOR. For this cruise each of the three transportation tanks was equipped with a powerful submerged rotary pump (2,400 L h^{-1}, Eheim) for strong water currents, an air-stone (50 mm, Sander) with an attached air-pump (2.7 m^3 h^{-1}, Medo Compressor) for fresh air circulation and a fibre glass lattice (50 × 50 mm grid size) on the bottom of the tanks for sample fixation. The water in the transportation tanks was natural seawater from offshore locations which had been pumped into the aquaria tanks of RV ALKOR beforehand. Due to biological processes and warming of the water, it had to be renewed at regular intervals or when water temperature reached levels uncomfortable for the corals (above 9° C).

For more details of this cruise see the RV ALKOR cruise report AL275 (Rüggeberg & Form 2007).

RV ALKOR cruise 316 – Sula-Reef, 2008

The collecting of viable coral samples during this cruise could be realised in only two JAGO dives on 15th March 2008 in the Sula Reef Complex (SRC).

Sampling site characteristics

The Sula Reef Complex consists of several closely neighboured *Lophelia* coral banks at 270 to 300 m depth off the west coast of mid-Norway. It is situated in a trough between two shallow banks, the Frøyabank in the south and the Haltenbank to the north (Fig. 9) (Freiwald *et al.* 2002). The *Lophelia*-reef structures are located on

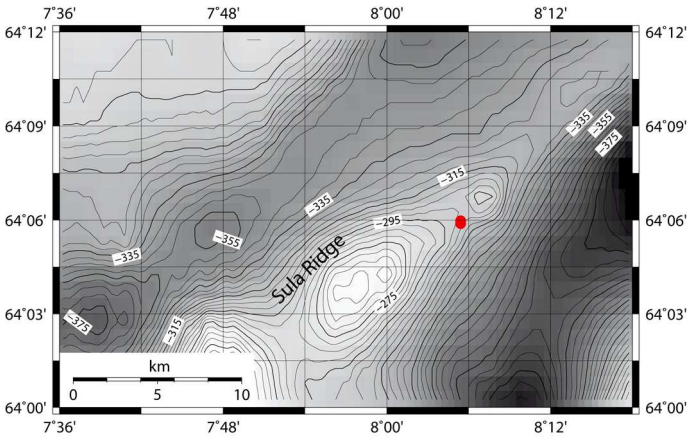

Fig. 9 Map of the central part of the Sula Ridge off mid-Norway. Red dods represent sampling site coordinates during JAGO dives. Image generated with GMT and bathymetric data from GEBCO_08 (2009).

top of the Sula Ridge whose topography is characterised by Palaeocene sedimentary stratified rocks and a thin layer (0 - 10 m) of subglacial till (Hovland *et al.* 1998; Freiwald *et al.* 1999). Overall the SRC is about 13 km long with a width ranging between 300 to 700 m. Estimations date the formation to be 8,060 years old (Hovland *et al.* 1998).

Sampling and maintenance on board

Sampling and cultivation on board were similar to the proceedings during the RV ALKOR cruise 275 (see above). Living *Lophelia pertusa* of both colour varieties (white and red), *Madrepora oculata* and one gorgonian (*Primnoa* spec.) were collected at the central part of the SRC in 275 to 285 m depth. Small coral pieces - only a few polyps each - were attached to PVC sockets (50 x 50 mm) with a two-component adhesive suitable for stony corals (Korallenkleber 9697, Rebie) for additional stabilisation. The exact sampling positions are listed in Appendix B.

For more details of this cruise see the RV ALKOR cruise report AL316 (Meyerhöfer *et al.* 2008).

2.1.2. The cold-water benthos rearing facilities

The IFM-GEOMAR cold-water benthos rearing facilities, designed and developed within the framework of this thesis, consist of six independent closed recirculating systems (CRS): two for general cultivation (the Cold-Water Coral Maintenance System; see 2.1.2.2), the Arctic Crustose Algae Maintenance System (not part of this work) and four identical independent CRS for experimental purposes (the Long-Term Experimental System; see 2.1.2.3).

2.1.2.1. Closed recirculating systems – main principles and components

In principle, a CRS consists of three main components: the organism tanks, a water reservoir and the water conditioning fixtures (Fig. 10). The water reservoir acts as a central supply unit for the other two components and the process water can be regarded as one water body connected through the piping.

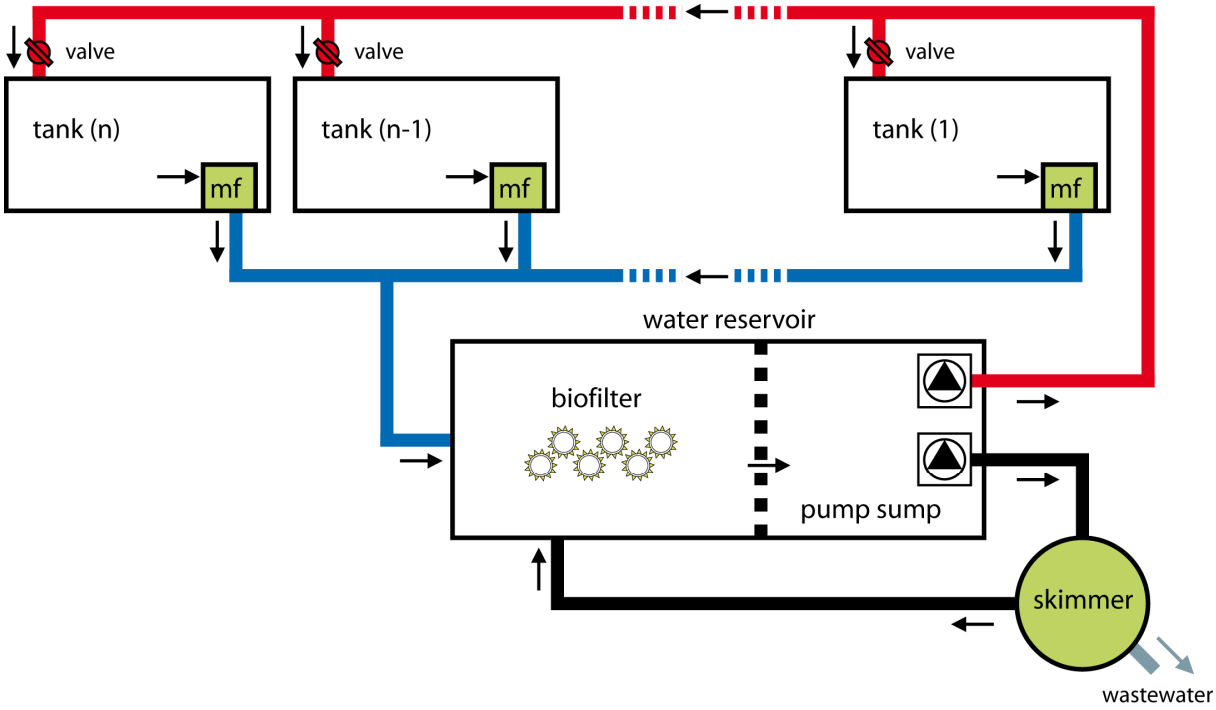

Fig. 10 Scheme of the main components and water flow (arrows) of an idealised closed recirculating system. Inflow (red) and outflow (blue) of each tank can be regulated independently by a valve. The filtering components are the mechanical filter (mf), the biofilter, and the skimmer.

From the pump sump of the water reservoir seawater is pumped into the tanks by a submerged rotary pump. Each tank is equipped with a valve for regulating the water flow which allows independent regulation or a complete separation of single tanks. After passing the tank, mechanical filters integrated on the outflow pipe of each tank pre-filter the water to extract all

large particulate compounds. Before finally flowing back into the reservoir the water is further processed by a biofilter. In a separate loop (bypass) the water is pumped from the reservoir into an optional skimmer. Loss of water is only possible in form of foam fraction (waste water) in the skimmer or due to evaporation.

2.1.2.2. Cold-Water Coral Maintenance System

After the cruises the CWC and accompanying reef fauna were placed in a large CRS with conditions as close to nature as possible for non-manipulative long-term cultivation (Fig. 11). The Cold-Water Coral Maintenance System (CWC-MS) consists of five main components: six rearing tanks, a water reservoir with an integrated biofilter, a large skimmer, and an external cooling aggregate. The total water capacity of the whole CRS amounts to ~ 1,600 L.

Tank design

The rearing tank array consisted of six glass aquaria (1,000 × 500 × 500 mm) with a capacity of ~ 220 L each. To prevent the water surface from air pollution the aquaria were covered with two juxtapositional glass plates (500 × 500 × 5 mm). For thermic isolation and shock-absorption Styrodur® plates (1,000 × 500 × 40 mm) were placed between the aquaria and the rack system (60 mm, V4A stainless steel). Water inflow was regulated by a valve which was normally set to flow-rates of 250 - 300 L h^{-1}. For additional water movement, especially during feeding (when the central water supply was shut off), an additional streaming pump (580 L h^{-1}, Rena Flow 600; later 270 L h^{-1}, Eheim) was positioned beneath the inflow pipe of each tank. The aquaria were equipped with a mechanical filter for cleaning the water of large particles before entering the pipes and the downstream filtering systems (pre-filtering). In addition, the mechanical filter protected the mobile fauna (e.g.,

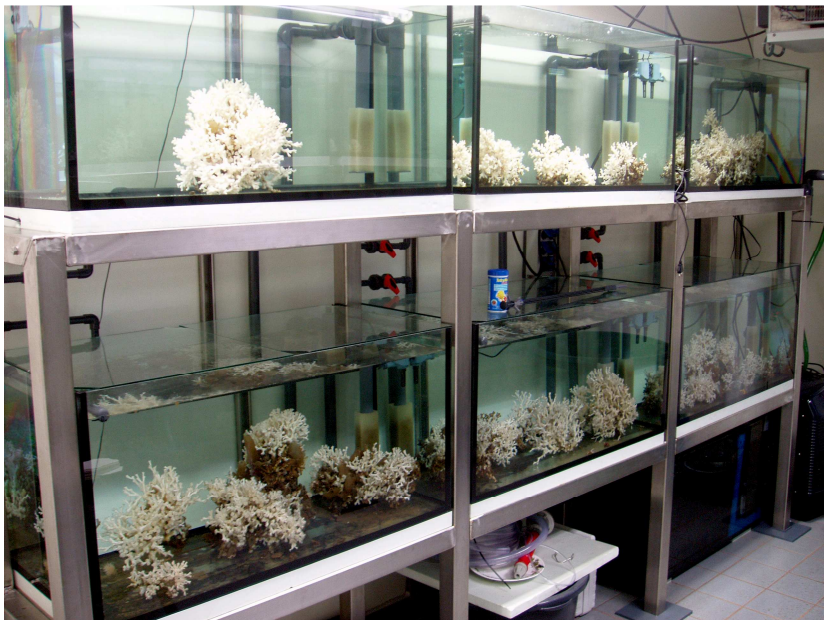

Fig. 11 The CWC-MS at the Leibniz Institute of Marine Sciences IFM-GEOMAR in Kiel. Light was only enabled during routine works in the climate chamber.

crabs, shrimps, gastropods, etc.) against filtering out or injury during the water recycling process. The filter material used in the CWC-MS systems consisted of reticulated open cell polyether foam (aquarium sponge, 150 × 50 × 50 mm) and was impermeable for particles larger than approximately 500 µm. The mechanical filter was mounted with a perforated PVC-C-tube (ø 32 mm) directly to the drainpipe and had to be rinsed in regular intervals. Due to its large surface area, the mechanical filter acted as an additional biofilter.

Biofilter, water reservoir, and process water

The main biofilter was constructed as a separate compartment of the water reservoir. It was housed in a glass aquarium (1,000 × 500 × 500 mm) with a capacity of ~ 220 L and comprised approximately 100 L of small 8 × 8 mm cylindrical polypropylene tubes (BNC tubes, 2H Kunststoff). The tubes had a complex three dimensional folded structure providing a specific surface of 0.963 m^2 L^{-1}. The whole biofilter therefore had a total surface area of ~ 212 m^2. This enlarged surface provided the preferred "settlement" conditions for the nitrifying bacteria species *Nitrosomonas* spp. and *Nitrobacter* spp., most responsible for the bacteriological degradation processes from ammonia to nitrate (nitrification).

The oxidative nitrification takes place in a two-step reaction:

1. *Nitrosomonas* oxidises ammonium (NH_4^+) to nitrite (NO_2^-):

$$NH_4^+ + \tfrac{1}{2}O_2 \rightarrow NO_2^- + 2H^+ + H_2O \qquad \textbf{Eq. 13}$$

2. *Nitrobacter* oxidises nitrite to nitrate (NO_3^-):

$$NO_2^- + \tfrac{1}{2}O_2 \rightarrow NO_3^- \qquad \textbf{Eq. 14}$$

The biofilter was situated beneath the drainpipes on the left side of the water reservoir separated from the pump sump by an aquarium sponge (500 × 500 × 40 mm).

The submerged rotary pumps for the central water supply of the tanks, the skimmer, and the cooling unit were mounted in the pump sump of the water reservoir. Each pump (type 1260, Eheim) had a flow-rate of 2,400 L h^{-1} and thus the whole water body was circulated through all compartments several times per day. The whole piping (tubes and fittings) consisted of PVC-C. A diameter of 32 mm was chosen both for the tank outlet (drainpipe) and for the main pipe while the inlet only measured 20 mm. In- and outlet of the cooling unit also

consisted of 32 mm (diameter) piping. The inlet for the skimmer consisted of 20 mm PVC hose while the outlet was constructed from 32 mm piping (tubes and fittings).

The initial process water was natural seawater sampled in direct vicinity of the CWC during the sampling cruises. In case of diminishing water quality (see 2.1.3) and to support the organisms with new micro nutrients, the used water was routinely replaced with new seawater.

Skimmer

Protein skimmers are highly effective in the removal of suspended wastes and dissolved organic matter (DOM) by foam fractionation. They are commonly used in marine aquaria and aquaculture systems (Sander 1998). In a perpendicular contact column large amounts of fine air bubbles are injected into the water providing a concentrated air/water interface. Surface-active suspended and dissolved organic material (e.g. proteins, particular wastes) congregates at the air/water interface during the migration of the air bubbles to the surface and was skimmed off as a coagulated foam fraction at the top of the skimmer. In addition to the "filter" mechanism, skimming enhances the oxygenation of the process water and provides an increased surface area for general gas exchange.

For the CWC-MS, a large external skimmer (type III/P AH 1500-1900, Sander) with an approximate air flow of 600 L h^{-1} - provided by an injection pump - was used. The contact column had a volume of about 50 L and the skimmer was able to process the water with a flow rate of about 1,200 L h^{-1}. The injection pump (venturi type) was supported by pressured air from the IFM-GEOMAR in-house gas supply and prevented the CRS from CO_2-fluctuations in the climate chamber. After passing the skimmer the oxygenated process water was injected back into the biofilter for maintaining oxic conditions.

Cooling

The CWC-MS was placed in a climatic chamber equipped with an air-cooling aggregate. The chamber environment was adjusted to temperatures between 6.0 and 7.5 °C all year round. For additional cooling and as an emergency device the CWC-MS was equipped with a separate water chiller (Titan 4000, Aqua Medic). The water temperature was adjusted to 7.0 - 7.5 ± 0.5 °C.

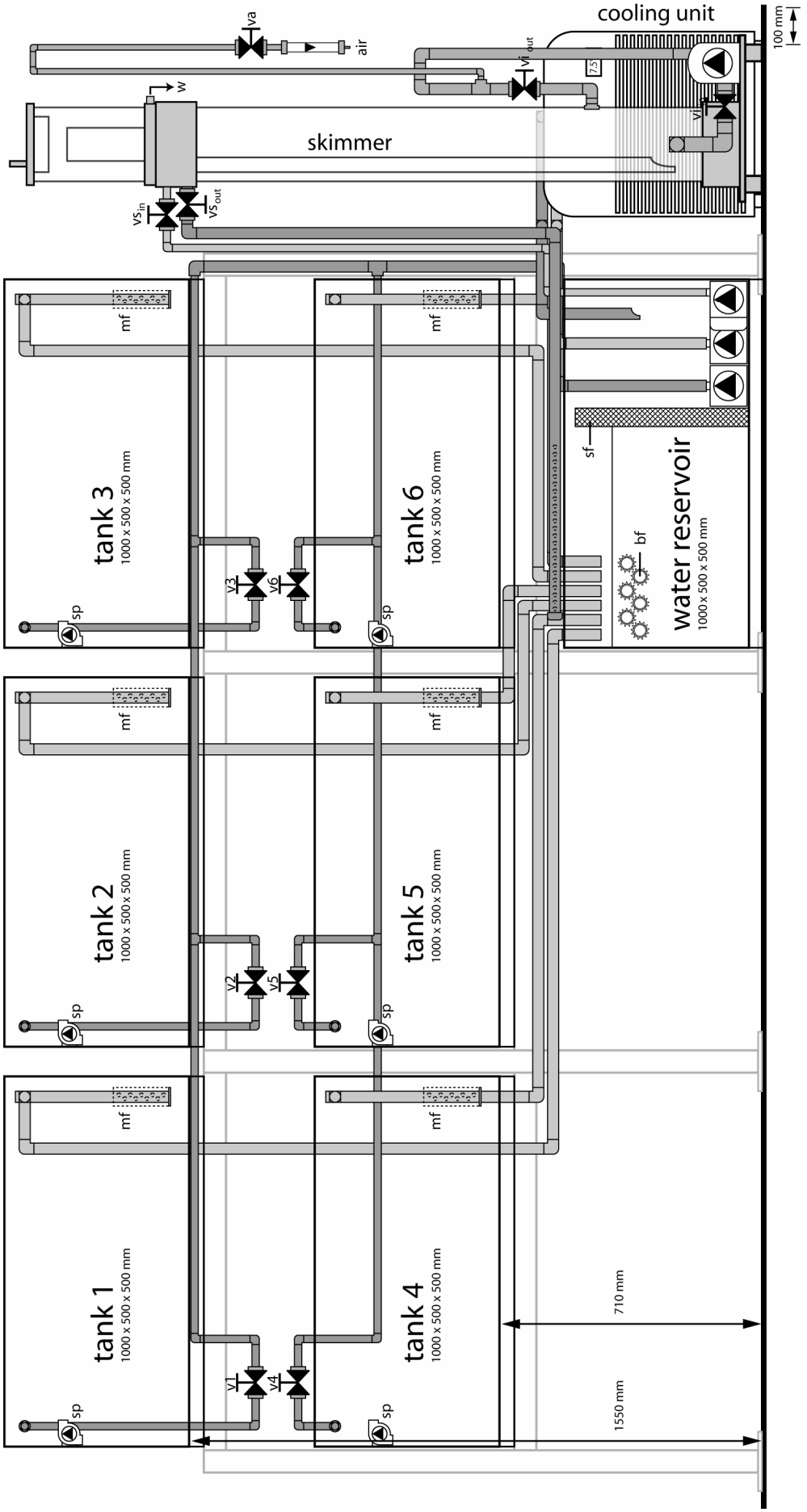

Fig. 12 Front view of the main components and piping of the Cold-Water Coral Maintenance System (CWC-MS). Abbreviations: mechanical filter (mf), biofilter (bf), sponge filter (sf), streaming pump (sp), valves for water inflow regulation to the tanks (v1, v2, ..., v6), valve for skimmer air regulation (va), valve for skimmer water inflow (vs_{in}), valve for skimmer water outflow (vs_{out}), valve for skimmer air-stream inflow (vi_{in}), valve for skimmer air-stream outflow (vi_{out}), waste water (w). See text for details.

2.1.2.3. Long-Term Experimental System

The Long-Term Experimental System (LTE-S) was designed for CO_2 incubation experiments with small coral branches (with up to 100 polyps) over a time period of several months with focus on constant and reproducible water conditions. The LTE-S consisted of four independent CRS (Fig. 13), each with an identical set of main components: six incubation tanks, a water reservoir with integrated biofilter and skimmer, and an additional temperature maintenance device. Each CRS could be aerated with pressured air or a gas mixture with predefined CO_2 concentration. The total water capacity of the LTE-S was about 2,000 L (4 × 500 L).

The following description represents the general configuration of one CRS of which four identical units composed the whole LTE-S.

Tank design

The six incubation tanks consisted of glass aquaria (400 × 400 × 400 mm) with a capacity of about 55 L each. The aquaria were covered with glass plates (400 × 400 × 5 mm) to prevent the contents from air pollution and to avoid a gas equilibration of the process water with the ambient air. For additional sealing during the CO_2 perturbation experiments, the aquaria were covered with a polyethylene foil. Styrodur® plates (400 × 400 × 40 mm) were mounted between the tanks and the rack system (60 mm, V4A stainless steel) for thermic isolation and shock-absorbing. Water inflow was regulated by a valve and set to flow-rates of 60 - 100 L h^{-1} (fine-adjusted depending on the polyps' individual behaviour). Each tank was equipped with a mechanical filter similar to those of the CWC-MS (2.1.2.2).

Water reservoir, integrated biofilter, and skimmer

Both, the biofilter and the skimmer were integrated into the water reservoir. A glass aquarium (1,200 × 400 × 400 mm) with a capacity of ~ 170 L was used as the most space-saving solution. The biofilter consisted of approximately 80 L of 8 × 8 mm cylindrical polypropylene tubes (BNC tubes, 2H Kunststoff) providing a total surface area of 77 m^2 (see above). Separated from the skimmer and the central water supply by an aquarium sponge (400 × 400 × 40 mm) the biofilter was placed on the left side of the water reservoir beneath the drainpipes. The skimmer (Bio-Compact Skim, Sander) was situated right next to the biofilter and had a contact volume of ~ 8.8 L and processed water with a flow rate of 150 - 250 L h^{-1}. An additional biofilter with a capacity of 5 L was connected to the drainpipe.

The skimmer could operate both with pressured air from the IFM-GEOMAR in-house gas supply or with the predefined CO_2-air gas mixtures that were used during the long-term CO_2 incubation experiments (see 2.3.2.2). The submerged rotary pump (2,400 L h^{-1}; type 1260, Eheim) for the central water supply was mounted next to the skimmer on the utmost right side of the water reservoir. As piping PVC-C tubes with a diameter of 20 mm for the inlet and 32 mm for outlet were used. As a deviation from this, the outlet pipes of one CRS were centralised in a main sewer with a diameter of 80 mm (Fig. 13, CRS # 0). During CO_2 incubation experiments the whole water reservoir was sealed air-tight with a specially trimmed polypropylene foil.

Temperature

The LTE-S was placed in the same climatic chamber as the CWC-MS. Under uncontrolled conditions, the temperatures in the CRS varied 0.5 to 1.2 °C. Thus, they reflected the local temperature gradient established by the air cooling aggregate. Therefore water temperature of each CRS was controlled by a digital thermostat with an accuracy of 0.1°C (UT100, Conrad) and a 300 W titanium heater (Schego) installed in the water reservoir (Fig. 13). During long-term incubation experiments the climate chamber temperature was set to 6.0°C and the LTE-S thermostats controlling the respective water temperatures were set to 7.5°C. As an emergency device, an optional cooling aggregate (Titan 4000, Aqua Medic) which was able to support all CRS simultaneously by a cooling hose filled with aqua dest. was installed in the LTE-S.

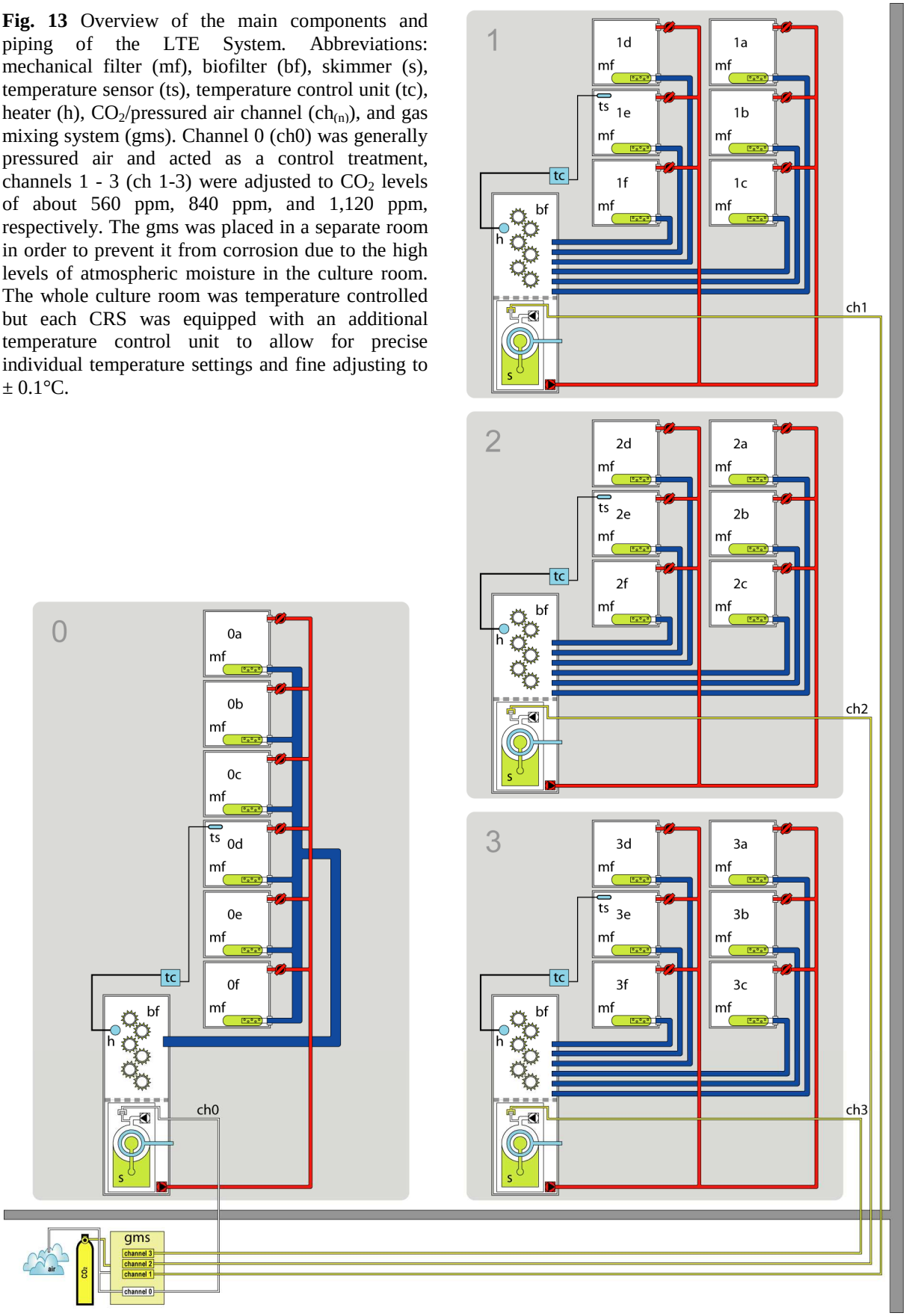

Fig. 13 Overview of the main components and piping of the LTE System. Abbreviations: mechanical filter (mf), biofilter (bf), skimmer (s), temperature sensor (ts), temperature control unit (tc), heater (h), CO_2/pressured air channel ($ch_{(n)}$), and gas mixing system (gms). Channel 0 (ch0) was generally pressured air and acted as a control treatment, channels 1 - 3 (ch 1-3) were adjusted to CO_2 levels of about 560 ppm, 840 ppm, and 1,120 ppm, respectively. The gms was placed in a separate room in order to prevent it from corrosion due to the high levels of atmospheric moisture in the culture room. The whole culture room was temperature controlled but each CRS was equipped with an additional temperature control unit to allow for precise individual temperature settings and fine adjusting to ± 0.1°C.

2.1.3. Water quality management

Especially in closed recirculation systems, regular measurements of the physicochemical water parameters and nutrient compositions are essential in order to keep the environmental conditions reproducible and in controlled margins (Losordo *et al.* 1998).

2.1.3.1. Physicochemical parameters

Salinity, pH, and temperature were measured usually twice a week. If something was out of range or attracted attention (fluctuations, high nutrients, water turbidity, etc.) measurements were taken daily. The measurements were performed with a portable measuring device (Multi 350i, WTW) equipped with specialised sensors: pH (SenTix®41 or SenTix®81, WTW), temperature and salinity (ConOx®, later TetraCon®, WTW). Calibration was conducted with three certified NIST/NBS buffer solutions (4.01, 7.00, and 10.01) with a three-point calibration applied each time before measurements. The conductivity sensor for salinity was adjusted after each sensor exchange with a certified conductivity standard (1413 µS cm^{-1} at 25 °C, Reagecon).

2.1.3.2. Monitoring of inorganic nutrients

Water samples of all CRS were measured weekly. Nitrate, nitrite, and phosphate were measured photometrically (Hitachi, U-2000) according to the standard methods by Hansen & Koroleff (1999) with precision levels of ± 0.5 µmol kg^{-1}, ± 0.02 µmol kg^{-1}, and ± 0.05 µmol kg^{-1}. Ammonium was measured fluorometrically (SFM 25, Kontron Instruments) according to Holmes *et al.* (1999) with a precision of ± 0.08 µmol kg^{-1}.

2.1.3.3. Ammonium sensitivity

In aquatic systems, ammonia is the principal nitrogenous compound excreted by animals (Colt & Armstrong 1981). In seawater, ammonia exists in unionised (NH_3) and ionised (NH_4^+) forms in a pH-, salinity-, and temperature dependent equilibrium (Bower & Bidwell 1978). Through extensive feeding or the death of specimens, the ammonium (and ammonia) concentration may on occasion rapidly increases in aquaria and aquaculture systems and can thus achieve levels detrimental for their inhabitants. For tropical warm-water scleractinian corals, ammonium concentrations up to 20 µmol L^{-1} are reported to be dangerous (Bassim & Sammarco 2003) and in marine reef aquaristics, levels above 5.5 µmol L^{-1} (0.1 mg L^{-1}) are

recommended to be prevented. The toxic relevance of ammonium for the cold-water coral *L. pertusa* is not known.

With a bioassay (Holtmann 2006) it was attempted to elucidate the influence of increasing concentrations of ammonium on the polyp behaviour of *L. pertusa* and whether a sustainable maximum concentration could be determined that should be avoided in the cultivation system.

Experimental Setup:

A small 20 L acrylic glass aquarium (400 × 200 × 250 mm) was segmented into two 10 L compartments by gluing a 5 mm thick PVC-panel into the middle of the tank. Each compartment was equipped with a submerged rotary pump (580 L h^{-1}; Rena Flow 600, Mars Fishcare Inc.) for supporting the corals with a continuous water flow and to enhance the water mixing during the ammonium-injections. On the upper part of each back wall, a small water outflow pipe was mounted. For daily water exchange, two 25 L water tanks (reserve tanks) were placed close above the aquarium - each connected with one of the two tank compartments. The water inflow rate was controlled by a valve. Both tank compartments were filled with natural seawater (8°C, 34.9 PSU). Approximately 20 coral polyps were placed in each compartment close to the front wall. For illumination, a cold-light source (KL150, Schott) was placed near the aquarium and two fibre-optic spotlights were directed towards the corals. In front of the aquarium, a CCD camera (GP-KR222, Panasonic) was mounted. The camera was connected through a shielded BNC cable (75 Ω) to a video recorder (DHR-1000VC, Sony), located in an adjacent laboratory room. In order to convert the analogue video signal into a digital streaming format (DV), a digital video camera recorder (DCR-TRV30E, Sony) was interconnected between the video recorder and a personal computer. Video capturing software was used (1-More Webcam, v. 1.03) to grab single images from the camera in 15 second intervals. An illustration of the experimental setup is shown in Fig. 14.

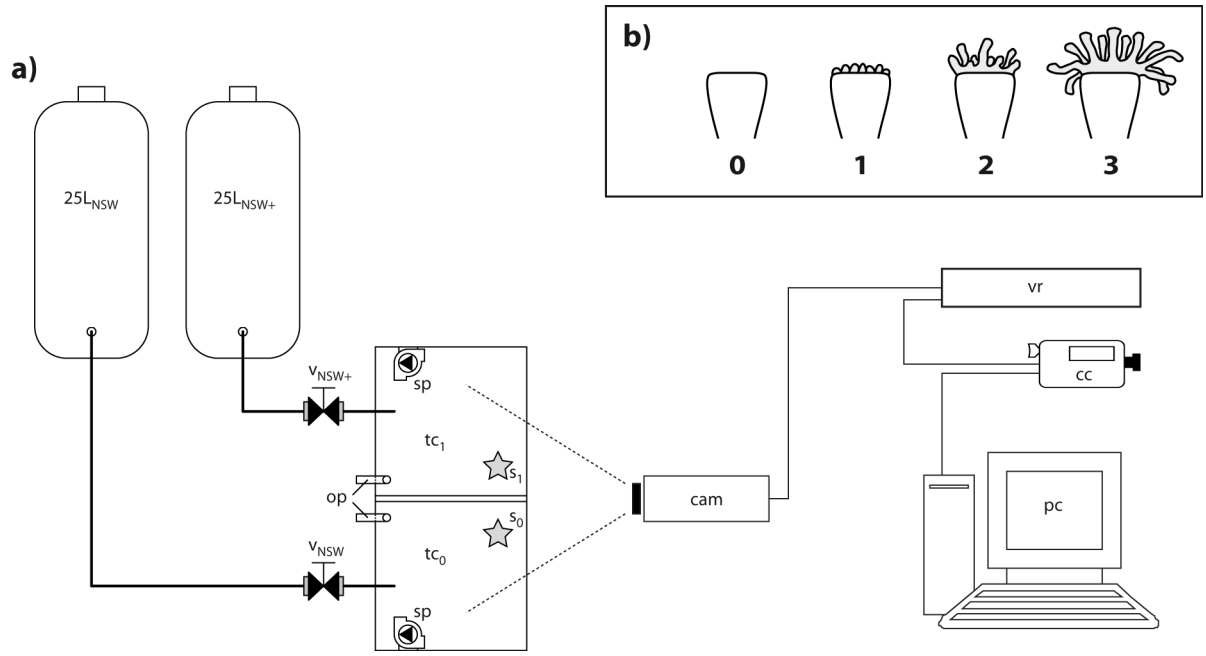

Fig. 14 a) Illustration of the experimental setup. Abbreviations: 25 L tank with natural seawater (25 L_{NSW}), 25 L tank with NH_4^+ enriched natural seawater (25 L_{NSW+}), valve for 25 L_{NSW} (v_{NSW}), valve for 25 L_{NSW+} (v_{NSW+}), streaming pump (sp), tank compartment (tc_1, tc_2), coral sample (s_1, s_2), water outflow pipes (op), CCD camera (cam), video recorder (vr), video camera recorder (cc), and personal computer (pc). For illumination, a cold-light source (not shown) was used. **b)** *L. pertusa* polyp expansion stages (see text for details).

At the beginning of the experiment, the reserve tanks were filled with natural seawater. During the 7 day experiment, water was renewed daily but one of the tanks was treated every day with increasing ammonia (NH_4Cl) according to following progression:

5.56 µmol L^{-1} → 11.11 µmol L^{-1} → 22.22 µmol L^{-1} → 44.44 µmol L^{-1} → 88.89 µmol L^{-1} → 188.89 µmol L^{-1} → 355.56 µmol L^{-1}.

Three times a day, water samples were taken from both compartments and the abiotic water parameters (temperature, salinity, and pH) were measured at the same time using a multi-sensor portable measuring device (WTW, Multi 350i, cf. 2.1.3.1). All water samples were frozen immediately after taking them and after the experiment they were analysed for ammonium, nitrite and nitrate in an autoanalyzer (AutoAnalyzer 3, Bran+Luebbe; for details see instruction manual). Although the video system was set up to record images in a 15 second interval, for the polyp behaviour measurements an interval of 5 minutes was applied. In each treatment, the polyp behaviour of 5 recorded polyps was measured from their side view on a scale based on Lasker (1979) ranging from 0 to 3 where (0) is full contraction of the polyp, (1) only the tips of the tentacles are visible, (2) the polyp is partly expanded, and (3) the polyp is fully expanded (Fig. 14 b).

2.1.4. Optimising Lophelia pertusa feeding regime

For heterotrophic organisms feeding is one of the main physiological parameters affecting survival, growth, and reproduction. Optimising the feeding regime was therefore an important aspect of successful cultivation and an essential precursor for all ecophysiological experiments.

Information about natural food sources and consumption of *L. pertusa* are sparse. Isotopic studies with $\delta^{15}N$ in the tissues of *L. pertusa* suggested a mixture of phytodetritus and zooplankton as main sources (Duineveld *et al.* 2004; Duineveld *et al.* 2007). In aquaria observations, *L. pertusa* catches particulate organic material and zooplankton up to a size of 20 mm (Mortensen 2001). In a series of bioassays (two student theses and one diploma thesis) it was attempted to find an optimal balance between the right food (organism, quality) and the maximum permissible food density for an effective water treatment. In the following only the key experimental setups and live food organisms are described. For detailed information, the reader is referred to the respective theses (Stratil 2006; Bach 2007; Moldzio 2008).

2.1.4.1. Live food organisms

2.1.4.1.1. Copepods: *Acartia tonsa* (Dana, 1849)

Acartia tonsa is a calanoid neritic copepod (Crustacea: Calanoida: Acartiidae) with a cosmopolitan distribution in the Atlantic, Indian, and Pacific oceans, and the Azov, Baltic, Black, Caspian, and Mediterranean seas (Marcus & Wilcox 2007). As a typical estuarine species, it is euryhaline and eurythermal with tolerances ranging from 1 to 38 in salinity and 0 °C to 30 °C in temperature, respectively (Mauchline 1998). It is mainly found inshore (0-20 m) but also depths up to 600 m have been reported (Marcus & Wilcox 2007). Adult *A. tonsa* (Fig. 15) are approximately 1,500 µm in length, and their N1 nauplii (first stage after hatching) are approx. 70 µm in length. Calanoid copepod nauplii are the primary first-food source for many marine vertebrates and invertebrates (Lee *et al.* 2005). In aquaculture they play an important role as early food for fish larvae and as adult food for many ornamental species such as seahorses or corals (Marcus & Wilcox 2007).

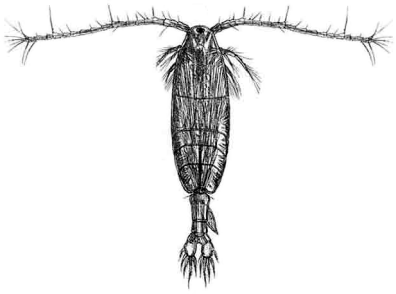

Fig. 15 Adult *Acartia tonsa* female. Image: from Marcus and Wilcox (2007).

A. tonsa population in Norwegian coastal waters is quite abundant and therefore it might be a potential natural food source for the cold-water coral reefs supported through estuarine influenced water masses.

Cultivation

For our experiments, eggs from a Baltic *A. tonsa* strain (IFM-GEOMAR stock strain) were hatched. In order to prevent osmotic stress due to the different salinities, the eggs were incubated in 5 µm filtered natural Baltic seawater enhanced to a salinity of 33 with artificial sea salt (Aqua Medic). Predetermined hatchery success was about 20 %. Four 20 L buckets were filled with 15 L of the above mentioned water and approximately 100,000 eggs to achieve an optimal density of 1 copepod per mL. During incubation the temperature was held constant at about 15 °C and a ligh regime of 16/8 light/dark (L/D) was performed. The copepods were fed daily with a suspension of 300 mL bucket^{-1} of the unicellular algae *Rhodomonas salina* (temporarily *Nanochloropsis* sp.). Under these conditions, adult *A. tonsa* fully developed in 16 days.

2.1.4.1.2. Mysidacea: *Neomysis integer* (Leach, 1814)

The opossum shrimp *Neomysis integer* is a pelagic mysid shrimp (Eumalacostraca: Peracarida: Mysidacea: Mysidae) with a global distribution from Arctic Norway to the Atlantic coast of Spain (Budd 2008). *N. integer* is also a euryhaline species and tolerates salinities from 1 to 40 (Vlasblom & Elgershuizen 1977; Roast *et al.* 2001). Preferred habitats are normally shallow water locations (5 - 10 m), usual estuaries or brackish water enclosures with lowered salinity. Under laboratory conditions, measured temperature tolerances ranges from 0 to 30°C (Mauchline 1980; Arndt & Jansen 1986). The gregarious species performs a diel vertical migration from the surface waters during the night to the deeper waters at daylight (Hough & Naylor 1992). Adult species sizes range from 10 to 18 mm (Fig. 16). *N. integer* is a substantial food source for many economically important fish species such as *Merlangius merlangus*, *Platichthys flesus*, *Pleuronectes platessa* or *Clupea harengus* (Hostens & Mees 1999) and thus has been studied as a potential food organism for aquaculture (Kuhlmann 1984).

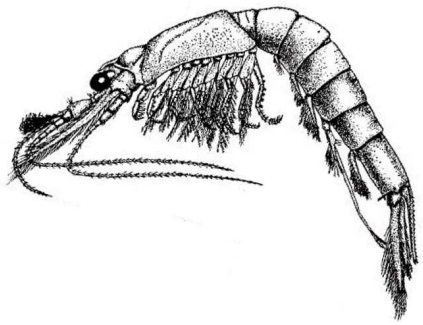

Fig. 16 Adult *Neomysis integer*. Image from Tatersall & Tatersall (1951).

Due to the species sensitivity to trace metals and organophosphate pesticides, *N. integer* has been studied with increasing interest as a toxicological test species for Western European estuarine systems (Roast *et al.* 1999; Verslycke *et al.* 2003).

Cultivation

Various *N. integer* of different sizes were captured with a dip net at the Kiel Canal (54.34° N, 9.97°E) in July 2006. After transfer to Kiel, the opossum shrimps were cultivated in a glass aquarium of 150 L connected with a Baltic Sea flow-through aquaculture system at the Aquarium of the IFM-GEOMAR. Water temperature was held constant at about 12 ± 1 °C and the shrimps were fed daily with grinded dried fish flakes (TetraMarine Flakes, Tetra).

2.1.4.1.3. *Artemia franciscana* (Kellogg, 1906)

The brine shrimps *Artemia* spec. belongs to the family Artemiidae (Branchiopoda: Anostraca: Artemiidae), which can be found worldwide in saltwater lakes and artificial salterns throughout the tropical, subtropical and temperate climatic zones (Dhont & van Stappen 2003). Due to their exceptional habitat, brine shrimps are an extremely euryhaline (3 - 300 PSU) and eurytherm (15 - 55 °C) species (Treece 2000). Normally, *Artemia* performs an ovoviviparous reproduction (fertilised eggs develop directly in the uterus of the females into free-swimming nauplii). Switching to oviparous reproduction (releasing of dormant embryos/cysts) occurs under deteriorating living conditions (e.g. high salinity, low oxygen levels). Dehydrated cysts are metabolically inactivated (diapauses) and can withstand several years and extreme environmental conditions. After hatching, their Instar I nauplii (first larval stage after "umbrella" stage) are 400 - 500 µm in length. Under optimal conditions, the larva maturates and differentiates through 17 larval stages in only one week to adults of about 8 - 12 mm in length (Fig. 17) (Hentschel 1968; Schrehardt 1987). Brine shrimps (primarily the Instar I and II nauplii) are the most common live food used in marine and freshwater aquaculture und aquaristics. Most commonly, *Artemia franciscana* (frequently misstated as *Artemia salina*) is used because a large part of the world market is supplied by harvests from the Great Salt Lake, Utah, where *A. franciscana* naturally occurs (Dhont & van Stappen 2003).

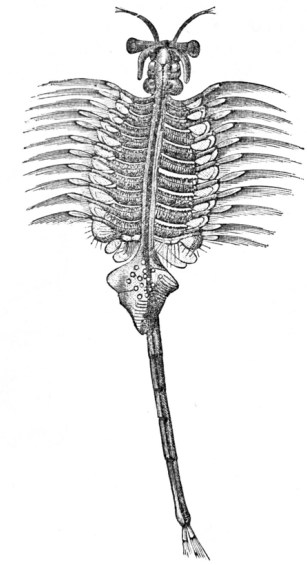

Fig. 17 Adult *Artemia salina* female. Image: from Joly (1873).

Cultivation

For both, experiments and regular feeding, *Artemia franciscana* (Great Salt Lake Artemia Cysts, Sander) Instar I and Instar II nauplii were used. Incubation of dried cysts (~ 0.8 g L^{-1} seawater) was performed in a cylindrical glass container with conical bottom. The hatching bottle was filled with Baltic seawater which was adjusted to salinities of approximately 24 - 28 with artificial sea salt (Seaquasal). Water temperature was kept in the recommended range of 25 - 28 °C (Dhont & van Stappen 2003). For maintenance of adequate oxygen levels, the hatching bottle was aerated from the bottom with pressured air from the IFM-GEOMAR in-house gas supply. A light source (80W; PAR38 Flood, Osram) was placed above the hatching bottle for triggering the start of embryonic development (Dhont & van Stappen 2003). Harvesting: After hatching (24 - 28 hours) the nauplii (Instar I) were separated from the hatching remains (empty cyst shell, unhatched cysts, debris, micro-organisms and hatching metabolites) (Dhont & van Stappen 2003) by switching off the bottom aeration and the top illumination. The positively phototactic nauplii then accumulated on the bottom and were filtered out with a fine mesh screen (150 µm) whereas the remains floated to the surface.

2.1.4.2. Natural food source experiments

Small mesozooplankton: Copepods

In this experimental approach (Stratil 2006) it was tried to elucidate the feeding rates of *Lophelia pertusa* with copepods, which are suggested to be a main natural food source of the corals (Duineveld *et al.* 2004; Thiem *et al.* 2006; Duineveld *et al.* 2007). As a representative test organism, the calanoid copepod *Acartia tonsa* (2.1.4.1.1.) was chosen.

Experimental design

Two *L. pertusa* branches (Oslofjord samples) of 67 and 85 polyps each were transferred into two independent perspex aquaria (320 × 170 × 190 mm) filled with 8 L natural seawater from the CWC-MS. Each aquarium was equipped with a submerged rotary pump (580 L h^{-1}; Rena Flow 600, Mars Fishcare Inc.) to ensure an appropriate water flow. Water temperature was held constant at 8.0 ± 0.2 °C. Before starting the experiment, the corals were acclimatised to this setup for 24 hours and were starved for 3 days. Adult *A. tonsa* of 830 µm in length had been harvested (2.1.4.1.1) and fed to *L. pertusa* in two different densities. Low density was appointed at 0.61 individuals mL^{-1} (Ind mL^{-1}), while high density was at four times as much with 2.44 Ind mL^{-1} (Fig. 18).

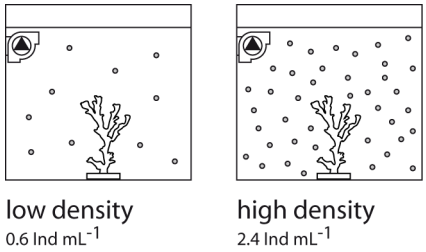

Fig. 18 Illustration of the feeding experiment with *L. pertusa* and two different food densities of *A. tonsa* (grey dots). See text for details.

After 24 hours, the densities of dead and remaining copepods were determined. Three 1 mL samples from the bottom (where the death copepods accumulated) and from the middle of the aquaria were counted and projected onto the total amounts. The number of *A. tonsa* consumed by the polyps was then determined by the difference of initial and final density:

$$Acartia_{consumed} = Acartia_{initial} - Acartia_{(remaining+death)} \quad \textbf{Eq. 15}$$

The feeding rate was calculated as the number of *A. tonsa* ingested per polyp per hour (Hii *et al.* 2008):

$$Feeding\ rate = \frac{density_{initial} - (density_{remaining} + density_{death})}{polyps \times time} \quad \textbf{Eq. 16}$$

Large mesozooplankton: Opossum shrimps

L. pertusa has been reported to be able to ingest large zooplankton up to a size of 20 mm (Mortensen 2001). While analysing the cold-water coral habitat video documentation (RV ALKOR cruise AL275; (Rüggeberg & Form 2007)), mainly euphausiad and mysiad shrimps, amphipods and chaetognaths could be observed as larger representatives of the mesozooplankton. As a second approach with natural food sources, a feeding experiment with *Neomysis integer* was conducted. *N. integer* was not regarded as a species naturally occurring in the cold-water coral ecosystem but morphologically it exhibits the same features and similar motility as the zooplankton observed in the habitat video documentation.

Experimental design

In a similar technical configuration and under the same environmental conditions as the previous experiment, *Neomysis integer* of approximately 15 - 18 mm in length was fed to *Lophelia pertusa* specimens for 24 hours in two different densities. Low density was

appointed at 5.6 Ind L^{-1} and high density at five times as much with 28 Ind L^{-1}. Additionally, to elucidate if prey capture is dependent on the polyp size, the experiment was conducted with two different *Lophelia* morphotypes. Two branches with 49 and 45 large and thick polyps (morphotype I) and two branches with 85 and 69 large but thin polyps (morphotype II) were chosen. For estimation of the mortality not caused by coral ingestion (e.g. cannibalism, rotary pumps) two aquaria without corals but with identical setup and mysidacean densities acted as control groups (Fig. 19).

Calculations were similar to those with the copepods (see above).

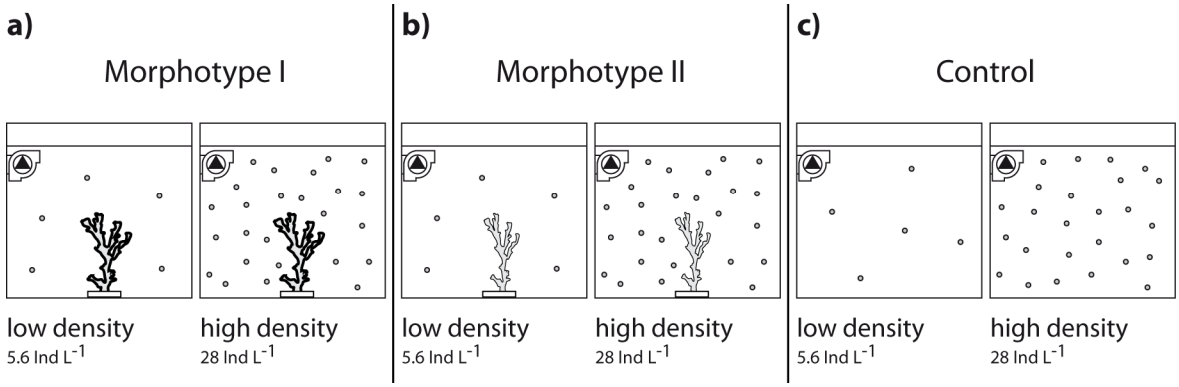

Fig. 19 Illustration of the feeding experiment with two different morphotypes of *L. pertusa* and two different food densities of *N. integer* (grey dots). See text for details.

2.1.4.3. Prey capture analysis

The prey capture of tropical corals is well documented (Sebens 1991; Sebens *et al.* 1996; Sebens *et al.* 1997). For the cold-water coral *Lophelia pertusa* only a few descriptions are available (Mortensen 2001). In this experiment (Bach 2007) the whole feeding process of *Lophelia pertusa* was investigated and documented in a real-time video for the first time.

Experimental design

A small *Lophelia pertusa* branch (Oslofjord sample) of about 15 polyps was transferred into a perspex aquarium filled with natural seawater from the CWC-MS (see above). The water temperature was "controlled" through the climate chamber and was held constant at 8.0 ± 0.2 °C. An appropriate water flow was supplied by a submerged rotary pump (580 L h^{-1}; Rena Flow 600, Mars Fishcare Inc.), placed directly beneath the water surface. In front of the aquarium, a CCD video camera system (see 2.1.3.3) was mounted and focused directly onto a large single polyp. Illumination was provided by a cold-light source (KL150, Schott) placed above the aquaria and directed onto the coral branch. After full expansion of the tentacles, the

coral was fed with living *Artemia franciscana* nauplii (approximately 5 Ind mL^{-1}). Polyp behaviour was recorded with a digital real-time video (25 fps, DV PAL) immediately after food was supplied and was stopped manually after 14 hours. Afterwards, the recorded video file was analysed by counting the uptake rates in 20 minute intervals. Only *Artemia* nauplii which were conveyed from the tentacles to the central mouth region and therefore not seen anymore were regarded as ingested by the polyp.

2.1.4.4. Food quality and uptake rates

Due to their relatively easy cultivation and high acceptance among several marine species, *Artemia franciscana* has been regarded as an adequate artificial food source for corals with reproducible quantity and quality (Hii *et al.* 2008). An additional advantage and one reason for their great success in aquaculture and aquaristics is that *Artemia* can be easily enriched to enhance their nutritional profile (Dhont & van Stappen 2003).

In a long-term experimental approach (Moldzio 2008), coral growth measurements and determinations of uptake rates from three different *Artemia franciscana* food qualities were conducted. The three food qualities were:

FQI freshly hatched *A. franciscana* nauplii (Great Salt Lake *Artemia* Cysts, Batch: 82128, Sander), Instar I

FQII as FQI, enriched with Lipovit® (Tropic Marin), Protein Selco Plus® (Selco), and Microplan® (Preis), Instar II and higher stages

FQIII adult frozen *A. franciscana* (Golden Gate Brine Shrimp, Batch: 69-0204, Kordon)

Experimental design

The feeding experiments were performed successively in a CRS, especially designed and developed for these studies. The CRS consisted of three cubic glass aquaria (400 × 400 × 400 mm) for the experiments and one aquarium (500 × 400 × 400 mm) for the water treatment. The experimental aquaria (stream tanks) were equipped with a cylindrical polycarbonate inlet (Ø 390 mm) and a central acrylic glass column (Ø 120 mm). The inlet was perforated with two diametrically opposed rows of six bores connected to the pipes from the water supply. The central column was hollowed bottom-side and connected to the water drainpipe (Fig. 20). Under non-feeding conditions, water was pumped from the water reservoir through the inlet

perforations thus providing a circular and laminar water flow around the corals (11.4 ± 1.6 mm s^{-1}) in the experimental aquaria. During feeding, the water supply was shut off but a lower constant water flow (66 ± 1.7 mm s^{-1}) was maintained by two air lifts, mounted on both of the other diametrically opposite positions of the inlet. Each air lift was provided with pressured air (~ 50 L h^{-1}) from the IFM-GEOMAR in-house gas supply and was only activated during the 27 hours feeding phase. The water reservoir was equipped with a skimmer (500 L h^{-1}; DOC Skimmer 9205, Tunze), and mechanical and biological filters (see 2.1.2.1). A submerged rotary pump (400 – 3,000 L h^{-1}; Master, Tunze) guaranteed the water supply while the water inflow to each aquarium was regulated by valves to 330 ± 30 L h^{-1}. The process water consisted of a mixture of 50 % natural seawater and 50 % artificial seawater (Classic, Tropic Marin) and was renewed three times during the experiment. Water salinity and temperature was held constant at 34.95 ± 0.57 PSU and 7.95 ± 0.87 °C, respectively.

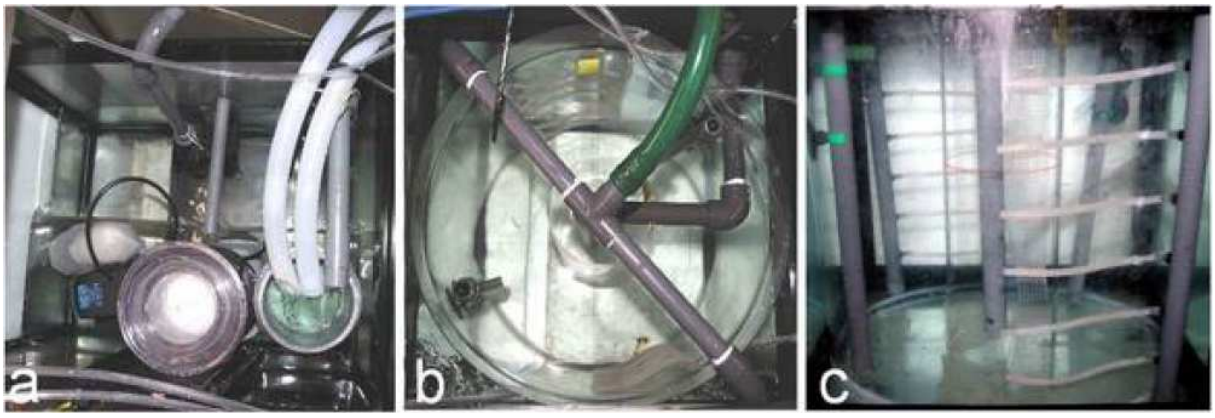

Fig. 20 Overview of the main components of the CRS. **a**) water treatment, **b**) top view of a stream tank, **c**) side-view of a stream tank. Images: from Moldzio (2008).

In each stream tank (replicate), three *L. pertusa* branches (Oslofjord samples) of approximately 30 polyps per branch (Ø 98.3 polyps $replicate^{-1}$) were placed equidistant from each other around the central column of their stream tank. For each of the three 45 days lasting treatment phases, the corals of all replicates were fed weekly with the same specific food quality (see above).

For growth determination, the corals were weighed before and after each treatment phase (buoyancy weight technique, see 2.2.1.1) and surplus growth was normalised to polyp number and polyp surface area.

The nauplii density for FQI and FQII was adjusted to 0.8 Ind mL^{-1}. For FQIII an equivalent amount of food (based on the uptake rates of FQI) was distributed directly to each polyp with a pipette (85 Ind $replicate^{-1}$). After the feeding periods, the uptake rate of each triplicate was determined and normalised to polyp number and polyp surface area. Prior to the feeding experiments, a series of blank tests were performed with the FQI and FQII by adding the same food densities to the not yet populated coral tanks. The aim of the blank tests was to determine the order of magnitude for the nauplii's natural mortality. The food uptakes reported from the experiments were subsequently corrected for the missing nauplii according to the natural mortality rate during the blank tests. For comparing the food qualities among each other, the energy content was measured with a calorimeter (C4000, IKA) according to DIN 51900 and normalised to dry weight.

The whole experimental design (in particular descriptions of the specific cultivation facility and the used measurement methods and calculations) is described comprehensively in Moldzio (2008).

2.2. Determination of ecophysiological variables

2.2.1. Growth rate determination and normalisation

2.2.1.1. Buoyancy Weight Technique (BWT)

For the measurement of the cold-water coral growth rates in long-term incubations an adaptation of the buoyancy weight technique (Jokiel *et al.* 1978; Davies 1989) was developed. The great advantage of this method is that it is non-detrimental for the corals because growth rates can be determined accurately through submerged coral weighing and algebraic transformations of the Principle of Archimedes. The method was introduced for coral growth measurements by Franzisket (1964) and Bak (1973, 1976). The algebraic background and technical solutions were explained in detail by Jokiel *et al.* (1978) and the method was further improved by Davies (1989). Here only the applied modifications and used materials for the cold-water coral growth measurements will be described.

Balances

From the beginning of the experiments in March 2006, buoyant weighings were made using an electronic balance (BP310P, Sartorius), reading to 1 mg with a balk construction above and a gondola below the water surface as described in Jokiel *et al.* (1978). Since summer 2008, a new digital balance (readability: 0.01 mg; CPA225D, Sartorius) with under-floor weighing capability was used, allowing the removal of the balk construction. An additional advantage of this balance was its "animal-weighing mode". In this mode the balance compensates weighing fluctuations normally caused by the animal's motions through calculating a mean value from a series of up to 100 fast weighings which were performed in a quick succession during one session.

Density of seawater

The density of seawater (ρ_{water}) has to be determined immediately before buoyant-weighing the corals and in intervals during the weighing because the density of seawater changes if mucus from the corals is released into the water or if the temperature changes (Davies 1989). By weighing an inert reference object of known air weight and density in seawater, the density of the seawater can be derived from Eq. 17.

$$\rho_{water} = \rho_{object} \times \left(1 - \frac{wt_{in\,water}}{w_{in\,air}}\right) \qquad \textbf{Eq. 17}$$

The reference object used was a glass embryo dish of 17.53 g air weight and with a density of 2.56 g cm^{-3}. The density of the reference objects was determined from Eq. 17 by weighing it in air and then in distilled water. The density of distilled water was obtained from Table F5-6 and F11 of the CRC Handbook of Chemistry and Physics (Weast 1979). In practice, the density of seawater was determined before and after weighing the corals and after each temperature change of 0.5 °C during the measurements. Due to the preceding acclimatisation of the corals an increased mucus production was not observed and therefore additional reference weighings were rarely done.

Density of skeleton and biomass correction

Four living branches with polyps in different sizes and morphologies were selected (107 polyps in total) in order to evaluate the biomass (tissue, biofilm, microorganisms, etc.) of their skeletons. First their buoyant weights were determined and then their aragonite skeletons were completely cleansed of their biomass by treating them in a 5 - 10 % NaOCl solution (sodium hypochlorite; commercial bleach) for 24 hrs. After carefully removing the organic residuals by stirring the coral branches in the solution, they were buoyant-weighed for a second time. The difference of both buoyant weighings resulted in a value for the biomass buoyant weight and was used to calculate a correction factor for biomass. The cleaned skeletons were dried to constant weight at 60 °C. Then the dried skeletons were weighed again and their specific densities were calculated from Eq. 18.

$$\rho_{object} = \frac{\rho_{water}}{\left(1 - \frac{wt_{in\ water}}{w_{in\ air}}\right)} \qquad \textbf{Eq. 18}$$

With the ascertained densities of seawater, skeleton, and the buoyant weights of the coral samples, their air weights could be derived using the following equation:

$$wt_{in\ air} = \frac{wt_{in\ water}}{\left(1 - \frac{\rho_{water}}{\rho_{sample}}\right)} \qquad \textbf{Eq. 19}$$

Calcification rates

In the long-term incubations (experiments and stock population monitoring) growth rate measurements using the BWT were calculated as a mass gain of $CaCO_3$ per time period:

$$G\ (mg\ CaCO_3\ \Phi^{-1}\ day^{-1}) = \frac{wt_{t2} - wt_{t1}}{\Phi \times (t2 - t1)} \quad \textbf{Eq. 20}$$

where wt_{t1} and wt_{t2} indicate the calculated dry weights (Eq. 19) at the start (t1) and the end (t2) of each period and Φ signifies the applied normalisation (see 2.2.1.3.1).

2.2.1.2. Total Alkalinity Anomaly Technique (TAAT)

The Total Alkalinity Anomaly Technique was suggested by Smith and Key (1975) and Kinsey (1978) as another non-destructive method for calcification measurements in marine environments. This method was later validated for the calculation of calcification and photosynthesis rates of scleractinian corals by Chisholm and Gattuso (1991). In principle, calcification can be estimated directly from changes in the total alkalinity (TA). The precipitation of one mole $CaCO_3$ lowers the total CO_2 content of seawater by one mole which is equivalent to lowering the TA by two molar equivalents (see definition of TA, p. 15):

$$Ca^{2+} + 2HCO_3^- \rightarrow CaCO_3 + CO_2 + H_2O \quad \textbf{Eq. 21}$$

TA is not affected by respiration, because every negative charged bicarbonate or carbonate ion is balanced by hydrogen:

$$CO_2 + H_2O \leftrightharpoons H_2CO_3 \leftrightharpoons H^+ + HCO_3^- \leftrightharpoons 2H^+ + CO_3^{2-} \quad \textbf{Eq. 22}$$

Also organic carbon production via photosynthesis does not change TA (Smith & Key 1975):

$$CO_3^{2-} + 2H^+ \rightarrow CH_2O + O_2$$
$$HCO_3^- + H^+ \rightarrow CH_2O + O_2$$
$$H_2CO_3 \rightarrow CH_2O + O_2$$
$$CO_2 + H_2O \rightarrow CH_2O + O_2 \quad \textbf{Eq. 23}$$

Correction for nutrients

Although respiration has no effect on TA, it is coupled through the assimilation and dissimilation of nitrogenic and phosphorous compounds which release or take up OH^- and H^+ (Kinsey 1978; Gattuso *et al.* 1999b). In samples of seawater with significant changes in

dissolved $CaCO_3$ and in nitrogen nutrients (due to excretion and nitrification), the precipitation or dissolution of $CaCO_3$ can be calculated from the following equation (Jacques & Pilson 1980):

$$\Delta CaCO_3 = ½ [\Delta TA - \Delta NH_4^+ + \Delta (NO_3^- + NO_2^-)] \quad \textbf{Eq. 24}$$

The effect of phosphorus (P) on the TA is difficult to evaluate because it will depend on which species of P is assimilated (Brewer & Goldman 1976). However, while it should be hardly detectable (Brewer & Goldman 1976) it can be disregarded in practice (Jacques & Pilson 1980).

Calcification rates

Using Eq. 24, net calcification rates (G) in the short-term incubation experiments were calculated by the following equation:

$$G\ (\mu mol\ CaCO_3\ \Phi^{-1}\ T^{-1}) = \frac{\left(\frac{\Delta TA - \Delta NH_4^+ + \Delta(NO_3^- + NO_2^-)}{2}\right) \times V_{sw} \times \rho_{sw}}{T \times \Phi} \quad \textbf{Eq. 25}$$

V_{sw} is the volume of the seawater (mL) with the corresponding density ρ_{sw}. T is the incubation time (hours or days) and Φ represents the chosen normalisation (e.g., polyp number, polyp volume).

The TA was measured in duplicate using a potentiometric, open-cell titration procedure according to Dickson *et al.* (2003). GF/F filtered seawater samples of 10 - 15 g were accurately weighed (1416B MP8-1, Sartorius). For the titration an automatic titrator (Titrando 808, Metrohm) was used. As titrand hydrochloric acid (HCl) with a concentration of 0.005 N was used. The average precision between duplicate measurements was ≤ 4 µmol kg^{-1}. All samples were poisoned with saturated $HgCl_2$ immediately after sampling to avoid further microbial activity. The nutrient measurements for the corrections were performed as described in section 2.1.3.2.

2.2.1.3. Normalisation and morphometrics

2.2.1.3.1. Normalisation of data

Normalisation of physiological rates (e.g. growth rates, feeding rates, oxygen consumption) is an important and necessary approach to scale to the size of an animal (Dodds 2007). Because of the complex variations in morphology, normalisation in scleractinian corals is quite difficult and highly dependent on the applied methods and species.

Studies on growth rates were often performed as ^{45}Ca-incorporation or as surplus-growth in length or weight during a specific period of time. For the latter two, typical normalisations were length or weight gain as a percentage of the initial measurement (Ferrier-Pagès *et al.* 2003; Lapid & Chadwick 2006). Other commonly used normalisations were surface area (Marubini & Davies 1996; River & Edmunds 2001), colony (Anthony 1999b) or biomass (Johannes & Wiebe 1970; Edmunds & Gates 2002). The wide range of possible units and normalisations makes comparisons between different studies and generalised statements very difficult.

In this study normalisation against polyp number was usually preferred. In order to compare gravimetric (BWT) based growth rates with calcification rates from other studies on scleractinian corals, a morphometric correlation analysis between the two parameters length and weight (see next section) was performed. The growth rates were subsequently calculated using the following equation:

$$G\ (\%\ day^{-1}) = \frac{x_{t2} - x_{t1}}{x_{t1} \times (t_2 - t_1)} \times 100 \qquad \textbf{Eq. 26}$$

where x is either the mass (in mg or µg $CaCO_3$) or the length (in mm) at the start (t_1) and the end (t_2) of each time period.

2.2.1.3.2. Length-weight relationship

Coral branches (approximately 20 - 80 polyps per branch) from different locations and morphologies were selected specifically to ensure a profile representative for our whole coral stock population. The skeletons were cleansed of their organic compounds and dried to constant weight as described above. After drying, single calices (n = 342) were dissected by cutting a calyx close to its budding zone with a side cutter. Any residues from the mother polyp were removed carefully. Each calyx was measured in its apical diameter and length

using a digital sliding caliper (Digimatic Series 500, Mitutoyo Ltd.) reading to 0.01 mm. If the diameter of a calyx was elliptical, the average of largest and smallest diameter was determined. Finally, the corresponding skeleton dry weight of each calyx was measured by double-weighing it on an analytical balance reading to 0.01 mg (CPA225D, Sartorius). The obtained data triplet of calyx length, diameter, and weight was then used for characterising the basic morphometry in a regression analysis (3.1.3.2).

2.2.2. Bioreactors for short-term experiments

The following section describes the materials and technical specifications of the incubation chambers (bioreactors) used for the short-term acidification experiments. For reasons of clarity, the experiments themselves are described separately in chapter 2.3 (Environmental change related experiments).

2.2.2.1. Hermetically closed bioreactors (HCB)

The first generation of bioreactors was especially designed for short-term incubation experiments with cold-water corals using hydrochloric acid (HCl) for seawater acidification. To avoid an outgassing of CO_2 during incubations, the chambers were constructed absolutely airtight and with an adjustable stamp as lid, allowing water sampling through a valve without opening the chamber (Fig. 21).

Bioreactor and rack design

Each of the 25 bioreactors consisted of a 5 mm thick acrylic glass tube of 195 mm in length and an inner diameter of 90 mm (1,240.5 cm^3). Five tubes each were combined to one unit on an acryl glass rack (480 × 310 × 140 mm). The rack was separated into a platform for the bioreactors and a small water bath (480 × 103 × 135 mm). On the inner bottom of each tube three fittings (Festo) were mounted. Two of them (G1/4) were connected by PVC hoses (Ø 5 mm) to the water bath (respectively rotary pumps) and the third (G1/8) was connected by a silicone hose (Ø 5 mm) with a valve in front of the rack.

The setup allowed the water in the bioreactor chamber to be hermetically sealed with an acrylic glass stamp. For temporary sensor measurements (e.g., pH, temperature, O_2) and in order to emit of the overhead air during closing, the stamp was provided with a large bore (Ø 18 mm) sealed with a rubber bung. Water movement in the bioreactor was provided by an external rotary pump (270 L h^{-1}; Universal Powerhead 1005, Eheim) which was placed

in a water bath for cooling and connected to the bioreactor through hoses and fittings (Festo) in the rack. Water flow was regulated by a valve and the direction of the water flow (in the bioreactor) was adjustable through a small PVC-tube (80 mm, Ø 5 mm) with lateral bores placed on the inner outflow fitting of the bottom of the bioreactor. For some experimental setups the net bioreactor water volume (~ 1 L) was regarded as insufficient. For such cases the bioreactors were interconnected. The rotary pump was attached to the inflow pipe of one reactor and the outflow pipe of the additional bioreactor. Then the outflow pipe of reactor one was short circuited with the inflow pipe from the second bioreactor (Fig. 21 a, optional piping).

Water sampling

Before opening the valves in front of the rack, the rotary pumps were shut off to avoid negative pressure (from the water reflux). Water samples (e.g. TA, DIC, nutrients) could then be obtained simply by moderately depressing the stamps of the bioreactors when the valves were open.

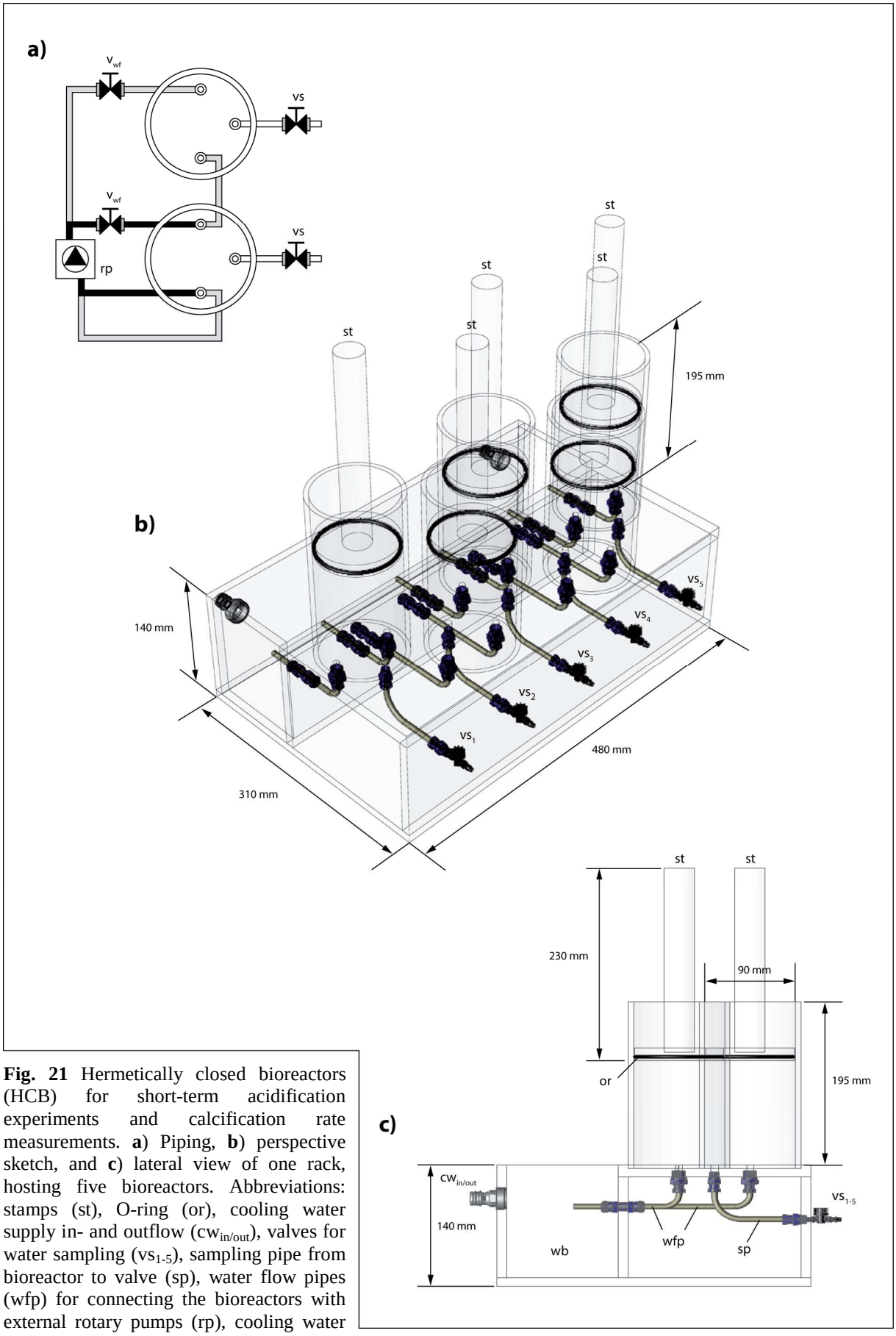

Fig. 21 Hermetically closed bioreactors (HCB) for short-term acidification experiments and calcification rate measurements. **a**) Piping, **b**) perspective sketch, and **c**) lateral view of one rack, hosting five bioreactors. Abbreviations: stamps (st), O-ring (or), cooling water supply in- and outflow ($cw_{in/out}$), valves for water sampling (vs_{1-5}), sampling pipe from bioreactor to valve (sp), water flow pipes (wfp) for connecting the bioreactors with external rotary pumps (rp), cooling water bath for the rotary streaming pumps (wb).

2.2.2.2. Semi-closed bioreactors (SCB) with gas exchange

Hermetically sealed bioreactors were only practicable in short-term experiments (minutes to hours), where the biochemical influence of the examined organism's physiology could be neglected. Or - in contrast - in short-term experiments (hours to days) where especially these influences were the designated variables (e.g. decreasing O_2 due to respiration). With the access to highly accurate gas-mixing systems (newly established IFM-GEOMAR infrastructure), a semi-closed bioreactor (SCB) for continuous seawater acidification with nearly constant CO_2/air gas mixtures was developed.

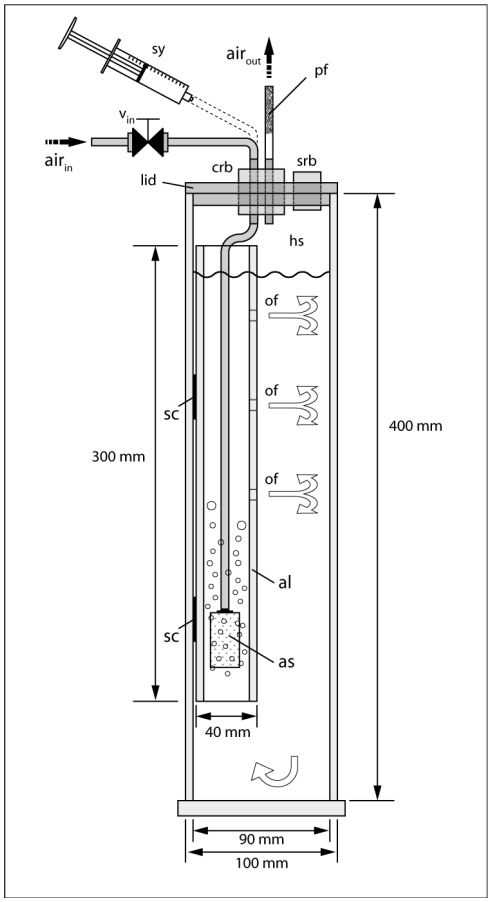

Fig. 22 Semi-closed bioreactor (SCB). Abbreviations: valve (v_{in}), sampling rubber bung (srb), central rubber bung (crb), headspace (hs), air lift (al), air stone (as), polyfill filter (pf), water outflow (of), double-sided suction cup (sc), syringe (sy).

Bioreactor design

The bioreactors consisted of a 5 mm thick acrylic glass tube - which measured 400 mm in length and had an inner diameter of 90 mm (2,545 cm^3) - mounted on an acrylic glass panel (110 × 110 × 10 mm). Both, water movement and water aeration were realised by an air-lift, consisting of a 300 mm acrylic glass tube (Ø 40 mm) with three lateral bores (Ø 7 mm) for water outflow in the upper half. Gas inflow was achieved by an air stone (type #1, Sander) placed in the lower half of the air-lift. The air stone was connected through a transparent PVC-hose (Ø 5 mm) to a fitting-tube in the bottom side of a rubber bung, plugged in the lid of the bioreactor. On the top side, the fitting-tube was connected through a valve to a channel of the gas mixing system. To ensure a constant outflow of the gases from the headspace while simultaneously preventing an equilibration with the atmosphere outside the bioreactor, a small additional fitting-tube (Ø 5 mm) was fixed in the rubber bung. The upper half of this tube was filled with Polyfill® in order to minimise water loss due to evaporation.

Sampling was realised by temporarily disconnecting the gas supply (Fig. 22, v_{in}) and attaching a syringe to the gas supply hose next to the fitting-tube.

2.2.3. Polyp Behaviour Monitoring tool (PoBeMon)

Polyp expansion/contraction has been well documented in tropical zooxanthellate corals and sea anemones (see introduction). Methods used for this ranged from direct observations with the naked eye (Lasker 1979; Levy *et al.* 2001; Levy *et al.* 2006) to photograph or video-assisted measurements (Mortensen *et al.* 2000; Brown *et al.* 2002). For deep-water corals, Roberts & Anderson (2002) suggested a semi-autonomous method based on time-lapsed video recordings and manual measurements of the polyps state on the video screen.

In this section, an advanced method for polyp expansion/contraction behaviour studies using computer image analysis is described. The method was applied within the experiments explained in section 2.3.1 after a series of verifications.

2.2.3.1. Hardware setup and pre-processing

In summary, the whole image analysis process consisted of three main steps: the real-time recording of selected coral branches in digital movie files (hardware), the extraction of single frames in a specified time interval (pre-processing) and the subsequent software image analysis of the frames.

Video recording

The basic hardware components consisted of a series of up to eight analogue CCD cameras connected to a PC through a multi channel framegrabber (Fig. 23). The black-white cameras (b/w plate camera A1-PRO, Conrad) used in the experiment had a very high photosensitivity of 0.1 lx (~ 1.37×10^{-3} µmol photons m^{-2} s^{-1}) and were mounted in a water resistant camera body. The cameras were placed in front of the aquarium tanks and a LED (0.12 W) for low grade illumination was mounted close to each camera and oriented towards the coral samples in the aquaria. The analogue signals from each camera were transmitted through BNC cables (75 Ω) to the framegrabber in an adjacent dry lab. The framegrabber (8CH PCI @ 25FPS, Eytron; video observation software: DigiProtect®) digitised each video channel with a sampling rate of 3.1 frames per second and stored the data as continuous compressed video-stream files (codec: MPEG4 or MJPEG) on an external 500 GB hard drive (HDD Professional, Iomega).

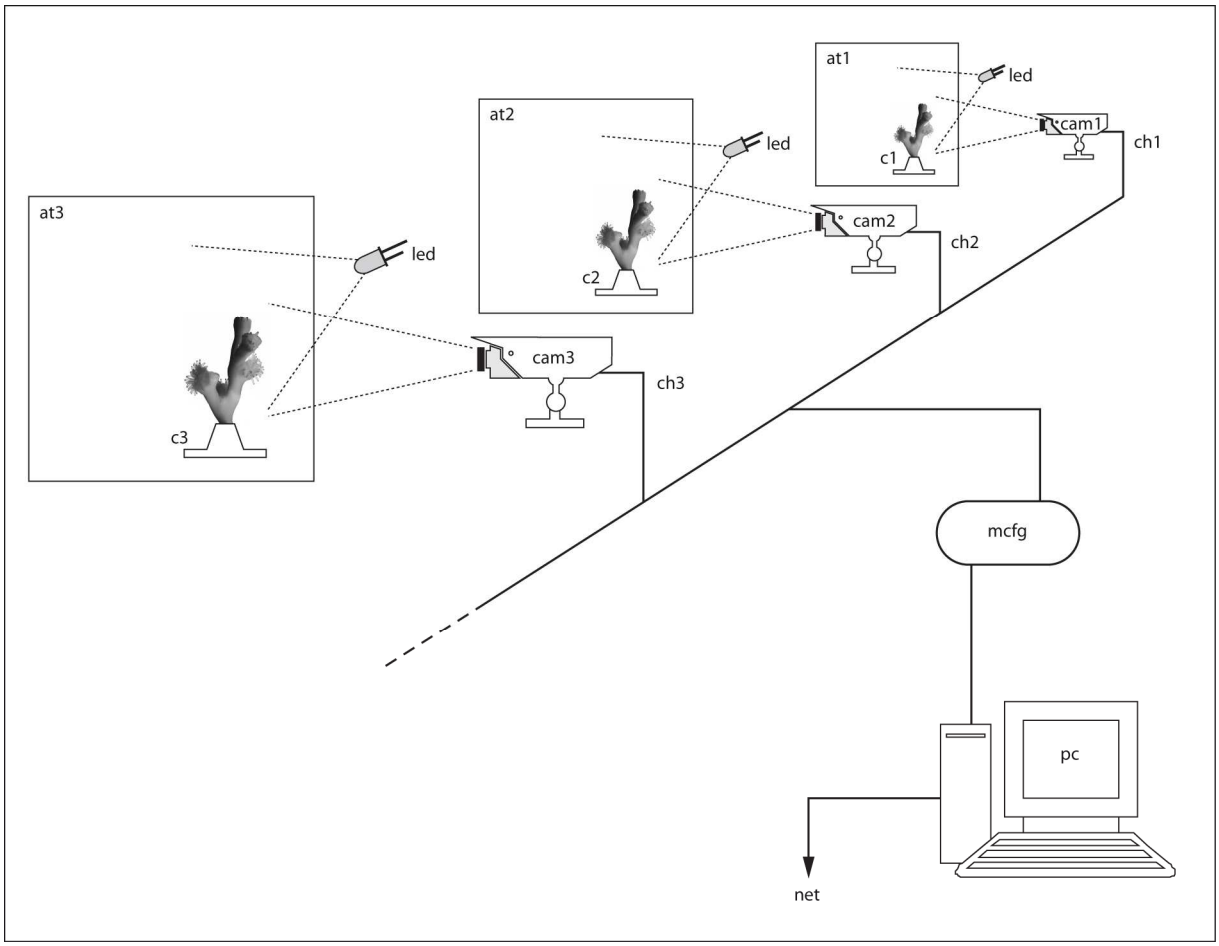

Fig. 23 Schematic diagram of the main hardware components used to record coral polyp behaviour simultaneously. In the diagram only three cameras are illustrated but the actual number depends only on the capacity of the framegrabber and PC. The distance between camera and framegrabber/PC is limited by the attenuation of the cables but can easily be extended (> 1,000 m) by using electronic amplifiers. For long-term recordings, the file storage on a large external hard drive or on the server of a LAN network is recommended. By using a LAN connection both the real time picture from the camera and the recorded videos can be viewed from each network access point. Abbreviations: aquarium tank (at), light-emitting-diode (led), CCD video camera (cam), multi-channel framegrabber (mcfg), personal computer (pc), network (net).

Pre-processing

In order to make the video files accessible for the image analysis, single frames from the video files (usually in AVI container) had to be extracted and saved as image files. Using the free software VirtualDub (v. 1.7.6) and a short processing script, images from the video streams were automatically extracted and saved as JPEG-files (24 bit, 640 × 480 pixel) in a predefined interval of five minutes.

2.2.3.2. Image analysis using ImageJ with scripting language macros

For the image analysis of the polyps' behaviour patterns, the open source software ImageJ was chosen. In addition to its strong and well established image analysis algorithms, ImageJ

was designed with an open architecture allowing the use and extension of the software with user-written Java plug-ins and macros.

By implementing an iterative recognition algorithm, as described below, the automatic measurements of extension/retraction of coral polyps in a series of images was realised.

2.2.3.3. Image analysis fundamentals

The measurement algorithm was based upon the differences of the grey intensities between the bright skeleton, the grey polyp, and the dark background. By using 24 bit images in the RGB colour mode (true colour) a colour is defined as the intensity of each of the three primary colours (red, green, blue). The intensities were represented by 8-bit unsigned integers (0 through 255), allowing a colour space of more than 16 million colours (256 × 256 × 256). In image analysis, the colour information can be converted to user-defined brightness-values representing the brightness of a colour on a monochromatic scale (8-bit greyscale). In our processing, the RGB pixel values were converted to brightness values (V) with the standard conversion equation (Rasband 2004):

$$V = \frac{(R + G + B)}{3} \qquad \textbf{Eq. 27}$$

resulting in the value 0 for absolute black, 255 for absolute white, and 254 values for the different shadings of grey.

2.2.3.4. Extension measurement algorithm (main macro)

2.2.3.4.1. Preparation and calibration

For each selected polyp of an image series, a few calibration values had to be determined and inserted into the macro script before the automatic measurements could be started. For reasons of simplicity, the procedure and subsequent analysis of only one single polyp is described.

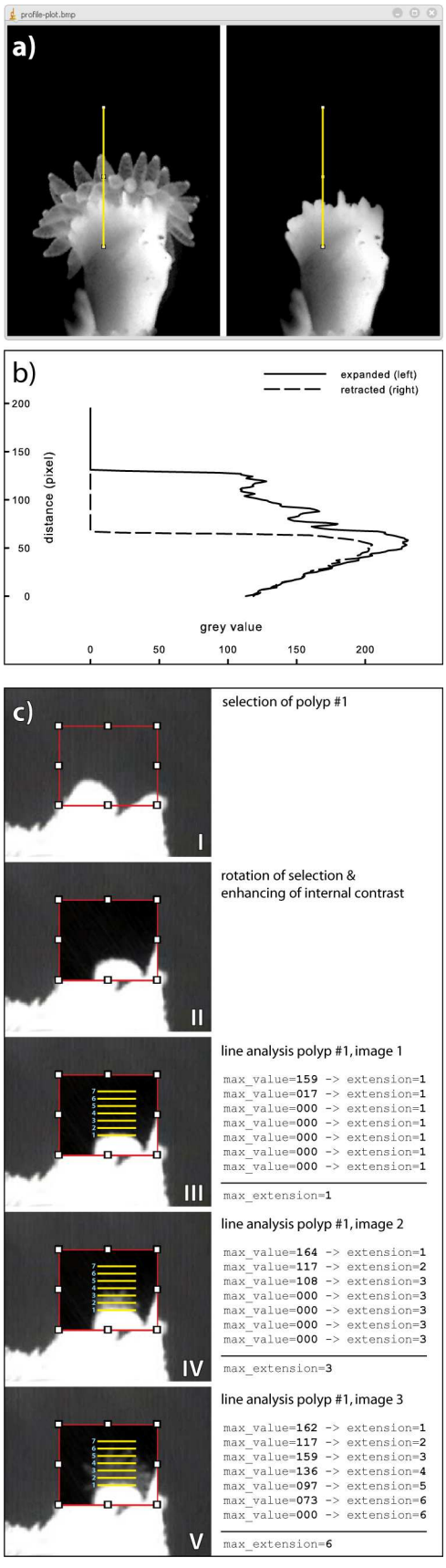

Fig. 24 Simplified PoBeMon analysis of a single polyp. **a**) profile scan of extended (left) and retracted (right) polyp, **b**) corresponding grey scale plot, **c**) sample processing sequence (left) and corre-sponding operations (right).

Detection limit

From the recorded image series, two frames had been loaded in ImageJ: one showing the polyp absolutely retracted and one showing the polyp at any expansion. With the 'Straight line selections' tool from the toolbar, a perpendicular line was drawn in both images from the distal part of the calyx to a point largely overestimated as the maximum polyp expansion (Fig. 24 a). By using the analysis function 'Plot Profile' (menu 'Analyze'), the software returns profile plots showing the distribution of grey values along the selections (lines drawn) for both images. When the plots were superimposed one above the other, the corresponding grey values of the skeleton (calyx), the tissue, and the background were made distinguishable (Fig. 24 b). As a detection limit necessary for the macro (Fig. 25, line 18) the lowest representative grey value for the tissue was chosen. Analysis on a selected polyp was rejected when background values were in the same range as the tissue values and no clear distinction was possible.

Polyp selection

If the polyp was not in a vertical position it had to be rotated before image analysis could start. For this, a rectangular selection (toolbox 'Rectangular selections') surrounding the polyp (in the expanded image) was performed and the coordinates of the selection were inserted into the macro (Fig. 25, line 21). The necessary rotation angle was determined with the 'Angle tool' from the toolbar and this value was also inserted into the macro (Fig. 25, line 22).

After rotating the selection (menu 'Image > Rotate > Arbitrarily…'), the coordinates for the line scanning were determined by drawing a horizontal line through the boundary between calyx and polyp with a length of the polyps' horizontal dimension. The x-values were entered into the 'makeLine()' command (Fig. 25, line 29) and the y-value was assigned to the 'arg' variable (Fig. 25, line 28). In the last step, the number of pixels above the horizontal line affected by the polyps' expansion were estimated (plus a buffer of about 20 - 30 %) and assigned to the condition statement (n < x) of the line scanning 'for'-loop (Fig. 25, line 27).

2.2.3.4.2. Running image analysis

The whole algorithm is highly iterative with a triply nested loop where the outer loop takes control of the number of complete repetitions of the inner loop (Fig. 25, flowchart). After starting the macro, the user only has to select the image directory where the raw image files from the pre-processing were saved and the program automatically proceeds with the measurements of the predefined polyps in all images in that directory. After enhancing the contrast in the selection (Fig. 25, line 23), the line scanning algorithm begins the process of detecting the actual polyp state in the selection. For this the grey values from a horizontal line on the boundary between calyx and polyp were measured and the maximum value was stored in the variable 'max_value' (Fig. 25, line 36 and Fig. 24 c, III). This variable was compared with the predefined detection 'limit' for tissue (Fig. 25, line 39) and if it was equal or larger than this a second variable 'extension' was set to the numerical value '1'. After this, the variable 'extension' was compared with a third variable 'max_extension' and in case of it being smaller than the initial value (0), the variable 'max_extension' was set to the 'extension's value. In the next iteration a second line was measured exactly one pixel above the previous line and the 'extension' variable was set to the next higher number (n + 1) if its maximum grey value was equal or higher than the 'limit'. Then, the 'maximum_extension' value (= the old 'extension') was compared with the new 'extension' and was set to the new value when it was higher or equal compared to the old value. This process was repeated for all iterations (Fig. 24 c, III). The number of respective line scannings was predefined (see above) and therefore an additional termination condition was not implemented. After processing all iterations, the variable 'max_extension' outputs the number of positively performed iterations along the y-axis. The data was temporally saved in an internal results table. If all polyps of an image were measured, the next image was loaded to memory and processed.

```
1   macro "multiPoBeMon_1" {
2   // global variables and data setup
3   dir = getDirectory("Choose Image Directory ");
4   list = getFileList(dir);
5   setBatchMode(false);
6   run("Colors...", "selection=red");
7   run("Colors...", "foreground=blue");
8   run("Clear Results");         // delete internal results table
9   row=0;                        // initial row number of results table
10  //
11  for (i=0; i<list.length; i++) { // open directory (recursive)
12  path = dir+list[i];
13  showProgress(i, list.length);
14  if (!endsWith(path,"/")) open(path);
15  if (nImages>=1) {
16  //
17  // P_1 Polyp Nr. 1
18  limit=40;             // detection limit
19  max_extension=0;      // reset initial maximal extension
20  //
21  makeRectangle(357, 92, 76, 62);       // selection of polyp P_1
22  run("Arbitrarily...", "angle=325 interpolate");
23  run("Enhance Contrast", "saturated=5"); // enhance selection
24  //
25  // START ANALYSIS
26  //
27  for (n=0; n<25; n++) {              // processed loops
28  arg = 138-n;                  // y-value - n
29  makeLine(393,arg,414,arg);    // makeLine(x1, y1, x2, y2)
30  profile = getProfile();
31  l = profile.length;
32  max_value=0;
33  for (k=0; k<l; k++) {
34  value = profile[k];
35  if (value>=max_value) {
36  max_value=value;
37  }; // end if
38  }; // end for loop
39  if (max_value>=limit) extension=n+1; else extension=0;
40  print("max_value: "+max_value+"    extension: "+extension);
41  run("Draw");
42  if (extension>=max_extension) max_extension=extension;
43  }    // end of loop (for) polyp nr 1
44  //
45  print("resulting maximal extension: "+max_extension);
46  setResult("ext 1",row,max_extension);
47  //
48  updateResults();
49  //
50  // INSERT POSITION (next Polyp)
51  // end of measurements
52  selectWindow("Results");
53  row++;
54  //
55  close();      // close active image
56  }    // end of analysis for image (n), next image (n+1)
57  }    // end of directory
58  saveAs("Measurements", "");
59  }    // end of macro
```

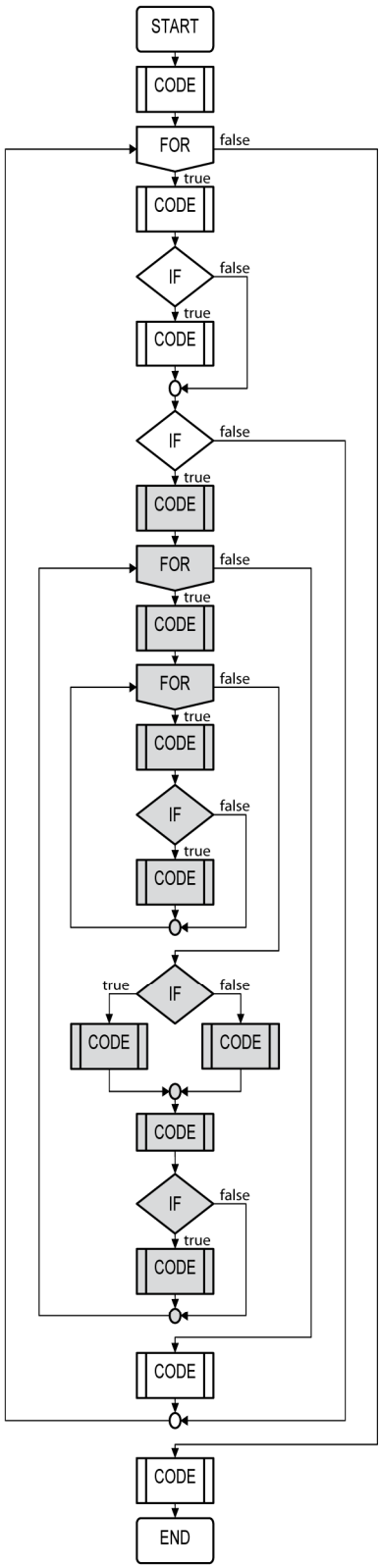

Fig. 25 Excerpt of the main algorithm from the PoBeMon image analysis using ImageJ JAVA-scripting language. Source code (left) and corresponding flowchart (right). For details see text.

Normalisation

At the end of the image analysis, the result table consisted of a time dependent series of 'max_extension' values from each measured polyp and the user was prompted to save the results in an external file (Fig. 25, line 58). To calculate the real expansion (in pixel) of a polyp, the minimum 'maximal_extension' value of all measurements from this polyp was subtracted from each 'maximal_extension' (for that polyp). If a polyp was completely retracted, the value for the real expansion was set to zero through this procedure. The value for the maximum real expansion however was dependent on the applied image resolution, camera angle and distance (camera - polyp). For standardised conditions only polyps showing at least one full expansion (see Fig. 14 b, 3) were used.

In order to make the individual expansion values (pixel) comparable, the maximum real expansion of a polyp was set to 100 % and normalised actual expansion ($Exp_{norm}(t)[\%]$) was calculated in percent of maximal expansion:

$$Exp_{norm}(t)[\%] = \frac{Exp(t)[px] \times 100}{Exp_{\max}(T)[px]} \qquad \textbf{Eq. 28}$$

where Exp(t)[px] is the expansion of a polyp at a specific time (t, i.e. the image number) and $Exp_{max}(T)[px]$ is the maximum expansion value of the same polyp in the entire time period (T).

2.2.4. Continuous optode-based respiration measurements

In close collaboration with the Institute for Polar Ecology Kiel, a novel method for continuous and parallel oxygen and pH measurements in small cold-water coral and arctic algae samples has been developed. The method is based on a new type of optical electrodes (optodes) and has several advantages compared to the conventional methods from Winkler (1888) and Clark (1956) as described in chapter 4.2.1.3.

2.2.4.1. Optodic measurement principles

a) Oxygen

For oxygen, the measurement principle is based on the effect of dynamic luminescence quenching by molecular oxygen depicted by a luminescent indicator (Fig. 26 a). Absorbed light energy from a blue LED elevates the indicator dye (luminophore) into an excited state. In the absence of oxygen the luminophore immediately emits a detectable luminescence (fluorescence). If an oxygen molecule collides with the luminophore in its excited state, an energy transfer takes place from the excited indicator to oxygen. In this case the indicator molecule does not emit luminescence and consequently the measurable total luminescence signal decreases.

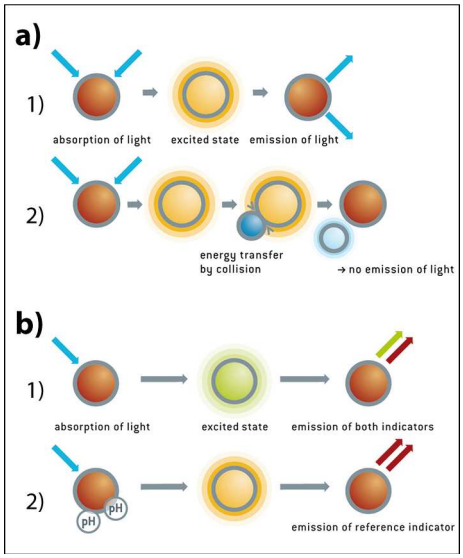

Fig. 26 Principles of dynamic quenching of luminescence by oxygen (**a**) and time dependent fluorescence intensity changes caused by pH (**b**). From PreSens GmbH (modified).

The relation between oxygen concentration, the luminescence intensity, and the luminescence decay time is described in the Stern-Volmer-Equation:

$$\frac{l_0}{l} = \frac{\tau_0}{\tau} = 1 + K_{SV} \times [O_2] \qquad \textbf{Eq. 29}$$

with luminescence intensity in the presence of oxygen (l), luminescence intensity in the absence of oxygen (l_0), luminescence decay time in the presence of oxygen (τ), luminescence in the absence of oxygen (τ_0), Stern-Volmer constant (K_{SV}), and the oxygen concentration ($[O_2]$). The Stern-Volmer constant quantifies the quenching efficiency and must be determined experimentally.

The oxygen meter measures the luminescence decay time of the immobilised luminophore as the oxygen-dependent parameter by phase modulation with sinusoidal modulated blue LED light. The decay time is thereby the phase angle between the excited and emitted signal.

b) pH

In contrast to the oxygen measurements with one specific luminescent dye, this application uses two luminophores with different decay times and similar excitation spectra. A pH-sensitive short decay luminophore (indicator dye) is combined with an analyte-insensitive long decay luminophore (reference dye). The fluorescence emissions from the reference luminophore give a constant background signal while the signal from the indicator luminophore depends on the pH concentration (Fig. 26 b). Hence, the overall signal (average decay time) is internally referenced and reflects the ratio of the two fluorescence intensities and its phase shift (Fig. 27).

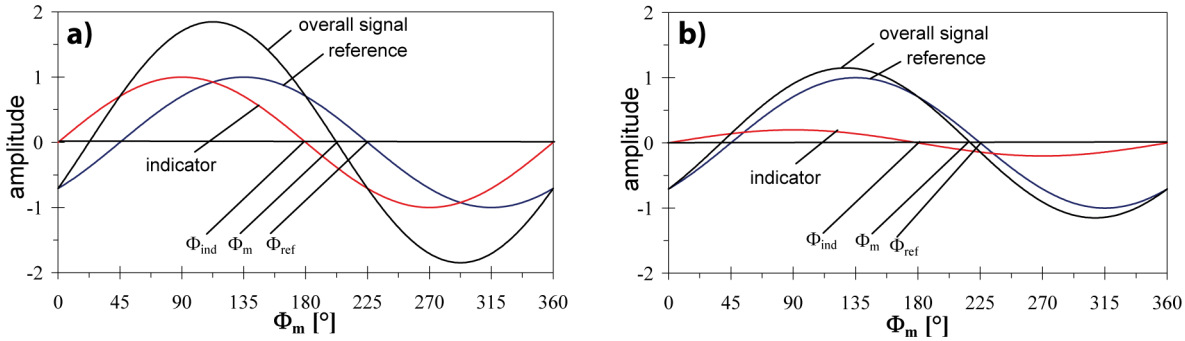

Fig. 27 Phase shift of the overall luminescence (Φ_m), the reference (Φ_{ref}), and the indicator (Φ_{ind}) in absence (**a**) and presence of protons (**b**). From PreSens GmbH (modified).

The overall luminescence decay time is measured by the pH meter through phase modulation with sinusoidal modulated blue LED light.

2.2.4.2. Combined pH and O_2 sensor spots in small respiration chambers

For parallel and simultaneous measurements of pH and oxygen, a temperature-controlled setup with 10 independent respiration chambers (RC) was developed (Fig. 28).

Respiration chamber design

The RC basically consisted of a water-resistant cylindrical PVC-box and the actual RC which was mounted on top of the PVC-box. The PVC-box was internally equipped with a low voltage electric motor (Fig. 28 b, M) that carried a miniature magnet bar and acted as a

magnetic stirrer. Power for the electric motor was controlled and supplied by a multi channel transformer, connected through a cable to the PVC-box. The RC consisted of a 5 mm thick acrylic glass tube with a length of 100 mm and an inner diameter of 110 mm (950 cm^3) - mounted on an acrylic glass panel (160 × 160 × 5 mm). On the bottom of the chamber, a small magnetic stir bar (25 mm) was placed. A removable round tripod PVC table (Ø 90mm, 28 mm in height) separated the magnetic stir bar from the samples. The lid of the RC consisted of an 18 mm thick cylindrical acrylic glass plate with an outer diameter of 120 mm and an inner diameter of 109 mm (Fig. 28 b). In order to seal the lid waterproof with the chamber tube, an o-ring was placed into a drilled nut in the inner diameter. On the top side of the lid, two plug-in connectors for the fibre optic wires were embedded and at the corresponding bottom side, two microscope slides were glued. The planar sensor spots for pH (SP-HP5-D7-US, PreSens) and oxygen (SP-PSt3-NAU-D7-YOP, PreSens) were attached to the slides with silicone glue opposite to the outside fibre optic wires. The centre of the lid was equipped with a continuous 3 mm bore to prevent excess pressure during the closing of the chamber. After closing the chamber, the bore was sealed with a plastic screw and an O-ring. In a closed RC, the gross water volume was ~ 875 mL.

General experimental setup

For the experiments the RC were placed completely submerged in a water bath filled with natural or artificial seawater. The water temperature was controlled by a digital thermostat with an accuracy of 0.1°C (UT100, Conrad) and a 300W titanium heater (Schego). The heater was located directly at the outflow of a streaming pump (1,500 L h^{-1}; Koralia 1, Hydor) which prevented the establishment of thermic gradients in the water bath. In order to control the water flow in the RC independently, the magnetic stirrer power supply cable of each RC was connected with a 10-channel transformer. Water bath temperature was logged in a predefined interval through a temperature logger (Fibox 3 LCD v. 3, PreSens) and the output data was archived (after the experiment) using OxyView software (v. 3.51, PreSens). Before sealing the RC with the lids, the fibre optic wires for the pH and oxygen sensor spots were plugged-in and thereby connected to their measurement devices (10 channel pH meter and 10 channel oxygen meter, PreSens) situated in an adjacent temperature adjusted room. The data was recorded online using a standard PC connected with the measurement devices. An illustration of the setup is shown in Fig. 28 a.

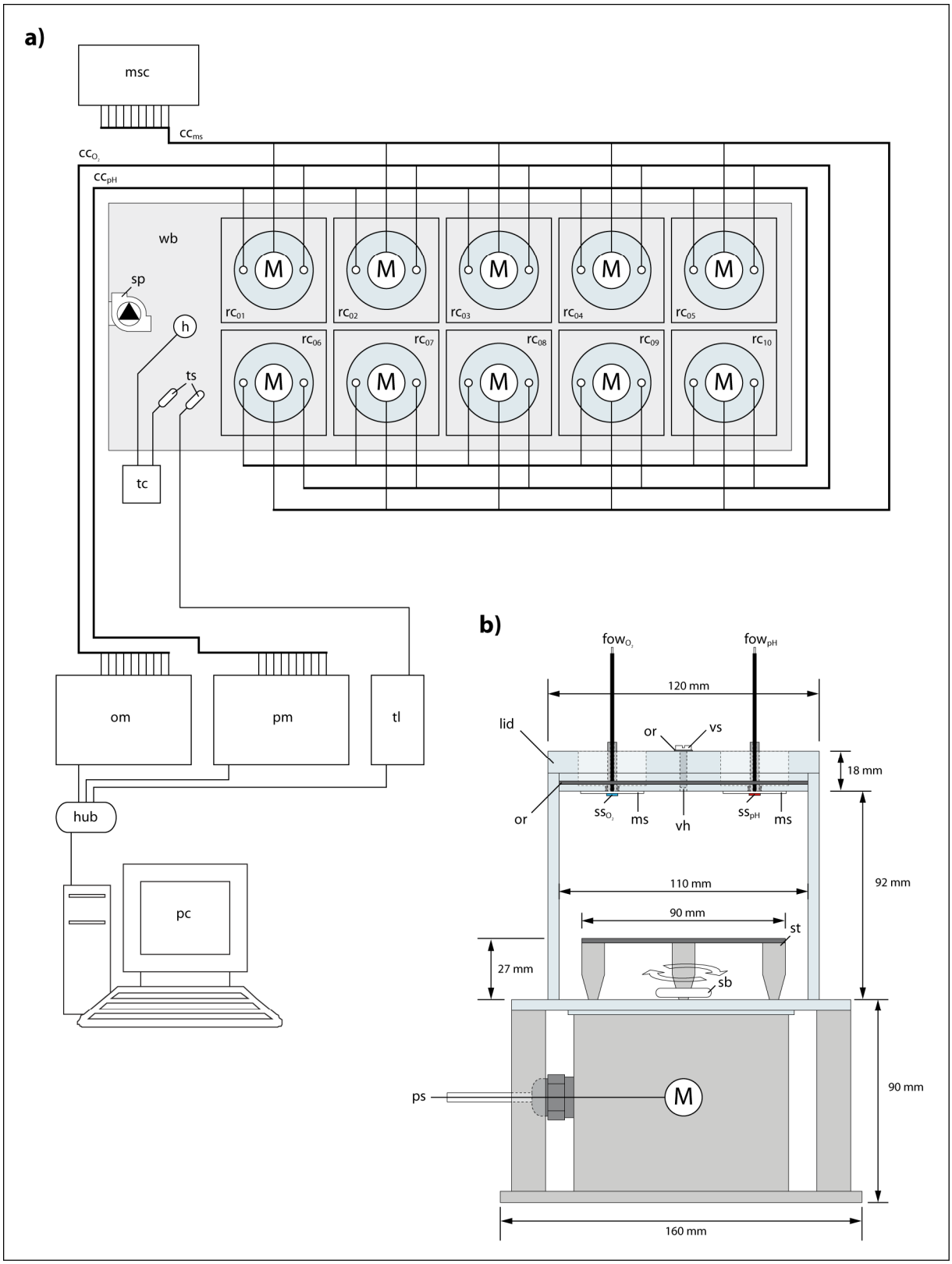

Fig. 28 Setup for simultaneous optodic measurements (a) and a depiction of a respiration chamber (b). Abbreviations: magnetic stirrer power control (msc), cable channel (cc), water bath (wb), streaming pump (sp), heater (h), temperature sensor (ts), temperature control unit (tc), respiration chamber (rc), oxygen meter (om), pH meter (pm), temperature logger (tl), personal computer (pc), fibre optic wire (fow), o-ring (or), magnetic stir bar (sb), sensor spot (ss), sample attachment table (st), microscope slide (ms), power supply for electromagnetic stirrer (ps), electric motor (M), ventilation hole (vh), ventilation screw (vs). See text for details.

2.2.4.3. Oxygen conversions and calculations

Per default, the oxygen meter measures the content of oxygen in pure water as % air-saturation. The solubility of oxygen in water is dependent on temperature, oxygen partial pressure, and water vapour pressure and can be described using the Bunsen absorption coefficient:

$$c_S(p,\theta) = \frac{p(O_2) - p_W(T)}{p_N}\alpha(\theta) \qquad \textbf{Eq. 30}$$

where $c_S(p,\theta)$ is the solubility of oxygen in water, $p(O_2)$ the oxygen partial pressure, p_N the standard pressure (1,013 mbar), $p_W(T)$ the temperature-dependent water vapour pressure, and $\alpha(\theta)$ the Bunsen absorption coefficient.

Water vapour pressure $p_W(T)$ can be calculated with a curve fitting function given by the Campbell equation:

$$p_W(T) = \exp\left(A - \frac{B}{T} - C - \ln T\right) \qquad \textbf{Eq. 31}$$

where T is the temperature in Kelvin, A = 52.57, B = 6,690.9, and C = 4.681 (PreSens GmbH 2005).

The Bunsen absorption coefficient $\alpha(\theta)$ can also be calculated with a curve fitting function or by using a thermodynamic correlation. In seawater, the oxygen solubility additionally depends on the salinity of the water (salting-out effect). Thus, for our calculations, a modified (compensated for salinity) thermodynamically based Bunsen absorption coefficient was used:

$$10^3 \times \alpha = \exp\left[\left(A + \frac{B}{T} + C \times \ln T + D \times T\right) - \left(\frac{\Psi - 0{,}03}{1.805}\right) \times \left(P + \frac{Q}{T} + R \times \ln T + S \times T\right)\right] \qquad \textbf{Eq. 32}$$

where T is the temperature in Kelvin, Ψ the salinity in ‰, A = -7.424, B = 4.417×10^3, C = -2.927, D = 4.238×10^2, P = -12.88, Q = 53.44, R = -4.442×10^2, and S = 7.145×10^4. The coefficients (A-D and P-S) are based on measurements at $273.1 \leq T \leq 308.18$ K and $0.03 \leq \Psi \leq 54.18$ ‰ (PreSens GmbH 2005).

Respiration data from the experiments was expressed as a relative decrease of oxygen saturation percentages (% saturation h^{-1}) or as absolute oxygen concentrations (µmol L^{-1} h^{-1}), calculated by combining Equations 30 - 32:

$$cO_2\left[\mu mol\ L^{-1}\ h^{-1}\right] = \frac{\frac{p_{atm} - p_W(T)}{p_N} \times \frac{\%air - saturation}{100} \times 0.2095 \times \alpha(T) \times 10^3 \times \frac{M(O_2)}{V_M} \times \frac{1000}{M(O_2)}}{RCV \times t_{inc}}$$

Eq. 33

where p_{atm} is the actual atmospheric pressure, p_N the standard pressure (1,013 mbar), 0.2095 the volume content of oxygen in air, $p_W(T)$ the calculated vapour pressure of water according to Eq. 31, $\alpha(T)$ the salinity compensated Bunsen absorption coefficient according to Eq. 32, $M(O_2)$ the molecular mass of oxygen (32 g mol^{-1}), V_M the molar volume (22.414 L mol^{-1}), *RCV* the water volume of the respiration chamber, and t_{inc} the incubation time in hours.

For further information about the thermodynamic background, the derivations of the equations and the constants used, the reader is referred to the instruction manual of the oxygen meter (PreSens GmbH 2005).

2.2.4.4. System validation (first experimental approaches)

Prior to experiments, the PreSens devices were calibrated with a two-point calibration for oxygen and a six-point calibration for pH according to their instruction manuals (PreSens GmbH 2005, 2007). The actual atmospheric pressure (p_{atm}) was obtained from the IFM-GEOMAR in-house weather station (west shore campus).

2.2.4.4.1. System reproducibility measurements

To evaluate the reliability of the setup developed and in order to find the optimal handling procedures, a series of test respiration measurements with identical seawater conditions for all respiration chambers was performed. Here, only the final one is described:

The experiment was performed under saturated oxygen conditions with open RC lids. The water bath was filled with new natural seawater of 5.7 °C and a salinity of 34.5. After the streaming pump had been switched on, seven RC (without lids) were placed equidistantly in the water bath and process water temperature was adjusted to 6.0 °C on the thermostat. Then, the fibre optic wires were connected to their corresponding sensor spots (pH and O_2, respectively) on the lids of the RC and submerged in the water bath close to their RC (not

being sealed). The power supply for the magnetic stirrers was switched on and adjusted to a similar rotation speed of the stir bars in all RC. Finally, the measuring devices were activated for data acquisition. Temperature was logged in 2-minute intervals, whereas pH and O_2 was recorded in 15-minute intervals. After about 70 hours, the experiment was terminated.

2.2.4.4.2. *L. pertusa* holobiont respiration at ambient and elevated temperature

Previous experiences have shown that a long lead time phase for the sensors and the overall system seems to be suitable to achieve a reproducible and temperature-stable setup. The aim of the next experiment was therefore to combine these experiences with first measurements of the cold-water coral *L. pertusa* at ambient (T, 7.5 °C) and elevated temperature of 11°C ($T_{+3.5°C}$) for a general characterisation of the corals respiratory physiology. Furthermore, the amount of bacterial "background respiration" in empty RC (blanks) was evaluated.

The water bath was filled with ambient seawater from the CWC-MS (7.5 °C, 35.2 PSU) and eight RC were placed equidistantly on the bottom of the tank. The thermostat was set to maintain temperature constantly at 7.5°C and the system was prepared and launched as described above. After three days (system stabilisation phase), five RC were equipped with small branches of *L. pertusa* (approx. 12 polyps branch^{-1}) from the CWC-MS (Sula Reef samples) and three RC were left empty (blanks) for measuring the general drift and bacterial "background respiration". Then, after an acclimatisation time of three hours with aerated seawater, the RC were closed airtight with their corresponding lids for the first respiration measurement (T).

After about 24 hours, the first respiration measurement was terminated by opening the lids and renewing the water both in the water bath and RC (~ 50 %). Then, the thermostat was set to 11 °C and seawater was aerated and pumped through all chambers. After about 40 hours of acclimatisation to the appropriate temperature, the RC were closed again for the second respiration measurement ($T_{+3.5°C}$). 24 hours later, the experiment was terminated and the corals were transferred into a vacuum freeze-dryer (Alpha 1-4, Christ) in order to determine their freeze-dried weight (FD) according to Dodds (2007). The water volume of each RC was determined by weighing the remaining water with a balance (Sartorius) and multiplying the weights with a calculated seawater density of 1.0269 (temp. 11.1 °C, salinity 35.2) (Lavigne & Gattuso 2009). During the experiment, one blank failed due to technical reasons (magnetic stirrer malfunctioned) and post-hoc evaluation of the measured phase angles led to the

decision, to discard the data from one *L. pertusa* replicate because of a 70 % higher standard deviation in its reproducibility. Oxygen consumption rates were calculated from the depletion of oxygen during its linear phase at normoxic conditions and were corrected for the microbial respiration from the blanks.

To assess the effect of temperature on oxygen consumption, the Q_{10} values according to van't Hoff were calculated from the oxygen consumption rates at both temperatures:

$$Q_{10} = \left(\frac{k_2}{k_1} \right)^{\frac{10}{(t_2 - t_1)}} \qquad \textbf{Eq. 34}$$

where k_1 and k_2 are the rates of oxygen consumption at the ambient (t_1) and elevated (t_2) temperature, respectively.

2.2.5. RNA/DNA-ratio measurements for stress diagnosis

Fluorometric RNA/DNA ratio measurements were performed on *L. pertusa* in the framework of the environmental change related experiments as explained in the next chapter (2.3). The method was applied after the procedures developed and described by Clemmesen (1993) and Belchier *et al.* (2004) and the adaptations to cold-water corals from Gutperlet (2008).

2.2.5.1. Sample preparation

Coral samples selected for the RNA/DNA ratio measurements were shock-frozen in liquid nitrogen (-196 °C) immediately after the termination of the experiment and afterwards stored at -80 °C. From the frozen samples, single calices were separated and thawed temporarily for transferring the polyps' tissues into Eppendorf vials. To separate the tissue from the carbonate skeleton, an airbrush apparatus filled with chilled natural seawater was used. After that the vials were immediately refrozen at -80 °C. The frozen vials were then transferred in a pre-cooled freeze dryer (Alpha 1-4, Christ) and freeze-dried at -54 °C for 12 hours with a consistent vacuum pressure of 0.1 mbar.

2.2.5.2. Measurement procedures

2.2.5.2.1. Homogenisation

Each vial of the samples was filled with glass beads of different sizes (0.2 - 2.0 mm) and a detergent (TE-SDS) was added to improve the extraction of nucleic acids. Then the vials were shaken for 15 minutes on a mill (MM-2, Retsch) for complete homogenisation of the tissues. Afterwards, the vials were centrifuged at 6,000 rpm (approximately 3,830 × g) for 8 minutes in a chilled centrifuge (3-18 K, Sigma) at 1 °C. Finally, the supernatant was transferred into a new vial and placed temporary in an ice bath.

2.2.5.2.2. Determination of nucleic acids

For the fluorometric determinations, the vials were placed into a microwell plate (Fig. 29). A control homogenate consisting of herring larvae with known RNA and DNA contents was added in a separate vial and treated in the same way as the coral samples. Then four calibration series (2, 5, 10, 20, 30, 40, and 50 µL)

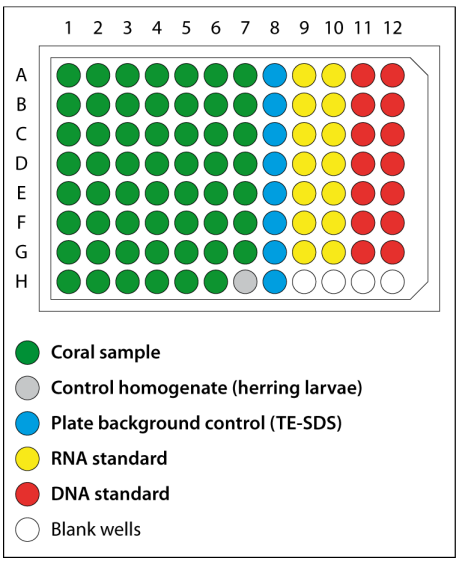

Fig. 29 Depiction of an example layout of a standard 96 microwell plate.

with RNA and DNA standards (2 × RNA, 2 × DNA) and eight blanks (130 µL TE-SDS) were added to the microwell plate. Subsequently the microwell plate was inserted into the flourometer (Fluoroskan Ascent®, Thermo) and an internal dispenser completed all vials with a TE buffer until a total volume of 180 µL per vial was reached. After shaking the plate for one minute, the fluorometer warmed up to 25 °C and shook the plate again for one minute.

a) Autofluorescence

The autofluorescence of the samples was measured at an excitation wavelength of 355 nm (λ_{exc}) and an emission wavelength of 590 nm (λ_{em}).

b) Total fluorescence

After the measurements of the autofluorescence, 20 µL ethidium bromide (0.1 mg mL^{-1}) was injected through a dispenser into the vials. Ethidium bromide is a fluorescent dye and intercalating reagent which reacts with based-paired regions of both RNA and DNA (Le Pecq & Paoletti 1966). Therefore it was used for total nucleic acids (RNA + DNA) determinations. For mixing, the plate was shaken for one minute and after a pause of two minutes again for another minute. Afterwards the total fluorescence of the vials was measured with the same excitation and emission wavelengths as used to measure the autofluorescence.

L. pertusa displays only a limited linear relationship between the sample size and the corresponding fluorescence (Gutperlet 2008). If the measured total fluorescence of a sample was higher than a certain limit, the sample was therefore diluted (Tab. 2) and both autofluorescence and total fluorescence were measured again.

Tab. 2 Dilution factors used to compensate high total fluorescence in *L. pertusa* RNA/DNA ratio samples.

Total fluorescence (*Tf*)	Dilution factor	Homogenate (µL)	TE-SDS Buffer (µL)
> 30	1:2	65	65
> 50	1:3	43	87
> 80	1:4	32.5	97.5
> 100	1:5	26	104

c) DNA fluorescence

The fluorescence of the DNA was measured after removing the RNA fluorescence. For this, all coral samples, the control homogenate, and four blanks were inoculated with 25 µL RNase whereas the other vials (four blanks and calibration series) were supplied with 25 µL TE buffer. The plate was shaken for two minutes and then incubated for 30 minutes at 37 °C. After cooling down for 30 minutes and an additional shaking for one minute, the DNA fluorescence was measured as described above.

2.2.5.3. Calculations

By subtracting the average fluorescence of the blanks (*Bf*) and the autofluorescence (*Af*) of the samples from the total fluorescence (*Tf*) and the DNA fluorescence (*DNAf*), the relative total (*rTf*) and relative DNA (*rDNAf*) fluorescence were calculated:

$$rTf = Tf - (Bf - Af) \quad \textbf{Eq. 35}$$

$$rDNAf = DNAf - (Bf - Af) \quad \textbf{Eq. 36}$$

The relative RNA fluorescence (*rRNAf*) was then calculated by subtracting the relative total fluorescence (*rTf*) from the relative DNA fluorescence (*rDNAf*):

$$rRNAf = rTf - rDNAf \quad \textbf{Eq. 37}$$

The absolute concentrations of DNA and RNA in the samples were calculated from comparisons with calibration curves made with the DNA and RNA standards:

$$DNA(\mu g\ L^{-1}) = a \times rDNAf \quad \textbf{Eq. 38}$$

$$RNA(\mu g\ L^{-1}) = b \times rRNAf \quad \textbf{Eq. 39}$$

where *a* and *b* are the slopes of the calibration curves.

2.2.5.4. Quality criteria

After measurements, the relative fluorescence of the samples was verified if they were in between the limits of the linear relationship between sample volume and fluorescence (see above). In order to categorise their different reliabilities, each measurement was assigned according to its proximity to the relationship (Tab. 3).

Tab. 3 Quality criteria to determine the degree of reliability of fluorometric measurements performed on cold-water coral *L. pertusa* samples. Abbreviations: rRNAf (relative RNA fluorescence), rDNAf (relative DNA fluorescence), and rTf (relative total fluorescence).

Quality	*rRNAf*	*rDNAf*	*rTf*
0 (very low)	< 1	< 1	< 5 and > 33
1 (low)	>16	< 12	< 5 and > 33
2 (acceptable)	> 15	> 10	< 5 and > 33
3 (optimal)	> 1 but < 15	> 1 but < 10	> 5 but < 33

For details concerning the definition of the quality criteria and for general in-depth information about methodology, the reader is referred to Gutperlet (2008).

2.3. Environmental change related experiments

The experiments described in this section were based on the techniques and methods developed in the framework of this thesis (and specified above). To provide greater accessibility for the reader and to prevent unnecessary repetitions the descriptions of the experimental designs were separated from the explanations of technical methods. An overview of the performed experiments and their related measurement methods is outlined in Tab. 4:

Tab. 4 Overview of the Climate Change related experiments performed on the heterotrophic cold-water coral *Lophelia pertusa* (Scleractinia).

Mode	Test variable	Method	Experiment
Temperature	Fitness	RNA/DNA (2.2.5)	TSRE (2.3.1)
	Behaviour	PoBeMon (2.2.3)	
	Respiration	Optodes (2.2.4)	
Acidification	Fitness	RNA/DNA (2.2.5)	STE (2.3.2.1)
	Calcification	TAAT (2.2.1.2)	
	Calcification	BWT (2.2.1.1)	LTE (2.3.2.2)

2.3.1. *L. pertusa* temperature stress response experiment (TSRE)

The temperature stress response experiment (TSRE) was conducted in two successive sub-experiments with three measurement phases (normal conditions, acute stress, acclimatised stress) each. Sub-experiment I (SE-I) was performed at 18 °C ($T_{+10°C}$) and acted as a methodological control and to elucidate maximum stress response reactions (see discussion). Sub-experiment II (SE-II) was performed at a moderate stress level of 11 °C ($T_{+3°C}$).

Experimental design

For the experiments two of the four closed recirculation systems from the LTE-S (2.1.2.3.) were used. The two LTE-S were filled with natural seawater (approximately 34 - 36 PSU) and initial water temperature was regulated to 8.0 ± 0.1 °C. From the CWC-MS (2.1.2.2) five coral branches (Oslofjord samples, approximately 30 - 40 polyps branch^{-1}) were transferred into each of the two LTE-S: two branches into the first tank (video corals) and three into the second tank (respiration corals). The other four tanks were left empty but were integrated into

the whole water body (~ 500 L). In front of the tank with the two video samples, two video cameras were mounted (one per branch) and connected with the PoBeMon Tool (2.2.3).

Sub-experiment I – Extreme stress response test

After an initial phase for general acclimatisation the video documentation system was enabled and the initial oxygen consumption of all respiration samples was measured by Winkler titration (Gutperlet 2008). Then, the water temperature of one LTE-S (stress group) was increased by a daily interval of 2 °C, whereas the other LTE-S was left unmanipulated (control group). When the target temperature of 18 °C had been reached (day 5), respiration was measured again.

The sub-experiment I (SE-I) was terminated early at day nine due to the observation of some detrimental effects on the corals (high mucus production).

Sub-experiment II – Moderate stress response test

This sub-experiment (SE-II) was performed similar to SE-I. The target temperature of 11 °C for the stress group had been reached after 1.5 days. After an incubation of 14 days, the sub-experiment was completed as planned. Respiration of both the acclimatised and the control groups was measured for a third time. At the end of each sub-experiment, all corals (video and respiration corals) were frozen and their RNA/DNA ratios were determined according to 2.2.5. In both sub-experiments and during all phases, the behaviour of the video corals was recorded continuously (SE-I: 9 days, SE-II: 22.5 days). From both groups (control and stress group) and both sub-experiments, the first 48 hours of each phase were extracted for the image analysis (2.2.3).

For methodology about the respiration measurements, performed in the framework of this experiment, the reader is referred to Gutperlet (2008).

2.3.2. *L. pertusa* acidification stress response experiments

During the past three years, quite a number of short- and intermediate-termed acidification experiments were conducted. The continuous improvement of the methods applied led to the eventual success of one short-term experiment and one long-term experiment which are both described below.

2.3.2.1. Short-term experiment (STE)

Twenty semi-closed bioreactors (SCB, 2.2.2.2.) were filled with 2,000 mL GF/F filtered (0.2 µ) natural seawater (salinity of 33.4) each and arranged in an acrylic glass tank. The tank was filled with tap water (approximately 175 L) and acted as a water bath in order to guarantee constant temperatures in all bioreactors. To avoid the establishment of thermic gradients in the tank, the tap water was circulated in a closed circuit by three submerged rotary pumps (270 L min^{-1}; Universal Powerhead 1500, Eheim). After water temperature was constant at 9.0 °C with a tolerance of ± 0.1 °C, the internal air lifts of the bioreactors were temporarily removed and 16 coral branches (Oslofjord samples, approximately 30 polyps $branch^{-1}$) were placed into the reactors. Then the air lifts were reattached close to the coral branches and the bioreactors were sealed.

Seawater acidification

Four bioreactors with coral samples (replicates) and one bioreactor without a sample (blank) were grouped together and linked to the same gas source. By this means, four different pCO_2 treatments were realised. For one of the gas sources, ambient air from the IFM-GEOMAR in-house gas supply ($pCO_2 \approx 406$ ppm) was used and for the other three groups, elevated CO_2-air mixtures with respective pCO_2 levels of 605, 856 and 981 ppm were applied. The elevated CO_2-air mixtures were supplied from three high precision gas mixing pumps (Digamix 5KA 36A/9, Wösthoff). The mixing pumps allow for the dynamical mixture of two gases in mixing ratios which were preset through a pair of cogwheels. In an optimal case, CO_2 free air and pure CO_2 would be used but due to the high amount of air needed for this experiment (~ 240 L h^{-1} $pump^{-1}$), the mixing pumps were operated with ambient air from the IFM-GEOMAR in-house gas supply. Hence, the gas mixtures supplied reflected the daily CO_2 fluctuations (± 50 ppm) in the ambient air.

Sampling & measurements

After 24 hours of bubbling, pH measurements revealed that the different pCO_2 levels were established and after six days of acclimatisation to the appropriate conditions (e.g. water flow, temperature) an initial water sample for dissolved inorganic carbon (DIC) and total alkalinity (TA) was taken from each bioreactor. A second water sample for the determination of the calcification rates was taken at day eight. Additionally, during each sampling, the physicochemical parameters (salinity, pH, temperature) of each reactor were monitored by inserting a multi sensor device (Multi350i, WTW) into a small opening in the lid. During incubations, pH and pCO_2 can change differently in each bioreactor depending on rates of respiration and calcification of the enclosed coral branches. Therefore, the carbonate system parameters (pH, pCO_2, Ω_{Ar}) and growth rates were calculated separately for each bioreactor.

At day ten, the experiment was terminated, the corals were frozen and their RNA/DNA ratios were determined according to 2.2.5.

Calculations

The carbonate system was determined by DIC and TA measurements using the thermodynamic constants of Mehrbach *et al.* (1973) as refitted by Dickson and Millero (1987) on the free scale and the DOS-based carbonate system calculation software CO2SYS (Lewis & Wallace 1998). The DIC was analysed photochemically according to Stoll *et al.* (2001) using an automated segment-flow analyzer (QuAAtro) equipped with an auto-sampler (± 5 µmol kg^{-1} precision) and TA was measured as described in 2.2.1.2.

The growth rates were calculated from changes in the TA values according to the total alkalinity anomaly technique (2.2.1.2). Before that, the TA values were corrected for evaporation based on the salinity measurements of the blanks.

2.3.2.2. Long-term acclimatisation experiment (LTE)

Short-term experiments can only reflect the principal physiological performance of an organism and, in an optimum case they can indicate the absence or presence of regulative or compensative mechanisms. Therefore, the goal of the long-term experiment was to determine growth rates for the cold-water coral *Lophelia pertusa*, acclimatised to different acidification scenarios for a long time.

Experimental design

For this experiment, all four LTE-S were implemented in the technical configuration as described above (2.1.2.3). In June 2008, the CRS were filled with new natural (North Atlantic) seawater with an initial salinity of 34.5. The average water temperature of all systems was set to 7.5 °C (similar to the CWC-MS). In one of the six tanks from each CRS ('a'-tank, Fig. 13), two Alizarin Red S stained coral branches (red and white colourmorphs, approximately 40 polyps branch^{-1}) were placed. In the remaining five tanks, single untreated coral branches (approximately 35 polyps branch^{-1}) were randomly arranged. The preparation of the stained corals was performed 20 days before the experiment started. The staining was conducted in a separate tank (120 L) after Barnes (1970, 1972) using Alizarin Red S (Fluka) in seawater with a concentration of 5 mg L^{-1} for an incubation period of eight days. All coral samples belonging to the Sula Reef corals and mother colonies were equally distributed among the four CRS allowing the analysis of differences in gene expression between the four treatments (not part of the thesis). The corals were fed twice a week with live *Artemia franciscana* nauplii (Premium, Sanders) and once a week with defrosted Cyclops (AD068, Amtra Aquaristik) and ground dried fish flakes (TetraMarine Flakes, Tetra).

Fig. 30 Alizarin Red S stained *L. pertusa* coral branch during the long-term cultivation experiment. The arrow indicates the incorporated staining dye. Scale bar: 10 mm.

At the beginning, all CRS were supplied with ambient air with a pCO_2 level of approximately 406 ppm. After taking initial water samples for TA, DIC, nutrients and measurements of the

physicochemical water parameters (temperature, pH, salinity), three of the four CRS were connected to the 560 ppm CO_2 channel of the IFM-GEOMAR in-house gas mixing system. After one week, two CRS were changed to the 840 ppm CO_2 channel and another week later, one CRS was connected to the 1,120 ppm CO_2 channel. At this stage (day 0 of the experiment) all CRS had reached their target CO_2 levels and the acclimatisation phase started.

During and after the acclimatisation, water quality and system performance were regularly monitored and maintained according to 2.1.3. Process water was renewed occasionally to avoid accumulation of inorganic nutrients and other metabolic waste products. Water exchanges with more than 40 % were performed by transferring the coral branches into one tank of the corresponding CRS. This tank was then disconnected from the water supply so that the water in the other five water tanks could be exchanged. The water supply of the isolated tank was slowly increased after the renewed water had acclimatised in terms of temperature and pH. The corals were repositioned after identical water conditions had been reached in all tanks. After 196 days, process water was slowly shifted from natural seawater (34.2 ± 1.1) to artificial seawater (adjusted to 35.2 ± 0.1; Seaquasal) due to a supply shortfall of natural seawater.

Calculations

The carbonate chemistry was monitored weekly based on TA and pH measurements. pH measurements were evaluated by monthly DIC and TA measurements. Measured and calculated pH estimates closely agreed with a deviation of ~ 0.03 pH. For the chemical analysis (TA, DIC) and the calculation of the carbonate system parameters the same procedures, thermodynamic constants and pH scale as in the STE were used (see above).

Growth rates for the incubation with natural seawater were measured using the buoyancy weight technique (2.2.1.1) on day 54 after the last CO_2 channel was set up (= end of acclimatisation phase; reference weight), on day 131 and 178. Weighings for the incubation with artificial seawater were conducted on day 241 (new reference weight) and on day 292.

3. Results

3.1. Cold-water corals - General cultivation

3.1.1. Water quality management

3.1.1.1. Physicochemical parameters

The process water of the CWC-MS was permanently controlled and readjusted with respect to temperature, salinity and pH. The control temperature during the Oslofjord-Incubation (April, 2006 - December, 2007) was set to 8.0 °C and to 7.5 °C for the Sula-Reef-Incubation (March, 2008 - March, 2009). The maximum fluctuation range allowed in both periods was ± 0.5 °C. Salinity depended on the actual value of the water used. In general - natural seawater from different North Atlantic locations with salinities ranging from 34.4 to 35.2 was used. The intended salinity was 35.0 but fluctuations of 1 - 2 PSU were accepted without taking corrective measures (addition of artificial sea salt or deionised water, respectively). Since December 2008, artificial seawater with a salinity of 35.2 ± 0.5 has been used to replace the previous process water in the CWC-MS successively. Average $pH_{free\ scale}$ was 7.95 ± 0.08 but fluctuations of ~ 0.15 pH units were tolerated.

The controlled physicochemical conditions and their measured minimum / maximum values during Oslofjord- and Sula-Reef-Incubation are summarised in Tab. 5:

Tab. 5 Physicochemical water parameters in the CWC-MS during the Oslofjord-Incubation (April, 2006 - December, 2007) and the Sula-Reef-Incubation (March, 2008 - March, 2009).

Parameter	Intended Value	Accepted Range	Minimum	Maximum
Temperature (°C)	8.0 / 7.5	7.5 - 8.5 / 7.0 - 8.0	5.8	8.5
Salinity (PSU)	35.0 / 35.2	34.0 - 36.0	33.1	37.3
$pH_{free\ scale}$	8.12	7.97 - 8.27	7.85	8.31

3.1.1.2. Nutrient measurement time series

The development of the inorganic nutrients reflected the bacterial degradation process from ammonia to nitrate (nitrification, see 2.1.2.2) in the course of time and the performed corrective measures (water exchanges, filter renewal, adsorber additions). The given time series were divided into the two incubation periods due to the different origins and quantities of the samples during both incubations.

Phase I (Oslofjord samples): April 2006 - December 2007

The ammonium concentrations during the first half year of the heltering varied strongly but exhibited a decreasing trend between 109.12 and 1.20 µmol L^{-1} NH_4^+. After this period the concentration remained relatively stable until the end of the incubation phase where it decreased to lower levels between 8.70 and 0.01 µmol L^{-1} with the only exception in November, 2007, where ammonium spontaneously increased to 37.44 µmol L^{-1} (see discussion).

A similar decreasing trend over time was found in the nitrite concentrations. The mean concentration was 0.76 µmol L^{-1} but varied between 4.43 and 0.20 µmol L^{-1} during the first third of the heltering period. Since December 2006, nitrite never reached concentrations above 1.00 µmol L^{-1}.

For nitrate and phosphate an opposite trend in a typical sawtooth pattern was recorded: Both nutrients increased continuously during the first year of heltering to maximum concentrations of 480.25 and 30.23 µmol L^{-1} respectively. After an exchange of approximately 70 % of the overall process water (Fig. 31, first blue line), nitrate concentration decreased gradually for four months while phosphate decreased strongly for three to four weeks. In the follwing sequel, nitrate concentrations remained constant at about 115 µmol L^{-1} and phosphate increased in a slope similar to the previous one - with a second maximum concentration of 15.87 µmol L^{-1}. After a total power blackout in the climate chamber in October 2007, a complete water exchange (> 95 %; Fig. 31, second blue line) had to be performed. As a result of this the nitrate and phosphate concentrations had been reset to nearby natural values of 26.98 and 1.41 µmol L^{-1}, respectively.

Phase II (Sula Reef samples): March 2008 – March 2009

In the second incubation phase with the Sula Reef samples, nearly constant low concentration levels of the main toxic nutrient compounds - ammonia and nitrite - could be realised (Fig. 32). The average ammonium concentration was 0.13 µmol L^{-1} and the maximum concentration never exceeded values above 0.33 µmol L^{-1}. Similarly low levels were monitored for nitrite, were mean and maximum concentration were 0.15 and 0.22 µmol L^{-1}, respectively.

For the non-degradable nutrients nitrate and phosphate the concentration increased continuously from April to November 2008 to maximum levels of 378.30 µmol L^{-1} NO_3^- and

15.75 µmol L^{-1} PO_4^{3-}. Average concentrations of nitrate and phosphate were 212.51 and 10.62 µmol L^{-1} and relatively low concentrations of 41.99 and 5.23 µmol L^{-1} could be achieved after a water exchange (approx. 70 %) in the first week of December, 2008 (Fig. 32, blue line).

Tab. 6 Descriptive statistics of the nutrient concentrations during the Oslofjord-Incubation (April, 2006 - December, 2007) and Sula-Reef Incubation (March, 2008 - March, 2009). The inconsistency in the sample size n was due to removed outliers. All concentrations in µmol L^{-1}.

Incubation	Nutrient	n	Mean	Median	Minimum	Maximum
Oslofjord	NH_4^+	71	9.92	1.03	0.01	109.12
	NO_2^-	71	0.76	0.38	0	4.43
	NO_3^-	67	189.33	168.53	26.98	480.25
	PO_4^{3-}	67	12.70	12.32	1.41	30.23
Sula Reef	NH_4^+	41	0.13	0.11	0	0.33
	NO_2^-	42	0.15	0.15	0.10	0.22
	NO_3^-	43	212.51	237.26	41.99	378.30
	PO_4^{3-}	43	10.62	10.83	4.72	15.75

Tab. 7 Physicochemical water parameters and nutrient compositions of the ambient seawater samples collected during both RV ALKOR cruises.

	Oslofjord, 2006	Sula Reef, 2008
Temperature (°C)	7.0	7.5
Salinity (PSU)	35.1	35.2
Depth (m)	100	285
Total Alkalinity (µmol kg^{-1})	2286.8	2313.7
DIC (µmol kg^{-1})	2170.0	2149.8
$pH_{free\ scale}$	7.98	8.08
NH_4^+ (µmol L^{-1})	-	0.58
NO_2^- (µmol L^{-1})	0.19	0.05
NO_3^- (µmol L^{-1})	9.40	0.80
PO_4^{3-} (µmol L^{-1})	0.58	0.21

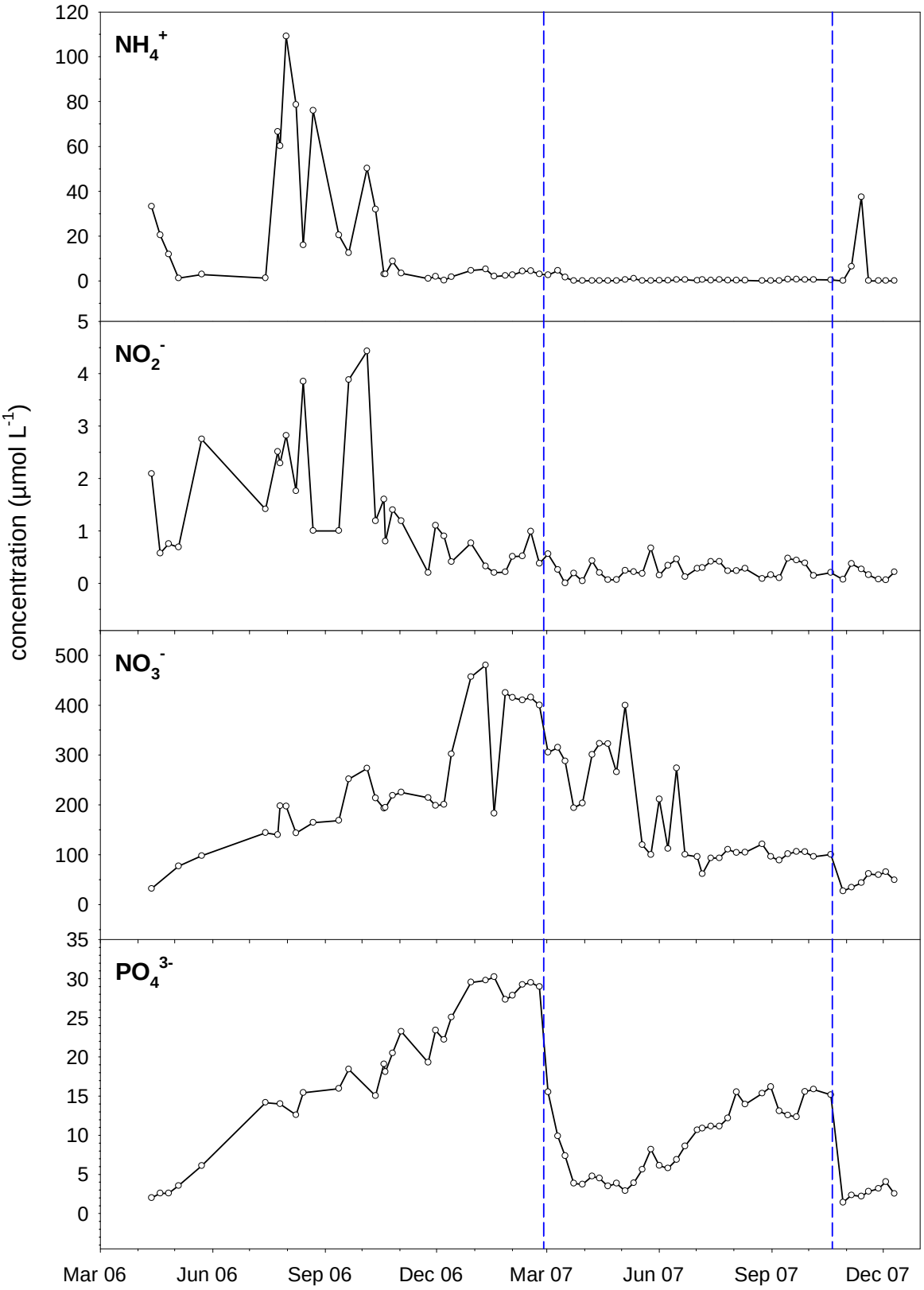

Fig. 31 Overview of the monitored nutrients levels during the cold-water coral incubation phase I (Oslofjord). The blue lines indicating large water exchanges of approximately > 70% of the whole water body.

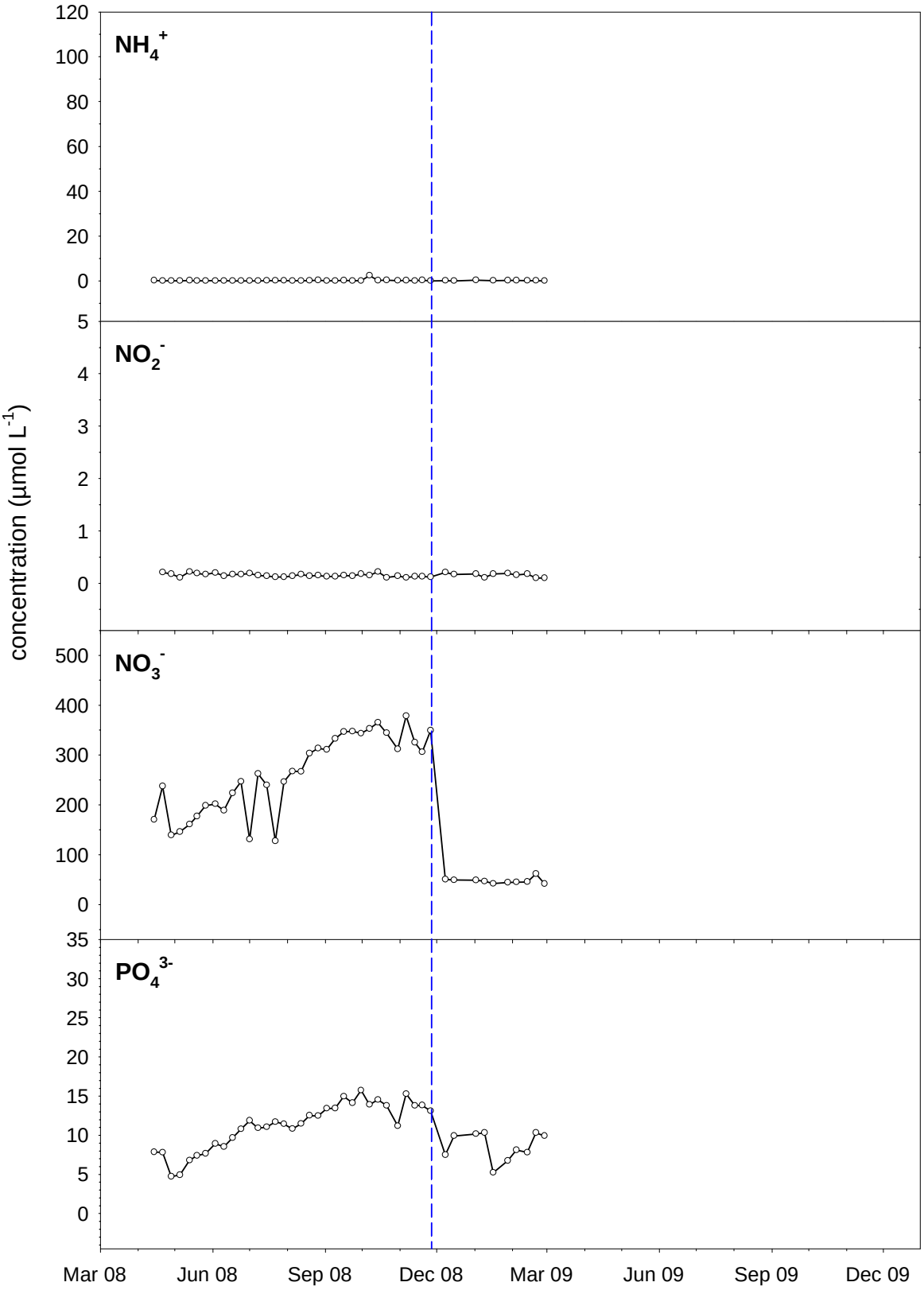

Fig. 32 Overview of the monitored nutrients levels during the cold-water coral incubation phase II (Sula Reef). The blue line indicates a large water exchange of approx. > 70% of the whole water body.

3.1.1.3. Ammonium sensitivity

Due to a leakage in the separating PVC-panel the water bodies of both compartments were mixed after the third day (Fig. A1-1; Appendix A1). However, the water bodies were well separated during the first 57 hours of the experiment and therefore results could still be analysed for this time interval.

The average ammonium concentration in the control tanks during the first 57 hours was 2.48 ± 1.80 µmol L^{-1} while the concentrations in the treatment tanks ranged from 5.53 to 43.20 µmol L^{-1} and reflected the intended concentration increase (with some fluctuations).

Fig. 33 shows the results of the polyp behaviour measurements from both groups (control and NH_4^+-treatment) in a 5 minute resolution (n = 648): The extension stages increased and decreased periodically with a slightly decreasing time trend. In both groups the maximum extension (of the means) was recorded during the first four hours (control: 3.4 hrs; NH_4^+: 4.0 hrs) and the minimum extensions between the 25^{th} and 28^{th} hour (control: 25.5 hrs; NH_4^+: 28.4 hrs). During the first 24 hours, the overall curve shapes suggest a synchronous behaviour pattern between both groups but this pattern seemed to be decoupled during the following 33 hours. Additionally to the decreasing trend in the polyp extensions, the amplitudes of the treatment also decreased in time.

For statistical analyses, the data was grouped in five time intervals of 9.5 hours each (Fig. 34): the median average extension stage of the control and the NH_4^+-treatment during the first 9.5 hours was 2.4 (n = 114) and 2.2 (n = 114) respectively. The median extension stages from of the control samples decreased over the next two intervals to a constant value of 1.6 (intervals IV to VI) whereas the values of the treatment group decreased continuously to 1.2 in the last interval (VI).

There was no significant difference between control and treatment samples in the first interval (Mann-Whitney Rank Sum Test: U = 6052, n = 114, T = 13499, P = 0.365). From the second time interval on, differences between control and treatment groups were highly significant (Tab. A1-2, Appendix A1) suggesting that extension behaviour is strongly related to elevated ammonium concentrations.

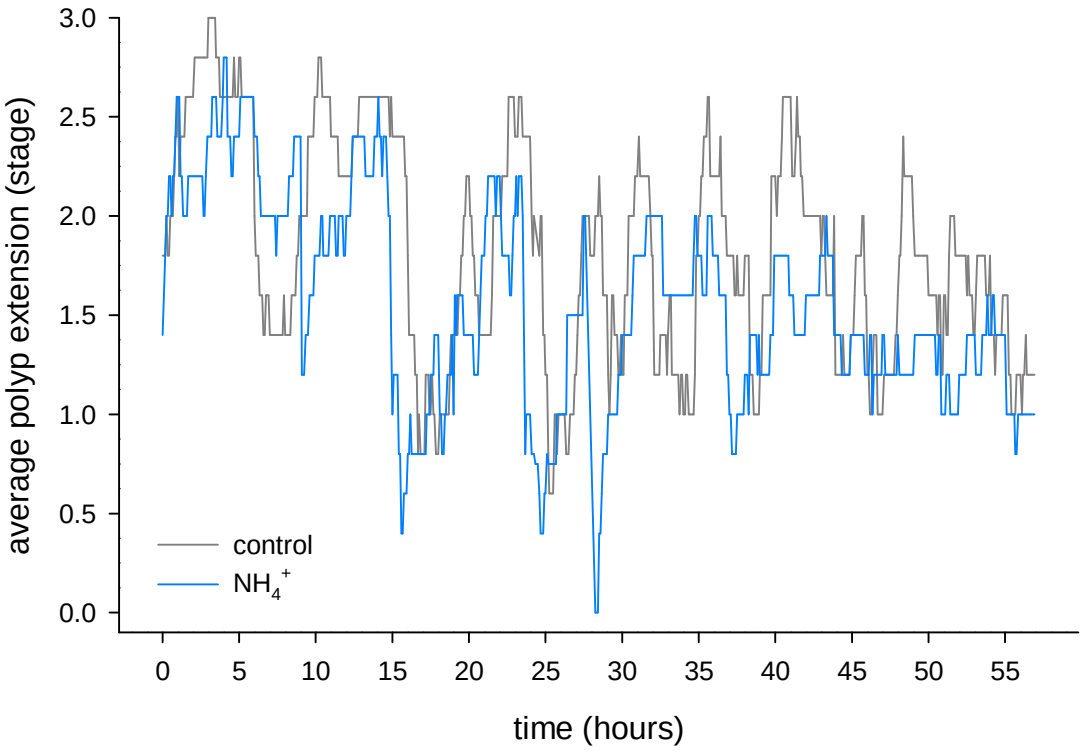

Fig. 33 Average polyp extension stages during the first 57 hours of observation. Dark grey line: polyp behaviour of the control group (constant ammonium concentration), blue line: behaviour of the treatment group (increasing ammonium concentration).

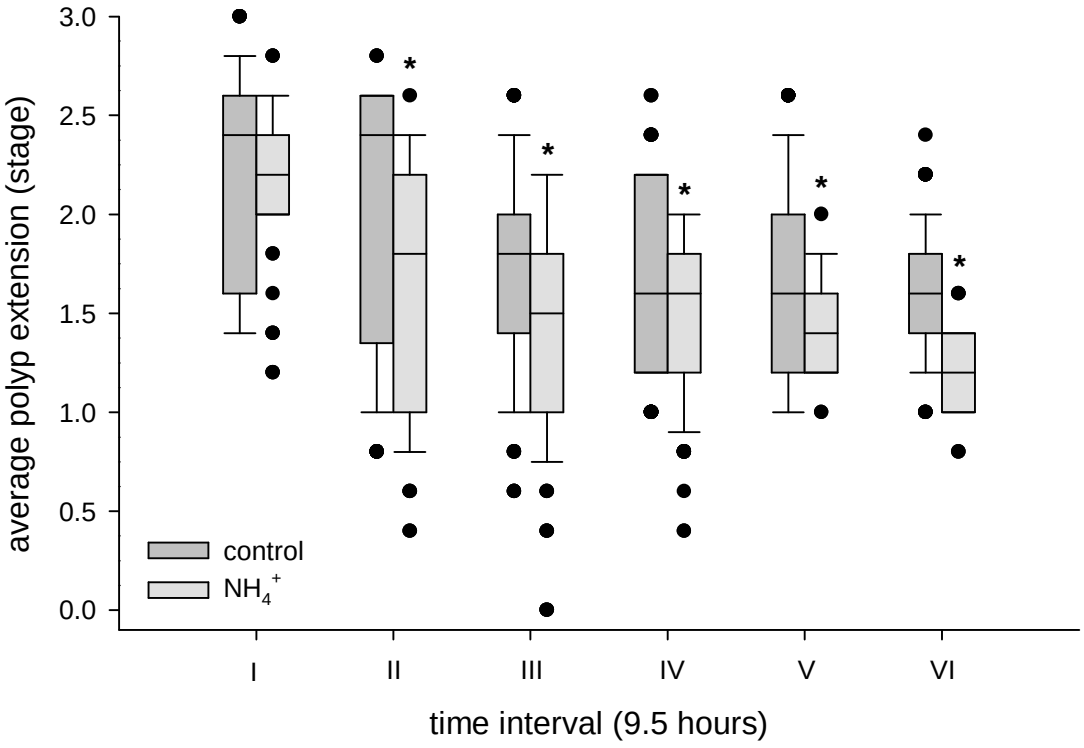

Fig. 34 Box-and-Whisker plots of the average polyp extension stages. Dark grey boxes: control group (constant NH_4^+ concentration), light grey boxes: treatment group (increasing NH_4^+ concentration). Box and whiskers are ± standard errors and standard deviations, respectively. Black dots: outliers. Asterisks indicating statistically significant differences between control and NH_4^+ treatment.

3.1.2. Optimising *Lophelia pertusa* feeding regimes

3.1.2.1. Natural food source experiments

Small mesozooplankton: Copepods (*Acartia tonsa*)

During the treatment with the low food density (0.61 Ind mL^{-1}) roughly one-third of the initial copepods could be recovered after the 24 hrs feeding period. Only 0.2 % of them were alive while 34.2 % were retrieved dead from the bottom of the aquarium. The missing 65.6 % were removed from the water column by the corals (Fig. 35 a). Similar amounts of copepods were consumed by the corals in the high density treatment (2.44 Ind mL^{-1}). The fractions of copepods being alive and dead were 0.2 % and 31.7 %, respectively. 68.2 % were removed from the water column by the corals (Fig. 35 b).

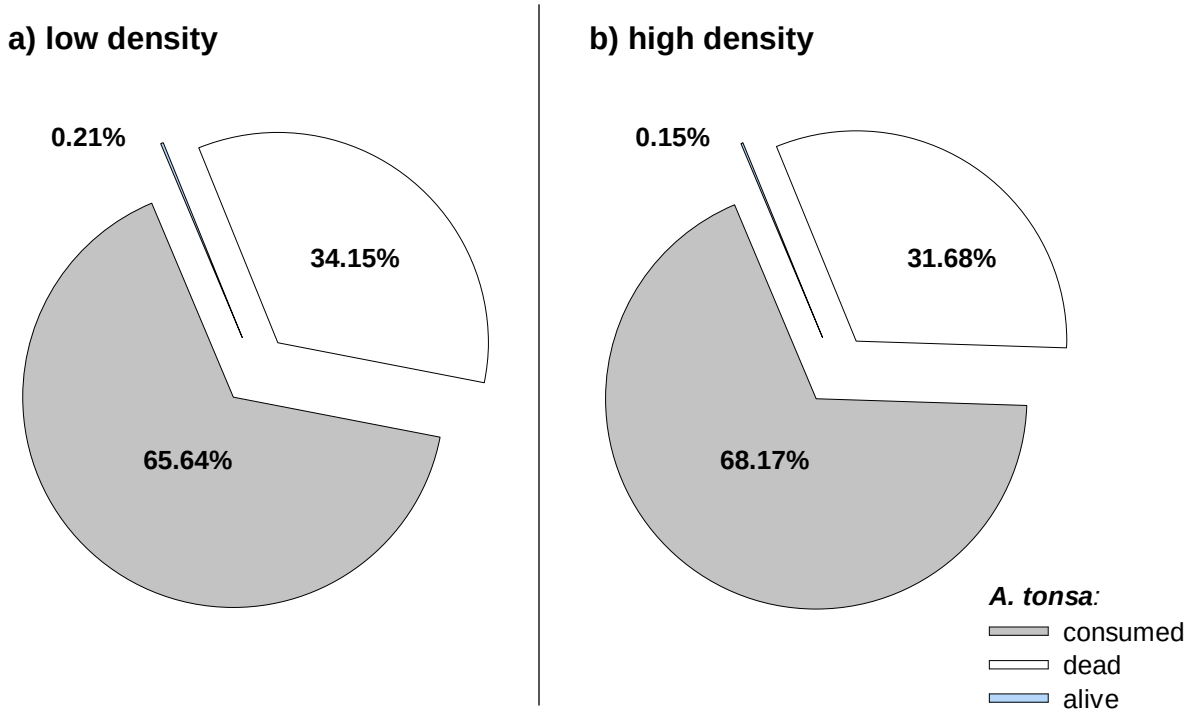

Fig. 35 Fractions of copepods (dead, alive, consumed) after a 24 hours feeding period. Low food density (**a**) was 0.61 Ind mL^{-1} and high food density (**b**) was 2.44 Ind mL^{-1}.

When corals were fed with the low *A. tonsa* density, the average feeding rate was 1.99 ± 0.15 Ind $polyp^{-1}$ h^{-1}, whereas the mean feeding rate under the high copepod density was 6.52 ± 0.52 Ind $polyp^{-1}$ h^{-1} (Fig. 36). Thus the cold-water coral *L. pertusa* feeding rate increased significantly with increasing food density (unpaired t-test: t-value: 14.519, $P < 0.001$).

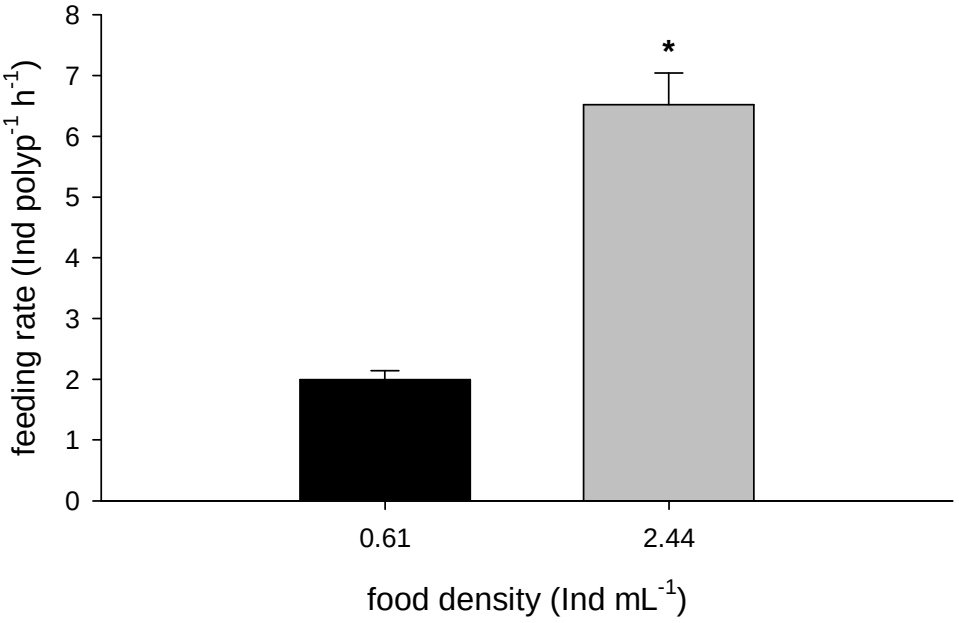

Fig. 36 Feeding rates of cold-water coral *L. pertusa* with low food density (black bar) and high food density (grey bar) of live copepods (*A. tonsa*). The error bars are the standard deviations and the asterisk indicates a statistically significant difference between both treatments (see text for details).

The corals total food uptake for the low copepod density was 47.81 ± 3.53 Ind polyp^{-1} d^{-1}. For the high copepod density, the total food uptake was 156.55 ± 12.48 Ind polyp^{-1} d^{-1}.

Assuming a dry weight of 4.5 ± 0.87 µg for adult female and male *A. tonsa* copepods (Pinho *et al.* 2007), the corals total dry mass uptake for low and high food density was 215.15 ± 47.80 µg polyp^{-1} d^{-1} and 704.47 ± 157.73 µg polyp^{-1} d^{-1}, respectively.

Large mesozooplankton: Opossum shrimps (*Neomysis integer*)

During the whole feeding experiment no direct observation of a successful prey capture was observed. *N. integer* avoided contact with the corals and even when it accidentally collided with the polyps it freed itself with convulsive body movements.

After the 24 hours feeding period most of the opossum shrimps were found dead at the bottom of the aquaria (Fig. 37). Only about 10 % of the initial food density was consumed in each aquarium - except for the treatment with low food density and morphotype II corals. In this treatment, 22 % of the opossum shrimps were removed. There was no significant food uptake due to coral consumption after subtracting the lost shrimps with the losses in their corresponding control groups. Mysidacean survival rates were very low and ranging from 0 (exception) to 14 % (low density, morphotype I corals).

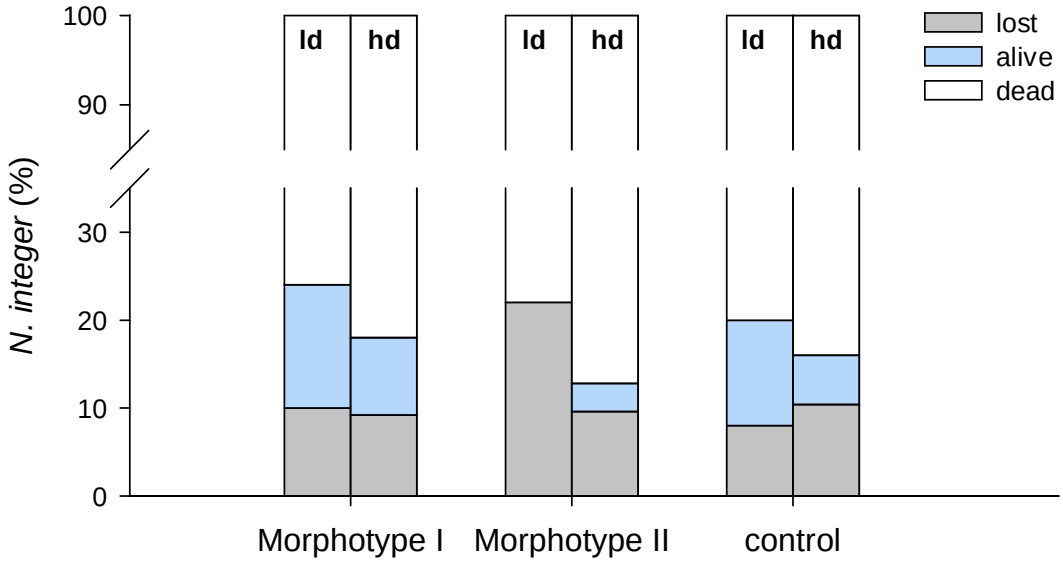

Fig. 37 Distribution of lost, alive, and dead fractions of *N. integer* (hd = high density, ld = low density) found after the feeding experiment with two different morphotypes of *L. pertusa* (morphotype I = thick polyps, morphotype II = thin polyps) and in an empty control group.

Additional observation:

The results from this experiment suggests that *L. pertusa* is neither able to catch nor to hold onto life mysidaceans. However, if dead shrimps were placed manually on the polyp tentacles, total ingestions of opossum shrimps (up to 20 mm in length) was observed.

3.1.2.2. Prey capture and feeding process video observation

Initially, the addition of food caused most of the polyps to perform a sudden total or partial retraction into their calices (Fig. 38 a). After about 4 minutes, the polyps began to expand again and active feeding started (Fig. 38 b).

Fig. 38 Sequence of three typical *L. pertusa* tentacle positions during a pulsed feeding with *Artemia franciscana* nauplii. **a**) initial retraction of whole polyp, **b**) active feeding phase: single tentacles were loaded with food particles which were transferred to the mouth, **c**) passive digestion phase: polyp maximal expanded, no tentacle activity. Photos: from Bach (2007).

The behaviour of the recorded single polyp during the 14 hours of video observation can be divided into three main phases (Fig. 39, I - III). During the first phase the polyp already started feeding even if it was not fully extended. If food particles (*A. franciscana* nauplii) collided with the coral tentacles, most of them (> 90 %) adhered to the tentacle surface (probably due to nematocyst adhesion). Loaded tentacles were sucked into the polyp's oral disc where the food particles were transferred through the pharynx into the gastrovascular cavity. Unloaded tentacles were left expanded as long as they were unaffected. The first phase lasted for about 140 minutes with an average feeding rate of 21.9 Ind polyp^{-1} h^{-1}.

In the second phase (140 - 320 minute) the highest feeding rates were measured: Average and maximum feeding rates for this phase were 40.3 Ind polyp^{-1} h^{-1} and 63 Ind polyp^{-1} h^{-1}, respectively. These high rates were realised by ingestion of whole packages (aggregations) of about 5 and more individuals per single tentacle at the same time. Water current sometimes dislodged these packages revealing the high influence of water currents on *L. pertusa* feeding rates and food supply in general.

In the last phase (320 - 500 minute) the feeding rate decreased to an average and minimum of 20.7 Ind polyp^{-1} h^{-1} and 6 Ind polyp^{-1} h^{-1}, respectively. Because of an extraordinary polyp extension during this phase, the contact rates between prey and polyp were the highest during this phase of the whole experiment. Nevertheless, the tentacles seemed not to be as active in

adhering food particles as they were during the former phases. After about 8 hours the polyp totally stopped feeding. Food particles still collided with the tentacles but were not adhered, or - if so - they were released after a few seconds. For a few hours the polyp was maximally expanded (Fig. 38, c) indicating a higher oxygen demand during the digestion process of the ingested food particles (see discussion).

The total food uptake was 234 Ind polyp^{-1}; thus the average feeding rate per day of this single *L. pertusa* polyp was 9.75 Ind polyp^{-1} h^{-1}.

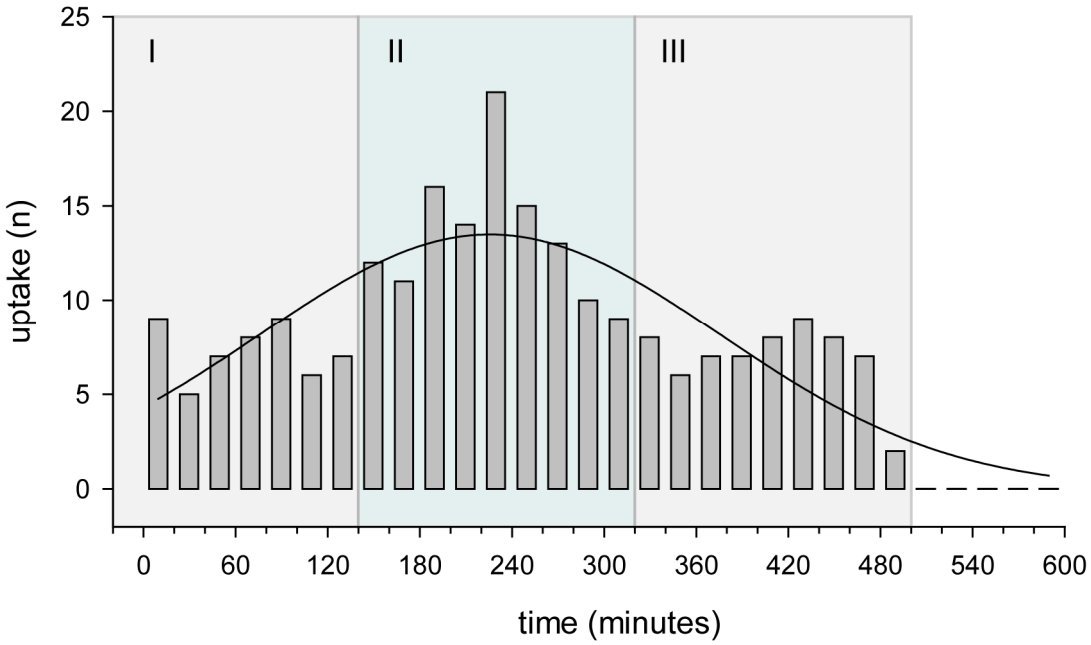

Fig. 39 Direct observation of food uptake of one single *L. pertusa* polyp measured in 20 minute intervals. Uptake quantities can be divided into three phases (I, II, and III) and followed an exponential Gaussian distribution (solid trend line, $R^2 = 0.72$). Active feeding was observed only during the first 500 (of 840) minutes.

Additional observations

In the last phase of the feeding and for several hours afterwards, the fed coral polyps could easily be distinguished from polyps without food uptake by a reddish gleam around the mouth region (Fig. 40). This gleam resulted most likely from the accumulated reddish *Artemia* nauplii in the gastrovascular cavity of the polyp.

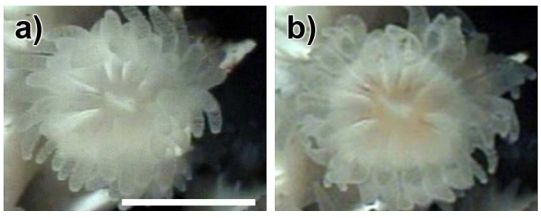

Fig. 40 *L. pertusa* before (**a**) and after feeding (**b**) with *A. franciscana* nauplii. Scale bar = 10 mm. Photos: from Bach (2007).

3.1.2.3. Food quality and uptake rates

Food quality characteristics

Tab. 8 summarises the measured dry weights and energy contents of the three food qualities (FQI - III) used in the feeding experiments. The enriched and eight hour older *A. franciscana* nauplii from FQ II were about 21 % heavier than the newly hatched nauplii of FQI (1.8 ± 0.1 µg Ind^{-1} vs. 2.2 ± 0.3 µg Ind^{-1}, respectively). Relatively similar energy contents (when normalised to dry weights) were found in all three food qualities. Lowest energy content was measured in the enriched *A. franciscana* nauplii (FQII).

Tab. 8 Dry weights and energy contents for three different *Artemia franciscana* food qualities. Mean values, standard deviation (s) and number of measurements (n).

Food quality	dry weight (µg Ind^{-1})			energy content (kJ g^{-1})		
	Mean	s	n	Mean	s	n
I (*A. franciscana* nauplii)	1.8	0.1	13	21.3	0.4	5
II (FQI, enriched)	2.2	0.3	18	18.5	0.4	4
III (adult *A. franciscana*)	236.2	34.0	5	21.7	0.2	4

Food uptake and feeding rates

The food uptake of the cold-water coral *L. pertusa* due to active prey capture was significantly different (paired t-test, $P \leq 0.001$, (Moldzio 2008)) between the life food qualities FQI and FQII (Fig. 41):

The average total food uptake during the 27 hours feeding periods varied for FQI between 70.6 and 141.3 Ind $polyp^{-1}$ or 1.9 and 3.9 Ind mm^{-2} (Tab. 9). This corresponds to the average total dry mass and total energy uptakes of 128.5 - 257.2 µg $polyp^{-1}$ and 2,735.2 – 5,474.3 mJ $polyp^{-1}$, respectively. Average food uptake for FQII was about 51 % higher than for FQI. Minimum and maximum total food uptake were 126.2 and 215.0 Ind $polyp^{-1}$ or 3.5 and 5.9 Ind mm^{-2} respectively. Corresponding average total dry mass uptakes were 278.9 - 475.2 µg $polyp^{-1}$ and total energy uptakes were 5,152.7 – 8,778.4 mJ $polyp^{-1}$.

FQIII was manually given to the corals after determining the average dry mass uptake of FQI (2.1.4.4) and therefore exhibited relatively similar dimensions regarding average total dry mass uptake (Fig. 41) or average total energy uptake (Tab. 9).

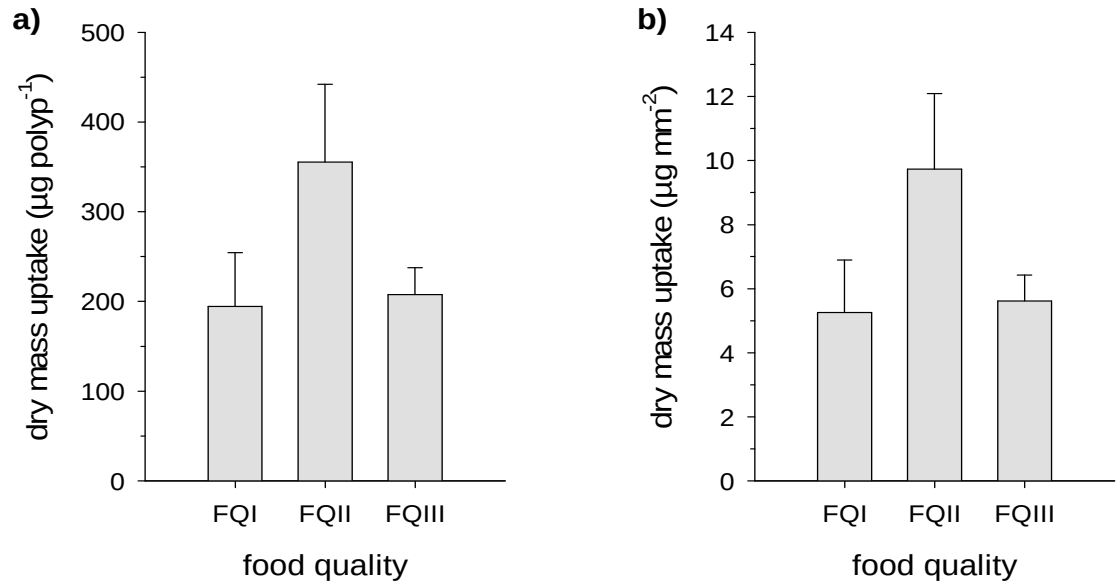

Fig. 41 Average total dry mass uptakes of *L. pertusa* during 27 hours feeding periods with two different *A. franciscana* nauplii food qualities (FQI and FQII) and adult *A. franciscana* (FQIII). Dry mass uptake was normalised to polyp number (**a**) and polyp surface area (**b**). Error bars are standard deviations.

The average *L. pertusa* feeding rate at the given food density of 0.8 Ind mL^{-1} for FQI and FQII amounted to 3.96 ± 1.22 Ind $polyp^{-1}$ h^{-1} and 5.96 ± 1.45 Ind $polyp^{-1}$ h^{-1}, respectively (Fig. 42).

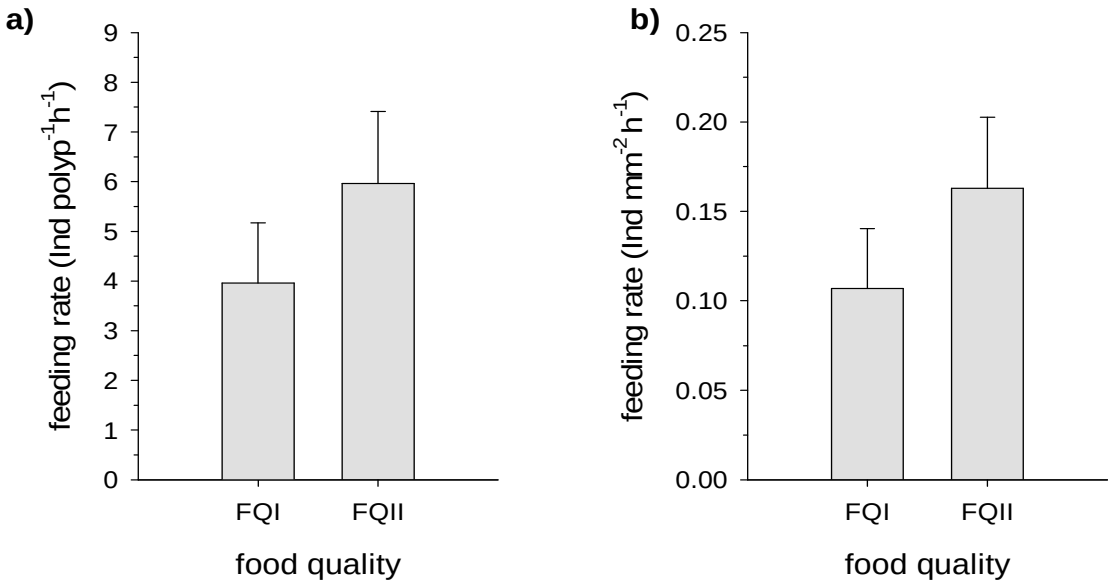

Fig. 42 *L. pertusa* feeding rates of two different *A. franciscana* nauplii food qualities (FQI and FQII) normalised to polyp number (**a**) and polyp surface area (**b**). Error bars are standard deviations.

Tab. 9 Average food uptake estimations from three different *Artemia franciscana* food qualities (I - III) normalised to polyp number and polyp surface area (as described in Moldzio (2008)). Mean, minimum and maximum values and standard deviations (s) were calculated in triplicates from five feeding intervals for each food quality. Food uptakes for food quality I and II (live *A. franciscana* nauplii) were due to active prey capturing of the coral polyps whereas food quality III (adult frozen *A. franciscana*) was manually given to the corals.

	Mean	s	Minimum	Maximum
Normalised to polyp				
Food Quality I				
total food uptake (Ind polyp^{-1})	106.8	32.9	70.6	141.3
total dry mass uptake (µg polyp^{-1})	194.4	59.8	128.5	257.2
total energy uptake (mJ polyp^{-1})	4138.8	1273.1	2735.2	5474.3
Food Quality II				
total food uptake (Ind polyp^{-1})	160.9	39.1	126.2	215.0
total dry mass uptake (µg polyp^{-1})	355.6	86.5	278.9	475.2
total energy uptake (mJ polyp^{-1})	6569.5	1597.7	5152.7	8778.4
Food Quality III				
total dry mass uptake (µg polyp^{-1})	207.9	29.9	180.9	247.9
total energy uptake (mJ polyp^{-1})	4499.2	646.7	3914.5	5364.3
Normalised to surface area				
Food Quality I				
total food uptake (Ind mm^{-2})	2.9	0.9	1.9	3.9
total dry mass uptake (µg mm^{-2})	5.3	1.6	3.5	7.1
total energy uptake (mJ mm^{-2})	112.0	34.9	73.6	151.1
Food Quality II				
total food uptake (Ind mm^{-2})	4.4	1.1	3.5	5.9
total dry mass uptake (µg mm^{-2})	9.7	2.4	7.7	13.0
total energy uptake (mJ mm^{-2})	179.7	43.7	142.9	240.9
Food Quality III				
total dry mass uptake (µg mm^{-2})	5.6	0.8	5.2	6.0
total energy uptake (mJ mm^{-2})	121.6	17.5	111.6	129.7

By analysing the different fractions of food particles (alive, dead, dying, eggs, and hatching nauplii) from the remains after the 27 hour feeding period relatively similar quantities of dead *A. franciscana* nauplii were found for FQI and FQII. However, by comparing the amounts of dead and dying nauplii of the FQI with results from the blank feeding tests (2.1.4.4) significantly higher quantities of remains were found in the coral tanks (Lord's test, $P < 0.01$). For FQII no significant differences were found between treatments with or without corals. These results suggest that the enriched, larger and older nauplii of FQII were more easily caught by the corals than the agile nauplii of the FQI tests.

For in-depth analysis of the different food fractions, *A. franciscana* nauplii mortality rates, and their statistical evaluations, the reader is referred to Moldzio (2008).

Growth measurements

Growth rates slightly decreased from treatment to treatment (Fig. 43). However, this was not statistically significant, regardless whether normalised against polyp number or polyp surface area (Appendix A2).

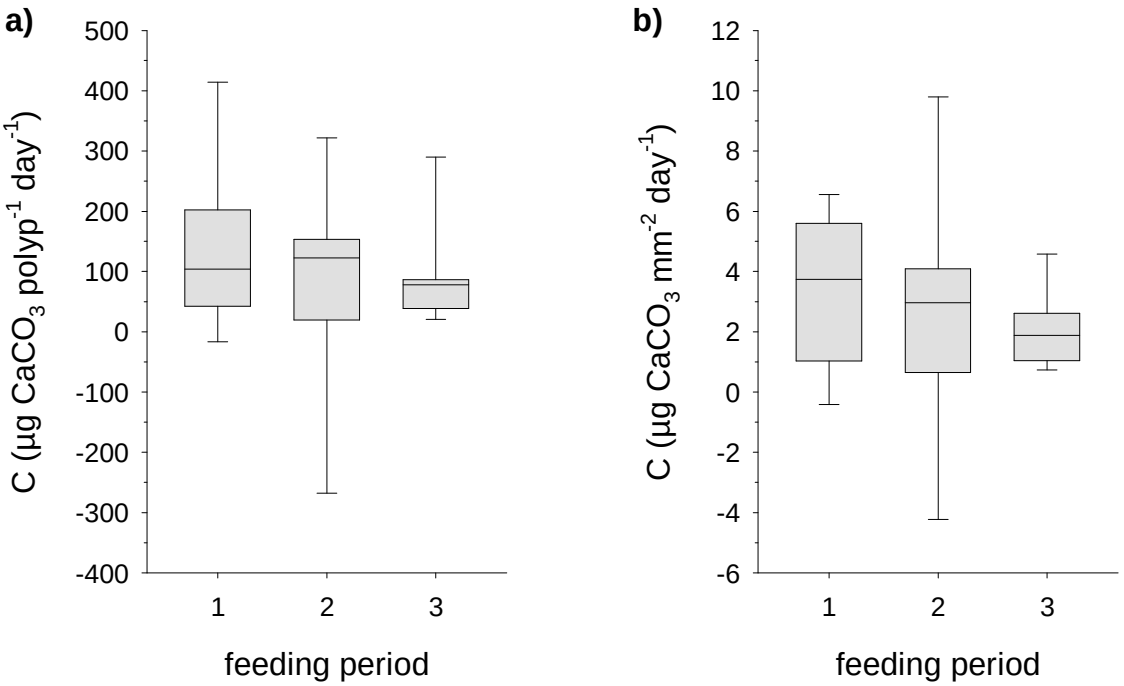

Fig. 43 Growth rates (C) during the three feeding periods (food qualities) normalised to polyp number (**a**) and polyp surface area (**b**). Box and whiskers are ± standard errors and standard deviations, respectively.

The median and mean growth rates for the three feeding periods and the two normalisation modes are given in Tab. 10. Negative growth rates were measured on two coral branches indicating a measurement error during the weighings or an accidental material loss during the general handling of the corals.

The maximum growth rate amounted to 414.4 µg $CaCO_3$ $polyp^{-1}$ day^{-1} (6.6 µg $CaCO_3$ mm^{-2} day^{-1}) whereas the average growth rate was 103.5 ± 125.0 µg $CaCO_3$ $polyp^{-1}$ day^{-1} (2.7 ± 2.6 µg $CaCO_3$ mm^{-2} day^{-1}). The high standard deviations reflect the high variability of the growth rates between the coral samples as well as the relatively small sample size.

Tab. 10 Median and mean growth rates (C) with standard deviations (s) measured at the end of each of the three experimental time periods (food qualities) and normalised against polyp number and polyp surface area (as described in Moldzio (2008)).

feeding period	C (µg $CaCO_3$ $polyp^{-1}$ day^{-1})			C (µg $CaCO_3$ mm^{-2} day^{-1})		
	Median	Mean	s	Median	Mean	s
1 (35 days)	104.1	140.9	129.5	3.7	3.4	2.5
2 (46 days)	122.8	82.5	159.1	3.0	2.6	3.7
3 (35 days)	77.6	87.1	79.6	1.9	2.0	1.2

The total carbonate production during the 116 day lasting experiment was 3.29 g resulting in a total relative calcification rate of 1.16×10^{-2} % day^{-1} (normalised as a percentage of the initial weight, see 2.2.1.3.1).

3.1.3. Basic morphometry and ambient calcification rates

The following chapter summarises measurements performed within the framework of the regulary coral growth measurements using the buoyancy weight technique (2.2.1.1) during the long-term incubations in the CWC-MS.

3.1.3.1. *L. pertusa* aragonite skeleton density and biomass

Measured *Lophelia pertusa* skeleton densities ranged from 2.746 to 2.780 g cm^{-3} with a mean density of 2.772 ± 0.011 g cm^{-3}. Corresponding fractions of the biomass buoyant weights (polyp tissue, mucus, associated epi- and endobionts) varied between 0.62 and 1.55 % from the total skeleton buoyancy weight (TBW) with an average of 0.88 ± 0.31 % TBW.

3.1.3.2. *L. pertusa s*keleton length-weight relationships

For characterising the basic morphometry - and in order to determine possible substitutions for subsequent weight measurements - the calyx lengths, diameters, and weights of 342 isolated *L. pertusa* calices were measured (2.2.1.3.2.). Results from descriptive statistics were summarised in Tab. 11:

Tab. 11 Descriptive statistics from 342 morphometric (calyx lengths and diameters) and gravimetric (weights) measurements on mechanically isolated single calices of *L. pertusa*.

	Mean	Median	Min	Max	25%	75%
Calyx diameter (mm)	5.8	5.6	3.0	10.3	4.7	6.7
Calyx length (mm)	13.8	13.2	5.5	28.9	10.6	16.6
Calyx weight (mg)	389	273	31	1997	153	506

Regression analysis

The relationship between calyx length and calyx weight is best described by a power regression equation with 2 parameters (Fig. 44). The coefficient of determination (R^2) of 0.72 indicates a good correlation with only 28% of uncertainties in the variation. Surprisingly, with a R^2 of 0.81 the calyx weight was better described by calyx diameter than calyx length (Fig. 45). But on closer inspection, an explanation for this is obvious: Due to the high variability of *L. pertusa* calices morphology (even within the same branch) a long calyx can be - for example - thin and lightweight with a small diameter or contrastively, very massive and heavy with a large diameter. However, a large diameter always needs - for geometrical reasons - more “material” than a small one. Finally, long and thick *L. pertusa* calices with small

diameters are unusual and a typical indication for a parasite infestation with bioeroding sponges (Beuck *et al.* 2007). If both parameters - calyx length and calyx diameter - are combined to a cylindrical surface area (Fig. 46) or volume based model, R^2 can be further increased up to nearly 10 %. In the latter case, calyx weight was even better described by a linear regression equation (Fig. 47).

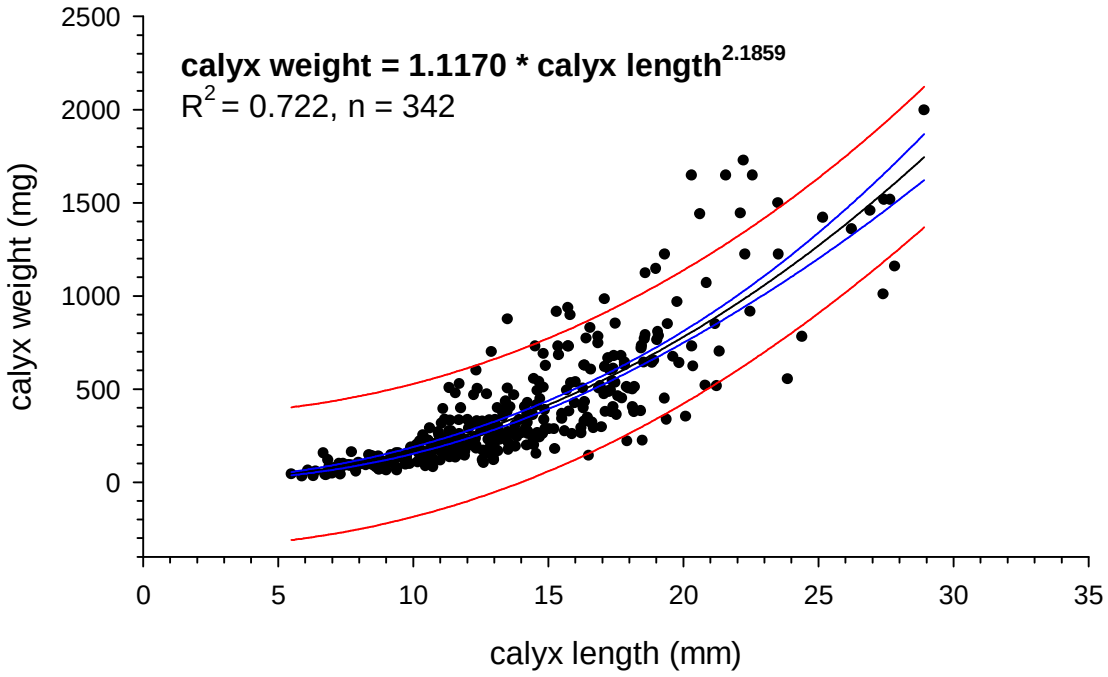

Fig. 44 Relationship between coral calyx length (x-axis) and weight (y-axis) measured on 342 *L. pertusa* calices (n). Coefficient of determination (R^2) was given for the computed power regression equation (equation and black line). 95 % confidence interval (between blue lines) and 95 prediction interval (between red lines).

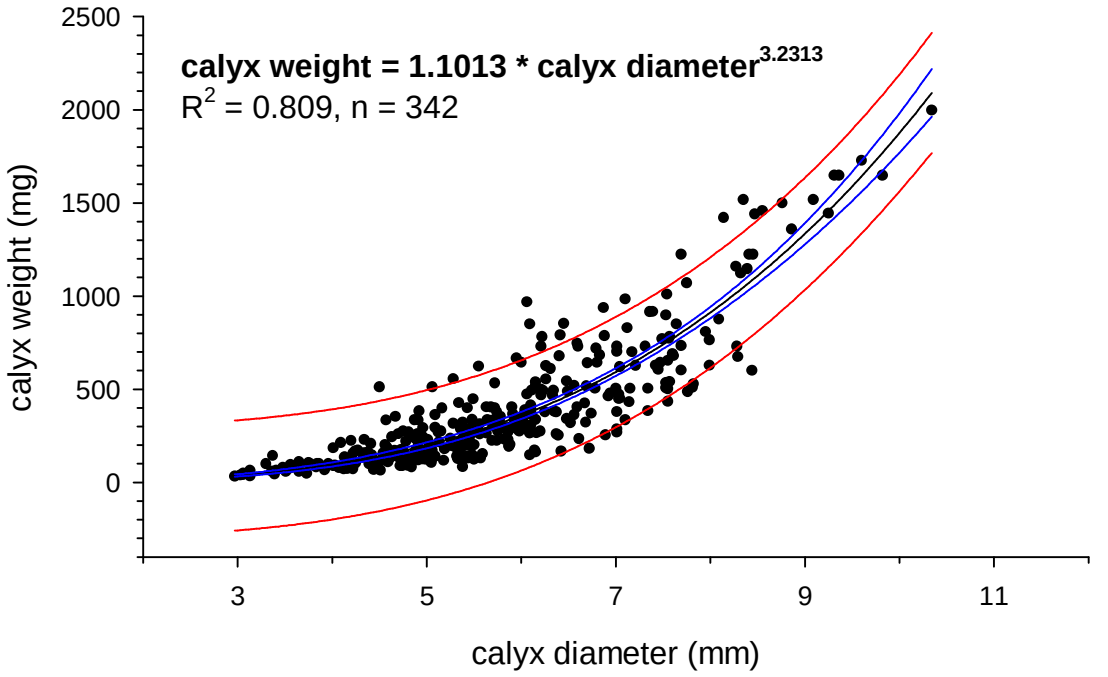

Fig. 45 Relationship between coral calyx diameter (x-axis) and weight (y-axis) measured on 342 *L. pertusa* calices (n). Coefficient of determination (R^2) was given for the computed power regression equation (equation and black line). 95 % confidence interval (between blue lines) and 95 prediction interval (between red lines).

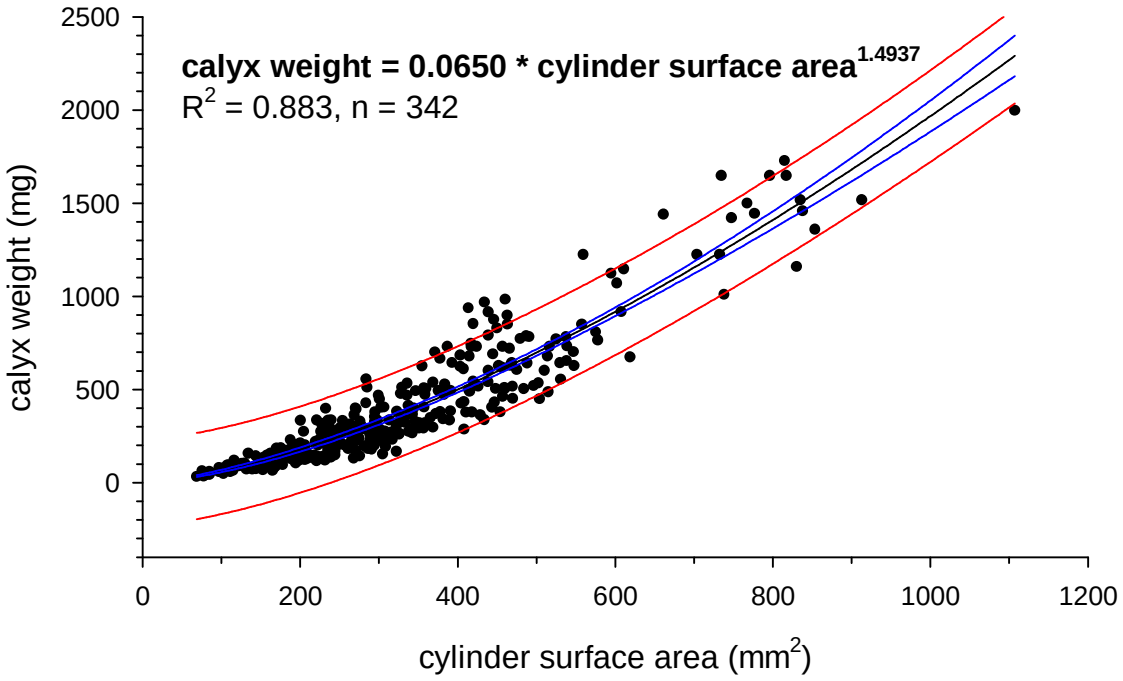

Fig. 46 Relationship between an idealised cylinder surface area (x-axis) and weight (y-axis) measured on 342 *L. pertusa* calices (n). Coefficient of determination (R^2) was given for the computed power regression equation (equation and black line). 95 % confidence interval (between blue lines) and 95 prediction interval (between red lines).

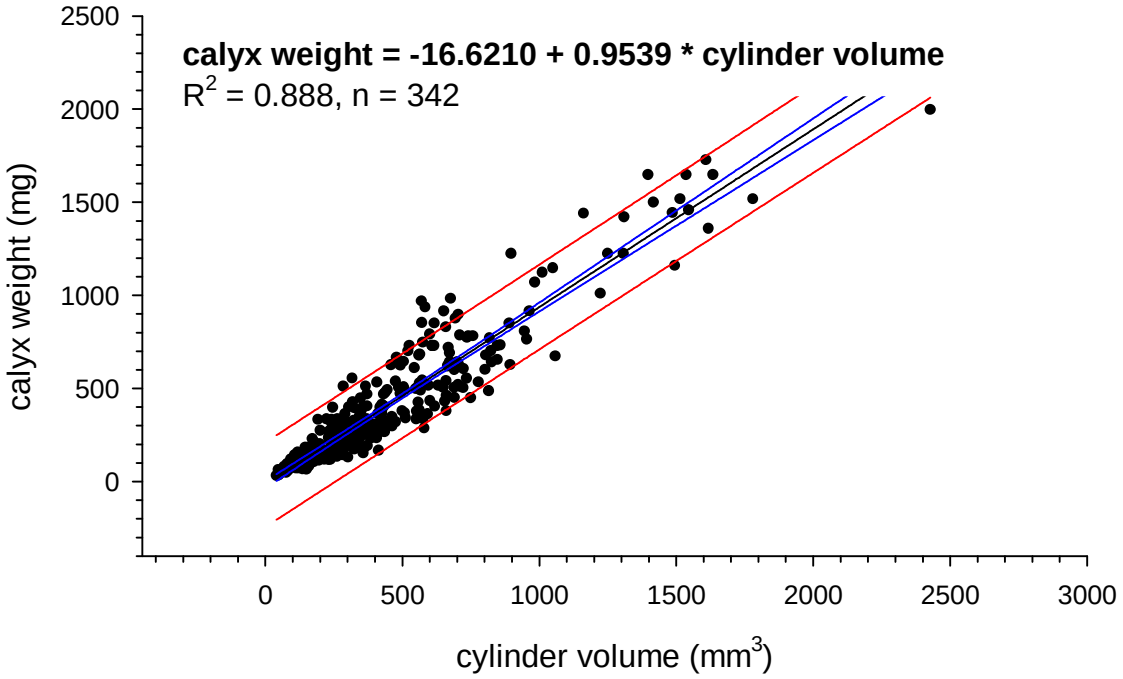

Fig. 47 Relationship between an idealised cylinder volume (x-axis) and weight (y-axis) measured on 342 *L. pertusa* calices (n). Coefficient of determination (R^2) was given for the computed linear regression equation (equation and black line). 95 % confidence interval (between blue lines) and 95 prediction interval (between red lines).

3.1.3.3. *L. pertusa* calcification rates (time series 2006-2008)

In January 2007 - after two months of acclimatisation to the CWC-MS - 34 coral branches from the Oslofjord samples with different weights and polyp numbers were buoyancy weighed for their initial skeleton weights (t_0). One month later ($t_{0+28days}$) and again after further 83 days ($t_{0+111days}$) they were reweighed in order to calculate their basic calcification rates (also referred to as bulk calcification). The whole dataset integrates over 1,850 live polyps with a total skeleton dry weight of 1,129 g. The average growth rate amounted to 57.3 ± 74.3 µg $CaCO_3$ $polyp^{-1}$ day^{-1} but the maximum growth rate was ca. 7.4 times higher (425.2 µg $CaCO_3$ $polyp^{-1}$ day^{-1}) revealing the high variation between the samples. Negative growth occurred in only 3 large and fragile branches and was attributed to a loss of skeleton "material" during the handling procedures. On a percentage basis (normalised to initial weight) growth rates range from -2.4×10^{-3} % day^{-1} to 7.1×10^{-2} % day^{-1} with an average of $8.7 \pm 11.7 \times 10^{-3}$ % day^{-1} (Tab. 12).

Tab. 12 Descriptive statistics and growth rates of 34 *L. pertusa* branches grown under unmanipulated conditions in the CWC-MS.

	Median	Mean	s	Max	Min
Dry weight (g $branch^{-1}$)	31.7	33.4	10.7	58.0	19.5
Polyps (n $branch^{-1}$)	53.0	54.4	18.9	109	28
C (µg $CaCO_3$ $polyp^{-1}$ day^{-1})	43.6	**57.3**	74.3	425.2	-14.1
C (% day^{-1})	7.2E-03	**8.7E-03**	1.2E-02	7.1E-02	-2.4E-03

While most of the corals were needed for subsequent experiments 10 of the 34 branches remained in the CWC-MS and were only disturbed for two repeated buoyancy weight measurement in September 2007 and February 2008. This way a nearby annual circle ($t_{0+28days}$, $t_{0+111days}$, $t_{0+240days}$, and $t_{0+384days}$) could be realised (Fig. 48).

The average annual growth rate exhibited was 25.1 ± 22.0 µg $CaCO_3$ $polyp^{-1}$ day^{-1} or 4.8 ± 3.4×10^{-3} % day^{-1}. For both kind of normalisations, the rates were about half of those from the originating 34 coral branches. An explanation for this could be found by looking into the dataset, more precisely into the individual calcification rates of each branch during the first collective buoyancy weight measurements: Calcification rates for the 10 branches were lacking in extraordinary high rates (G_{max}: 99.9 µg $CaCO_3$ $polyp^{-1}$ day^{-1} / 1.1×10^{-2} % day^{-1}) and seemed to be more homogenous. Growth in winter months tended to be lower than during

the summer but due to the high variation there was no statistical significance between the different time intervals (ANOVA on ranks, see Appendix A3).

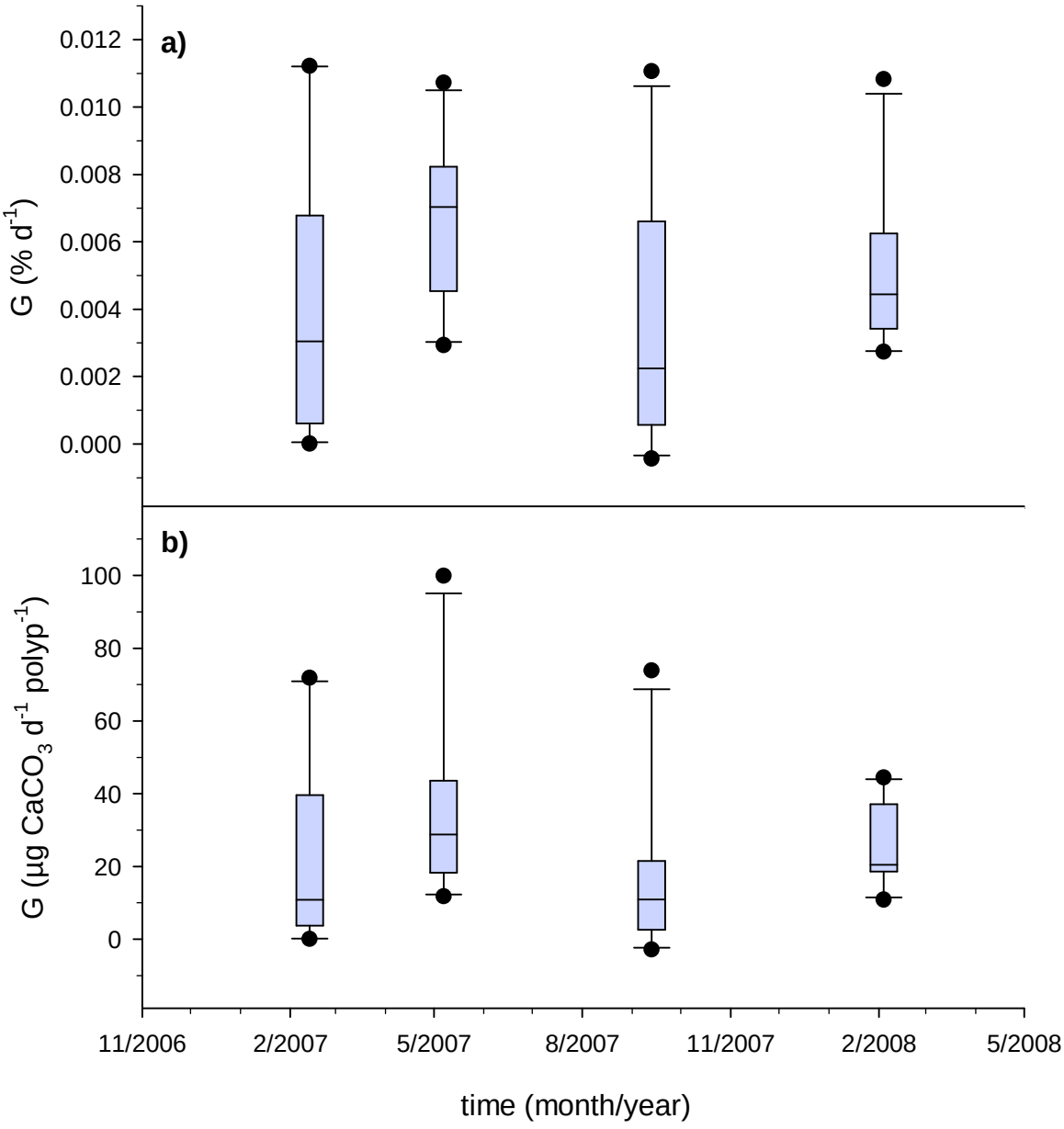

Fig. 48 Calcification rates (G) of 10 *L. pertusa* branches measured with buoyancy weight technique during unmanipulated long-term incubation between November 2006 and February 2008. **a**) normalised to percentage surplus growth to initial weight per day, **b**) normalised to surplus growth in µg per polyp and day. Box and whiskers are ± standard errors and standard deviations, respectively. Black dots: outliers.

3.1.4. Continuous optodic-based respiration measurements

3.1.4.1. System reproducibility test measurements

General observations

After 28 hours the water bath reached its target temperature (Fig. 49 a). Discrepancy between intended and achieved value was only 0.1 °C and subsequent temperature fluctuations were less than 0.1 °C (out of the scope of the temperature measurement device, ≤ 0.1 °C). Remarkably the initial temperature shift of only 0.4 °C was sufficient to decrease the measured phase angles for the oxygen and pH sensor spots significantly (Fig. 49). This emphasises the necessity for extremely constant temperature conditions in order to avoid an overlaying noise. In the continuation of the experiment a constant decreasing drift in both sensor spot types (O_2/pH) was measured. For the oxygen and pH sensor spots the average drift rate was $-5.14 \pm 0.62 \times 10^{-3}$ ° h^{-1} (n = 5) and $-4.27 \pm 3.03 \times 10^{-3}$ ° h^{-1} (n = 5) respectively. Because of the non-linear relationship between phase angles and corresponding pH values (2.2.4.1), future corrections for pH drift have to be performed on the measured raw data for the different phase angles. Theoretically all sensor spots of the same type should reflect a measurement of the same sample (like it was the case here) with "identical" phase angles because of their cloned origin (same sensor foil/batch). In practice, measured phase angles were phase shifted (max. 1°) which was attributed to methodical reasons (e.g. relatively long fibre-optic wires, differences in the layer thickness of the implanted sensor-spot carrying slides). Thus the phase shift of each sensor spot had to be corrected by trimming it to the phases from the initially calibrated sensor spot. Note: a phase shift correction is not necessary if only relative developments or changes are of interest!

Reproducibility

Reproducibility (precision) for oxygen and pH sensor spot measurement in the experimental set-up (system reproducibility) was calculated from the averaged standard deviations of the respective sensor spots (n = 5 for each sensor type) after performing an individual correction for drift and phase angle shifts (baseline trimming):

- Oxygen sensor spot reproducibility was $3.86 \pm 0.4.8 \times 10^{-2}$ ° or 0.13 ± 0.02 %
- pH sensor spot reproducibility was 0.22 ± 0.03 ° or 1.17 ± 0.16 %

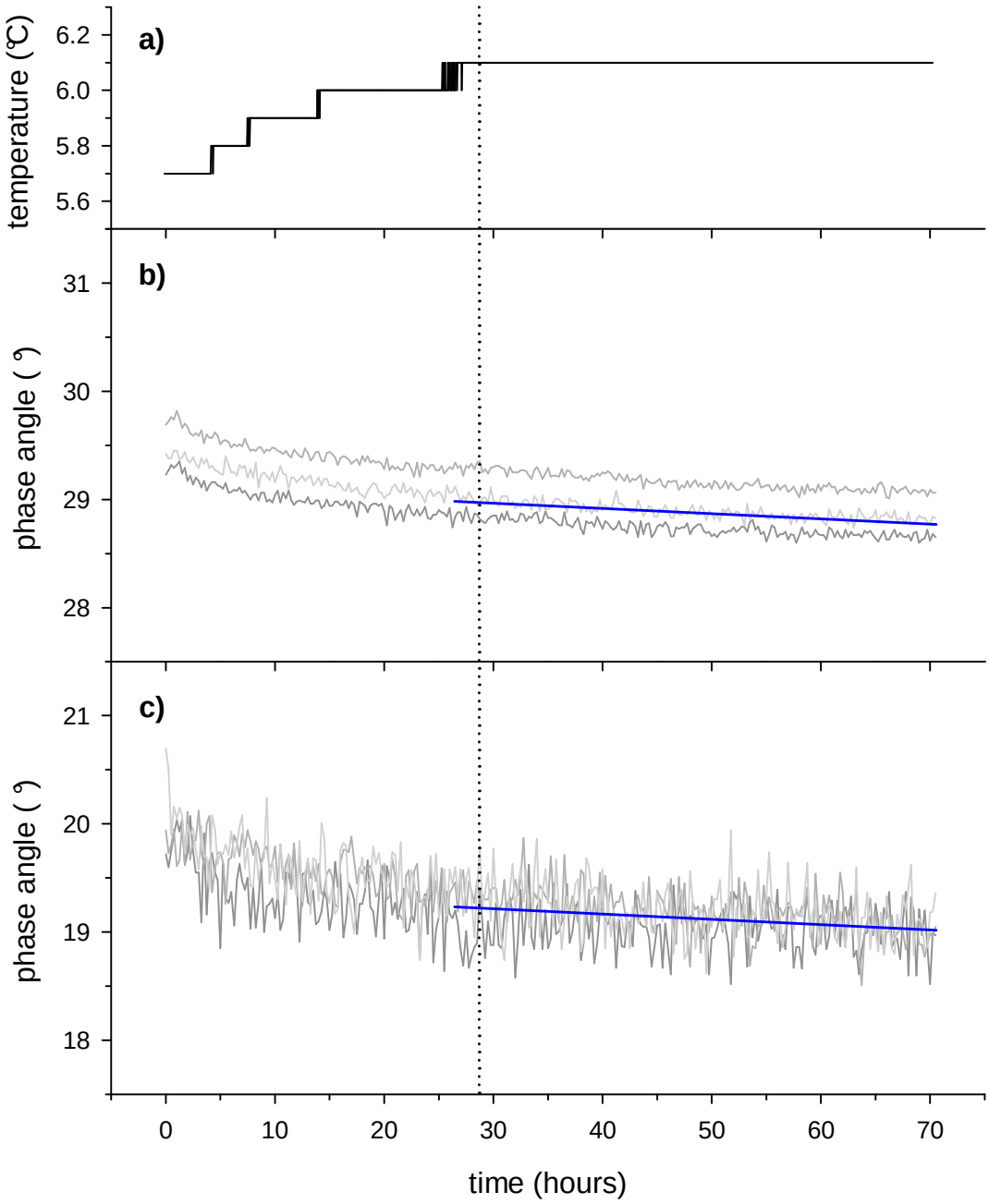

Fig. 49 Phase angles of optodic sensor spots for oxygen (**b**) and pH (**c**) mounted in respiration chambers and submerged in an air-saturated water bath (see text for details). Temperature was set to 6.0 °C but initial temperature of the water bath was 5.7 °C (**a**). For reasons of clarity, only three representative channels of each sensor type were plotted. Blue lines: linear decreasing trend (drift) in sensor spot phase angles after stabilisation of temperature (vertical dotted line).

3.1.4.2. *L. pertusa* holobiont respiration at ambient and elevated temperature

At ambient conditions of 7.5 °C an approximately linear decrease of the available oxygen was measured for the whole measurement period of 24 hours (Fig. 50). At an elevated temperature of 11 °C, the decrease / slope was about 58 % higher than under ambient temperature but also approximately constant during the first 12 hours. In three of the four *L. pertusa* replicates at 11 °C, oxygen consumption slightly increased hyperbolically after oxygen concentrations depleted to less than ~ 190 µmol L^{-1} (~ 70 % O_2 saturation) indicating this concentration a "critical" pO_2 level below a constant oxygen consumption rate could not be maintained. At 7.5 °C no "critical" oxygen concentrations were reached during the 24 hours measurement phase.

Oxygen consumption rates (MO_2) under normoxic conditions at 7.5 °C varied between 0.21 and 0.34 µmol g^{-1} h^{-1} with an average of 0.30 ± 0.06 µmol g^{-1} h^{-1}. At 11 °C measured maximum and minimum MO_2 were 0.55 and 0.34 µmol g^{-1} h^{-1}, respectively. The average oxygen consumption rate at 11 °C was 0.47 ± 0.09 µmol g^{-1} h^{-1} and was significantly higher (paired t-test , $P \leq 0.01$) than for ambient conditions (Fig. 51, Tab. 13).

Tab. 13 Overview of oxygen consumption rates of *L. pertusa* measured at ambient (T = 7.5 °C) and elevated temperatures (T = 11 °C) and normalised to skeleton dry weight (g^{-1} h^{-1}), polyp number ($polyp^{-1}$ h^{-1}) and modelled cylinder volume (cm^{-3} h^{-1}). Comparative statistics between both temperatures was performed with a paired t-test after verifying the data for normal distribution.

MO_2 (Oxygen consumption)	Temp. (°C)	Mean	s	t	P
µmol g^{-1} h^{-1}	7.5	0.30	0.06	-7.802	0.004
	11	0.47	0.09		
µmol $polyp^{-1}$ h^{-1}	7.5	0.29	0.11	-6.431	0.008
	11	0.45	0.15		
µmol cm^{-3} h^{-1}	7.5	0.97	0.25	-5.384	0.013
	11	1.54	0.44		

The average Q_{10} value according van't Hoff (2.2.4.4.2) was 3.65 ± 0.69.

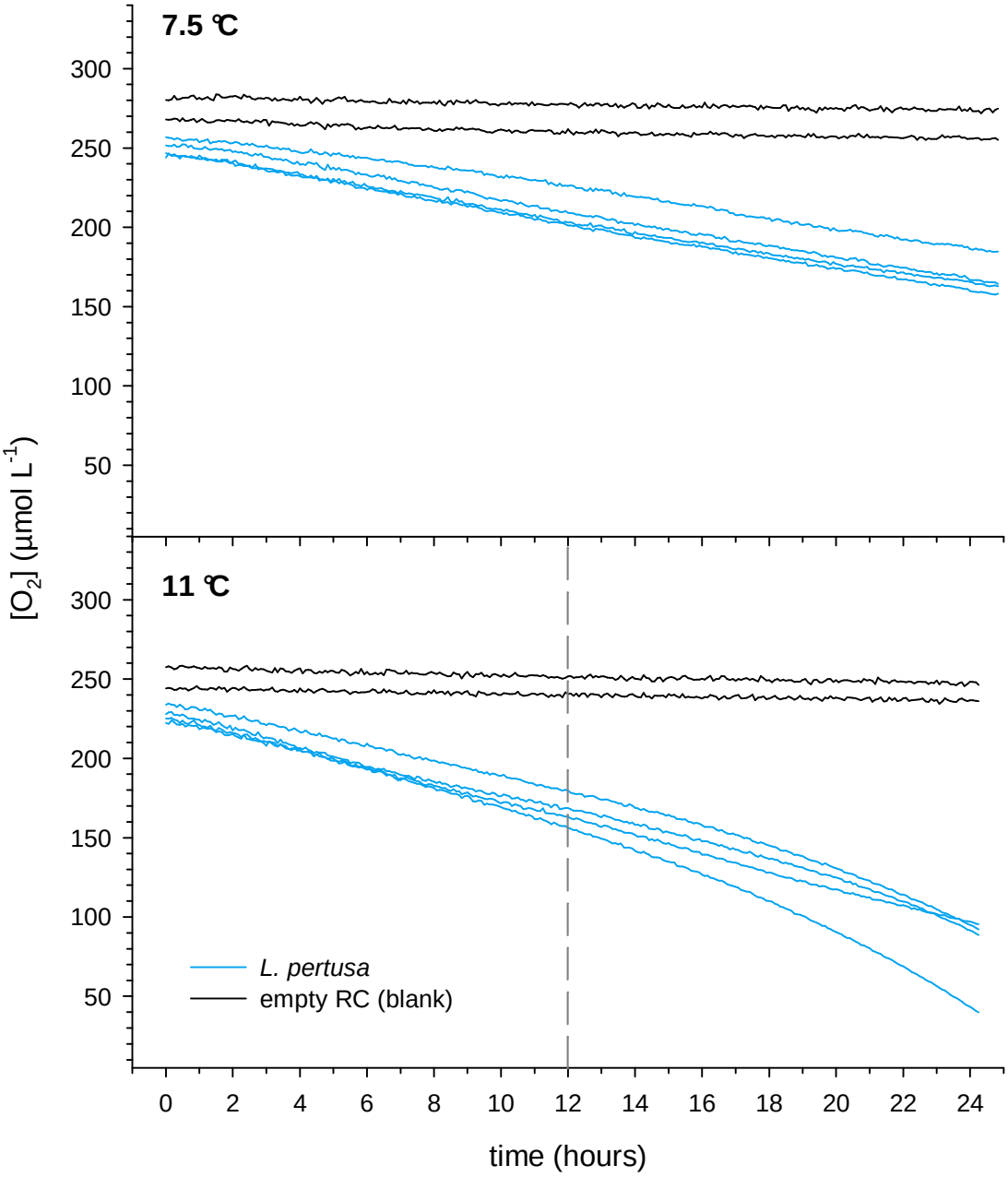

Fig. 50 Four *L. pertusa* samples (blue lines) during 24 hour respiration measurements at ambient and elevated temperatures of 7.5 °C and 11 C°, respectively. For calculation of oxygen consumption rates at 11 °C only the first 12 hours were used (normoxic conditions, linear maintenance of respiratory independence from pO_2). In both phases initial oxygen concentrations were saturated (~ 105 %). The two empty RC (blanks) were used for corrections (bacterial background respiration).

The average microbial background respiration in the two empty RC for 7.5 and 11 °C amounted to 0.41 ± 0.10 and 0.44 ± 0.11 µmol O_2 L^{-1} h^{-1}, respectively.

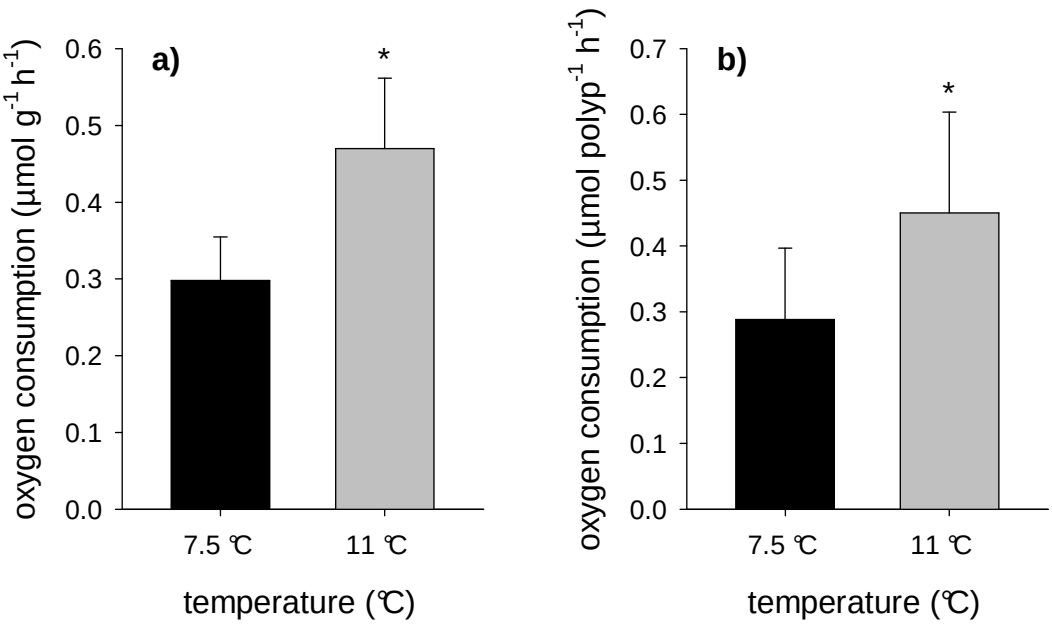

Fig. 51 Average oxygen consumption rates (± standard deviations) for 4 samples of *L. pertusa* measured at ambient and elevated temperature of 7.5 and 11 °C, respectively. Oxygen consumption was normalised to skeleton dry weight (**a**) and polyp number (**b**). The asterisk indicates a statistically significant difference between both treatments.

3.2. Environmental change related experiments

As a result of the rise in anthropogenic CO_2 emissions ocean temperatures and the carbonate system have begun to alter (see introduction, 1.2.2). In the following section results of experiments focused on environmental change related issues are reported. An overview of the performed experiments and their applied methods can be found summarised in Tab. 4 (p. 76).

3.2.1. *L. pertusa* temperature stress response

In the temperature stress response experiment the RNA/DNA ratios, respiration and coral polyp behaviour was studied under ambient (8 °C, T), moderately elevated (11 °C, $T_{+3\,°C}$), and extremely elevated (18 °C, $T_{+10\,°C}$) temperatures (see 2.3.1). The results of the respiration measurements are not part of this work and the reader is referred to Gutperlet (2008).

3.2.1.1. Fitness (RNA/DNA ratio measurements)

At an ambient seawater temperature RNA/DNA ratios for *L. pertusa* varied from 0.97 to 7.85, with an average ratio of 2.99 ± 1.20. RNA/DNA ratios for $T_{+3°C}$ and $T_{+10°C}$ ranged from 1.22 to 3.89 and 0.47 to 3.42, respectively (Tab. 14). Although the ratios for both elevated temperatures were in between those from the ambient treatment (Fig. 52) a nonparametric ANOVA on ranks (with subsequent post-hoc Tukey HSD test for unequal n) revealed a statistically significant effect of both temperatures on the RNA/DNA ratios (see Appendix A4).

Tab. 14 Overview of RNA/DNA ratios measured after a long-term incubation of *L. pertusa* exposed to ambient seawater temperature (8°C, T), and two elevated temperatures (11 °C, $T_{+3°C}$ and 18 °C, $T_{+10°C}$). Standard deviation (s), number of samples (n).

Treatment	n	Mean	Median	s	Minimum	Maximum
T	207	2.99	2.92	1.20	0.97	7.85
$T_{+3°C}$	40	2.34	2.25	0.68	1.22	3.89
$T_{+10°C}$	44	1.57	1.37	0.87	0.47	3.42

For details and results on methodical issues, the reader is referred to Gutperlet (2008).

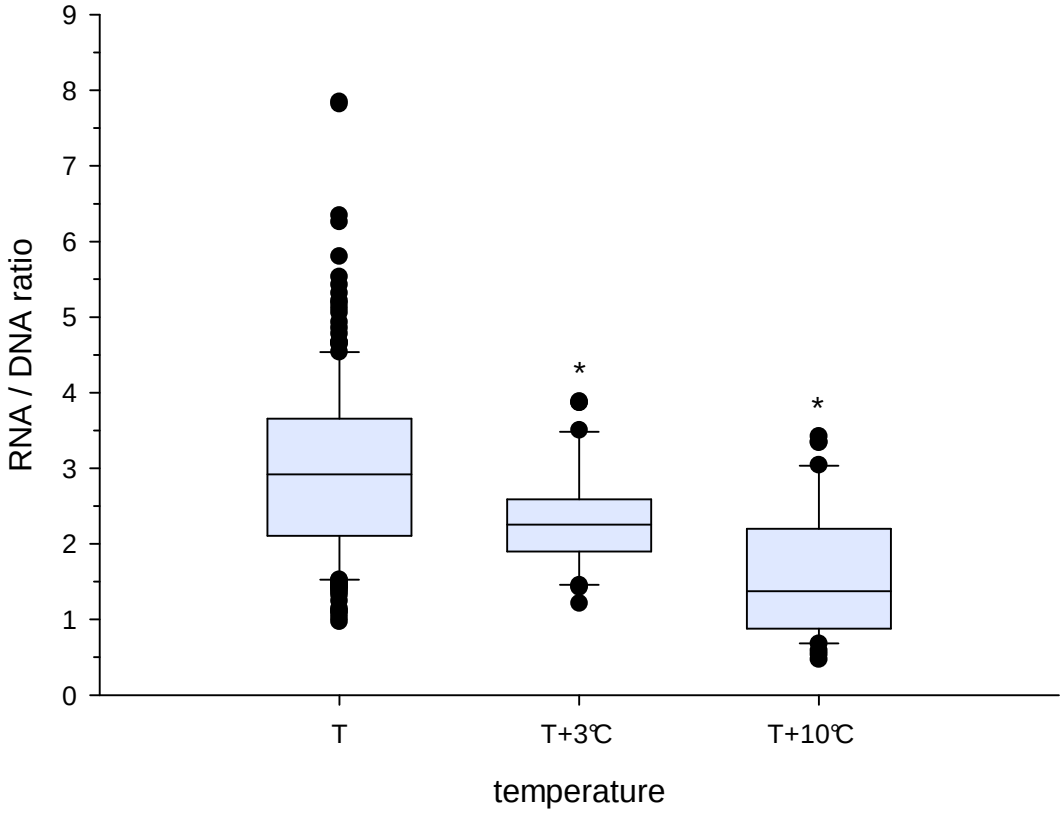

Fig. 52 RNA/DNA ratios of *L. pertusa* measured after a long-term incubation exposed to ambient seawater temperature (8°C, T), and two elevated temperatures (11 °C, $T_{+3°C}$ and 18 °C, $T_{+10°C}$). Box and whiskers are ± standard errors and standard deviations, respectively. Black dots: outliers. The asterisks indicate statistically significant differences between the control and the treatments.

3.2.1.2. Behaviour (PoBeMon studies)

Using the PoBeMon tool, polyp behaviour can be described as a function of polyp extension with 100 % meaning a fully extended and 0 % indicating a fully retracted polyp (2.2.3). In the framework of the Temperature Stress Response Experiment *L. pertusa* polyp behaviour of 39 polyps (distributed to eight coral branches) was recorded in two subexperiments.

Data visualisation & behaviour studies

For visualisation of the polyps' individual behaviour during the different observation periods one representative polyp was chosen from each coral group and sub-experiment (Fig. 53 - 56). Additionally - in subexperiment II - a second polyp from the stress group was selected to illustrate the specific behaviour during the three observation periods (Fig. 57).

"Normal" behaviour at ambient conditions varied strongly (Fig. 53 - 56, a) between individual polyps and between branches. The average and median extension for all polyps measured during the initial phase (t_0) was 52.1 ± 32.8 % and 58.8 %, respectively. For individual polyps median extensions of > 90 % have been documented whereas some other polyps only expanded their polyps for a few minutes (median of < 1 %). There was no diurnal rhythm found between maximum and minimum amplitudes and frequency of expansion / retraction (in the following only frequency). Nevertheless, at least one total retraction (> 80%) was documented by all polyps during the 48 hours of observation revealing a general cycle of expansion and retraction. A temporal synchronisation of these cycles was sometimes observed within the polyps of the same branch. However, this intra-colonial synchronisation was only "stable" for about three or four cycles and needs to be validated statistically with a pattern recognition system.

In subexperiment I (18 ° C) the polyps' behaviour from the stress groups after the temperature elevation (t_{acute}) was characterised consistently by a higher frequency and a general retraction reaction to lower (Fig. 54 b) or zero extension levels. Short-term maximum extension levels (of approx. 70 - 80 %) were sometimes achieved by some polyps whereas other polyps' maximum extension never exceeded 7 %. However, frequency and maximum extensions subsided from day to day which led to the decision to terminate the first sub-experiment ahead of schedule.

Polyp behaviour from the stress groups in subexperiment II (11 °C) was characterised by higher (up to 100 %) or normal extensions and frequency during the first 24 hours followed by a considerable depression (only extension) during the second part of the observation period (Fig. 56 b and Fig. 57 (t_{acute})). 14 days later the polyps had balanced their frequency back to normal intensity. Average extensions were also at a high level or sometimes exceeded the initial measurements (Fig. 56 c and Fig. 57 ($t_{acclimatised}$)).

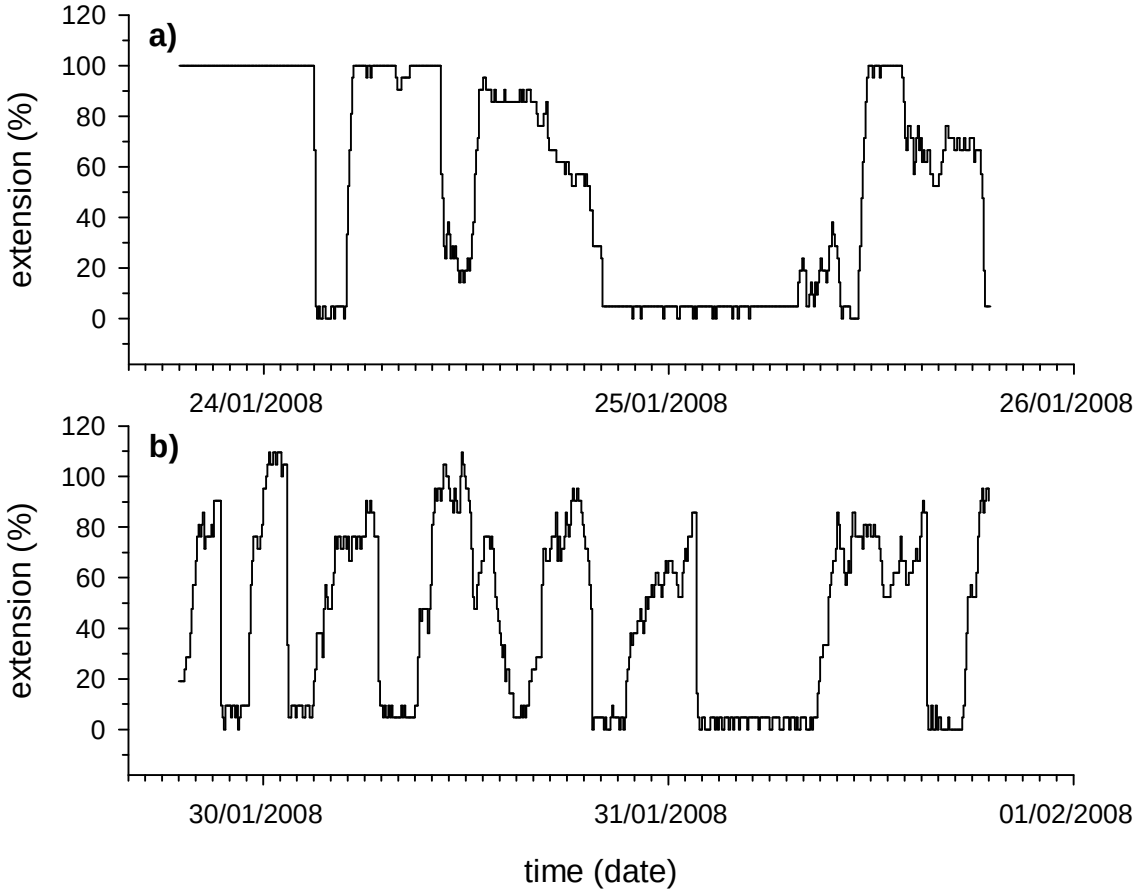

Fig. 53 Subexperiment I: Single *L. pertusa* polyp extension behaviour at constant temperature conditions (8 °C) during all observational periods (**a**, **b**) (control group).

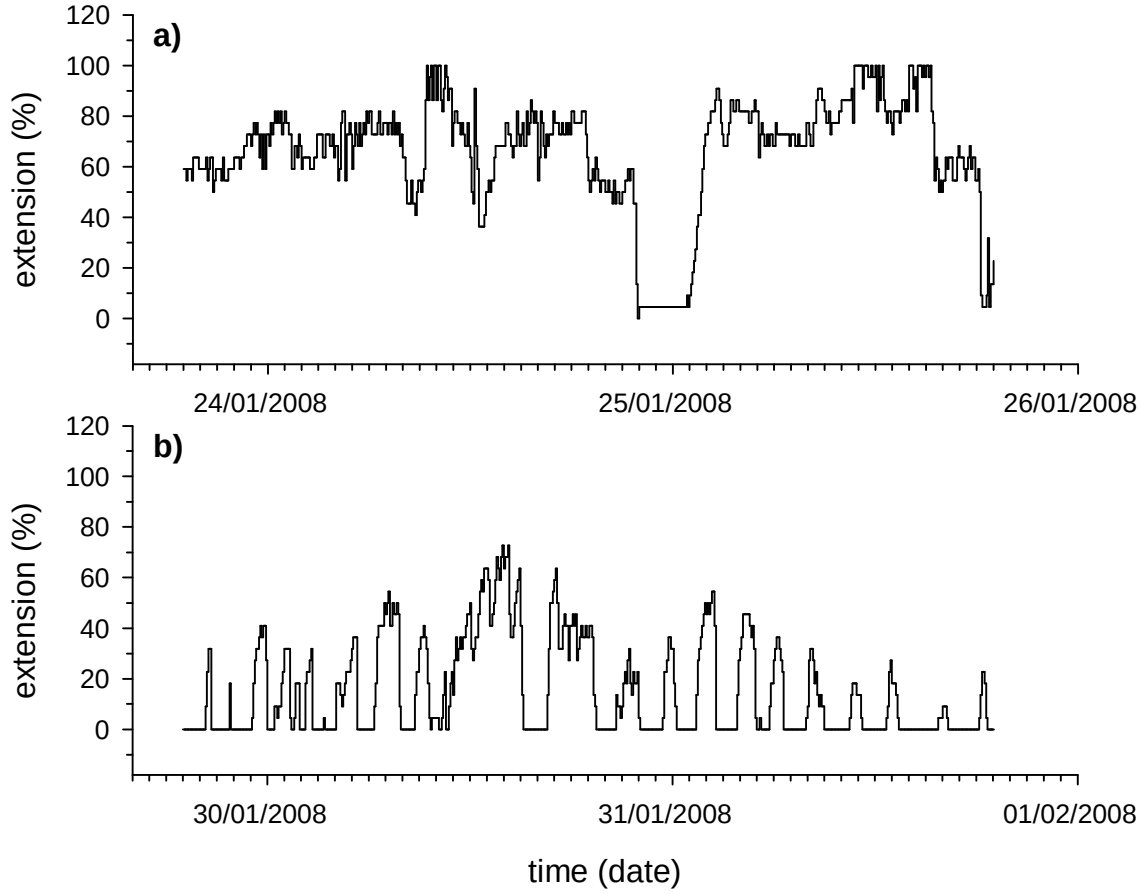

Fig. 54 Subexperiment I. Single *L. pertusa* polyp extension behaviour at unmanipulated temperature of 8 °C (**a**) and directly after a temperature shift to 18 °C (**b**).

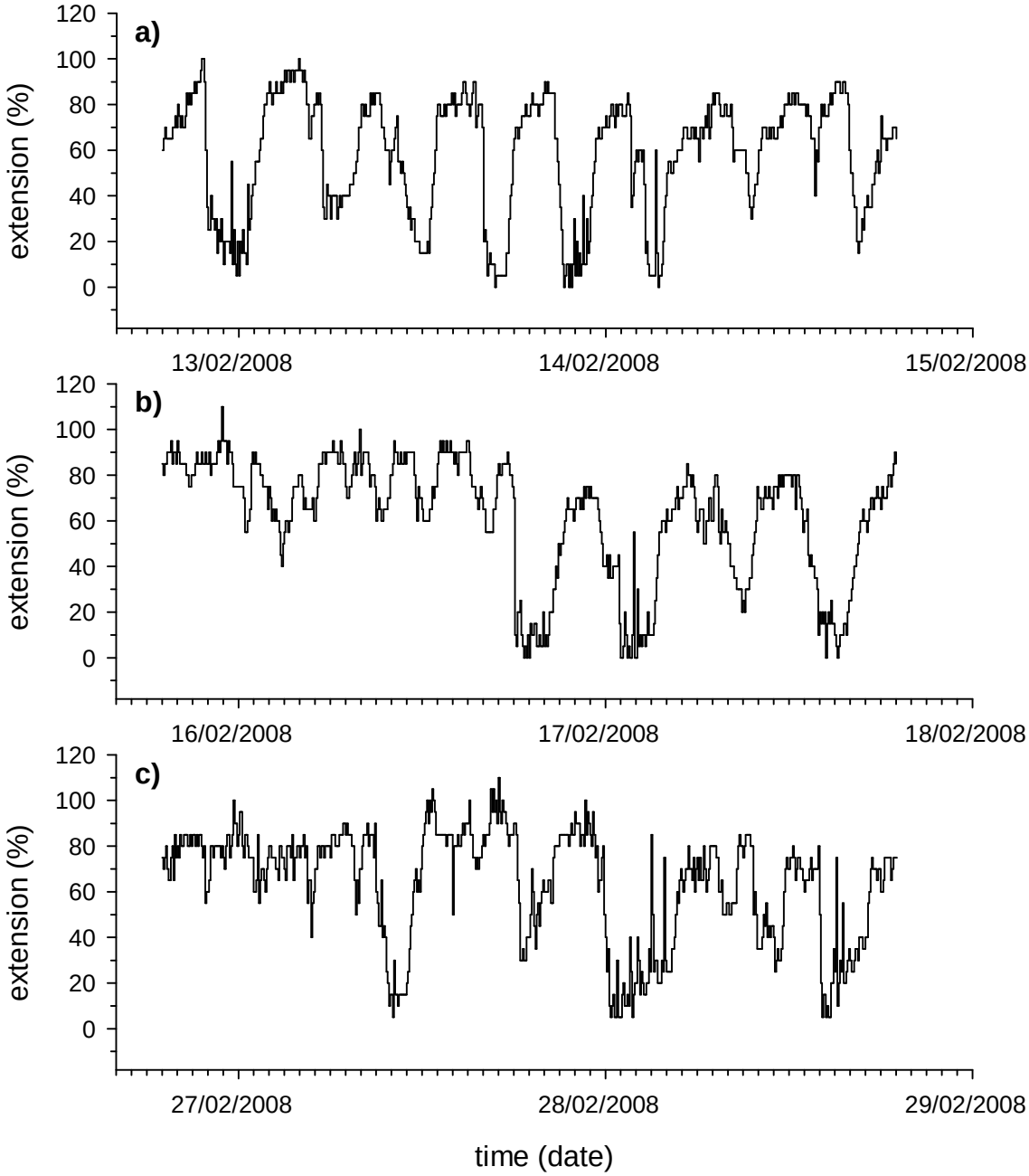

Fig. 55 Subexperiment II. Single *L. pertusa* polyp extension behaviour at constant temperature conditions (8 °C) during all observational periods (**a**, **b**, **c**) (control group).

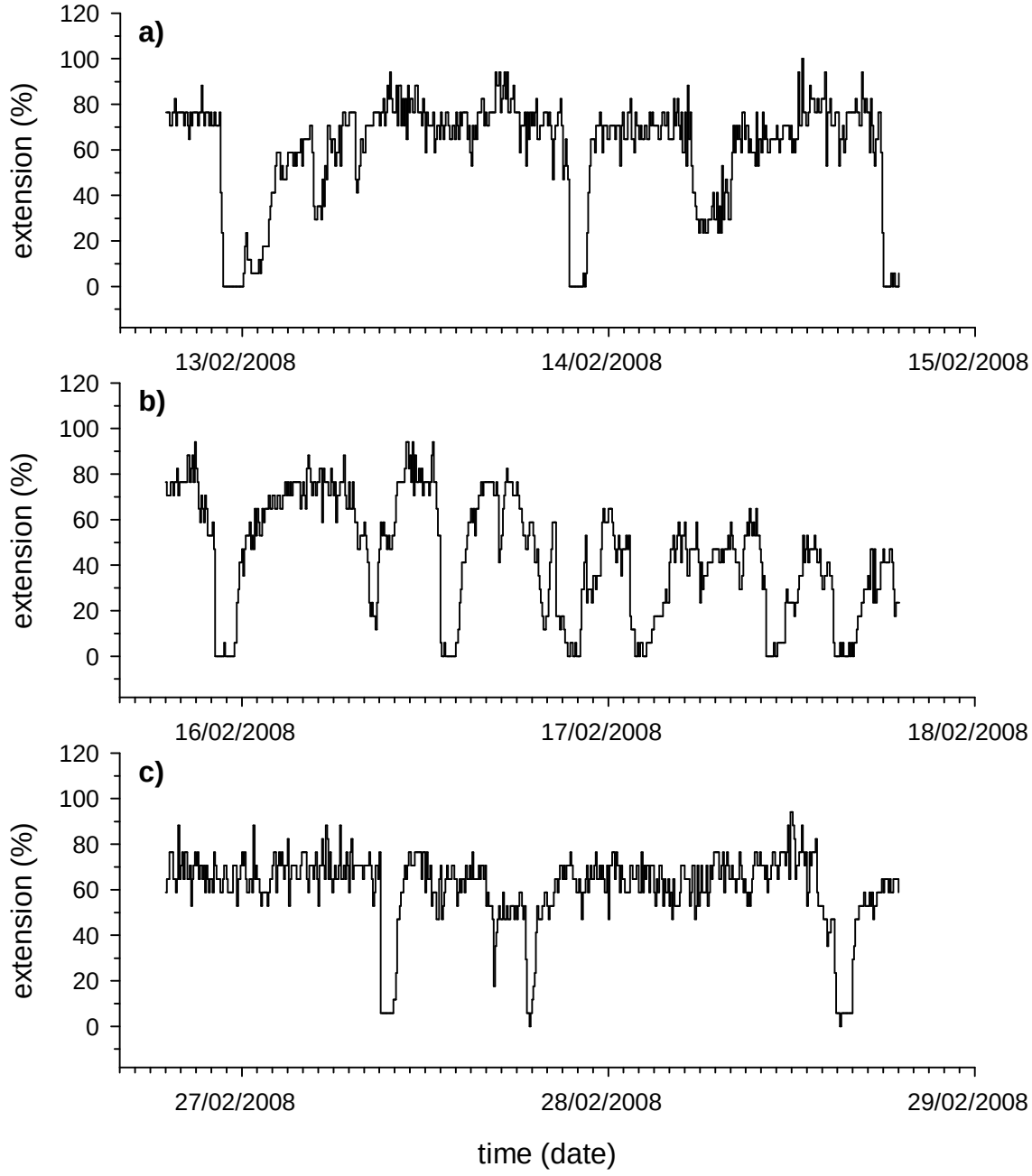

Fig. 56 Subexperiment II. Single *L. pertusa* polyp extension behaviour at unmanipulated temperature of 8 °C (**a**), directly after a temperature shift to 18 °C (**b**), and 14 days later (**c**).

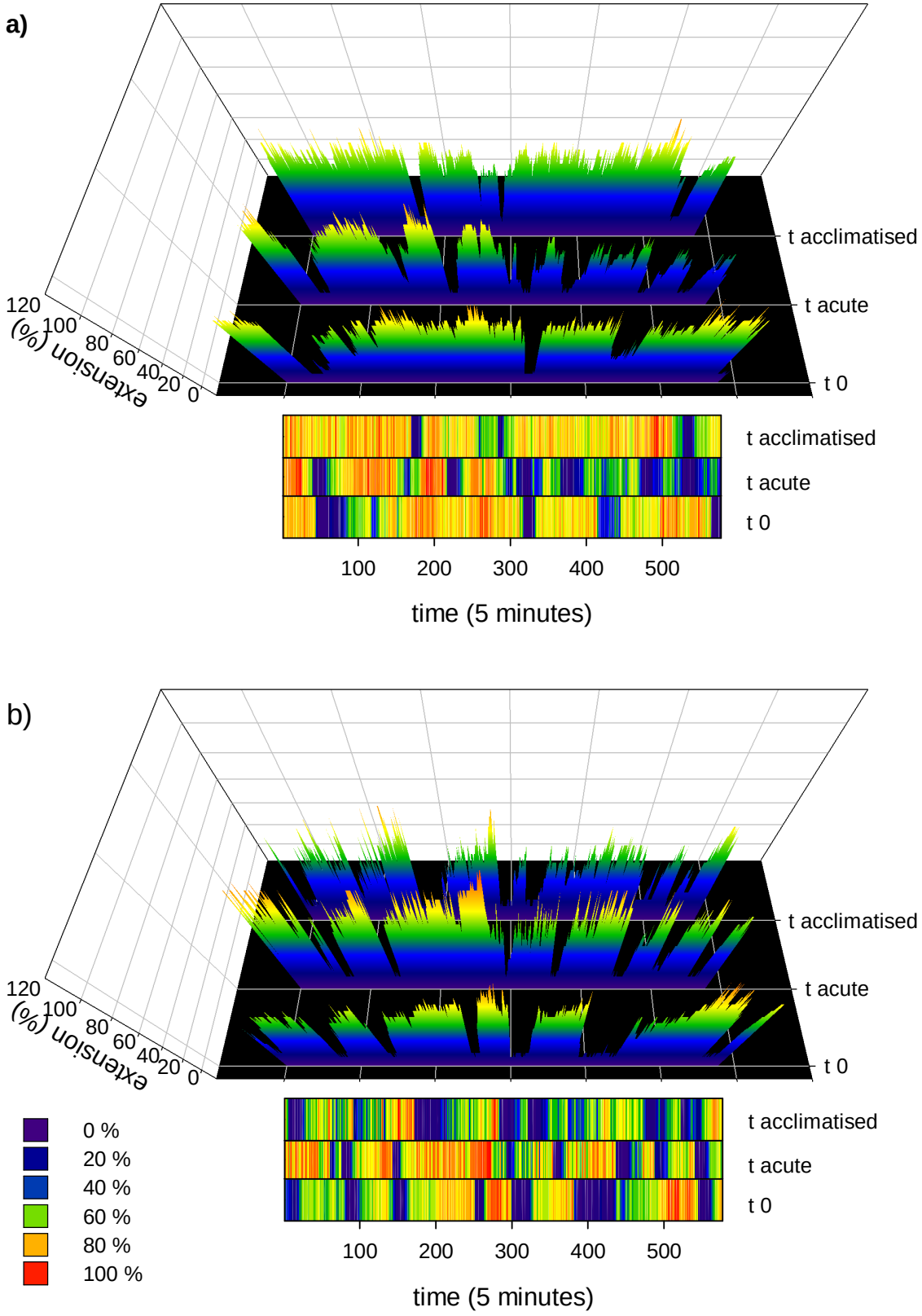

Fig. 57 Extension behaviour of two *L. pertusa* polyps (**a**, **b**) from subexperiment II visualised in intervals of five minutes as 3D Scatter Plot and Contour Plot.

Statistical data analysis

Subsequent statistics were focused on the question if there was a significant change in behaviour immediately after the temperature was shifted from ambient (8°C) to extreme (18 °C) or moderate regimes (11 °C). Also of interest was the possibility of another change after 14 days of "acclimatisation" to the new temperature conditions (only examinable in sub-experiment II).

Statistical testing was problematic due to the irregular nature of the polyps' extension behaviour and frequency even within the same branch (see above). As a result of this a high significance between most of the phases (to the polyps' individual behaviour) was the general case and not the exception to the rule (Friedman ANOVA). In order to harmonise the data for an ANOVA on ranks (Kruskal-Wallis) with subsequent multiple post-hoc comparisons, individual polyps' behaviour was condensed to "group extension" for each branch under the following assumptions:

(1) Median extension of each polyp had to be ≥ 50 % during the first observational period (t_0, ambient temperature for all polyps).

(2) At least three polyps of a branch had to pass (1) otherwise grouping failed for this branch.

(3) Level of significance (critical P-value) was set to 0.01 for ANOVA and for post-hoc procedures.

(4) Post-hoc comparisons were performed with Dunn's Method (multiple comparisons versus control group) on an averaged community extension (see below) at t_0 for control.

As a result of the grouping rules some polyps were removed from further considerations leading to a loss of stress group 1 and control group 2 in the subexperiment II (because of assumption (2)).

At ambient conditions the average and median extension for all groups (in the following called as "community extension") measured during the initial phases (t_0) was 62.3 ± 19.4 % and 63.2 %, respectively. In the control groups of both subexperiments lower extension rates were measured in each subsequent observation period, revealing a significant overlaying decreasing effect of time (Fig. 58). For subexperiment I and the first repeated

measurement (t_{acute}) the average decrease for the control groups compared with the community extension (t_0) was -9.6 ± 0.4 % (significant). In subexperiment II corresponding decreases for t_{acute} and $t_{acclimatised}$ were -6.8 ± 1.8 % (not significant) and -14.7 ± 2.4 % (significant) respectively.

In subexperiment I a substantive decrease of the stress group extensions was observed during the second observation period (t_{acut}) (Fig. 58 a). In comparison to the community extension the decrease was highly significant with -53.9 ± 13.1 %. A moderate but also highly significant decrease of -19.5 ± 6.4 % was calculated for the corresponding “stress group 2” extensions in subexperiment II. After 14 days of incubation at the elevated temperature a significant increase of 10.2 % in the average extension level was measured for the last observation period ($t_{acclimatised}$) (Fig. 58 c). Compared to the community extension the time-related decrease was only -11.3 ± 7.6 % and consequently in the same range as the control group.

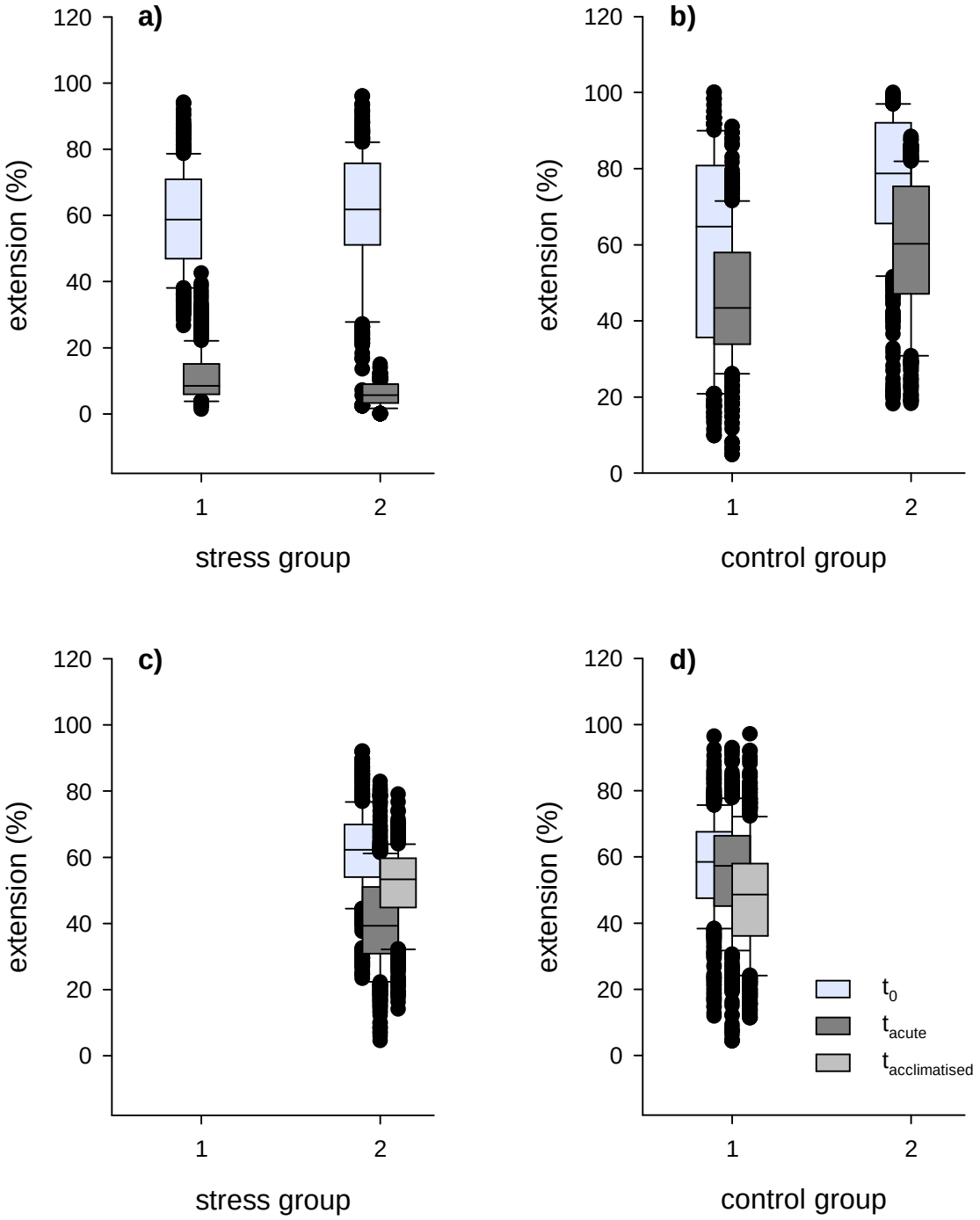

Fig. 58 *L. pertusa* extension behaviour of whole coral branches (group extension) during subexperiment I (**a**, **b**) and subexperiment II (**c**, **d**). Group extension was generated by averaging the polyps' behaviour of each coral branch according to predefined rules (see text for details). Box and whiskers are ± standard errors and deviations, respectively. Black dots indicate outliers.

3.2.2. *L. pertusa* ocean acidification stress responses at different time scales

3.2.2.1. Short-term incubation experiment (STE)

3.2.2.1.1. Water conditions and carbonate system

Physicochemical water parameters and nutrients

Temperature was measured every second day in each bioreactor and averaged at 9.0 ± 0.1 °C. Initial salinity was 33.4 but due to evaporation, salinity increased continuously to a maximum value of 34.1 (mean: 33.5 ± 0.3) in some of the replicates on the last sampling day.

Nutrients were measured at the beginning and the end of the experiment. Calculations based on the two day time interval for the delta alkalinity measurements revealed that they could be negligible in the subsequent calculations of the growth rates (2.2.1.2). For delta nitrate and nitrite $\Delta(NO_3^- + NO_2^-)$ and delta ammonium $\Delta(NH_4^+)$ average contributions were only 1.21 ± 1.06 µmol L^{-1} and 0.21 ± 0.49 µmol L^{-1}, respectively.

Carbonate system

Results from the total alkalinity and DIC measurements and calculations of the corresponding carbonate system parameters (pH, pCO_2, Ω_{Ar}) are summarised in Tab. 15:

Tab. 15 Overview of the carbonate system parameters after one week incubation of *L. pertusa* in the semi-closed bioreactors. All values are mean values ± standard deviations. pH, pCO_2 and aragonite saturation state (Ω_{Ar}) were calculated according to methods given in the text.

treatment	TA (µmol kg^{-1})	DIC (µmol kg^{-1})	$pH_{total\ scale}$	pCO_2 (ppm)	Ω_{Ar}
1 (ambient)	2392.6 ± 46.2	2249.8 ± 45.7	7.969 ± 0.023	509 ± 32	1.722 ± 0.086
2 (pH - 0.1)	2377.6 ± 47.3	2263.0 ± 38.1	7.900 ± 0.024	605 ± 26	1.478 ± 0.101
3 (pH - 0.2)	2390.7 ± 85.6	2319.1 ± 98.2	7.766 ± 0.062	856 ± 162	1.140 ± 0.119
4 (pH - 0.3)	2391.8 ± 38.5	2340.3 ± 33.4	7.708 ± 0.021	981 ± 40	0.997 ± 0.057

3.2.2.1.2. Growth rates

The average growth rate in the treatment with the highest aragonite saturation state (treatment 1: Ω_{Ar} = 1.72 ± 0.09, pCO_2 = 509 ± 32 ppm) was 6.80 × 10^{-3} % d^{-1} and varied strongly between 4.86 × 10^{-3} and 1.17 × 10^{-2} % d^{-1} (Tab. 16). Average growth rates at decreased aragonite saturation states were about 74, 89, and 81 % lower for treatment 2, 3, and 4, respectively. No statistically significant differences were found for growth rates of the four treatments when the normalisation against daily percentage weight increase (% d^{-1}) was used (Kruskal-Wallis ANOVA on ranks, H = 6.176, P = 0.103).

The average growth rate normalised to precipitated $CaCO_3$ per day and polyp for treatment 1 was 57.35 ± 25.05 µg $CaCO_3$ d^{-1} $polyp^{-1}$ (Tab. 16). The maximum growth rate peaked at 79.84 µg $CaCO_3$ d^{-1} $polyp^{-1}$ while the minimum growth rate in the same treatment was 66 % lower (27.49 µg $CaCO_3$ d^{-1} $polyp^{-1}$). This demonstrated the generally high variability of the corals' growth pattern (see discussion). However, a one-way ANOVA reveals a highly significant effect of pCO_2 on growth rate ($F = 8.579$, $P < 0.01$). Statistical posthoc comparisons (Tukey HSD, Holm-Sidak method) revealed also that growth was significantly different between treatment 1 and the treatments under elevated pCO_2 levels (see Appendix A5) while the differences between themselves were not significant.

Tab. 16 *L. pertusa* growth rates and normalisations of the short-term experiment with four pCO_2/pH treatments. Experiments were carried out in semi-closed bioreactors with filtered seawater of 34.4 and temperatures of 9.0 ± 0.2 °C (see text for details). Growth rates (G) were measured using the total alkalinity technique (2.2.1.2) and were normalised to percentage skeleton weight increase per day (% d^{-1}) and precipitated $CaCO_3$ per day and polyp (µg $CaCO_3$ d^{-1} $polyp^{-1}$). At the end of the experiment, polyps per branch were counted visually and skeleton dry weight (Skeleton DW) was measured using the buoyancy weight technique (2.2.1.1). Reported values are mean rates (n = 4), standard deviation (±), standard error of the means (sem), minimum (min), and maximum (max).

treatment	G (% d^{-1})		G (µg $CaCO_3$ d^{-1} $polyp^{-1}$)		Skeleton DW (g)		Polyps (n $branch^{-1}$)	
1 (ambient)	6.80E-03	± 3.24E-03 sem: 1.62E-03 min: 4.86E-03 max: 1.17E-02	57.35	± 25.05 sem: 12.53 min: 27.49 max: 79.84	26.50	± 6.35 sem: 3.18 min: 19.18 max: 31.89	32.00	± 8.04 sem: 4.02 min: 23 max: 41
2 (pH - 0.1)	1.78E-03	± 2.90E-03 sem: 1.45E-03 min: -2.80E-05 max: 6.11E-03	8.65	± 13.50 sem: 6.75 min: -0.76 max: 28.67	27.13	± 12.72 sem: 6.36 min: 17.83 max: 45.91	32.50	± 15.11 sem: 7.56 min: 17 max: 51
3 (pH - 0.2)	7.30E-04	± 3.14E-03 sem: 1.57E-03 min: -1.14E-03 max: 5.42E-03	-0.31	± 18.69 sem: 9.35 min: -15.01 max: 26.91	26.28	± 3.99 sem: 2.00 min: 21.04 max: 29.79	31.75	± 14.45 sem: 7.23 min: 16 max: 51
4 (pH - 0.3)	1.27E-03	± 2.60E-03 sem: 1.30E-03 min: -4.86E-04 max: 5.07E-03	3.41	± 14.04 sem: 7.02 min: -8.57 max: 22.86	28.75	± 8.47 sem: 4.23 min: 19.84 max: 39.10	33.00	± 14.09 sem: 7.05 min: 18 max: 46

Additionally, in all treatments with elevated pCO_2 conditions a negative growth (dissolution) of some replicates was measured, indicating a stress response of these corals to the elevated treatment pCO_2 conditions.

The seawater carbonate system in the relatively small bioreactors was highly influenced by coral respiration (DIC) and calcification (DIC and TA). Evaporation was also different between indivicual bioreactors (see above) leading to an additional interference factor. For these reasons a simple grouping of the treatments to their target pCO_2 does not reflect their real carbonate system at a given point in time. Hence, a linear regression analysis which correlates the individual calcification rates to their individual measured pCO_2 values was

performed (Fig. 59). Coefficients of determination for the resulting linear regressions were $R^2 = 0.31$ and $R^2 = 0.41$ for G (% d^{-1}) and G (µg $CaCO_3$ d^{-1} $polyp^{-1}$), respectively. For the first regression the relationship between growth rate and pCO_2 was statistically significant ($P = 0.03$) and for the latter one highly significant ($P < 0.01$).

In terms of future ocean acidification the results of the short-term experiment indicate that a drop of 0.1 pH units decreases *L. pertusa* growth up to 26 - 29 % (depending on the normalisation and pH range). The critical threshold pCO_2 concentration above which the corals cannot maintain positive growth is in the range between 721 and 1,299 ppm (1,010 ± 289 ppm or 933 ± 189 ppm for G (% d^{-1}) and G (µg $CaCO_3$ d^{-1} $polyp^{-1}$), respectively).

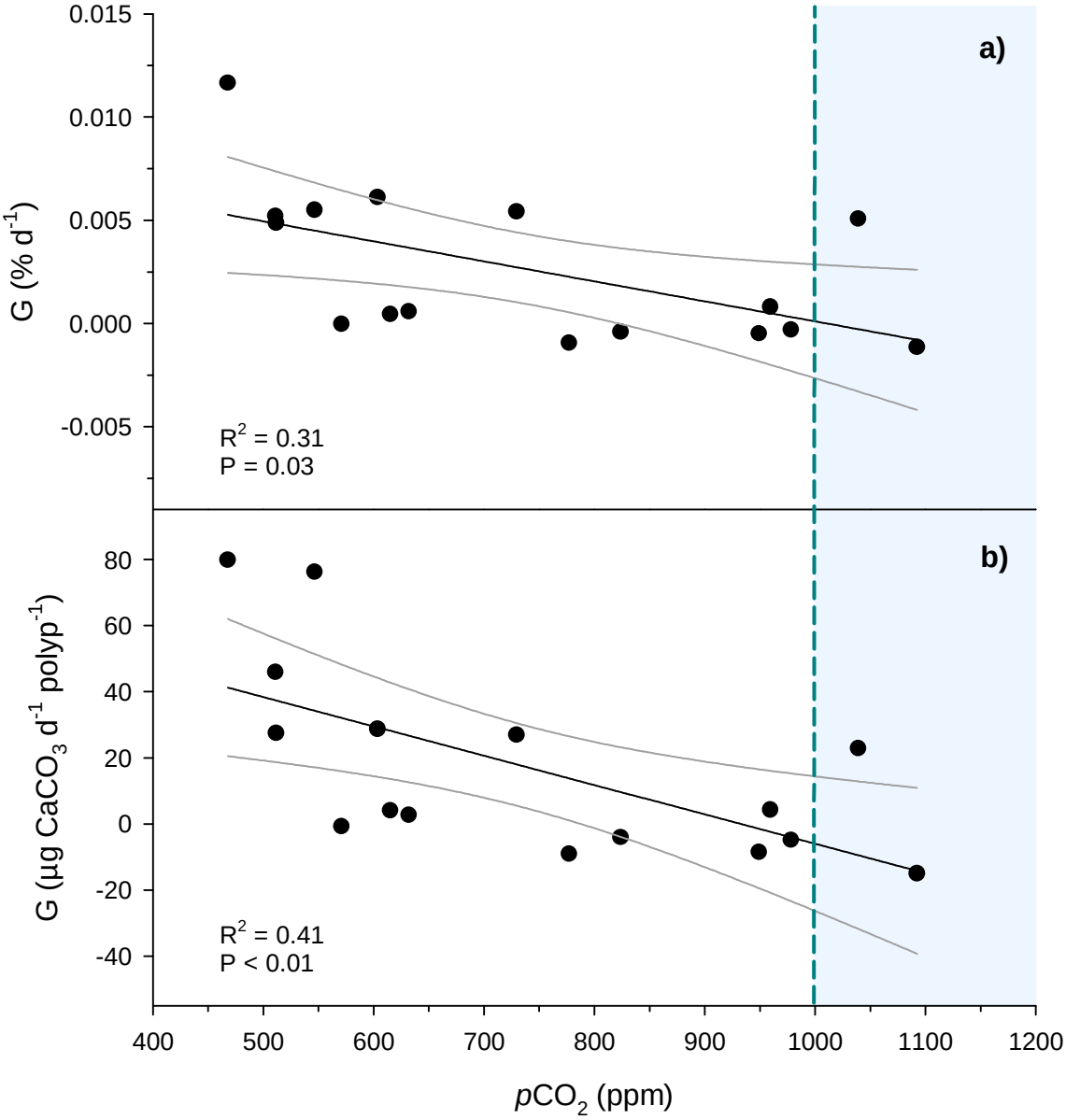

Fig. 59 *L. pertusa* growth rates (data points) from the short-term experiment normalised to percentage weight increase per day (**a**) and to precipitated $CaCO_3$ per day and polyp (**b**). Coefficient of determination (R^2) and significance level (P) were given for both linear regression analyses. Black and grey lines indicate the linear trend and the 95 % confidence intervals, respectively. The vertical dashed line marks the aragonite saturation equilibrium ($\Omega_{Ar} = 1$) below which unprotected aragonite skeleton structures are expected to dissolve (blue area).

3.2.2.1.3. Fitness (RNA/DNA ratios)

After 10 days of incubation a significant relationship between the RNA/DNA ratios and pCO_2 levels was only observed in the 651 ppm treatment ($P < 0.05$; multiple comparisons versus control group (Dunn's Method) after Kruskal-Wallis ANOVA on ranks, see Appendix A5). Average RNA/DNA ratios for the three elevated treatments ranged from 2.86 ± 0.64 to 3.51 ± 0.99 and were in the same range or even higher than the control group data with an average of 3.35 ± 1.02 (Fig. 60).

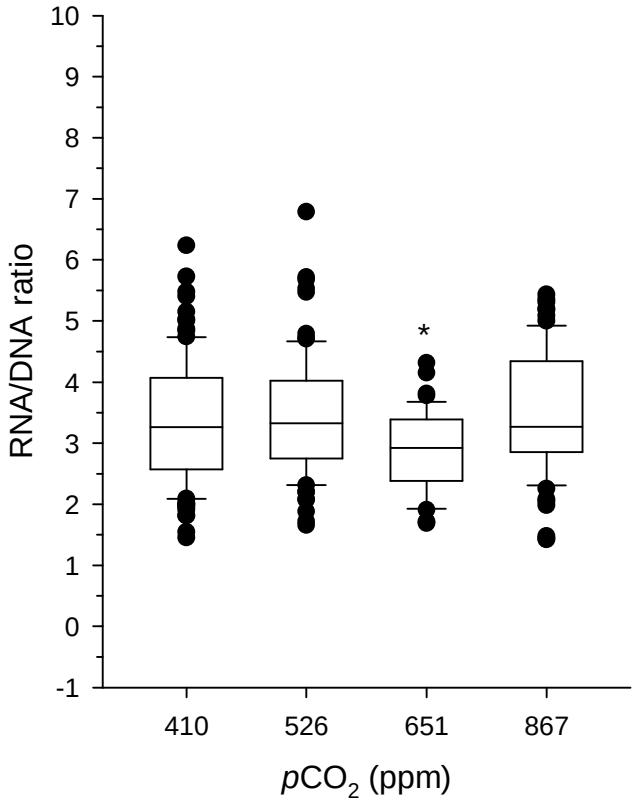

Fig. 60 RNA/DNA ratios of *L. pertusa* samples incubated for 10 days under four different CO_2 concentrations. Box and whiskers are ± standard errors and deviations, respectively. Black dots indicate outliers and the asterisk indicates a statistically significant difference between treatment (651 ppm) and control group (410 ppm).

3.2.2.2. Long-term acclimatisation experiment (LTE)

3.2.2.2.1. Water conditions and carbonate system parameters

Physicochemical measurements

The average salinity during the first half-year of incubation with natural seawater (06/2008 - 12/2008) was 35.0 ± 0.43. In the second incubation period (02/2009 - 04/2009) after a gradual exchange of the process water to 100 % artificial seawater, salinity stabilisation was further improved to 35.2 ± 0.10. Initially, temperature varied during the first two months between 6.6 and 7.9 °C (6.9 ± 0.3 °C on average) but was stabilised at 7.5 + 0.2 °C for the rest of the experiment after replacing the temperature control units in all CRS. An overview of the individual measured physicochemical parameters is shown in (Fig. 62).

For pH measurements as well as for the whole carbonate system four phases need to be distinguished and regarded separately:

- Adjustment phase 1 (A1): during this phase the pCO_2-treatments were set-up and pH was characterised by some fluctuations and a general lowering to the new pH levels. Initially measured pH of untreated water was 8.023. After about four weeks the new carbonate system was established (Fig. 62) and for the corals' acclimatisation to the new conditions an additional month (07/2008) was assigned to A1.
- Natural seawater incubation phase (I1 & I2): during the next four months of acclimatised incubation (08/2008 - 12/2008) a slightly increasing pH trend of 6.722×10^{-4} units d^{-1} in all three CRS was observed. The average "treatment pH-values" for CRS 1 - 3 were 7.944 ± 0.064, 7.829 ± 0.053, and 7.755 ± 0.056, respectively (Tab. 17).
- Adjustment phase 2 (A2): the switch from natural to artificial seawater was accompanied by a steep decrease of the pH values. Two weeks after the last water exchange to 100 % artificial seawater (indicated with a black line in Fig. 62) pH levels reached a steady state at the end of A2 (02/2009).
- Artificial seawater incubation phase (I3): the last time period (02/2009 - 04/2009) was characterised by an intense regulation of the total alkalinity in all CRS in order to maintain the carbonate system as constant as possible. Measured average treatment pH-values for CRS 1 - 3 were 7.777 ± 0.037, 7.675 ± 0.041, and 7.598 ± 0.046, respectively (Tab. 17).

Carbonate system

Carbonate system parameters for the LTE were shown in Tab. 17. In Fig. 63 the chronological sequence of the main carbonate species (CO_2, CO_3^{2-}, and HCO_3^-) and the derived pCO_2 and aragonite saturation levels (Ω_{Ar}) are plotted.

Tab. 17 Calculated parameters of the carbonate chemistry of the three pCO_2-treatments established in three independent closed recirculating systems (CRS) with natural (NSW) and artificial (ASW) seawater. All values are mean values ± standard deviations. pH, pCO_2 and aragonite saturation state (Ω_{Ar}) were calculated according to methods given in the text.

CRS		TA (µmol kg^{-1})	DIC (µmol kg^{-1})	pH$_{free\ scale}$	pCO_2 (ppm)	Ω_{Ar}
1	$NSW_{(I1+I2)}$	2298.5 ± 73.0	2185.8 ± 82.6	7.944 ± 0.064	604 ± 105	1.366 ± 0.156
	I3 / ASW	2270.1 ± 21.1	2214.9 ± 21.3	7.777 ± 0.037	888 ± 78	0.936 ± 0.079
2	$NSW_{(I1+I2)}$	2232.4 ± 61.4	2161.1 ± 71.2	7.829 ± 0.053	778 ± 112	1.035 ± 0.090
	I3 / ASW	2268.0 ± 15.2	2242.6 ± 20.0	7.675 ± 0.041	1139 ± 109	0.752 ± 0.070
3	$NSW_{(I1+I2)}$	2349.9 ± 79.5	2300.1 ± 89.2	7.755 ± 0.056	982 ± 146	0.932 ± 0.097
	I3 / ASW	2272.2 ± 17.8	2269.6 ± 22.8	7.598 ± 0.046	1377 ± 146	0.639 ± 0.067

Nutrient composition

The development of the nutrient concentrations during the approximately one year incubation period illustrates the effectivity but also the slowness of the bacterial degradation processes in the biofilters at low temperatures (nitrification, see 2.1.2.2). Within the first two months of the experiment ammonium and nitrite reached their highest concentrations of 1.67 and 0.35 µmol L^{-1} (in CRS 1), respectively. Initial concentrations of nitrate and phosphate were relatively low (NO_3^-: 23.05 ± 13.22 µmol L^{-1}; PO_4^{3-}: 1.12 ± 0.20 µmol L^{-1}) but increased continuously to maximum values of 164.61 µmol L^{-1} and 6.49 µmol L^{-1} about three months after the ammonium/nitrite peak (Fig. 61). Nitrification was fully established at the fifth month and from this time forth (11/2008) average concentrations of ammonium and nitrite concentrations were only 0.13 ± 0.15 µmol L^{-1} and 0.11 ± 0.04 µmol L^{-1}, respectively.

Tab. 18 Nutrient concentration ranges during long-term ocean acidification experiment. The value for each nutrient represents an average or median (n = 120) from all three CRS integrated over the experimental period (06/2008 - 04/2009) with the standard deviation (s). All values in µmol L^{-1}.

Nutrient	Mean	Median	s	Minimum	Maximum
NH_4^+	0.29	0.21	0.31	0	1.67
NO_2^-	0.13	0.12	0.06	0.05	0.35
NO_3^-	59.34	51.58	30.36	9.20	164.61
PO_4^{3-}	3.33	3.23	1.41	0.89	6.49

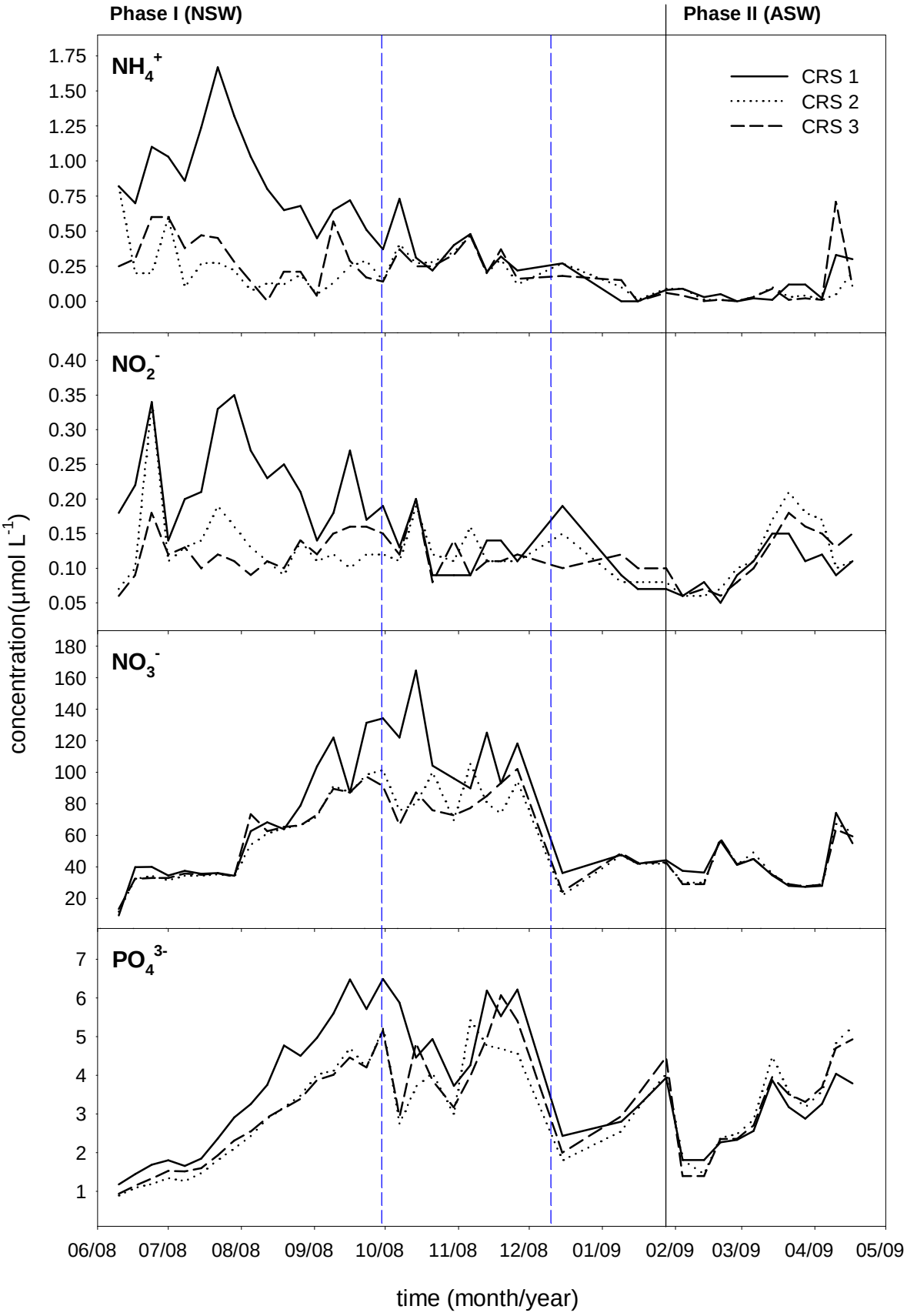

Fig. 61 Nutrient concentrations during long-term incubation. Blue dashed lines indicate a water exchange of more than 40 % and the black line marks the start of the second incubation period after a gradual switch from natural seawater (NSW) to artificial seawater (ASW). Legend: CRS 1 - 3: closed recirculating systems 1 - 3.

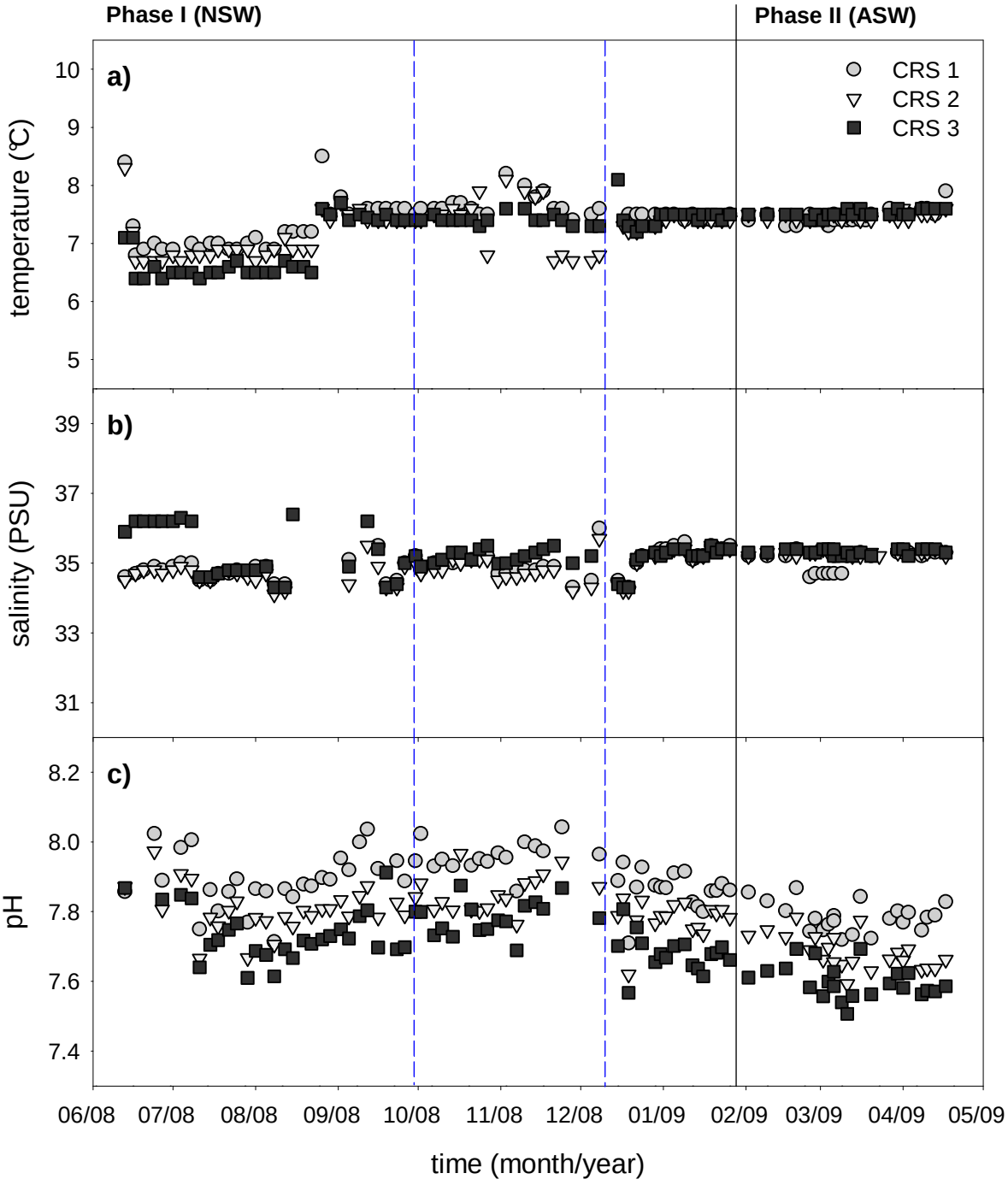

Fig. 62 Physicochemical water parameters measured during long-term incubation. Blue dashed lines indicate a water exchange of more than 40 % and the black line marks the start of the second incubation period after a gradual switch from natural seawater (NSW) to artificial seawater (ASW). Legend: CRS 1 - 3: closed recirculating systems 1 - 3.

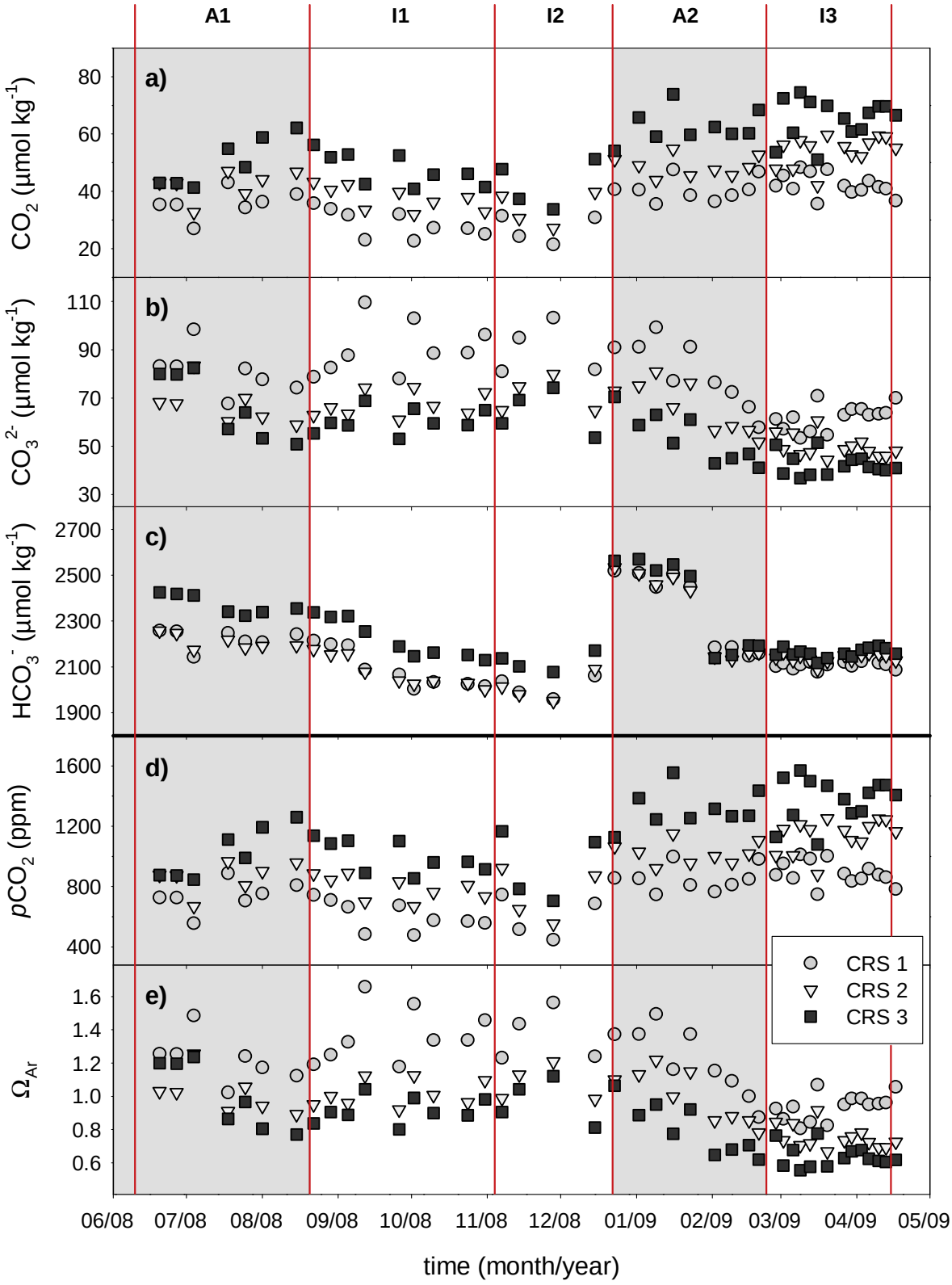

Fig. 63 Calculated carbonate system parameters during the long-term experiment. Red lines indicate buoyancy weight measurements. Grey boxes indicate phases of intense adjustments at the water parameters. Calcification measurement phases (I1 - 3) were only performed between the adjustment phases (A1, A2). Legend: CRS 1 - 3: closed recirculating systems.

3.2.2.2.2. Growth rates

Although the Alizarin Red S stained corals visually looked healthy the measured growth rates which were illustrated in Fig. 64 were not integrated into the following calculations of averaged treatment growth rates and subsequent statistical analysis. An impact of the staining procedure on growth could not be excluded as it was documented for tropical warm-water corals (Dodge *et al.* 1984).

Measured growth rates varied strongly between 1.60×10^{-3} and 3.99×10^{-2} % d^{-1} or 8.76 and 397.32 µg $CaCO_3$ d^{-1} $polyp^{-1}$ (Tab. 19, Fig. 64), respectively. Average growth rate for the first incubation period with natural seawater and saturated aragonite levels (Ω_{Ar} = 1.37, CRS 1) was $8.70 \pm 3.18 \times 10^{-3}$ % d^{-1}. The corresponding growth rate for the same CRS measured at the end of the second incubation period with artificial seawater was significantly lower (5.11×10^{-3} % d^{-1}) (paired t-test; t = -2.847, P = 0.047). A statistically significant reduction of growth rates between NSW and ASW was also calculated for CRS 3 (paired t-test; t = -2.927, P = 0.043) whereas changes in CRS 2 were not significant (paired t-test; t = -2,142, P = 0.099).

Interestingly, average growth rates in both seawater phases were highest in the group exposed to the undersaturated conditions (CRS 3, Fig. 65). For NSW and ASW the average growth rate in this system was $1.88 \pm 1.34 \times 10^{-2}$ % d^{-1} and $8.60 \pm 8.12 \times 10^{-3}$ % d^{-1}, respectively. No statistically significant relationship between average growth rates and pCO_2 concentrations during the NSW incubation phase (Kruskal-Wallis ANOVA on ranks; H = 1.46, P = 0.482) as well as the ASW incubation phase (Kruskal-Wallis ANOVA on ranks; H = 0.42, P = 0.812) were detected. Although there was no statistical evidence a linear regression analysis suggests an increasing trend of coral growth with increasing pCO_2 concentration (R^2 = 0.22, P = 0.077; see Appendix A6). A reason for this unexpected trend can be found in the increasing coefficients of variances (e.g. a 95 % increase from CRS 1 to CRS 3) which could also be regarded as a physiological reaction of the cold-water corals to increasing pCO_2 concentrations (see discussion).

The lowest aragonite saturation state during the NSW phase was Ω_{Ar} = 0.80 (0.93 ± 0.10, on average) and Ω_{Ar} = 0.56 (0.64 ± 0.07, on average) for the ASW phase (Tab. 17, CRS 3). Thus a second surprising result of the long-term incubation experiment was the absence of negative growth rates due to dissolution of skeleton material in these undersaturated treatments (Fig. 65). Only in one of the stained branches a loss of weight was measured at an

intermediate buoyancy weighing (I2). In the next measurement the same branch exhibited positive growth leading to the conclusion that in the former case a miss weighing must have occurred. Seawater chemistry measurements also confirmed no corrosive effects on the corals' skeletons due to undersaturated conditions (in the given range). The total alkalinity was expected to increase due to dissolution of the skeletons but in praxis total alkalinity as well as Ω_{Ar} decreased continuously.

Tab. 19 *L. pertusa* growth rates measured at three specified intervals (I_{1-3}) during the long-term ocean acidification experiment. Growth rates (G) were normalised to percentage weight increase per day (% d^{-1}), precipitated calcium carbonate per day and polyp (µg $CaCO_3$ d^{-1} $polyp^{-1}$). Corals were heltered in three independent closed recirculating systems (CRS 1 - 3) representing the three pCO_2-treatments (see text for details). Measurement interval I1 and I2 were combined to one group for summarising the first incubation period with natural seawater (NSW_{I1+I2}). In contrast, during interval I3, the cold-water corals were maintained in artificial seawater (I3 / ASW). Reported values are mean rates (n=5), standard deviation (±), standard error of the means (sem), minimum (min), and maximum (max).

	CRS 1		CRS 2		CRS 3	
			G (% d^{-1})			
I1	8.04E-03	± 3.26E-03 sem: 1.46E-03 min: 3.75E-03 max: 1.22E-02	1.16E-02	± 8.02E-03 sem: 3.59E-03 min: 1.60E-03 max: 2.39E-02	1.77E-02	± 1.28E-02 sem: 5.71E-03 min: 5.37E-03 max: 3.50E-02
I2	9.67E-03	± 3.19E-03 sem: 1.43E-03 min: 6.37E-03 max: 1.44E-02	1.11E-02	± 4.21E-03 sem: 1.88E-03 min: 5.81E-03 max: 1.55E-02	2.02E-02	± 1.41E-02 sem: 6.29E-03 min: 6.07E-03 max: 3.99E-02
NSW (I1+I2)	8.70E-03	± 3.18E-03 sem: 1.42E-03 min: 5.06E-03 max: 1.31E-02	1.14E-02	± 6.12E-03 sem: 2.74E-03 min: 4.14E-03 max: 2.08E-02	1.88E-02	± 1.34E-02 sem: 6.00E-03 min: 5.65E-03 max: 3.73E-02
I3 / ASW	5.11E-03	± 2.44E-03 sem: 1.09E-03 min: 2.50E-03 max: 7.96E-03	5.37E-03	± 2.52E-03 sem: 1.13E-03 min: 2.95E-03 max: 8.23E-03	8.60E-03	± 8.12E-03 sem: 3.63E-03 min: 2.88E-03 max: 2.29E-02
			G (µg $CaCO_3$ d^{-1} $polyp^{-1}$)			
I1	68.02	± 27.67 sem: 12.38 min: 32.56 max: 104.49	115.53	± 120.40 sem: 53.84 min: 14.47 max: 318.32	148.09	± 125.00 sem: 55.90 min: 22.30 max: 339.41
I2	83.76	± 28.09 sem: 12.56 min: 40.66 max: 107.84	113.15	± 79.89 sem: 35.73 min: 24.06 max: 210.63	173.94	± 146.79 sem: 65.64 min: 25.18 max: 397.32
NSW (I1+I2)	74.11	± 26.32 sem: 11.77 min: 35.69 max: 105.79	114.61	± 101.03 sem: 45.18 min: 34.72 max: 276.63	158.09	± 133.26 sem: 59.60 min: 23.42 max: 361.83
I3 / ASW	50.05	± 30.37 sem: 13.58 min: 9.91 max: 84.03	54.85	± 39.50 sem: 17.66 min: 13.51 max: 108.53	80.02	± 89.66 sem: 40.10 min: 8.76 max: 236.94

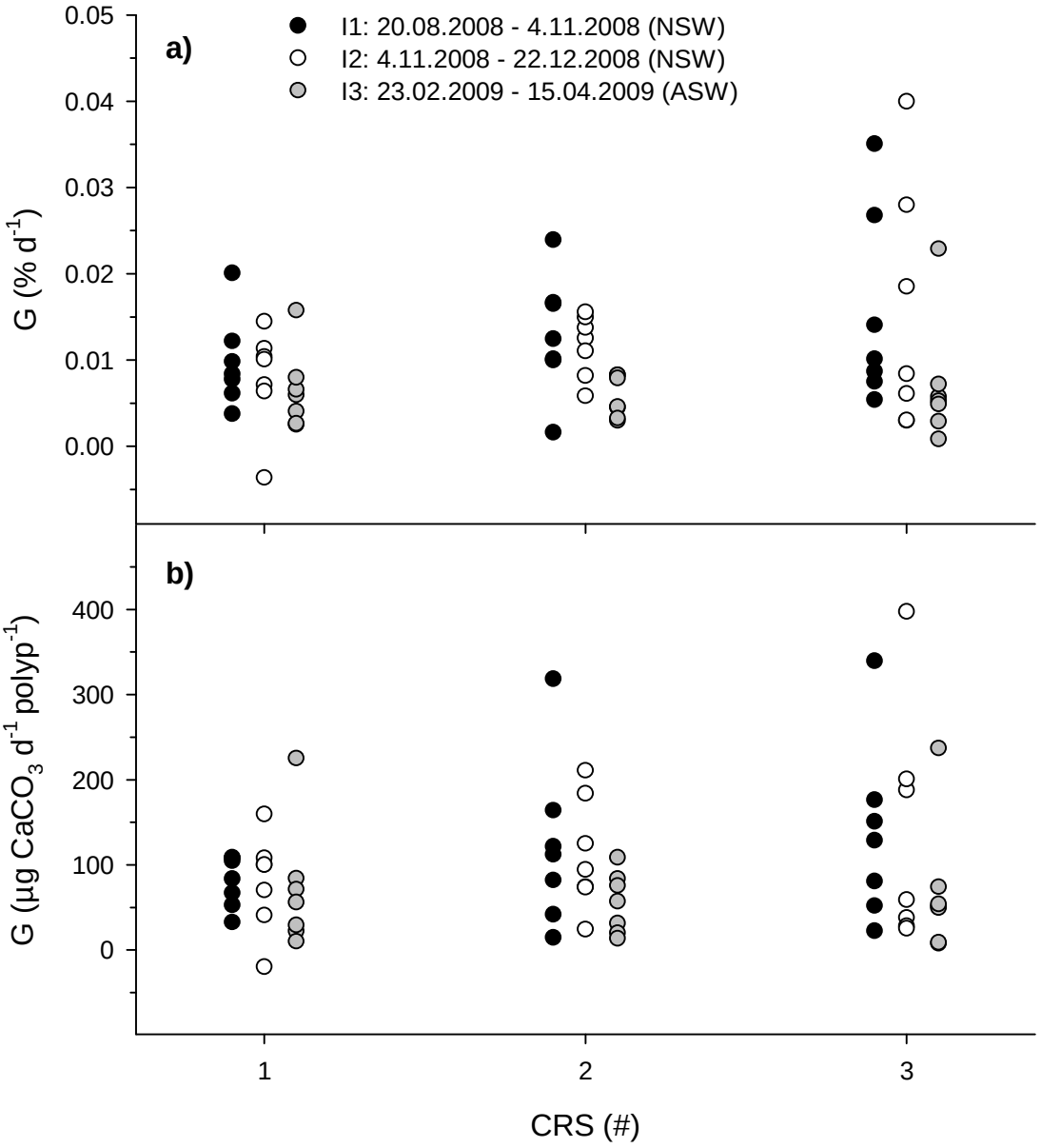

Fig. 64 Growth rates of *L. pertusa* measured during long-term incubation in three closed recirculating systems (CRS). Growth rates were calculated from repeated buoyancy weight measurements (see text for details). Intervals I1 and I2 were carried out with natural seawater (NSW), whereas interval I3 was carried out with artificial seawater (ASW) of the same salinity but deviating carbonate system. Growth rates were normalised to a percentage weight increase of each coral branch per day (**a**) and to precipitated $CaCO_3$ in each branch per day and polyp (**b**).

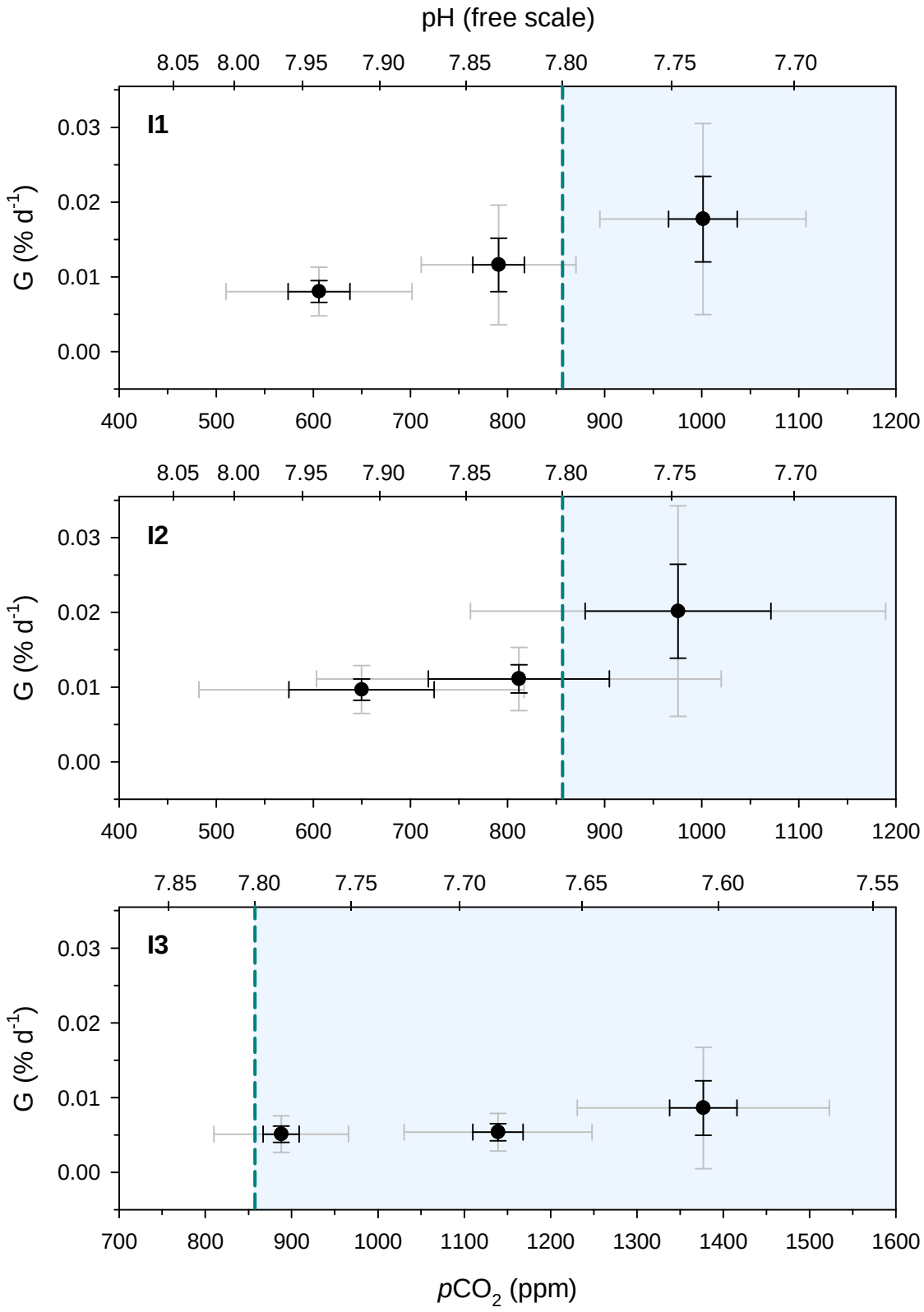

Fig. 65 *L. pertusa* growth rates during the three incubation phases vs. experimental treatment pCO_2-levels (bottom x-axis) and corresponding pH (top x-axis). Incubation phase 1 (I1) was carried out from August 20, 2008 to November 4, 2008 and incubation phase 2 (I2) from November 4, 2008 to December 22, 2008. After a switch from natural seawater to artificial seawater a third incubation phase (I3) was carried out from February 23, 2009 to April 15, 2009. Data points are mean values (n = 5), light grey and black error bars are the corresponding standard deviations and standard errors of the means, respectively. The vertical dashed line marks the aragonite saturation equilibrium (Ω_{Ar} = 1) below which unprotected aragonite skeleton structures are expected to dissolve (blue area).

4. Discussion

4.1. System setup and general cultivation

4.1.1. Closed Recirculating Systems: opportunities and limitations

General considerations

The quality and quantity of seawater is generally one of the most essential aspects of aquaculture. The advantages and disadvantages of culturing corals and other seawater animals in closed recirculating systems (CRS) have already been discussed in detail (Atkinson *et al.* 1995; Losordo *et al.* 1998). Therefore only the main points of view will be outlined here for a general understanding of the topic (sensu Boletzky and Hanlon (1983)):

Open or semi-closed systems:

- proven, reliable, and convenient
- not realisable without access to coastal waters
- water quality (e.g. nutrient concentrations, contaminants) depends on the quality of the local access point for the seawater
- influence of disease-causing agents can not be totally excluded

Closed recirculating systems:

- stable, controllable and reproducible marine environment
- independent from access to natural seawater
- high initial and running costs for water maintenance

For the cultivation and the experiments with the CWC *Lophelia pertusa* at the IFM-GEOMAR only the development of a CRS design was feasible due to the geographical location of the institute. Limited access to natural seawater was most of the time provided by collecting seawater during cruises of RV ALKOR in the North Atlantic.

During the last four years of CWC cultivation much experience was gained with the new facility and some general considerations can be made in retrospective:

Tank design: Because of a limitation in horizontal space, all CRS were build in two levels of glass aquaria on top of each other. From an optical point of view this was convenient because

it allowed a fast overview of all heltered organisms (corals and accompanying fauna). From a practical position handling of the corals as well as routine work (e.g. exchanges of the mechanical filters, removing food or detritus) - especially on the upper level - was cumbersome. The glass walls tended to mist up during the daily routine work in the climate chamber leading to a permanently moist steel framework which has to be dried regularly in order to prevent corrosion.

Framework: As mentioned above, the steel framework was permanently affected by corrosion. For future systems, an aluminium based framework is highly recommended.

Biofilter: A culturing system is regarded to be conditioned when the nitrifying bacteria in the biofilter rapidly oxidise all incoming ammonia / ammonium to nitrate without a significant accumulation of the intermediate nitrite (Bower & Turner 1983). Even though the biofilters of the CWC-MS and LTE-S were inoculated with substrata (old filter balls with a thick biofilm) from a CRS of the Kiel Aquarium, conditioning needed more time than previously estimated. This was because of the apparent inability of the inoculum to cope with the new water conditions. Maybe there are temperature-specific strains amongst the nitrifying bacteria or the low temperatures are far below their physiological optimum. Consequently, growth of an adequate biofilm and establishment of full nitrification lasted about seven months (Fig. 31).

Skimmer: Initially the large skimmer for the CWC-MS was considered to be oversized (recommended water volum: > 2000 L) but in practice the larger water-flow rate was scaled appropriately. During the feedings the water-flow through the skimmer was short-circuited and after reintegration turbidity within the aquaria was removed within a few hours. In contrast, the smaller skimmers used in the LTE-S CRS proved to be a slightly undersized even though their foam-fractionation seemed to be effective.

Temperature and cooling: The CWC-MS and the LTE-S were set up in a climate chamber of the IFM-GEOMAR. During the long-term cultivation several routine maintenances on the cooling aggregate and one total replacement led to large fluctuations in the room temperature. Thus the installed back-up water-cooling aggregates rescued the aquaria organisms more than once by keeping the water temperature low.

Light: During the first weeks the corals were cultivated in almost complete darkness and for the routine work illumination was only supplied through blue low-intensity LED spot lights (~ 1 W / LED). After repeated observations and trials, it was concluded that *L. pertusa* did not seem to be affected by light at all. This was confirmed by aquarium observations from Mortensen (2001) and later Dodds (2007) who both reported that no polyps reaction was recognised in respone to illumination. Additionally, during the dives with the submersible JAGO it was also observed that a spontaneous bright illumination with the spot lamps caused no visual reaction of the polyps. As a consequence and in order to make the routine works more safe and comfortable room lighting was enabled temporarily thenceforth.

4.1.2. Water quality management

4.1.2.1. Water quality during long-term incubations

Measured *in situ* nutrient concentrations in the Oslofjord were significantly higher than those from the Sula Reef (Tab. 7) but still within the eco-environmental range reported for the North-east Atlantic (Davies *et al.* 2008). For nitrate and phosphate Davies *et al.* (2008) calculated environmental tolerance levels based on an Ecological-Niche Factor Analysis (ENFA) and found that *L. pertusa* lives in areas with lower concentrations of all nutrients than the global means but interestingly not in areas with lowest nutrient concentrations (Davies *et al.* 2008). To date no information about the physiological tolerance levels for CWC with respect to elevated nutrient concentrations are available.

For tropical shallow-water scleractinian corals the effects of elevated inorganic nutrients on corals and coral reef health are still being controversially discussed (Koop *et al.* 2001). Many studies demonstrate negative effects of highly enriched nutrients on coral growth (Stambler *et al.* 1991; Marubini & Davies 1996; Ferrier-Pagès *et al.* 2000) while some other studies reveal positive (Atkinson *et al.* 1995; Edinger *et al.* 2000) or species-dependent effects (Zhu *et al.* 2004). However, findings for tropical shallow-water corals can not simply be transferred to cold-water corals:

- For some species ammonia is the toxic component of the nitrogen waste while for others ammonium leads to detrimental effects.
- Elevated nutrient concentrations enhance zooxanthellate photosynthetic activity leading to an increase of algal and coral tissue biomasses (Muller-Parker *et al.* 1994; Marubini & Davies 1996) and sometimes also to a decrease of calcification due to an imbalance of

tissue growth and skeletogenesis (Tanaka *et al.* 2007). CWC like *L. pertusa* lack zooxanthellae and thus a nutrition of algae and a competition for the internal DIC pool between photosynthesis and calcification does not exist.

- Tropical shallow-water reefs are typically oligotrophic marine environments while cold-water coral reefs are most commonly located in nutrient and organic matter-laden waters. Consequently ecology and environmental conditions of both ecosystems are completely different from each other - leading to a different ecophysiology and evolutionary background of their scleractinian corals and most likely to different sensitivities towards inorganic nutrients.

On account of these considerations and the lack of available experimental or field data about the specific tolerance levels of *L. pertusa* the water treatment in the CRS was balanced between an appropriate technical effort and keeping the corals at nutrient concentrations close to nature (Tab. 7).

One part of the daily routine work was to observe possible changes in the behaviour of the coral polyps as well as the accompanying invertebrates (mainly the polychaete *Eunice norvegicus*, some crustaceans (*Pandalus borealis* and *Munidopsis* spec.) and the abundant brittle stars) at an early stage. Shrimps are well documented bioindicators for water quality (Lorenzon *et al.* 2000) and therefore special focus was given to their appearance. A total power blackout in the climate chamber in October 2007 led to curious behaviour patterns (e.g. swimming in a circle) and an increase of the shrimps mortality only a few hours after reactivation of the water treatment. A reason for this was supposed to be derived from a spontaneous release of formerly bounded nitrogenic compounds from the biofilter (see ammonium peak in the monitored nutrients for November 2007, Fig. 31). After exchanging approximately 40 % of the process water and the removal of accumulated detritus the situation recovered and some of the Pandalidae even survived both incubation periods (Oslofjord- and Sula Reef -Incubation).

Fig. 66 Female deep-sea shrimp *Pandalus borealis* sitting on top of retracted cold-water coral *L. pertusa* polyps. Photo: W. Holtmann.

4.1.2.2. Ammonium tolerances by warm- and cold-water corals

During the start-up phase rising ammonium concentrations in the CRS were not preventable (see above). Generally ammonium is known to cause a broad range of detrimental effects which can result in mortality including changes in membrane permeability that affect iono- and osmoregulation, inhibition of Na^+ uptake by a Na^+-NH_4^+ exchange pump, effects of carbohydrate metabolism and effects on the acid-base balance (Withers 1992). In tropical shallow-water corals different effects of elevated ammonium concentrations alone - or in combination with other stressors - are well documented (Muller-Parker *et al.* 1994; Ferrier-Pagès *et al.* 2000; Cox & Ward 2002; Bassim & Sammarco 2003; Zhu *et al.* 2004). The aim of this early bioassay was therefore to study whether increasing ammonium concentrations have a visual effect on the CWC behaviour which was thought to be an indicator for the corals health (Roberts & Anderson 2002).

Despite several methodical limitations (e.g. only one treatment and control group) some conclusions can be drawn from the results. As shown in Fig. 33 and Fig. 34 the average extension for both groups decreased during the first three time intervals (28.5 hrs). This behaviour was only expected for the polyps from the treatment group and would in this case suggest that the acclimatisation time to the setup was too short (2 days). Since both groups exhibited a stress reaction in form of hyperextension it was more probable that both groups experienced an additional stressor. Reasons for additional stressors were manifold: the experiment was carried out under relatively bright illumination. Even though Mortensen's (2001) and our own observations suggest that light has no influence on the normal behaviour of the corals it could make a difference if corals were illuminated only a few minutes or permanently. Although the experiment was carried out in a climate chamber, disturbances due to the daily routine work could not be fully avoided. This may also explain the synchronised polyp retractions during the first 24 hours. Hyperextension is a common behaviour for coral polyps and was typically regarded as an indicator for higher demand of metabolite-exchange by increasing the tissue surface area (Dodds 2007).

However, from the second time interval onwards, differences in the polyps' behaviour between blank and the treatment specimens were statistically significant indicating the corals sensitivity to detect ammonium in elevated concentrations of > 17 µmol L^{-1} (corresponding NH_4^+ of the control: < 4 µmol L^{-1}). Unfortunately, water of the control and treatment group was mixed at the third day, making further considerations problematic. The continuation of

the experiment was illustrated in Fig. A1-1 (Appendix A1). Increasing ammonium concentrations seemed to evoke no further depressions in the average polyp extension states until a concentration of ~ 80 µmol L^{-1} was reached on the fifth day (129^{th} hour). From this time onwards the maximum polyp extension states (white triangles in Fig. A1-1) decreased to final extension levels of 1.8 and 1.6 for the former control and treatment group, respectively. After the experiment was terminated, the corals were brought back into their aquaria and after a few days a complete recovery of the polyps back to full extension states were observed.

In conclusion a maximum tolerable concentration for ammonium could not be determined in the study but a fast increasing concentration evokes a clear retraction of the coral polyps, suggesting that higher concentrations may lead to detrimental effects for the corals and should be avoided during the long-term incubation of *L. pertusa* because of their unknown physiological effects.

4.1.3. Feeding regimes – ecophysiological considerations

To date very little is known about *L. pertusa's* feeding ecology in its natural habitat. Aquarium observations, isotopic measurements of coral tissue samples and *in situ* zooplankton assemblages suggest a mixed food spectrum of zooplankton (e.g. copepods, amphipods, chaetognaths) and particulate organic matter (Frederiksen *et al.* 1992; Mortensen 2001; Duineveld *et al.* 2004; Duineveld *et al.* 2007; Dodds *et al.* 2009).

In the following discussion the results are discussed with respect to their ecophysiological relevance only. For a discussion about methodological issues or other aspects not mentioned in the text, the reader is referred to the corresponding discussion sections of the cited studies (see section Cooperations).

4.1.3.1. Natural food sources

Small mesozooplankton: copepods (*Acartia tonsa*)

Marine mesozooplankton is commonly dominated by copepods with *Calanus finmarchicus* as the most abundant species in Norwegian marine zooplankton communities (Wiborg 1976; Helle 2000). In the Norwegian Sea, *C. finmarchicus* migrates to depths of > 600 m in autumn to overwinter (Østvedt 1955; Hirche 1991) and may play an important role in the North Atlantic *Lophelia* reef food-webs. *A. tonsa* - as used in this study - is a calanoid copepod which occurs in estuaries all along the Atlantic coasts (see 2.1.4.1.1) which also makes it a

potential food source for *L. pertusa* especially on reef sites located within or nearby the Norwegian fjords (e.g. Oslofjord, Trondheim Fjord).

An indirect evidence for the importance of calanoid copepods in the diet of the cold-water coral *L. pertusa* was obtained from lipid signatures of several *L. pertusa* from different areas in the North Atlantic. High lipid content and large wax ester fractions with a prevalence of copepod lipid biomarkers indicate that *L. pertusa* feeds predominantly on calanoid copepods (Dodds *et al.* 2009).

Although Mortensen (2001) has observed food uptake and ingestion of live copepods he did not determine any feeding rates nor the total food uptake. Thus, the results of this study demonstrate for the first time quantitatively that live and adult copepods can be captured and ingested by the cold-water coral *L. pertusa*. This is not obvious because copepods are known for their effective predator avoidance behaviour ("escape jumps") enabling them to escape away even from mobile predators like fish larvae or scyphomedusae (Suchman 2000). Generally it can be assumed that higher water currents lead to higher contact rates and that strong currents diminish the copepods radius of movement. Even though water currents in this experiment were not explicitly measured they were visually adjusted to mimic intermediate field conditions as measured during dives with the submersible JAGO and were estimated to be largely < 500 mm s^{-1} (max. current speed for JAGO operations). *A. tonsa's* maximum speed during escape jumps is > 800 mm s^{-1} (Buskey & Hartline 2003). Predator avoidance was therefore possible in principle. Additionally, average current speeds for *L. pertusa* North-east Atlantic habitats were modelled to be 7 mm s^{-1} (Davies *et al.* 2008) and thus one order of magnitude below *A. tonsas'* maximum speed. It is therefore conceivable that even though some escape jumps prevented the copepods from being harvested for a certain time predator avoidance could not be maintained by them for the whole duration of the experiment.

In both treatments with the adult copepods relatively similar amounts of 66 % and 68 % for the low and high densities, respectively, were ingested by the corals (Fig. 35). However, the absolute feeding rate (Ind $polyp^{-1}$ h^{-1}) in the treatment with high density was 228 % greater than for the low density. This suggests a strong correlation between capture efficiency and food density. Increasing feeding rates with increasing food densities are typical for suspension feeders and are well documented for tropical and temperate corals and other cnidarians (Clayton & Lasker 1982; Lasker *et al.* 1982; Ferrier-Pagès *et al.* 1998; Ferrier-Pagès *et al.* 2003; Picciano & Ferrier-Pagès 2007). Sometimes they are also described by a Michaelis-

Menten model (Hii *et al.* 2008). At high food densities a feeding plateau was reported for some corals (Ferrier-Pagès *et al.* 1998; Anthony 1999a; Hii *et al.* 2008) whereas others gave no indication for saturation of food uptake over the range of prey densities (Clayton & Lasker 1982; Anthony 1999a; Picciano & Ferrier-Pagès 2007).

Comparisons between the different studies and coral species are problematic because in addition to methodological differences coral feeding rates were generally affected by several factors e.g. differences in their feeding mechanisms, morphology, number of tentacles and polyps, satiety, differences in coelenterates cnidom, prey type and size, water flow, depth, temperature, and light availability. However, measured feeding rates of 1.99 - 6.52 Ind polyp^{-1} h^{-1} for *L. pertusa* (this study) were of the same dimension as reported feeding rates for tropical or temperate scleractinian coral species (Tab. 20), indicating a high physiological adaptation of the cold-water corals to low temperatures.

In both treatments < 0.5 % of the copepods survived the experiment. Copepods which were not caught by the corals accumulated dead at the bottom of the aquaria. This was most likely a methodological issue suggesting that only live copepods could maintain position in the water column of the aquaria while POM accumulated at water-current depleted sites. Nevertheless, pooling the data for ingested and dead copepods indicates that virtually all copepods which encountered the tentacles of a coral polyp were harvested or died of the nematocyst venom. In a large and healthy *L. pertusa* reef with a vertical depth of several polyp generations it can therefore be assumed that all copepods that had direct contact with live corals on the surface of the reef would be captured directly or by polyps at deeper levels. The latter aspect can be regarded as “passive nursing” of the older proximal polyps in a reef by increasing the available POM pool and may help to explain the longevity and survival of the species.

Large mesozooplankton: opossum shrimps (*Neomysis integer*)

In contrast to the copepods, adult life mysidacean do not seem to be an appropriate food source for *L. pertusa*. Although the mysidacean population was diminished by approx. 10 % after the feeding experiments relatively similar amounts were also absent in the control group without corals (3.1.2.1) indicating either a methodological artefact (e.g. sucked into the pump) or cannibalism. Cannibalism in mysidacean shrimps is well documented (Abdussamad & Thampy 1994; Quirt & Lasenby 2002) and may also be responsible for the higher losses in the treatment with the morphotype II corals (“exception”, see 3.1.2.1).

In contrast to the copepods the *N. integer* were cultivated at lower salinities (according to their ambient conditions at the collecting site). Thus the generally high mortalities in the treatments as well as in the control group revealed that the opossum shrimps were either not able to compensate for the abrupt changes in salinity or that the experimental conditions (especially the permanent relatively high water currents) prevented a successful acclimatisation to the experimental setup.

Interestingly *N. integer* actively avoided contact with the coral polyps and were able to free themselves from the tentacles by convulsive abdomen movements. Like copepods predator avoidance is also a common feature in mysidacean shrimps (Lindén *et al.* 2003). However, it can also be assumed that predator avoidance will only secure the shrimps live as long as they don't get in touch with the coral nematocysts. Because of the high mortality in the control group it was unfortunately not possible to distinguish between the different causes of their death.

Mortensen (2001) also reported that live mysidaceans avoid contact with *L. pertusa* tentacles and that they were never ingested except if dead specimens were placed manually onto the polyps. In the latter case shrimps up to 20 mm in size could be fed to the corals. This observation was also confirmed in this study - suggesting that less defensive or injured large mesozooplankton may also be a potential (minor) food source for the corals and that *L. pertusa* is capable of handling a wide range of food particles with respect to their size.

4.1.3.2. Prey capture and feeding process video observation

Only few authors have outlined the feeding process of *L. pertusa* which makes the observation report provided by this study (3.1.2.2) the most detailed description to date. To the authors best knowledge this was also the first time that the whole feeding process was video-documented scientifically (2.1.4.3).

Generally, anthozoans and corals use two mechanisms for prey capture: nematocyst adhesion for large prey (Muscatine 1973), and cilia with mucus entrapment for small non-motile particles (Goreau *et al.* 1971). The size of the polyps therefore determines the size and type of the preferred prey (e.g. zooplankton, phytoplankton, bacterioplankton) as it was well demonstrated for shallow-water reef corals and anthozoans (Porter 1976; Sebens 1987). In the framework of this study the observed *L. pertusa* polyp only used nematocyst adhesion to capture prey. Interestingly the polyp was even able to capture the *Artemia* nauplii when only a

few tentacles were extended - demonstrating the high efficiency of the nematocysts adhesion. Similar observations were reported from Tsounis *et al.* (2010) after feeding *L. pertusa* from the Mediterranean Sea with *Artemia* nauplii. These authors also reported that the polyps remained saturated and unable to ingest more prey for the next 12 to 24 h after a feeding period of 2 hours. This finding is substantiated by our observation. After the active feeding phase we observed approximately 10 - 15 % higher-than-average polyp expansion. This high degree of polyp extension results in a maximum surface to volume ratio (S/V ratio). A dependency between polyp extension state and respiration rate was examined by Brafield and Chapman (1967) on pennatulid octocorals (*Pteroides griseum*). In their study, respiration rates increased about 70 % if the polyps returned from a retracted to an extracted state (Brafield & Chapman 1967). Therefore we attributed the high polyp expansion of *L. pertusa* to an enhanced need for a gas exchange during the digestion of the food particles (dissimilation).

The maximum feeding rate for *L. pertusa* was 63 Ind polyp^{-1} h^{-1} and was in the same range as the reported maximum feeding rates of 76.9 Ind polyp^{-1} h^{-1} for *Galaxea fascicularis*[1] - a common scleractinian zooxanthellate coral from the tropics (Hii *et al.* 2008) - suggesting the physiological adaptation of the catching mechanism of *L. pertusa* to the cold-water environment. A feeding plateau, as it was described for several tropical species (see above), could not be observed

4.1.3.3. Food quality, carbon uptake and growth

Although enriched the measured energy content of food quality II was about 13 % less than that of food quality I (Tab. 8). At first glance one could conclude that this may indicate a failure in the enrichment of the *Artemia* nauplii (see 2.1.4.4). However, during the 24 hrs of larval development from instar I (FQI) to instar II (FQII) dry weights and energy contents of starved *Artemia* nauplii are known to decrease by 16 - 34 % and 22 - 37 %, respectively (Vanhaecke *et al.* 1983). Thus the lesser energy content decrease of the FQII *Artemia* nauplii proves that supplying the FQII with the highly enriched lipids of the food additives was successful.

On average *L. pertusa* polyps have ingested about 50 % more *Artemia* nauplii of FQII than FQI. This corresponds to an additional energy and dry mass uptake of 58 % and 83 %, respectively, indicating a high preference for FQII. As the analysis of the different remains (in

[1] measured under dark conditions. Maximum feeding rate under light conditions for *Galaxea fascicularis* was 113.6 Ind polyp^{-1} h^{-1} (Hii *et al.* 2008).

particular dead nauplii) suggested, the instar II nauplii of FQII were caught with a higher efficiency than the instar I nauplii of FQI (Moldzio 2008). Nevertheless, growth rates measured at the end of each feeding phase were comparable with those obtained from the CWC-MS and revealed no relationship between food quality and growth (Fig. 43, Tab. 10).

This could indicate:

(1) that FQI was of higher nutritional value for the corals and that it was necessary to enhance food uptake in the second feeding phase (FQII) for the replenishment of important nutrition pools (e.g. specific fatty acids or wax esters) or

(2) that if a minimum food quality is guaranteed the precipitation of $CaCO_3$ is unaffected by the food quantity.

In the latter case the additional energy and dry mass uptake could be used by the coral polyps for tissue growth, reproduction or other physiological pathways not measured in the framework of this study.

As outlined above, comparisons of feeding rates from different studies are problematic and can only highlight general trends and dependencies. However, feeding rates of *L. pertusa* with *Artemia* nauplii seemed to be consistent with the feeding rates obtained from the video observation study and the natural plankton study (copepods) indicating a dominant role of the prey density rather than the prey size or prey quality (Tab. 20). The differences in feeding rates between *Artemia* spec. and the copepod *Acartia tonsa* were most likely based on the physical characteristics of both prey animals. *Artemia* spec. are weak swimmers and behave more like passive particles than actively swimming zooplankton. In all stages of development *Artemia* spec. lack effective predator avoidance (e.g., escape jumps)[1] (Léger *et al.* 1987). Capturing success therefore seems to be a direct function of the encounter rates between coral polyp and prey.

To date only the study of Tsounis *et al.* (2010) reported feeding rates for *L. pertusa* and three other cold-water scleractinian coral species from the Mediterranean. For *L. pertusa* fed with *Artemia* spec. nauplii a feeding rate of ~ 280 Ind polyp^{-1} h^{-1} was measured (Tab. 20). The authors have not determined a total food uptake but based on the duration of the experiment

[1] *Artemia* spec. are living in hypersaline environments (salt lakes, brines) on top of a flat food chain. A predator avoidance mechanism was therefore evolutionary not manifested.

(2 hours) a maximum food uptake of 567.5 ± 260.2 Ind polyp^{-1} h^{-1} can be calculated. Based on the limited space of the polyps coelenteron and our measured maximum total food uptake of 234 *Artemia* spec. nauplii (video observation) a food uptake of ~ 560 *Artemia* nauplii seemed to be overestimated. Unfortunately the authors failed to describe their methods appropriately. It is not clear whether feeding rates were calculated from missing food particles in general or only from missing food particles in the water column. In the latter case *Artemia* nauplii which were killed but not captured and ingested by the polyps were also counted when tallying the feeding rate.

Tab. 20 Comparison of feeding rates by scleractinian corals from cold-water, temperate, and tropical habitats.

Species	Feeding rate (Ind polyp^{-1} h^{-1})	Prey	Prey density (Ind mL^{-1})	Temp. (°C)	Reference
Lophelia pertusa	2.0 ± 0.2	*Acartia tonsa*	0.6	8	this study
Lophelia pertusa	6.5 ± 0.5	*Acartia tonsa*	2.4	8	this study
Lophelia pertusa	9.8	*Artemia* spec. nauplii	~ 5	8	this study (video observation)
Lophelia pertusa	4.0 ± 1.2	*Artemia* spec. nauplii FQI	0.8	8	this study
Lophelia pertusa	6.0 ± 1.5	*Artemia* spec. nauplii FQII	0.8	8	this study
Lophelia pertusa	283.7 ± 130.1	*Artemia* spec. nauplii	10 - 20	12	(Tsounis *et al.* 2010)
Madrepora oculata	47.9 ± 33.3	*Artemia* spec. nauplii	10 - 20	12	(Tsounis *et al.* 2010)
Desmophyllum cristagalli	8.5 ± 3.0	*Artemia* spec. adults	10 - 20	12	(Tsounis *et al.* 2010)
Pavona gigantea	2 - 18	Natural plankton	-	25 - 27	(Palardy *et al.* 2006)
Galaxea fascicularis	0.8	*Artemia* spec. nauplii	0.1	28	(Hii *et al.* 2008)
Galaxea fascicularis	46.6	*Artemia* spec. nauplii	10	28	(Hii *et al.* 2008)
Madracis mirabilis	6 - 15	Natural plankton	< 0.03	25 - 27	(Sebens *et al.* 1996)
Montastrea cavernosa	30	Natural plankton	< 0.03	25 - 27	(Sebens *et al.* 1996)

For discussion about feeding efficiency, methodological considerations and statistical analysis, the reader is referred to Moldzio (2008).

4.1.4. *L. pertusa* basic morphometry and ambient calcification rates

4.1.4.1. Aragonite skeleton density and biomass contents

$CaCO_3$ exists in many crystalline polymorphs with calcite and aragonite as the most important (Medeiros *et al.* 2006). Pure aragonite is a translucent mineral with a density of 2.947 g cm^{-3} (Ralph & Chau 2010). Measured skeleton densities for *L. pertusa* were up to 6.8 % lower, ranging from 2.746 to 2.780 g cm^{-3}, revealing the presence of residual organic matrix within the skeleton. Deviations from the density of pure aragonite in marine biological skeleton structures are well documented. Measured densities for *L. pertusa* are intermediate to densities reported for tropical shallow-water scleractinian corals (Tab. 21):

Tab. 21 Scleractinian coral skeleton densities.

Species	Density (g cm^{-3})	Reference
Acropora humilis	2.622	Davies (1989)
Favia fragum	2.82	Mann (1994)
Lophelia pertusa	2.746 - 2.780	this study
Lophelia pertusa	2.75 ± 0.07	Dodds (2007)
Pocillopora damicornis	2.703	Spinaze *et al.* (1996)
Porites australiensis	2.810 - 2.819	Barnes & Devereux (1988)
Porites lutea	2.737 - 2.802	Barnes & Devereux (1988)

For acroporid corals the effect of different colonies and locations on the skeleton density was examined and results revealed that the density was relatively constant within a colony and even between sites (Bucher *et al.* 1998). The *L. pertusa* samples from Dodds (2007) were collected at the Mingulay Reef Complex (for a comprehensive site description see Roberts *et al.* (2005)) 600 nm north-west of the sample-site of this study (Oslofjord). Although the sample sizes of both studies were very limited, measured densities are comparable and suggest that site-specific variations in density are also very low for *L. pertusa*.

The measured fraction of biomass as a percentage of the whole buoyancy weight for *L. pertusa* was 0.88 ± 0.31 %. This is comparable with reported biomass fractions of 0.81 ± 0.17 % for *Pocillopora verrucosa* - an imperforate coral from the tropics (Davies 1989). For *L. pertusa* there are no biomass fractions published to date.

4.1.4.2. Skeleton length-weights relationships

Corallites length of this study (Oslofjord samples) were 1.4 cm on average and are intermediate to reported lengths from Fedje / Osterfjorden and Sula Reef corals with 1.0 and 1.7 cm, respectively (Mortensen 2001). The linear relationship between corallites diameter and length from the Oslofjord corals was highly significant ($R^2 = 0.56$, $P < 0.001$) and stronger than the correlation of the corallites from the Osterfjorden ($R^2 = 0.43$, $P < 0.001$) and Fedje corals (no significant correlation) but weaker than for the Sula reef corals ($R^2 = 0.68$, $P < 0.001$) (Mortensen 2001).

Based on the high variability of *L. pertusa* phenotypes Freiwald *et al.* (1997) defined different morphotypes but it is actually not known whether these morphotypes are genetically or environmentally controlled (Mortensen 2001).

The calculated relationships between corallite weights, length and - respectively - diameter are unique for *L. pertusa*. Therefore comparisons with published data were not possible. However, the strong linear relationship between calyx weight and a hypothised cylinder volume ($R^2 = 0.89$) reveals that a cylinder describes the morphotype of *L. pertusa* adequately. Additionally if both diameter and length of a corallite are known the corresponding dry weight can be determined sufficiently. In laboratory experiments the morphometric measurements can be used for normalisations of the metabolic processes (especially respiration rates where the exhibited tissue surface plays an important role). Very recent approaches in order to find geometric based normalisations for scleractinian corals (including *L. pertusa*) were performed using computer tomography (CT) and subsequent 3-dimensional surface reconstruction (Naumann *et al.* 2009). But even if this method reveals excellent accuracy its usability in practice is limited to the access of CT and 3D postprocessing routines. Furthermore a CT detects only coral carbonate skeleton and thus over- or underestimates the live tissue surface area composed by the polyps and the coenosarc (Naumann *et al.* 2009).

For future field studies the found equations are suggested to be used for an enhanced estimation of the carbonate budgeting of *L. pertusa* reef structures by high-precision video-mapping.

4.1.4.3. Ambient calcification rates

Growth rates for scleractinian corals have been typically reported in linear skeleton extension (LSE) or in weight gain as a percentage of the initial weight (G) according to the different methods (2.2.1.3). Commonly LSE rates were used for an estimation of how high a colony may develop above the seafloor over time (Roberts *et al.* 2009) while G was typically used in laboratory experiments for examining physiology based issues.

The earliest LSE measurement for *L. pertusa* was published in 1877 by Peter M. Duncan (1824-1891) who examined newly formed colonies on a trans-Atlantic telegraph cable (Duncan 1877). His reported average LSE of 7.0 mm yr^{-1} was in between the range of actual studies - specifying annual LSE growth rates for *L. pertusa* from 2.6 to 34 mm yr^{-1} (Mortensen & Rapp 1998; Gass & Roberts 2006) (Tab. 22). A comparably high variation in LSE was also reported for *Madrepora oculata*, (3 - 18 mm yr^{-1}; Orejas (2008)) another cosmopolitan scleractinian cold-water coral frequently associated with *Lophelia* reefs (Freiwald *et al.* 2004).

Mass-gain related growth rates (G) for *L. pertusa* are scarce. To date only one peer-reviewed short-term study (Maier *et al.* 2009) and one PhD-thesis (Dodds 2007) have reported growth rates for bulk calcification (whole branches). Their range encompasses more than two orders of magnitudes from 1.6×10^{-4} to 6.7×10^{-2} % d^{-1} (Dodds 2007; Maier *et al.* 2009). In this study the rates of calcification (Tab. 12 and 22) varied over time and between measurement methods (BWT or TAAT) but were - on average - on the same dimension. Maximum growth rates (7.1×10^{-2} % d^{-1}, Tab. 12) were comparable with mean calcification rates from Maier *et al.* (2009) while mean rates (8.7×10^{-3} % d^{-1}, Tab. 22) range exactly between the rates from Maier *et al.* (2009) and Dodds (2007).

The high variation in growth rates has motivated an discussion about the reasons and drivers determining cold-water corals growth and distribution. Generally azooxanthellate corals were regarded to have low growth rates due to the absence of symbiotic algae which are suggested to enhance calcification in zooxanthellate coral species (Goreau 1959; Pearse & Muscatine 1971; Allemand *et al.* 1998; Al-Horani *et al.* 2003a). In all studies (Tab. 22) bulk growth rates (G) of *L. pertusa* were indeed low compared to shallow-water zooxanthellate branching species with growth rates of 0.2 - 2.3 % d^{-1} (Erez 1978; Ferrier-Pagès *et al.* 2000; Reynaud *et al.* 2003). For young *L. pertusa* polyps however, maximum growth rates of 1 % d^{-1} were measured which are fairly similar to those of tropical zooxanthellate corals (Maier *et al.*

2009). Additionally the LSE for most of the zooxanthellate coral species were also on the same range (e.g. 6.0 - 24.0 mm yr^{-1} for *Montastrea annularis* - a dominant hermatypic Caribbean scleractinian coral (Huston 1985)) as for *L. pertusa.* Some extreme fast growing zooxanthellate acroporid species may even yield grow rates of > 150 mm yr^{-1} (Huston 1985).

A positive correlation between temperature and growth rates for zooxanthellate corals is extensively documented (Weber *et al.* 1975; Nie *et al.* 1997; Lough & Barnes 2000; De'Ath *et al.* 2009) and various reasons were suggested as explanation (e.g. higher Ω_{Ar} saturation states in warmer waters promoting $CaCO_3$ accretion, enhanced physiological exchange processes between host coral and zooxanthellae, etc.). However, examined temperature ranges were according to the corals natural warm-water environment and physiological tolerances. The range was far more narrow (only a few °C) than the wider scope of cold-water corals ecoenvironmental ranges (e.g. 4 - 12 °C for *L. pertusa*). But surprisingly, the highest LSE rates for *L. pertusa* (26 ± 5 mm yr^{-1}) were measured on conductors (wide-diameter pipes) of oil-platforms in the northern North Sea at 95 - 106 m water depth coinciding with cold Atlantic waters of 7 - 11 °C (Gass & Roberts 2006). It has therefore been suggested that even though temperature has an important influence on the distribution of *L. pertusa* habitats (Dons 1944; Freiwald 2002; Roberts *et al.* 2003) water-mass properties and food supply could be of even higher significance (Frederiksen *et al.* 1992; Gass & Roberts 2006). Feeding frequency has been demonstrated to positively affect growth rates of both, tropical shallow-water scleractinian corals (Ferrier-Pagès *et al.* 2003; Hii *et al.* 2008; Houlbrèque & Ferrier-Pagès 2009) and the cold-water coral *L. pertusa* (Mortensen 2001). Generally nutrient (biomass) input into the deep-sea decreases exponentially with increasing depth (Rex 1981) - making the deep-sea a food-depleted environment (Thiel 1979; Wilson & Hessler 1987). Accordingly *L. pertusa* was found most frequently on the continental margins where high currents provide enhanced nutrient and food availability (Spiro *et al.* 2000).

A distinctive feature of *L. pertusa* is its occurrence in two colour varieties and several different morphotypes (Freiwald *et al.* 1997). The fast growing *L. pertusa* colonies from the oil-platforms were attributed to the *tabular* morphotype (trumpet-like tabular shaped corallites, deep calices and a thin stereome) whereas corals from Dodds (2007) and those used in this study have much thicker skeletons with more widely interspersed polyps (*brachycephala* and *gracilis* morphotypes). It is therefore possible that weight gain based growth rates from oil platform corals were on a comparable range than for other areas and that

the faster growth could also be a response to exceptional environmental conditions (e.g. high sedimentation rates).

Another important source of variation comes from the suggested allometric and pulsed growth pattern of *L. pertusa*. The highest linear growth was measured in the early growth stages of the polyps (Mortensen & Rapp 1998; Mortensen 2001; Brooke & Young 2009). Inversely linear extension rates decreased drastically with increasing age of the corallites (Mortensen 2001; Brooke & Young 2009). The maximum calcification rate of 1 % d^{-1} in the study of Maier *et al.* (2009) was also only measured on young and isolated polyps (see above). The comparatively low bulk calcification rates in contrast support the allometric growth pattern model. Mortensen (2001) also observed that linear growth occurred as episodic events with rapid growth (max. 1.2 mm d^{-1}) followed by longer time intervals (> 4 weeks) with nearly zero growth. Interestingly during the two years of observation no significant correlation was found between linear extension rates and changing seawater temperatures or salinities (Mortensen 2001). Allometric as well as episodic / pulsed growth is typical for solitary, massive and branching scleractinian corals and for example responsible for the density banding patterns in cross-sections of coral skeletons (Emiliani *et al.* 1978; Barnes & Devereux 1988; Nagelkerken *et al.* 1997). Episodic growth can also be regarded as an explanation for the high and inhomogeneous variations in the growth rates of the unmanipulated long-term incubations in this study.

In summary bulk calcification depends strongly on the proportion of older and younger polyps in a branch (Maier *et al.* 2009) and was affected by several interconnected factors including time. Additionally a progressive growth did not necessarily reflect optimum life conditions and to date it is unknown to what extent calcification is controlled environmentally and / or genetically.

Tab. 22 Linear skeleton extension growth rates (**a**) and calcification rates measured as weight gain in a percentage of the initial weight (**b**) for the main bioherm forming cold-water coral *Lophelia pertusa*.

Growth rate	Method	Origin depth (m)	Reference
a) Linear skeleton extension (mm yr^{-1})			
7.0	man-made structure of known age	955 - 1006	Duncan (1877)
6.0	man-made structure of known age	800	Wilson (1979)
25.0	C/O stable isotopes	300	Mikkelsen *et al*. (1982)
19.0	C/O stable isotopes	250	Freiwald *et al.* (1997)
5.5	C/O stable isotopes	200 - 350	Mortensen & Rapp (1998)
2.6	aquarium grown corals	200 - 350	Mortensen & Rapp (1998)
26.0	man-made structure of known age	60 - 109	Bell & Smith (1999)
9.4	aquarium grown corals		Mortensen (2001)
5.0	man-made structure of known age	100	Roberts (2002)
19.0 - 34.0	man-made structure of known age	95 - 106	Gass & Roberts (2006)
15.0 - 17.0	aquarium grown corals	Mediterranean 214 - 218	Orejas *et al*. (2008)
2.4 - 3.8	*in situ* field study with stained corals	Gulf of Mexico 430 - 520	Brooke & Young (2009)
b) Percentage weight gain (% d^{-1})			
1.6 E-04	Buoyancy weight	Rockall Banks 600	Dodds (2007)
3.7 E-04	Buoyancy weight	Mingulay reef 130	Dodds (2007)
6.7 ± 1.9 E-02	^{45}Ca labelling	Mingulay reef 150	Maier *et al*. (2009)
3.3 ± 2.4 E-02	^{45}Ca labelling	Oslofjord 109	Maier *et al*. (2009)
8.7 ± 11.7 E-03	Buoyancy weight	Oslofjord 100	this study
6.8 ± 3.2 E-03	Delta total alkalinity	Oslofjord 100	this study
8.7 ± 3.2 E-03	Buoyancy weight	Sula reef 285	this study

4.2. Environmental change related experiments

4.2.1. *L. pertusa* ocean warming stress response

4.2.1.1. RNA/DNA ratio measurements

This method is based upon the assumption that in a common tissue cell the amount of DNA is fixed, whereas the amount of RNA depends on the actual activity of protein biosynthesis. Progressively growing or differentiating somatic cells are associated with active protein production and therefore the RNA/DNA ratio is higher than in cells with low metabolic activity. The RNA/DNA ratio method has therefore been used in a wide variety of organisms as an indicator for growth rate, biomass, or general metabolic status. In marine animals this technique was applied for example to fish larvae (Bullow 1987; Kawakami *et al.* 1999; McNamara *et al.* 1999; Clemmesen *et al.* 2003; Tanaka *et al.* 2008), copepods (Nakata *et al.* 1994; Wagner *et al.* 1998; Biegala *et al.* 1999) and other marine invertebrates (Wright & Hetzel 1985; Frantzis *et al.* 1992; Pierce *et al.* 1999; Wo *et al.* 1999) as well as to bacteria and microbial communities (Kerkhof & Kemp 1999; Yu & Mohn 1999). In zooxanthellate corals RNA/DNA ratio measurements were demonstrated to be an appropriate indicator of metabolic activity (Buckley & Szmant 2004) and of acclimatisation / adaptation along altered environmental gradients (Bak & Meesters 2002; Meesters *et al.* 2002). In this study the RNA/DNA measurements were used for the first time on a cold-water coral (see section Cooperations).

Based on the coefficients of variation derived from measurements on control homogenates with unmanipulated corals (n = 30) a methodological precision of ± 3 % was determined. However, due to a relatively high autofluorescence of the coral tissue reliable data was only obtained in a small range where a linear correlation between measured fluorescence and sample size existed (for details, see Gutperlet (2008)).

Temperature stress response experiment

RNA/DNA ratios from the corals in the control group (T, 8 °C) varied over a wide range reducing the discriminatory power of the stress groups ratios. A strong variation in RNA/DNA ratios was also observed in the zooxanthellate coral *Madracis mirabilis* suggesting generally large intrinsic metabolic differences among scleractinian corals (Gates & Edmunds 1999). Other reasons may cohere with those suggested to be responsible for the variations in the growth rates (mainly different proportions of young and old polyps).

Despite the high variations in the control groups the RNA/DNA ratios of the stress groups were significantly lower revealing the corals sensitivity towards elevated temperatures as well as the practicability of the RNA/DNA ratio method as an indicator for "temperature stress" with respect to metabolic activity. These results are consistent with the findings of Buckley & Szmant (2004) in reporting a decrease of the RNA/DNA ratios at elevated temperatures in the tropical scleractinian coral *Montastrea annularis*.

In a methodical evaluation (Gutperlet 2008) *L. pertusa* polyps were incubated at ambient seawater conditions identical to those of the control groups (placed in the same CRS) for 5 months without any nutrition. *L. pertusa* is known to withstand several months of starvation (up to 22 months!). Adverse effects like an increasing mortality and deterioration of the polyp's condition[1] can be observed on polyps starving for 3 months or more (Mortensen 2001). RNA/DNA ratios of the starved polyps were therefore assumed to represent the lowest metabolic activity and thus a good proxy for lowest levels of fitness in *L. pertusa* specimens (Fig. 67). In account of this the median RNA/DNA ratio of the $T_{+10°C}$ treatment lies below the median ratio of the starved polyps. This may indicate that a temperature of 18 °C is far beyond the compensatory capabilities for thermal stress in *L. pertusa*. Additionally, the polyps in this treatment looked increasingly worse (e.g. low expansion, high mucus production) and the disintegration of tissue led to a termination of this treatment after an incubation time of only three days (2.3.1.).

Median RNA/DNA ratios from the $T_{+3°C}$ (= 11 °C) treatment were in between those measured in the control group (T) and the starved corals (Fig. 67) suggesting that this temperature was also above the physiological optimum of this species or that the time allotted for acclimatisation (to recover higher ratios) was too short. The polyps in this treatment visually looked healthy and studies on the polyps' behaviour demonstrated an acclimatisation of the expansion-retraction behaviour pattern (see 4.2.1.2). However, measurements of the respiration rates performed at the end of the experiment (14 days) where lower than immediately after raising the temperature (acute stress) but still higher than the initial respiration rate measured at ambient temperature at the beginning of the experiment (Gutperlet 2008). Hence it can not clearly be stated to what extent the corals were acclimatised or still under thermal stress at the time of the RNA/DNA ratio measurements.

[1] Polyps showing poor condition were retracted and changed colour from transparent to more yellow-brownish (Mortensen 2001).

In the Ionian See (Mediterranean basin) *L. pertusa* was found in water temperatures of 13.8 °C (Taviani *et al.* 2005) which marks the maximum of the actually known ecoenvironmental range normally reported between 4 and 12 °C (Rogers 1999; Freiwald *et al.* 2004; Roberts *et al.* 2009). Thus, the experimental temperature was in the normal thermal range of *L. pertusa* and future studies should address the question whether an increased acclimatisation time would balance the RNA/DNA ratios or not. In the latter case the hypothesis that an evolutionary adaptation of the Mediterranean cold-water corals has made them physiologically and genetically separated from their relatives in the North Atlantic can be proposed.

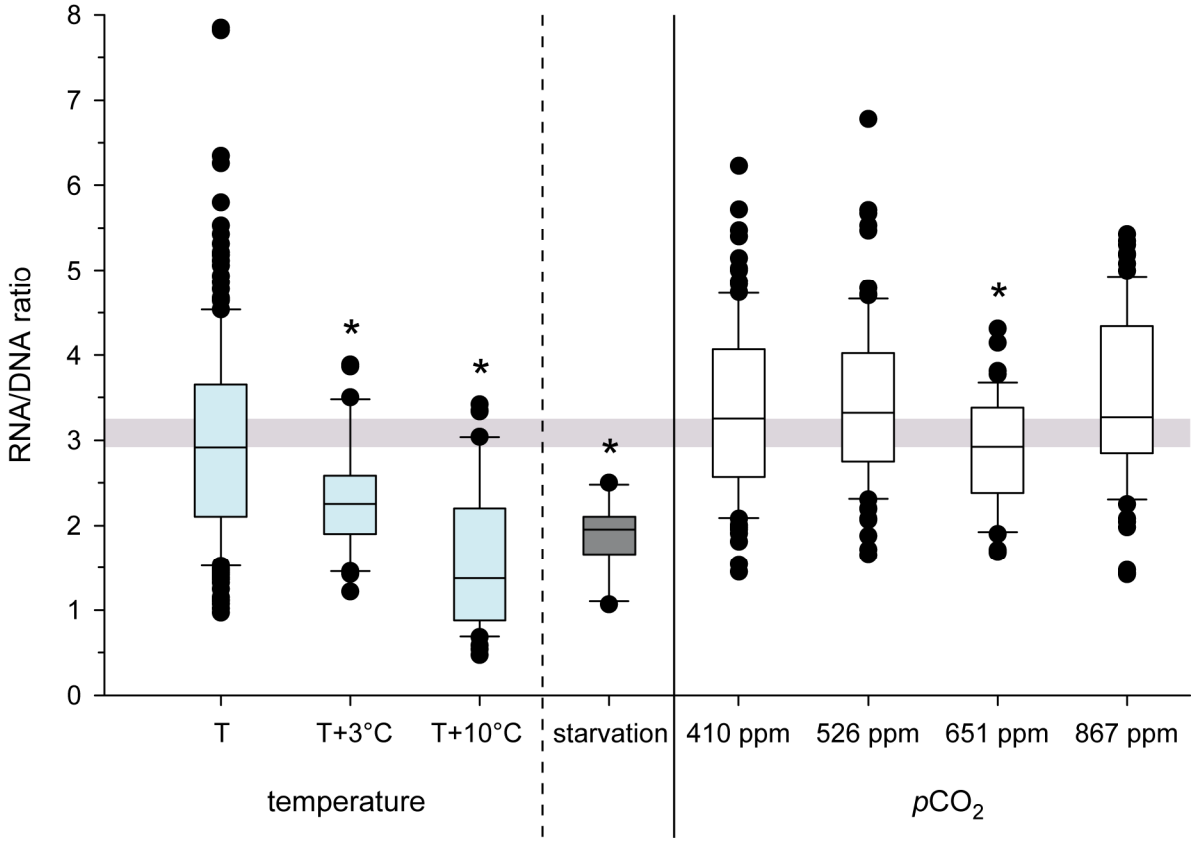

Fig. 67 RNA/DNA ratios of *L. pertusa* from three experiments separated by vertical lines. The horizontal grey bar indicates the RNA/DNA-ratio area which was determined by the medians of the unmanipulated control corals from the temperature (T) and pCO_2 (410 ppm) experiment. Corals in the experiment "starvation" were incubated identical to "T" but without feeding them for 152 days. Box and whiskers are ± standard errors and deviations, respectively. Black dots indicate outliers and the asterisks indicate statistically significant differences between treatments and the control groups (T, 410 ppm).

Ocean acidification stress response

Surprisingly RNA/DNA ratios seemed not to be negatively affected by elevated pCO_2 conditions whereas growth rates of the same corals decreased significantly with increasing pCO_2 concentrations. Moreover, a temperature increase of only 3 °C seems to be more problematic for *L. pertusa*'s fitness than a doubling in the pCO_2 concentration (corresponding to aragonite undersaturated conditions) (Fig. 67)!

It is therefore possible that for *L. pertusa* and other scleractinian corals calcification is more dependent on the seawater chemistry and the polyps capability to react / acclimatise to changes than the corals general state of fitness. The experiment of Fine and Tchernov (2007) in which two scleractinian species from the Mediterranean Sea survived at highly undersaturated conditions in form of entirely decalcified anemones-like polyps (referred to as ecophenotypes) give further evidence for the strong plasticity of the calcification process and the corals survivability towards large-scale environmental changes with respect to ocean acidification.

4.2.1.2. Polyp behaviour studies using PoBeMon tool

Polyp behaviour is an important factor with respect to the polyp's health. To check the "polyp status" regularly is one of the most important tasks in marine reef aquaristics. The polyps react to changes in water quality or other disturbances immediately and long before complex or time-consuming analysis may point out the possible causes. In scientific studies expansion / contraction behaviour patterns have been extensively examined on tropical shallow-water corals (Kawaguti 1954; Abel 1963; Lewis & Price 1975; Lasker 1979; Brown *et al.* 1994; Levy *et al.* 2001; Levy *et al.* 2006) and sea anemones (Gladfelter 1975; Sebens & Deriemer 1977). Depending on the question and habitat of the examined corals, most of these studies attributed their polyp behaviour patterns to diel cycles of food availability, tidal water currents or solar irradiance. Due to the high technical efforts needed to investigate cold-water corals to date only a few descriptions of their behaviour exists (Shelton 1980; Mortensen 2001; Roberts & Anderson 2002). For laboratory studies Roberts & Anderson (2002) developed a method based on time-lapse video recordings of *L. pertusa* polyp silhouettes using a Freznel lens and indirect infrared illumination. The method developed in the framework of this thesis is a technical advancement of the one used by Roberts & Anderson (2002) with the main advantages of being autonomous with respect to the image analysis and to being independent from an experimental apparatus (see also 5.2.1).

Normal polyp behaviour patterns

At "normal" conditions (e.g., constant water flow, stable water properties, absence of epibionts, etc.) *L. pertusa* polyps exhibit a variable periodicity of retractions and extensions without any diurnal pattern (Fig. 53 - 56, a). None of the polyps showed a permanent expansion during the 48 hours of monitoring. These observations are in accordance with Roberts & Anderson (2002). They also describe a variable rhythm of expansions and retractions. As a result of both observations the description from Shelton (1980) that polyps of *L. pertusa* would remain permanently expanded unless mechanically disturbed should therefore be regarded as outdated. However, Shelton's observation that there is no continuous nerve net connection between individual adult polyps within the same colony was supported by Roberts & Anderson (2002) with their description of asynchronous behaviour of adjacent polyps. In this study most of the time expansion and retraction of adjacent polyps were asynchronous but sometimes a synchronisation for a few cycles was observed. Unfortunately it could not be determined whether these "synchronisations" were intrinsic or caused by external disturbances (e.g. small temporal vibrations in the climate chamber). To date the reason for the periodic contraction and re-expansion is unknown but Robert & Anderson (2002) suggested that it could reflect the polyps need to exchange water within the coelenteron or expel undigested food remains. Interestingly, a total polyp extension of 100 % was mostly a short-time event of a few minutes. During the expanded phases the polyps stayed between 60 - 80 % in the majority of cases. This may indicate that a full expansion is exhausting for the polyp and not necessary to maintain the basic vital functions (mainly "filtrating", gas exchange and excretion). The apparent absence of a diurnal pattern further suggests that in azooxanthellate corals behaviour is rather linked with changing water conditions and food availability than the time of day[1].

Polyp behaviour pattern under thermic stress

In subexperiment I (18 °C) the results were consistent with those from the RNA/DNA ratio measurements of the same specimens. It has therefore been demonstrated, that lowest metabolic fitness corresponds to decreased polyp expansion behaviour. In this context it is worth mentioning that frequency of extension / retraction immediately increased after elevation of the temperature (Fig. 54) but that frequency declined the longer the corals were exposed to the new temperature. Hence, in a future approach the software should be extended

[1] The time of day corresponds to the solar irradiance which is known to be an important trigger in the host - symbiont interactions of zooxanthellate corals (Lasker 1979).

by a pattern recognition algorithm in order to use this parameter as an additional indicator for polyp behaviour under acute stress conditions (see also 5.2.1). Corals in the subexperiment II (11 °C) behaved relative similar to those of the subexperiment I during the first 24 hours after the temperature change: after a phase with increased frequency and average extension states their group extensions (see p. 118) decreased significantly. Despite a decreasing trend with time the corals group extension increased back to a state comparable with those of the non-manipulated corals of the control group after 14 days of incubation at 11 °C (Fig. 58 c). This indicates an acclimatisation process of *L. pertusa* towards moderately elevated temperatures.

The fact that extension behaviour completely contrasted the RNA/DNA ratio measurements (significant differences in the polyps fitness between the stress and control group) may suggest that:

(1) polyp extension behaviour does not necessarily reflect the metabolic state at low to moderate levels of stress,

(2) the experimental time was too short and the physiological acclimatisation was not finished yet, or

(3) the temperature was too high for a successful acclimatisation with the consequence of a degraded metabolic activity.

Further work should therefore focus on improvements of the methods as well as longer acclimatisation times in order to assess the reason(s) for the difference between behaviour and RNA/DNA ratios.

4.2.1.3. Respiration measurements using advanced optode technology

Methodological considerations

For the study of the ecophysiology of a species precise measurements of oxygen concentrations are required for calculating rates of consumption and production. In the past two methods have been widely used and established: iodometric titration after Winkler (1888) and electrochemical measurements using Clark electrodes (1956). In short, the titration after Winkler yields the highest accuracy but measuring is time consuming. Additionally for each measurement a water sample is needed which is sometimes problematic (especially when the water volume of an experiment is limited or has to be constant). The Clark electrodes are adequate in their accuracy and reproducibility and can be used without diminishing the water

volume. However for reliable results the water sample has to continuously circulate around the electrodes and in long-term measurements they are subjected to a remarkable drift. For a comprehensive comparison of both methods in small volumes of seawater, the reader is referred to Peck & Uglow (1990).

In the framework of this thesis advanced optode technology was applied as an alternative method to measure oxygen concentrations without the potential problems outlined above. General advantages of optodes are:

- they are small (no sensor head needed, only a flat spot),
- they do not consume O_2,
- detection limit up to 15 ppb
- measurements are possible over a temperature range wider than for classical methods
- accuracy of ± 1 % (air saturation)
- long-term stability with nominal drift
- autoclavable / gamma-sterilised
- no cross sensitivity (CO_2, H_2S, NH_3, pH)

In the planned respiration measurements on *L. pertusa*, only relative rates (as a function of oxygen consumption) were of interest. Thus, for evaluating the methodological reliability, only the determination of the reproducibility and the sensor drift was of relevance. For a methodological comparison between optodic and Winkler based oxygen measurements, see Hydes *et al*. (2007).

At nearly constant environmental conditions (temperature and oxygen saturation) measured drift rates for oxygen and pH sensor spots were extremely low (see 3.1.4.1). For example, in 24 hrs, phase angles for oxygen and pH sensor drifts depleted only about 0.12° and 0.10°, respectively. In terms of "percent air saturation" and pH the drift corresponds to a rate of about -1.1 % d^{-1} and -0.03 pH d^{-1} respectively. Additionally during the 40 hours of measurements, the drift in both sensor types was strongly linear (Fig. 49), allowing precise corrections for drift if necessary. Precision in the pH sensor spots was acceptable (± 0.09 pH) if pH is used only for monitoring reasons (e.g. to follow trends) but needs further improvements (e.g. modified calibration routines) if the pH measurements were to be used for calculations of the carbonate system parameters. Precision of the oxygen sensors was very high (± 1.1 µmol L^{-1} or ± 0.36 % air saturation) and on a comparable size to classical Winkler

titrations (1.5 - 2.2 µmol L^{-1}; Hydes *et al.* (2007)) which demonstrates their successful application in long-term continuous oxygen measurements.

L. pertusa holobiont respiration at ambient and elevated temperatures

The rising concern about climate warming and weather phenomena like El Niño / La Niña has motivated an extensive research effort on tropical coral ecophysiology. Shallow-water hermatypic corals from the tropics are commonly found in a symbiotic relationship with dinoflagellates (zooxanthellae) and evolved to become dependent upon a very narrow temperature range. Thus reported sensitivities as well as metabolism pathways can not be easily transferred or compared with cold-water corals such as *L. pertusa*.

Although *L. pertusa* are important deep-sea ecological engineers (Jones *et al.* 1994) this thesis is only the second attempt to assess their respiratory physiology and the first study examining respiration rates on any cold-water coral using optode technology.

Respiration rates of this study measured at *in situ* temperature (7.5 °C) were in the same range as reported rates for *L. pertusa* samples from two other North Atlantic locations (Tab. 23). The fact that both studies revealed relatively similar rates at two different temperatures ($_{\Delta}T$ = 1.5 °C) may indicate that a value of ~ 0.3 µmol O_2 g^{-1} h^{-1} represents an oxygen consumption specific for *L. pertusa* living in the North Atlantic.

Tab. 23 Mean rates of oxygen consumption of *Lophelia pertusa* from three different North Atlantic locations normalised to skeleton dry weight.

Location	Rate (µmol O_2 g^{-1} h^{-1})	(CV)	n	Temperature (°C)	Reference
Rockall	0.25 ± 0.02	(25.68)	8	9.0	Dodds (2007)
Mingulay	0.36 ± 0.09	(51.36)	4	9.0	Dodds (2007)
Sula Reef	0.30 ± 0.06	(19.05)	4	7.5	this study

When the temperature was modified the oxygen consumption of *L. pertusa* was clearly affected. Respiration rate at 11 °C was about 58 % higher when compared to the rate measured at control temperature of 7.5 °C (see 3.1.4.2). This result is in good accordance to the findings of Dodds *et al.* (2007), reporting a 50 % increase in response to a temperature change from 9 to 11°C and to studies on tropical scleractinian corals, which also demonstrated the interrelation of respiration rates with temperatures (Coles & Jokiel 1978; Edmunds 2005).

The results are also in agreement with the findings of the behaviour studies. As an immediate measure for regulation of oxygen consumption the polyps can increase their surface to volume ratio through expansion (see feeding regimes). Although respiration was not quantified during the behaviour studies, measured polyp expansions were highest during the first hours after the temperature increase what strongly suggests higher rates of oxygen consumption during this phase (Dodds 2007). The high Q_{10} values (3.65) are above the upper limit of the van't Hoff Q_{10} rule of 2-3. This suggests that *L. pertusa* may not be able to compensate for changes in temperature, thus being sensitive to climate-change driven ocean warming. This would lead to enhanced food requirements and would have severe implications for the overall energy budget of the animals and therefore their growth, calcification performance, and competitiveness.

Preliminary results from respiration measurements performed at the end of the long-term ocean acidification experiment revealed that respiration rates decreased significantly with increasing pCO_2 by an average of 20 - 30 % within the range of 400 to 1,200 ppm pCO_2, suggesting that mean metabolic rates may decline with ocean acidification. Thus ocean warming and ocean acidification will have diverging impacts on the metabolism of *L. pertusa*, the physiological causes of which have yet to be studied in greater detail.

4.2.2. *L. pertusa* ocean acidification stress response

4.2.2.1. Short-term incubation experiment (STE)

Methodological considerations

The permanent bubbling with ambient or pCO_2-enriched pressured air in the bioreactors lead to an increase of the salinity in all bioreactors - especially in the blanks. For unknown reasons evaporation in the blanks was on average 5 % higher than in the replicates with the corals. It is possible that the intensity of bubbling in the blanks was higher than in the replicates because the bubbling was fine-adjusted with particular care on the bioreactors containing corals in order to prevent them from surrounding air-bubbles (which could be misinterpreted from the polyps as food-particles as previous aquarium observations indicate). However, salinity measurements of the blanks and their corresponding TA revealed a quasi perfect regression ($R^2 = 0.99$) allowing precise corrections for evaporation in the replicates with the corals[1].

Initial nutrient concentrations for nitrate, nitrite, ammonium, and phosphate were compared with their final concentration and measured on water samples gathered at day 10 after removing the corals for the subsequent RNA/DNA ratio determinations. As expected all nutrients increased their concentrations due to biological activity (especially permanent release of mucus) but final concentrations were in the same range or even lower than concentrations reported for CWC habitats in the North-east Atlantic (Davies *et al.* 2008). An influence of the nutrients on the corals as well as on alkalinity measurements was therefore unlikely.

The corals for the STE were taken from the CWC-MS in February 2008. At this time *L. pertusa* samples from the Oslofjord were cultivated in the CRS at a temperature of 8.0 ± 0.5 °C. Even though the climate chamber was set to lower air temperatures (~ 6 °C) the measured water temperatures in the bioreactors and the water bath increased spontaneously to a constant 9.0 ± 0.1 C°. A reason for this was found in the permanent bubbling with ambient or pCO_2-enriched pressured air which was imported from a gas-mixing system situated in an adjacent and well-temperated room. Although this temperature was slightly elevated compared to the CWC-MS or the *in situ* winter temperatures at the reef-site (7.0 °C, (Rüggeberg & Form 2007)) the applied temperatures were well within the range of

[1] In practice, the corrections for evaporation were limited by the precision of the salinity measurements (± 0.1‰) leading to an overall reproducibility in the TA of ~ 6 - 7 µmol kg^{-1}.

environmental tolerances for *L. pertusa*. in the North-east Atlantic (6.7 - 14.9 °C, see introduction or Davies *et al*. (2008)).

For accurate working the WÖSTHOFF gas mixing pumps need to be supported with the right amounts of CO_2 free air and pure CO_2. For example a single pump needs per hour about 240 litres of CO_2 free air to mix it with a few ppm of pure CO_2. Projected onto the 3 pumps and the duration of the experiment more than 170,000 litres of CO_2 free air were needed. This went beyond the scope of CO_2 scrubbers and therefore it was decided to use ambient air as a substitute and to accept fluctuations in the mixed gases due to CO_2 variations in the air (± 30 - 40 ppm).

As a consequence of respiration and calcification the carbonate system developed individually in all bioreactors. The given carbonate system (Tab. 15) reflected only the established mean parameters at the seventh day integrated over the respective pCO_2-channels for the predefined treatments. pH-measurements on every second day revealed a general shift to lower pH levels in the course of time. This could also explain the relatively high pCO_2-value of the "ambient" treatment (506 ppm). A perturbation of the bioreactors with higher flow-rates / pressures in order to compensate for the respiratory CO_2 was not practicable due to the corals sensitivity to air bubbles (see above).

The statistical level of significance was higher when growth (weight gain) was normalised against polyp number ($P < 0.01$) instead of initial weight ($P = 0.03$) revealing a better fit of the data and therefore the first normalisation as a preferable choice. However, trends in both normalisations were on a comparable dimension and for comparisons with other studies on corals, the well established second normalisation can be used safely.

Ambient calcification rates

Measured calcification rates at unmanipulated pCO_2 conditions ranged from 4.86×10^{-3} to 1.17×10^{-2} % d^{-1} (mean 6.80×10^{-3} % d^{-1}). While the maximum rate was in the same range as the average bulk calcification rate for *L. pertusa* reported in the short-term study of Maier *et al*. (2009) - average calcification rate of this study was about one order of magnitude lower than in the previous study. However, replicates in the study of Maier *et al.* (2009) consisted only of about 2.86 ± 0.24 g $branch^{-1}$ (6.55 ± 0.32 polyps $branch^{-1}$) whereas replicates of this study were much heavier with 27.17 ± 7.68 g $branch^{-1}$ (32.31 ± 11.85 polyps $branch^{-1}$) revealing different proportions of fast growing young - and slow to stagnant growing adult

polyps. Additionally calcification rates of both studies were measured with different techniques (^{45}Ca labelling and BWT in Maier *et al.* (2009) and this study, respectively) and on different time horizons (one and nine days in Maier *et al*. (2009) and this study, respectively). In a more comparable approach (sample sizes of 28.93 - 60.55 g branch^{-1}, duration: 7 days) average bulk calcifications rates of 1.55 - 3.74 × 10^{-4} % d^{-1} were measured (Dodds 2007). Thus our ambient calcification rates were intermediate in the broad range spanned from both studies and considered to represent characteristic values for the cold-water coral *L. pertusa*.

Calcification rates in response to elevated pCO_2 conditions

Calcification rates for *L. pertusa* significantly decreased with increasing pCO_2 (3.2.2.1.2). A pH drop of 0.1 pH unit slowed down the corals growth by up to 26 - 29 %. Moreover, the critical threshold value with respect to aragonite saturation below which *L. pertusa* is not able to maintain positive growth was Ω_{Ar} = 0.99 - 1.06 (depending on the normalisation used).

Results of this study suggest a strong impact of rising atmospheric CO_2 concentrations on the growth of the cold-water coral *L. pertusa.* They exceed previous findings of Maier *et al.* (2009), reporting a decline of calcification in *L. pertusa* of more than 50 % for the end of the century.

4.2.2.2. Long-term acclimatisation experiment (LTE)

Methodological considerations

When the long-term experiment started a CRS supplied with ambient air (pCO_2 = 385 ± 30 ppm) was set-up to act as a control group (CRS 0). In order to aerate the water as much as possible with ambient air the pump sump was not completely covered with foil (as described in section 2.1.2.3). Unfortunately a technical failure of the cooling aggregate in the climate chamber during the first weeks of the experiment led to an intoxication of the biofilter in the pump sump with refrigerant fluid (which was sprayed into the climate chamber as an aerosol). As a result of this more than 80 % of the corals in CRS 0 died within the subsequent two weeks and the remaining corals did not recover to their former appearance within the next months. Some measured growth rates and water properties were therefore regarded to be unusable and due to a limitation of new samples (for restarting the treatment) the control group was discarded. However, all treatments with elevated pCO_2 conditions worked well and were unaffected by the incident because they were completely covered with lids and foil (see above).

Each aquarium of a CRS was supplied with water from the pump sump thus all corals of a treatment were exposed to the same water body. In terms of statistics the single coral branches in the aquaria of the whole CRS have to be regarded as pseudoreplicates sensu Hurlbert (1984) because an interaction amongst the corals could not be excluded. Pseudoreplication in CRS is a known issue and statistical comparisons between the replicates are problematic (Hurlbert 1984). In this study therefore only the mean values of all (pseudo)replicates of a treatment were compared with the mean values of the independent other treatments.

For the growth measurements the corals were buoyancy weighed at predefined intervals before, during, and after the experiment. A negative influence of the methodical procedures on corals growth rates could not be excluded but was regarded to be negligible because of the relatively large time intervals between repeated measurements and the absence of a decreasing trend in the growth rates of the corals maintained in the CWC-MS at unmanipulated conditions. In a methodical evaluation, Davies (1989) measured growth increments on a tropical shallow-water scleractinian coral (*Porites porites*) using the buoyancy weight technique in 24 hours intervals and compared the results with a control group, which remained untouched for 7 days. No significant difference was observed between the two approaches (Davies 1989). In contrast to other methods (e.g., ^{45}Ca labelling, Alizarin Red S staining), the buoyancy weight technique was stated as a non-destructive method not affected by handling artefacts (Davies 1989).

Although Mortensen (2001) did not find a significant relation between growth rates and seasonally-caused changes in temperatures and salinities during his two-year incubation of *L. pertusa*, both parameters have been suggested to determine *L. pertusa* growth and distribution patterns (see 4.1.4.3). In order to avoid unknown synergistic effects and shifts in the carbonate system (esp. in the ASS) temperature and salinity were decided to be kept as constant as possible. For temperature an accuracy of more than 97 % could be achieved after the replacement of all temperature control units during the initial adjustment phase. Small fluctuations in the salinity (± 0.4) occurred during the first incubation phase with natural seawater. This was due to some minor water exchanges with seawater from different North Atlantic locations with different salinity profiles. In the second incubation period with artificial seawater, fluctuations in the salinity were close to the detection limit of the conductivity measurement device (± 0.1).

Even though the first treatment (CRS 1) could not be considered as a control group due to its relatively high pCO_2 of 604 ppm, the corresponding ASS was adequately saturated (Ω_{Ar} = 1.4) and in the range of *L. pertusa* environmental tolerance of Ω_{Ar} = 0.6 - 1.8 (Davies *et al.* 2008). Also treatment two (Ω_{Ar} = 1.0) and three (Ω_{Ar} = 0.9) were in the same range and therefore the experimental gradient can be regarded as an established ecoenvironmental range showing *L. pertusa'*s sensitivity towards decreasing aragonite saturations.

Calcification rates in response to elevated pCO_2 conditions

The mean calcification rate in the first treatment with the well saturated aragonite levels was $8.70 \pm 3.18 \times 10^{-3}$ % d^{-1} and therefore in the same range as growth rate for the unmanipulated corals in the short-term experiment ($6.80 \pm 3.24 \times 10^{-3}$ % d^{-1}, see above) and for unmanipulated corals in the long-term observation of the CWC-MS ($8.68 \pm 11.7 \times 10^{-3}$ % d^{-1}, n = 34). Thus growth rates for the first treatment were considered to be representative for cold-water coral *L. pertusa* living at ambient aragonite saturation states. Surprisingly, average and maximum growth rates increased with decreasing aragonite saturation to $1.14 \pm 0.61 \times 10^{-2}$ % d^{-1} and $1.88 \pm 1.34 \times 10^{-2}$ % d^{-1} for treatment 2 and 3, respectively (Fig. 65). The increasing mean values were accompanied by an increasing variance and therefore no statistical significance could be found for the relationship between growth rates and pCO_2 concentrations. However, the highest growth rate (3.73×10^{-2} % d^{-1}) was found in treatment 3 featuring the lowest aragonite saturation state and no negative trend in growth due to elevated pCO_2 levels.

This is therefore the first study showing a positive response in calcification with respect to increasing pCO_2 concentrations for the main reef-forming cold-water coral *L. pertusa* and to the author's knowledge to any scleractinian coral in general. For tropical zooxanthellate corals an approximately linear decreasing trend in calcification rates with increasing pCO_2 concentrations was extensively documented (Gattuso *et al.* 1998; Marubini *et al.* 2003; Langdon & Atkinson 2005; Schneider & Erez 2006; De'Ath *et al.* 2009). Increasing pCO_2 concentration to 720 ppm, as projected for the end of the century, causes coral calcification to decrease by up to 80 % (Albright *et al.* 2008) and will cause bioerosion to exceed coral growth in many reef systems (Hoegh-Guldberg *et al.* 2007; Silverman *et al.* 2009). In contrast, calcification rates in two zooxanthellate temperate coral species from the Mediterranean were recently demonstrated to remain unaffected by comparable pCO_2 concentrations (Ries *et al.* 2009; Rodolfo-Metalpa *et al.* 2010). As an explanation it has been

suggested that the carbonate requirement of slow growing corals is low and that therefore the concentration of carbonate ions does not become limiting (Rodolfo-Metalpa *et al.* 2010). Even though these studies and the results of the LTE are contradictious to the majority of coral research published to date, they substantiate actual findings that marine calcifiers exhibit different responses to rising pCO_2 concentrations (Ries *et al.* 2009). For some species increasing calcification rates were also observed (Wood *et al.* 2008; Gooding *et al.* 2009; Ries *et al.* 2009) or calcification was maintained even though seawater was undersaturated with respect to $CaCO_3$ (Cohen *et al.* 2009; Miller *et al.* 2009). Positive net calcification at undersaturated conditions were also observed for *L. pertusa* by Maier *et al.* (2009) and in the STE and LTE of this study which suggests that *L. pertusa* is adapted to low aragonite saturation states. Although most of the currently known *L. pertusa* habitats are located in aragonite saturated conditions (Guinotte *et al.* 2006; Davies *et al.* 2008), they are horizontally distributed at depths close to and even below saturated horizons (Davies *et al.* 2008). Moreover, some solitary scleractinian deep-sea coral species can commonly be found in highly undersaturated waters (Fautin *et al.* 2009). Therefore it is not really surprising that *L. pertusa* was able to evolve to these conditions by evolutionary adaptation. An adaptation to low $CaCO_3$ saturation states was also suggested as an explanation for the different trends in calcification rates found in sea urchin larvae: growth rates in tropical and temperate species were, similar to tropical corals, positively correlated with aragonite saturation states whereas for slow-growing arctic species no significant relationship could be found (Clark *et al.* 2009). However, for the common brittlestar *A. filiformis* it was demonstrated that increasing calcification rates in response to elevated pCO_2 concentrations were accompanied by an increased metabolism and a loss of arm muscle mass (Wood *et al.* 2008). Hence it was emphasised that even though increased calcification could be compensated its physiological costs may reduce survival and fitness.

Although *L. pertusa* is capable to withstand several months without food supply (Mortensen 2001), specimens in the LTE were regularly fed and thus thought to be in good physiological condition, which probably enforces their capacity to cope with acidified conditions. Very little is known about the nutrition of *L. pertusa* in their natural habitat but $\delta^{15}N$ signatures (Duineveld *et al.* 2004; Duineveld *et al.* 2007) and fatty acid composition in *L. pertusa* tissues (Dodds *et al.* 2009) indicate that it predominantely relies on food supplied from surface production. Vertical flux of surface-derived food to deeper waters varies greatly in time and magnitude, both on a seasonal and inter-annual basis. Thus, in their natural habitat cold-water

corals are likely to experience strong fluctuation in their nutritional status, which will need to be considered in assessing their ability to cope with corrosive waters. Moreover, even though actively growing branches of *L. pertusa* might be able to withstand corrosive conditions, older parts of the coral stock not covered by polyps are mostly unprotected and may experience dissolution in undersaturated waters. This would weaken the reef structure with potentially severe consequences for overall reef integrity. Another critical aspect to be considered is the sensitivity of corals to ocean acidification during early life stages, as recently demonstrated by Albright *et al.* (2008). While the settlement of larvae of the shallow-water scleractinian *Porites astreoides* was not significantly affected at pCO_2 levels of 560 and 720 ppm, growth rates after settlement decreased by 50 % and 78 %, respectively, compared to the present day CO_2 concentration (Albright *et al.* 2008).

This was also the first time that different trends between a short-term and a long-term acidification experiment have revealed an acclimatisation effect on the calcification rate of a scleractinian coral. Even though results of the LTE give a little hope that - to a certain degree - *L. pertusa* will be able to cope with future ocean acidification the most important result of the present study was the highlighted necessity to scale experiments to the "size" of the organism. This has significant implications because the response of corals to elevated pCO_2 has mostly been measured during short- and mid-term experiments (hours to weeks) and therefore exclude any potential acclimatisation/adaptation to the altered conditions (Rodolfo-Metalpa *et al.* 2010).

5. Significance and Outlook

5.1. Final considerations

With the completion of this study after three years it was proven for the first time that it is possible to successfully cultivate and maintain *L. pertusa* - an important representative of the reef forming cold-water corals - in closed recirculating systems. The observed development of the water properties was highly predictable. This made it possible to maintain the system parameters (e.g. ammonium concentration) in predefined ranges. The reported values for the dissolved organic nutrients can be regarded as "safe" limits in respect to long-term cultivation which makes them an important baseline information for future research in this field.

The feeding experiments reported in this thesis have contributed significantly to our understanding of the nutritional requirements of *L. pertusa*. For the first time the whole feeding process was video-documented and nematocyst adhesion was confirmed as the exclusive mode of ingestion for mesozooplankton. A few authors have reported feeding rates of nonnatural life food (*Artemia* spec.) but this thesis is the first publication to report feeding rates of live copepods which are expected to be the main food source of *L. pertusa* in the field. Moreover, the observation that - even at moderate water currents - only a small fraction of the live food particles remains attached to the polyp after initial contact but that the prey is subsequently killed by the cnidocyst activity has led to the formulation of the "passive nursing hypothesis": In an open reef, polyps located on the upper layer of the framework kill a certain amount of the passing live zooplankton making it easier to catch them for the coral polyps situated several generations deeper in the framework. This hypothesis should be verified in the field by working with labelled live and dead copepods and combined with studies addressing the general dynamics of zooplankton in the deep-sea bottom layer. Such an approach would significantly improve our understanding of biogeochemical fluxes on *L. pertusa* bioherms.

The experiments with two different food qualities of the same food source have revealed that *L. pertusa* is able to differentiate between different nutritional qualities. Moreover, there is some evidence that under sufficient nutrition, skeleton growth depends neither on the quality nor the quantity of the food. This could indicate that calcification in *L. pertusa* is not directly dependent on the heterotrophic food supply. Future feeding experiments should therefore include isotopic measurements to trace the pathways of carbon from the ingestion to its

excretion or incorporation into the tissue and / or skeleton. These studies would help to identify the carbon source(s) for calcification, a controversially discussed issue in today's coral research with respect to calcification mechanisms.

The biomorphometric measurements and relationships obtained as part of this study provide valuable information that will help to scale and normalise the existing data. In combination with the weight based growth rates from the unmanipulated cultivations, it is now possible to compare gravimetric growth with length growth. This is important from an ecological point of view since all growth rates reported from the field were given as linear skeleton extensions (Tab. 22).

The major aim of this thesis was to investigate the influence of anthropogenic climate change on the ecophysiology of *L. pertusa*. In view of this, several new methods and techniques to measure ecophysiologically important parameters under various environmental conditions were developed and successfully applied to *L. pertusa*. RNA/DNA ratio measurement have revealed that *L. pertusa* is sensitive to elevated temperatures, even if they are still in the range of its ecoenvironmental distribution. To date it is not clear whether a longer acclimatisation time would change these results but the response is consistent with the findings from the optodic based respiration measurements. This strongly suggests that *L. pertusa* is a stenothermic species and thus sensitive to rising seawater temperatures.

However, the present thesis has also demonstrated that *L. pertusa* exhibits converse trends in its growth rates, when experiments with increased concentrations of CO_2 were carried out on different time spans and with different experimental approaches. Unexpectedly the highest calcification rates were measured in corals maintained at undersaturated seawater concentrations with respect to aragonite ($\Omega_{Ar} < 1$). Hence this is the first study showing a positive response in calcification to increasing pCO_2 for an important bioherm-forming cold-water coral species and - to the author's best knowledge - for scleractinian corals in general. The fundamental difference in the observed responses between warm- and cold-water corals likely reflects an evolutionary adaptation to the carbonate chemistry prevailing in their respective environments. Seasonal variation in Ω_{Ar} values in surface waters, with generally lower values in winter time, and advective transport of undersaturated waters from deeper parts of the ocean may temporarily expose cold-water corals to conditions corrosive for their unprotected skeletons. Therefore tolerance to temporary exposure to undersaturated waters appears to be a prerequisite for cold-water corals to colonise these environments. The high

variability in net calcification rates in the short-term incubation experiment - with occasional net dissolution in oversaturated conditions - implies that factors other than the external saturation state may be equally or more important in determining the momentary calcification rate of a given polyp or coral branch. Moreover, the differences in observed responses between short- and long-term exposure experiments highlight the importance of long-term incubation studies which allow for complete acclimation of the test organisms.

5.2. Future developments and experiments

5.2.1. Some methodological improvements

Cultivation

Although the established long-term cultivation facilities have demonstrated their applicability, further developments should replace the angular shaped tank design with cylindrical tanks. This would allow a better control of the water currents and thus would reduce the number of places in the tanks which are unattractive for *L. pertusa* because of a stagnant water movement. Water treatment should be further improved by adding anoxic denitrification zones and temporary phosphate absorbers to the CRS. This would reduce the frequency of partial water exchanges by decreasing the accumulation of nitrates and phosphates in the process water. This would in turn allow to feed and cultivate more corals within the same amount of water.

RNA/DNA ratios

Further improvements of the RNA/DNA ratio measurements may be achieved, if ratios would be normalised according to the polyp rank in the skeleton-framework. Maier *et al*. (2009) and our own observations have indicated that growth rates of *L. pertusa* were highest in young apical standing polyps of a coral branch. Progressive growing should be accompanied by a higher proteinbiosynthesis und thus by higher RNA/DNA ratios compared to stagnant growing adult polyps. This inherent source of variation is believed to be minimised by assigning the measured ratio of a polyp to its polyp rank (age).

PoBeMon

The observation of coral polyp extension behaviour is generally a time- and manpower consuming affair. An improvement of this process has been realised by the author through the automation of the measurements on the actual polyp extension state with the aid of an image

recognition algorithm. In the present setup only real-time or recorded digital video-data was used and no Freznel lens or other experimental apparatus were needed. It is therefore believed that - after some improvements - the software will have the potential to analyse corals' *in situ* behaviour, recorded from ROV or manned submersibles. Proposed improvements are

- the programming of a graphical user interface (GUI) which should allow the user to select polyps by mouse instead of giving their positions in x-y-coordinates,
- enhancing the stabilisation algorithms for keeping the corals in a steady position,
- the use of high definition (HD) video material (1920 × 1080 pixels versus 720 × 576),
- the implementation of a virtual perspective modus (3D) for analysing of polyps which are not perfectly recorded in their profile view.

With these improvements and appropriate background data it should be possible to examine, if behaviour of single polyps is synchronised to a colonial behaviour ("superorganism CWC reef"), how environmental conditions affect behaviour and if there is any interaction with the associated reef fauna (sponges, brittle stars, polychaetes).

5.2.2. Experimental challenges

Climate change - From organism to cellular level, an outlook

Cold-water corals, such as *Lophelia pertusa*, do not contain photosynthetic symbionts, making them ideal study objects to solely consider calcification related ion transport. In future studies within the framework of the BMBF funded project BIOACID the physiological functioning of the calicoblastic epithelium from corals cultivated under different pCO_2 concentrations will be determined in *ex-vivo* measurements. The use of a Ussing chamber and patch-clamp techniques will allow the determination of transepithelial voltage, transepithelial resistance and equivalent short-circuit currents as characteristics of epithelial and / or cellular function. With pharmacological tools and changes in the solute composition on either site of the corals epithelium, it is aimed to uncover the transepithelial pathways for calcium and carbon during the calcification process and their sensitivities towards ocean acidification by identifying the involved ion transport proteins. In this context it is further addressed how corals can regulate pH in the calicoblastic cells and how they remove protons produced during the calcification process (see introduction) respectively. These studies should contribute to a

comprehensive mechanistic view about the effects of ocean acidification on the calcification of scleractinian corals.

Climate change - From organism to ecosystem level, a vision

A crucial question which remains unanswered by the climate change-related experiments is whether the ability to maintain high calcification rates over six months when incubated in undersaturated waters also enables *L. pertusa* to withstand permanent exposure to corrosive waters. Moreover, the fact that a temperature increase of only about 3 °C seems to be of higher relevance with respect to fitness and metabolism activity than a doubling of the pCO_2 emphasises the problem of synergistic impacts between ocean warming and ocean acidification. So the key question is, how "*adaptable to change*" *L. pertusa* is. Addressing this question requires a holistic approach, accounting for whole organism responses including respiration, fitness, defence, behaviour, growth, feeding, reproduction, dispersal and settlement along the ecoenvironmental gradients for both, temperature and CO_2.

To realise this aim, laboratory experiments like the present studies are important pillars of research, especially for deep-sea organisms. However, if we want to transfer our knowledge to the level of an ecosystem or higher we need to classify fieldwork as of equal, or even higher importance. Techniques for *in situ* pCO_2 perturbation experiments are suggested (Barry *et al.* 2010) and could be adapted to cold-water coral reef specific conditions. In this context it is noteworthy that in an open reef system, the formation of new framework is a permanent struggle between production (growth) and degradation (bioerosion). Future laboratory and field experiments therefore should also examine, how changing seawater properties affect biogenic carbonate stability and bioerosion.

Cooperations

The present work only became possible by cooperations with other institutions and through intense collaborations with students in the framework of their education.

In the following table these partners and their area of contribution are listed and assigned to the corresponding chapters:

Tab. 24 List of partners during the different phases in the frame-work of the dissertation.

Partner / *Institution*	**Related experiment(s)**	**Chapter(s)**	**Type of cooperation**
Michael Gruber Uwe Waller Ralf Traulsen *Aquarium Kiel*	Rearing facilities, food stock cultivation	2.1.2. 2.1.4.1.	Cooperation
Wiebke Holtmann *FB2*	Ammonium sensitivity	2.1.3.3.	Student thesis
Dirk Wehrend *TLZ*	HCB construction	2.2.2.1.	Cooperation
Catriona Clemmesen Helgi Mempel *FB3*	RNA/DNA-ratio method adaptation	2.2.5.	Cooperation
Jan Büdenbender *FB2*	SCB improvement	2.2.2.2.	Student thesis Diploma thesis
Stephanie Stratil *FB3*	Food density experiments with natural food sources	2.1.4.2.	Student thesis
Lennart Bach *FB2*	Feeding process observations	2.1.4.3.	Student thesis
Stephan Moldzio *FB2*	Food quality and uptake estimations	2.1.4.4.	Diploma thesis
Ruth Gutperlet *FB2*	Temperature stress experiments; RNA/DNA-ratios, PoBeMon	2.2.3. 2.2.5. 2.3.1.	Diploma thesis
Dieter Piepenburg Michael Bartz Frank-Peter Rapp *Inst. for Polar Ecology*	Respiration chamber development and optodic respiration measurements	2.2.4.	Cooperation

Acknowledgements

First of all, I would like to thank my supervisor Prof. Dr. Ulf Riebesell (IFM-GEOMAR, Kiel) for support, encouragement and most of all for the great privilege to let me work and research on these fascinating species.

I am also very grateful to Prof. Dr. Dieter Piepenburg (Institute for Polar Ecology, Kiel) for co-correcting this thesis and for helpful discussions concerning respiratory physiology of marine animals.

My colleague Dipl.-Biol. Wiebke Holtmann (now Institute for Physiology, Kiel) is deeply thanked for encouragement, support and uncountable discussions. She was one of the first people learning with me about the corals' needs and behaviour.

My student workers Janina Büscher and Claudia Gersdorf are thanked for their ambitious support, flexibility and for never once complaining, despite my increasing absence of mind.

The team from the Aquarium Kiel, namely Michael Gruber, Prof. Dr. Uwe Waller (now HTW, Saarbrücken) and Ralf Traulsen, is acknowledged for its technical assistance and help on all questions concerning marine animal cultivation and water quality management.

I would like to thank "my" students for their support and the opportunity to learn how to teach and attract young people in science. Namely, I would like to acknowledge Stephanie Stratil, Jan Büdenbender, Lennart Bach, Stephan Moldzio, Ruth Gutperlet, Janett Voigt, and Stefanie Sokol.

Dr. Michael Meyerhöfer (IFM-GEOMAR, Kiel) is thanked for his DIC analyses but most of all for several discussions helping me organising and managing my scientific course of life.

I am grateful to our technicians Andrea Ludwig and Peter Fritsche for their high-quality water analyses and for their great flexibility.

I would also like to acknowledge Dr. Kai Schulz (IFM-GEOMAR, Kiel) for teaching me the secrets of the carbonate system and for the discussions that helped me to correctly interpret the data.

Dr. Catriona Clemmeson, Helgi Mempel (both IFM-GEOMAR, Kiel), Michael Bartz (Institute for Polar Ecology, Kiel), Dirk Wehrend (TLZ, Kiel) are thanked for an excellent and close collaboration, allowing the development or adaptation of new research methods on cold-water corals.

Dr. Andres Rüggeberg (now Renard Centre of Marine Geology; University of Ghent, Belgium) is thanked for helping me in managing the ship cruises and for sharing his deep knowledge about cold-water corals with me.

I am also very grateful to Dipl.-Biol. Christina Oettmeier (now Bremen University), Dr. Sven Neulinger (IFM-GEOMAR), and Dr. Vera Thiel (IFM-GEOMAR) for support, advice and helping me to see things from another perspective.

The crew of the vessel RV ALKOR is acknowledged for sampling assistance and good fieldwork. Special thanks goes to the team from the submersible JAGO, Dr. Karen Hissmann and pilot Jürgen Schauer (both IFM-GEOMAR, Kiel) for allowing me to be among the few who have seen cold-water coral habitats with their own eyes.

And a cohort of student apprentices is deeply acknowledged for their voluntary collaboration and for their catching curiosity.

Last, but definitely not least, I would like to thank my parents, sisters and my wife for always being there for me and my two children for giving everything its right dimensions. I love you!

This research was funded by the Deutsche Forschungsgemeinschaft - DFG (RI598/4-1) and the Kiel Cluster of Excellence (CP07A45 and CP07A54).

References

Abdussamad, E. M. & Thampy, D. M. (1994) Cannibalism in the tiger shrimp *Penaeus monodon* Fabricius in nursery rearing phase. *Journal of Aquaculture in the Tropics* **9**(1), 67-75.

Abel, E. (1963) Rhythmik bei Anthozoen. *Neptun* **12**, 331-333.

Adkins, J. F., Boyle, E. A., Curry, W. B. & Lutringer, A. (2003) Stable isotopes in deep-sea corals and a new mechanism for "vital effects". *Geochimica et Cosmochimica Acta* **67**(6), 1129-1143.

Ahnert, A. & Borowski, C. (2000) Environmental risk assessment of anthropogenic activity in the deep-sea. *Journal of Aquatic Ecosystem Stress and Recovery* **7**(4), 299-315.

Al-Horani, F. A., Al-Moghrabi, S. M. & de Beer, D. (2003a) The mechanism of calcification and its relation to photosynthesis and respiration in the scleractinian coral *Galaxea fascicularis*. *Marine Biology* **142**(3), 419-426.

Al-Horani, F. A., Al-Moghrabi, S. M. & de Beer, D. (2003b) Microsensor study of photosynthesis and calcification in the scleractinian coral, *Galaxea fascicularis*: active internal carbon cycle. *Journal of Experimental Marine Biology and Ecology* **288**(1), 1-15.

Albright, R., Mason, B. & Langdon, C. (2008) Effect of aragonite saturation state on settlement and post-settlement growth of *Porites astreoides* larvae. *Coral Reefs* **27**(3), 485-490.

Allemand, D., Ferrier-Pagès, C., Furla, P., Houlbreque, F., Puverel, S., Reynaud, S., Tambutte, E., Tambutte, S. & Zoccola, D. (2004) Biomineralisation in reef-building corals: from molecular mechanisms to environmental control. *Comptes Rendus Palevol* **3**(6-7), 453-467.

Allemand, D., Tambutte, E., Girard, J. P. & Jaubert, J. (1998) Organic matrix synthesis in the scleractinian coral *Stylophora pistillata*: Role in biomineralization and potential target of the organotin tributyltin. *Journal of Experimental Biology* **201**(13), 2001-2009.

Andersson, A. J., Kuffner, I. B., Mackenzie, F. T., Jokiel, P. L., Rodgers, K. S. & Tan, A. (2009) Net loss of $CaCO_3$ from a subtropical calcifying community due to seawater acidification: mesocosm-scale experimental evidence. *Biogeosciences* **6**(8), 1811-1823.

Anthony, K. R. N. (1999a) Coral suspension feeding on fine particulate matter. *Journal of Experimental Marine Biology and Ecology* **232**(1), 85-106.

Anthony, K. R. N. (1999b) A tank system for studying benthic aquatic organisms at predictable levels of turbidity and sedimentation: Case study examining coral growth. *Limnology and Oceanography* **44**(6), 1415-1422.

Arndt, E. A. & Jansen, W. (1986) *Neomysis integer* (LEACH) in the chain of boddens south of Darss/Zingst (Western Baltic): ecophysiology and population dynamics. *Ophelia* **4**, 1-15.

Atkinson, M. J., Carlson, B. & Crow, G. L. (1995) Coral growth in high-nutrient, low-pH seawater: a case study of corals cultured at the Waikiki Aquarium, Honolulu, Hawaii. *Coral Reefs* **14**(4), 215-223.

Bach, L. (2007) *A first estimation of optimal food density for Lophelia pertusa (L. 1758) and observations of general feeding behaviour*. Student Thesis (Semesterarbeit), IFM-GEOMAR, Kiel: Christian-Albrechts-University, 13 pp.

Bak, R. P. M. (1973) Coral weight increment in situ. A new method to determine coral growth. *Marine Biology* **20**(1), 45-49.

Bak, R. P. M. (1976) The growth of coral colonies and the importance of crustose coralline algae and burrowing sponges in relation with carbonate accumulation. *Netherlands Journal of Sea Research* **10**(3), 285-337.

Bak, R. P. M. & Meesters, E. H. (2002) Acclimatization/adaptation of coral reefs in a marginal environment. *Proceedings of the Ninth International Coral Reef Symposium*, Bali.

Barcelos e Ramos, J., Biswas, H., Schulz, K. G., LaRoche, J. & Riebesell, U. (2007) Effect of rising atmospheric carbon dioxide on the marine nitrogen fixer *Trichodesmium*. *Global Biogeochemical Cycles* **21**(GB2028), 1-6.

Barker, S. & Elderfield, H. (2002) Foraminiferal calcification response to glacial-interglacial changes in atmospheric CO_2. *Science* **297**(5582), 833-836.

Barnes, D. J. (1970) Coral skeletons: an explanation of their growth and structure. *Science* **170**(3964), 1305-1308.

Barnes, D. J. (1972) The structure and formation of growth-ridges in scleractinian coral skeletons. *Proceedings of the Royal Society B: Biological Sciences* **182**, 331-350.

Barnes, D. J. & Devereux, M. J. (1988) Variations in skeletal architecture associated with density banding in the hard coral *Porites*. *Journal of Experimental Marine Biology and Ecology* **121**(1), 37-54.

Barnett, T. P., Pierce, D. W., AchutaRao, K. M., Gleckler, P. J., Santer, B. D., Gregory, J. M. & Washington, W. M. (2005) Penetration of human-induced warming into the world's oceans. *Science* **309**(5732), 284-287.

Barry, J. P., Buck, K. R., Lovera, C. F., Kuhnz, L., Whaling, P. J., Peltzer, E. T., Walz, P. & Brewer, P. G. (2004) Effects of direct ocean CO_2 injection on deep-sea meiofauna. *Journal of Oceanography* **60**(4), 759-766.

Barry, J. P., Hall-Spencer, J. M. & Tyrell, T. (2010) *In situ* perturbation experiments: natural venting sites, spatial / temporal gradients in ocean pH, manipulative *in situ* pCO_2 perturbations. In *Guide to best practices in ocean acidification research and data*

reporting (eds. U. Riebesell, V. J. Fabry, L. Hansson & J. P. Gattuso) Luxembourg: Publications Office of the European Union, pp. 123-136.

Bassim, K. M. & Sammarco, P. W. (2003) Effects of temperature and ammonium on larval development and survivorship in a scleractinian coral (*Diploria strigosa*). *Marine Biology* **142**(2), 241-252.

Bates, N. R., Samuels, L. & Merlivat, L. (2001) Biogeochemical and physical factors influencing seawater fCO_2, and air-sea CO_2 exchange on the Bermuda coral reef. *Limnology and Oceanography* **46**(4), 833-846.

Belchier, M., Clemmesen, C., Cortes, D., Doan, T., Folkvord, A., Garcia, A., Geffen, A., Høie, H., Johannessen, A. & Moksness, E. (2004) Recruitment studies: manual on precision and accuracy of tools. In *ICES Techniques in Marine Environmental Sciences*, vol. 33: International Council for the Exploration of the Sea, 44 pp.

Bell, N. & Smith, J. (1999) Coral growing on North Sea oil rigs. *Nature* **402**(6762), 601-601.

Berrridge, M. J. & Oschman, J. L. (1972) *Transporting Epithelia*. New York: Academic Press.

Beuck, L., Vertino, A., Stepina, E., Karolczak, M. & Pfannkuche, O. (2007) Skeletal response of *Lophelia pertusa* (Scleractinia) to bioeroding sponge infestation visualised with micro-computed tomography. *Facies* **53**(2), 157-176.

Biegala, I. C., Harris, R. P. & Bergeron, J. P. (1999) ATCase activity, RNA:DNA ratio, gonad development stage, and egg production in the female copepod *Calanus helgolandicus*. *Marine Biology* **135**(1), 1-10.

Bijma, J., Spero, H. J. & Lea, D. W. (1999) Reassessing foraminiferal stable isotope geochemistry: Impact of the oceanic carbonate system (experimental results). In *Use of Proxies in Paleoceanography: Examples from the South Atlantic* (eds. G. Fischer & G. Wefer) Berlin: Springer, pp. 489-512.

Boletzky, S. v. & Hanlon, R. T. (1983) A review of the laboratory maintenance, rearing and culture of cephalopod molluscs. *Memoirs of the National Museum Victoria* **44**, 147-187.

Bower, C. E. & Bidwell, J. P. (1978) Ionization of ammonia in seawater: effects of temperature, pH, and salinity. *Journal of the Fisheries Research Board of Canada* **35**(7), 1012-1016.

Bower, C. E. & Turner, D. T. (1983) Nitrification in closed seawater culture systems: Effects of nutrient deprivation. *Aquaculture* **34**(1-2), 85-92.

Brafield, A. E. & Chapman, G. (1967) The respiration of *Pteroides griseum* (Bohadsch) a pennatulid coelenterate. *Journal of Experimental Biology* **46**(1), 97-104.

Brewer, P. G. & Goldman, J. C. (1976) Alkalinity changes generated by phytoplankton growth. *Limnology and Oceanography* **21**(1), 108-117.

Broecker, W. S. (2003) The Ocean $CaCO_3$ Cycle. In *The Oceans and Marine Geochemistry* (eds. H. Elderfield) Oxford: Elsevier Pergamon, pp. 1-21.

Brooke, S. D. & Young, C. M. (2009) *In situ* measurement of survival and growth of *Lophelia pertusa* in the northern Gulf of Mexico. *Marine Ecology Progress Series* **397**, 153-161.

Brown, B. E., Downs, C. A., Dunne, R. P. & Gibb, S. W. (2002) Preliminary evidence for tissue retraction as a factor in photoprotection of corals incapable of xanthophyll cycling. *Journal of Experimental Marine Biology and Ecology* **277**(2), 129-144.

Brown, B. E., Letissier, M. D. A. & Dunne, R. P. (1994) Tissue retraction in the scleractinian coral *Coeloseris mayeri*, its effect upon coral pigmentation, and preliminary implications for heat balance. *Marine Ecology Progress Series* **105**(3), 209-218.

Bucher, D. J., Harriott, V. J. & Roberts, L. G. (1998) Skeletal micro-density, porosity and bulk density of acroporid corals. *Journal of Experimental Marine Biology and Ecology* **228**(1), 117-136.

Buckley, B. A. & Szmant, A. M. (2004) RNA/DNA ratios as indicators of metabolic activity in four species of Caribbean reef-building corals. *Marine Ecology Progress Series* **282**, 143-149.

Budd, G. C. (2008) *Neomysis integer*. An opossum shrimp. *Marine Life Information Network: Biology and Sensitivity Key Information Sub-programme*, Plymouth: Marine Biology Association of the United Kingdom, http://www.marlin.ac.uk/species/Neomysisinteger.htm.

Bullow, F. J. (1987) RNA:DNA ratios as indicators of growth in fish: A review. In *Age and growth of fish* (eds. R. C. Summerfelt & G. E. Hall) Ames: Iowa State University Press, pp. 45-64.

Burton, E. A. & Walter, L. M. (1987) Relative precipitation rates of aragonite and Mg calcite from seawater: Temperature or carbonate ion control. *Geology* **15**, 111-114.

Buskey, E. J. & Hartline, D. K. (2003) High-speed video analysis of the escape responses of the copepod *Acartia tonsa* to shadows. *The Biological Bulletin* **204**(1), 28-37.

Cairns, S. D. (1984) New records of ahermatypic corals (Scleractinia) from the Hawaiian Islands and Line Islands. *Occasional Papers of the Bishop Museum* **25**, 1-30.

Cairns, S. D. (2007) Deep-water corals: an overview with special reference to diversity and distribution of deep-water scleractinian corals. *Bulletin of Marine Science* **81**(3), 311-322.

Cairns, S. D. & Macintyre, I. G. (1992) Phylogenetic implications of calcium carbonate mineralogy in the Stylasteridae (Cnidaria: Hydrozoa). *Palaios* **7**, 96-107.

Cairns, S. D. & Stanley, G. D. (1982) Ahermatypic coral banks: living and fossil counterparts. *4th International Coral Reef Symposium*, Manila, The Philippines, 611-618.

Caldeira, K. & Wickett, M. E. (2003) Anthropogenic carbon and ocean pH. *Nature* **425**(6956), 365-365.

Chisholm, J. R. M. & Gattuso, J. P. (1991) Validation of the alkalinity anomaly technique for investigating calcification and photosynthesis in coral-reef communities. *Limnology and Oceanography* **36**(6), 1232-1239.

Clark, D., Lamare, M. & Barker, M. (2009) Response of sea urchin pluteus larvae (Echinodermata: Echinoidea) to reduced seawater pH: a comparison among a tropical, temperate, and a polar species. *Marine Biology* **156**(6), 1125-1137.

Clark, L. C. J. (1956) Monitor and control of blood and tissue oxygen tensions. *Transactions - American Society for Artificial Internal Organs* **2**, 41-46.

Clayton, W. S. & Lasker, H. R. (1982) Effects of light and dark treatments on feeding by the reef coral *Pocillopora damicornis* (Linnaeus). *Journal of Experimental Marine Biology and Ecology* **63**(3), 269-279.

Clemmesen, C. (1993) Improvements in the fluorometric-determination of the RNA and DNA content of individual marine fish larvae. *Marine Ecology Progress Series* **100**(1-2), 177-183.

Clemmesen, C., Buhler, V., Carvalho, G., Case, R., Evans, G., Hauser, L., Hutchinson, W. F., Kjesbu, O. S., Mempel, H., Moksness, E., Otteraa, H., Paulsen, H., Thorsen, A. & Svaasand, T. (2003) Variability in condition and growth of Atlantic cod larvae and juveniles reared in mesocosms: environmental and maternal effects. *Journal of Fish Biology* **62**(3), 706-723.

Cohen, A. L. & McConnaughey, T. A. (2003) Geochemical perspectives on coral mineralization. *Biomineralization* **54**, 151-187.

Cohen, A. L., McCorkle, D. C., de Putron, S., Gaetani, G. A. & Rose, K. A. (2009) Morphological and compositional changes in the skeletons of new coral recruits reared in acidified seawater: Insights into the biomineralization response to ocean acidification. *Geochemistry Geophysics Geosystems* **10**(Q07005), 1-12.

Coles, S. L. & Jokiel, P. L. (1978) Synergistic effects of temperature, salinity and light on the hermatypic coral *Montipora verrucosa*. *Marine Biology* **49**, 187-195.

Colt, J. E. & Armstrong, D. A. (1981) Nitrogen toxicity to crustaceans, fish, molluscs. *Bioengineering Symposium for Fish Culture* **1**, 34-47.

Cooper, T. F., De 'Ath, G., Fabricius, K. E. & Lough, J. M. (2008) Declining coral calcification in massive Porites in two nearshore regions of the northern Great Barrier Reef. *Global Change Biology* **14**(3), 529-538.

Costello, M. J., McCrea, M., Freiwald, A., Lundälv, T., Jonsson, L., Bett, B. J., van Weering, T. C. E., de Haas, H., Roberts, J. M. & D., A. (2005) Role of cold-water coral *Lophelia pertusa* coral reefs as fish habitat in the NE Atlantic. In *Cold-Water Corals and Ecosystems* (eds. A. Freiwald & J. M. Roberts) Berlin, Heidelberg: Springer, pp. 979-1001.

Cox, E. F. & Ward, S. (2002) Impact of elevated ammonium on reproduction in two Hawaiian scleractinian corals with different life history patterns. *Marine Pollution Bulletin* **44**(11), 1230-1235.

CSA International Inc. (2007) Characterization of northern Gulf of Mexico deepwater hard bottom communities with emphasis on *Lophelia* coral. New Orleans: U.S. Department of the Interior, Minerals Management Service, Gulf of Mexico OCS Region, 169 pp.

Cuif, J. P. & Dauphin, Y. (2005) The two-step mode of growth in the Scleractinian coral skeletons from the micrometre to the overall scale. *Journal of Structural Biology* **150**(3), 319-331.

Dauphin, Y., Cuif, J. P. & Williams, C. T. (2008) Soluble organic matrices of aragonitic skeletons of Merulinidae (Cnidaria, Anthozoa). *Comparative Biochemistry and Physiology B - Biochemistry & Molecular Biology* **150**(1), 10-22.

Davies, A. J., Roberts, J. M. & Hall-Spencer, J. (2007) Preserving deep-sea natural heritage: Emerging issues in offshore conservation and management. *Biological Conservation* **138**(3-4), 299-312.

Davies, A. J., Wisshak, M., Orr, J. C. & Roberts, J. M. (2008) Predicting suitable habitat for the cold-water coral *Lophelia pertusa* (Scleractinia). *Deep-Sea Research Part I - Oceanographic Research Papers* **55**(8), 1048-1062.

Davies, P. S. (1989) Short-term growth measurements of corals using accurate buoyant weighing technique. *Marine Biology* **101**(3), 389-395.

De'Ath, G., Lough, J. M. & Fabricius, K. E. (2009) Declining coral calcification on the great barrier reef. *Science* **323**(5910), 116-119.

Delille, B., Harlay, J., Zondervan, I., Jacquet, S., Chou, L., Wollast, R., Bellerby, R. G. J., Frankignoulle, M., Borges, A. V., Riebesell, U. & Gattuso, J. P. (2005) Response of primary production and calcification to changes of pCO_2 during experimental blooms of the coccolithophorid *Emiliania huxleyi*. *Global Biogeochemical Cycles* **19**(GB2023), 1-14.

Dhont, J. & van Stappen, G. (2003) Biology, tank production and nutritional value of *Artemia*. In *Live feeds in marine aquaculture* (eds. J. G. Støttrup & L. A. McEvoy) Oxford: Blackwell Science Ltd, pp. 145-195.

Dickson, A. G., Afghan, J. D. & Anderson, G. C. (2003) Reference materials for oceanic CO_2 analysis: a method for the certification of total alkalinity. *Marine Chemistry* **80**(2-3), 185-197.

Dickson, A. G. & Millero, F. J. (1987) A comparison of the equilibrium constants for the dissociation of carbonic acid in seawater media. *Deep Sea Research Part I - Oceanographic Research Papers* **34**, 1733-1743.

Dickson, A. G., Sabine, C. L. & Christian, J. R. (2007) *Guide to best practices for ocean CO_2 measurements*. PICES Special Publication. Sidney: North Pacific Marine Science Organization.

Dodds, L. A. (2007) *The ecophysiology of the cold-water coral Lophelia pertusa (Scleractinia).* Doctoral Thesis, Scottish Association for Marine Science, Aberdeen: University of Aberdeen, 206 pp.

Dodds, L. A., Black, K. D., Orr, H. & Roberts, J. M. (2009) Lipid biomarkers reveal geographical differences in food supply to the cold-water coral *Lophelia pertusa* (Scleractinia). *Marine Ecology Progress Series* **397**, 113-124.

Dodds, L. A., Roberts, J. M., Taylor, A. C. & Marubini, F. (2007) Metabolic tolerance of the cold-water coral *Lophelia pertusa* (Scleractinia) to temperature and dissolved oxygen change. *Journal of Experimental Marine Biology and Ecology* **349**(2), 205-214.

Dodge, R., Aller, R., Thomsom, J. & 577. (1974) Coral growth related to resuspension of bottom sediments. *Nature* **247**, 574-577.

Dodge, R. E. & Szmant-Froelich, A. (1985) Effects of drilling fluids on reef corals: a review. In *Wastes in the Ocean* (eds. I. W. Duedall, D. R. Kester, P. K. Park & B. H. Ketchum) New York: Wiley InterScience, pp. 341-364.

Dodge, R. E., Wyers, S. C., Frith, H. R., Knap, A. H., Smith, S. R., Cook, C. B. & Sleeter, T. D. (1984) Coral calcification rates by the buoyant weight technique: Effects of alizarin staining. *Journal of Experimental Marine Biology and Ecology* **75**(3), 217-232.

Doney, S. C. & Schimel, D. S. (2007) Carbon and climate system coupling on timescales from the Precambrian to the Anthropocene. *Annual Review of Environment and Resources* **32**, 31-66.

Donner, S. D., Skirving, W. J., Little, C. M., Oppenheimer, M. & Hoegh-Guldberg, O. (2005) Global assessment of coral bleaching and required rates of adaptation under climate change. *Global Change Biology* **11**(12), 2251-2265.

Dons, C. (1944) Norges korallrev. *Det Kongelige Norske Videnskabers Selskabs Forhandlinger* **16**, 37-82.

Duineveld, G. C. A., Lavaleye, M. S. S. & Berghuis, E. M. (2004) Particle flux and food supply to a seamount cold-water coral community (Galicia Bank, NW Spain). *Marine Ecology Progress Series* **277**, 13-23.

Duineveld, G. C. A., Lavaleye, M. S. S., Bergman, M. I. N., De Stigter, H. & Mienis, F. (2007) Trophic structure of a cold-water coral mound community (Rockall Bank, NE Atlantic) in relation to the near-bottom particle supply and current regime. *Bulletin of Marine Science* **81**(3), 449-467.

Dullo, W. C., Flögel, S. & Rüggeberg, A. (2008) Cold-water coral growth in relation to the hydrography of the Celtic and Nordic European continental margin. *Marine Ecology Progress Series* **371**, 165-176.

Duncan, P. M. (1877) On the rapidity of growth and variability of some Madreporaria on an Atlantic cable, with remarks upon the rate of accumulation of foraminiferal deposits. *Proceedings of the Royal Society of London* **26**, 133-137.

Edinger, E. N., Limmon, G. V., Jompa, J., Widjatmoko, W., Heikoop, J. M. & Risk, M. J. (2000) Normal coral growth rates on dying reefs: Are coral growth rates good indicators of reef health? *Marine Pollution Bulletin* **40**(5), 404-425.

Edmunds, P. J. (2005) The effect of sub-lethal increases in temperature on the growth and population trajectories of three scleractinian corals on the southern Great Barrier Reef. *Oecologia* **146**, 350-364.

Edmunds, P. J. & Gates, R. D. (2002) Standardizing physiological data for scleractinian corals. *Coral Reefs* **21**, 193-197.

Edwards, M., Reid, P. & Planque, B. (2001) Long-term and regional variability of phytoplankton biomass in the Northeast Atlantic (1965-1995). *ICES Journal of Marine Science* **58**, 39-49.

Emiliani, C., Hudson, J. H., Shinn, E. A. & George, R. Y. (1978) Oxygen and carbon isotopic growth record in a reef coral from the Florida Keys and a deep-sea coral from Blake Plateau. *Science* **202**(4368), 627-629.

Engel, A., Zondervan, I., Aerts, K., Beaufort, L., Benthien, A., Chou, L., Delille, B., Gattuso, J. P., Harlay, J., Heemann, C., Hoffmann, L., Jacquet, S., Nejstgaard, J., Pizay, M. D., Rochelle-Newall, E., Schneider, U., Terbrueggen, A. & Riebesell, U. (2005) Testing the direct effect of CO_2 concentration on a bloom of the coccolithophorid *Emiliania huxleyi* in mesocosm experiments. *Limnology and Oceanography* **50**(2), 493-507.

Erez, J. (1978) Vital effect on stable-isotope composition seen in foraminifera and coral skeletons. *Nature* **273**(5659), 199-202.

Erez, J., Silverman, J., Schneider, K., Reynaud, S. & Allemand, D. (In press) Coral calcification under ocean acidification and global change. In *Coral and Coral Reefs* (eds. Z. Dubinsky): Springer.

Fautin, D. G., Guinotte, J. M. & Orr, J. C. (2009) Comparative depth distribution of corallimorpharians and scleractinians (Cnidaria: Anthozoa). *Marine Ecology Progress Series* **397**, 63-70.

Feely, R. A., Sabine, C. L., Lee, K., Berelson, W., Kleypas, J., Fabry, V. J. & Millero, F. J. (2004) Impact of anthropogenic CO_2 on the $CaCO_3$ system in the oceans. *Science* **305**(5682), 362-366.

Ferrier-Pagès, C., Allemand, D., Gattuso, J. P., Jaubert, J. & Rassoulzadegan, F. (1998) Microheterotrophy in the zooxanthellate coral *Stylophora pistillata*: Effects of light and ciliate density. *Limnology and Oceanography* **43**(7), 1639-1648.

Ferrier-Pagès, C., Gattuso, J. P., Dallot, S. & Jaubert, J. (2000) Effect of nutrient enrichment on growth and photosynthesis of the zooxanthellate coral *Stylophora pistillata*. *Coral Reefs* **19**(2), 103-113.

Ferrier-Pagès, C., Witting, J., Tambutté, E. & Sebens, K. P. (2003) Effect of natural zooplankton feeding on the tissue and skeletal growth of the scleractinian coral *Stylophora pistillata*. *Coral Reefs* **22**(3), 229-240.

Fine, M. & Tchernov, D. (2007) Scleractinian coral species survive and recover from decalcification. *Science* **315**(5820), 1811-1811.

Fosså, J. H., Lindberg, B., Christensen, O., Lundälv, T., Svellingen, I., Mortensen, P. B. & Alvsvåg, J. (2005) Mapping of *Lophelia* reefs in Norway: experiences and survey methods. In *Cold-Water Corals and Ecosystems* (eds. A. Freiwald & J. M. Roberts) Berlin, Heidelberg: Springer, pp. 359-391.

Fosså, J. H., Mortensen, P. B. & Furevik, D. M. (2000) *Lophelia* korallrev langs norskekysten. Forekomst og tilstand. *Fisken og Havet* **2**, 1-94.

Fosså, J. H., Mortensen, P. B. & Furevik, D. M. (2002) The deep-water coral *Lophelia pertusa* in Norwegian waters: distribution and fishery impacts. *Hydrobiologia* **471**, 1-12.

Frantzis, A., Gremare, A. & Vetion, G. (1992) Growth rates and RNA:DNA ratios in *Paracentrotus lividus* (Echinodermata: Echinoidea) fed on benthic macrophytes. *Journal of Experimental Marine Biology and Ecology* **156**(1), 125-138.

Franzisket, L. (1964) Die Stoffwechselintensität der Riffkorallen und ihre ökologische, phylogenetische und soziologische Bedeutung. *Zeitschrift für vergleichende Physiologie* **49**, 91-113.

Frederiksen, R., Jensen, A. & Westerberg, H. (1992) The distribution of the scleractinian coral *Lophelia pertusa* around the Faroe Islands and the relation to internal tidal mixing. *Sarsia* **77**, 157-171.

Freiwald, A. (2002) Reef-forming cold-water corals. In *Ocean Margin Systems* (eds. G. Wefer, D. Billett, D. Hebbeln, B. B. Jørgensen, M. Schlüter & T. C. E. van Weering) Heidelberg: Springer, pp. 365-385.

Freiwald, A., Fosså, J. H., Grehan, A., Koslow, T. & Roberts, J. M. (2004) Cold-water coral reefs: Out of sight - no longer out of mind. In *UNEP-WCMC Biodiversity Series*, vol. 22: UNEP World Conservation Monitoring Centre, 86 pp.

Freiwald, A., Heinrich, R. & Pätzold, J. (1997) Anatomy of a deep-water coral reef mound from Stjernsund, west Finnmark, northern Norway. In *Cool-Water Carbonates*, vol. 56 (eds. N. P. James & J. A. D. Clarke): Society for Sedimentary Geology, pp. 141-161.

Freiwald, A., Hühnerbach, V., Lindberg, B., Wilson, J. B. & Campbell, J. (2002) The Sula Reef Complex, Norwegian shelf. *Facies* **47**, 179-200.

Freiwald, A. & Wilson, J. B. (1998) Taphonomy of modern deep, cold-temperate water coral reefs. *Historical Biology* **13**, 37-52.

Freiwald, A., Wilson, J. B. & Heinrich, R. (1999) Grounding Pleistocene icebergs shape recent deep-water coral reefs. *Sedimentary Geology* **125**, 1-8.

Fukuda, I., Ooki, S., Fujita, T., Murayama, E., Nagasawa, H., Isa, Y. & Watanabe, T. (2003) Molecular cloning of a cDNA encoding a soluble protein in the coral exoskeleton. *Biochemical and Biophysical Research Communications* **304**(1), 11-17.

Furla, P., Galgani, I., Durand, I. & Allemand, D. (2000) Sources and mechanisms of inorganic carbon transport for coral calcification and photosynthesis. *Journal of Experimental Biology* **203**(22), 3445-3457.

Gass, S. E. & Roberts, J. M. (2006) The occurrence of the cold-water coral *Lophelia pertusa* (Scleractinia) on oil and gas platforms in the North Sea: Colony growth, recruitment and environmental controls on distribution. *Marine Pollution Bulletin* **52**(5), 549-559.

Gates, R. D. & Edmunds, P. J. (1999) The physiological mechanisms of acclimatization in tropical reef corals. *American Zoologist* **39**(1), 30-43.

Gattuso, J. P., Allemand, D. & Frankignoulle, M. (1999a) Photosynthesis and calcification at cellular, organismal and community levels in coral reefs: A review on interactions and control by carbonate chemistry. *American Zoologist* **39**(1), 160-183.

Gattuso, J. P., Frankignoulle, M., Bourge, I., Romaine, S. & Buddemeier, R. W. (1998) Effect of calcium carbonate saturation of seawater on coral calcification. *Global and Planetary Change* **18**(1-2), 37-46.

Gattuso, J. P., Frankignoulle, M. & Smith, S. V. (1999b) Measurement of community metabolism and significance in the coral reef CO_2 source-sink debate. *Proceedings of the National Academy of Sciences of the United States of America* **96**(23), 13017-13022.

Gazeau, F., Quiblier, C., Jansen, J. M., Gattuso, J. P., Middelburg, J. J. & Heip, C. H. R. (2007) Impact of elevated CO_2 on shellfish calcification. *Geophysical Research Letters* **34**(L07603), 1-5.

GEBCO_08. (2009) General Bathymetric Chart of the Oceans: The GEBCO_08 Grid: Intergovernmental Oceanographic Commission (IOC) of UNESCO and of the International Hydrographic Organization (IHO).

Genin, A., Dayton, P. K., Lonsdale, P. F. & Speiss, F. N. (1986) Corals on seamount peaks provide evidence of current acceleration over deep-sea topography. *Nature* **322**, 59-61.

Gladfelter, W. B. (1975) Sea anemone with zooxanthellae: Simultaneous contraction and expansion in response to changing light intensity. *Science* **189**(4202), 570-571.

Glasby, G. P. (2000) Economic geology: Lessons learned from deep-sea mining. *Science* **289**(5479), 551-553.

Gooday, A. J. & Hughes, J. A. (2002) Foraminifera associated with phytodetritus deposits at a bathyal site in the northern Rockall Trough (NE Atlantic): seasonal contrasts and a comparison of stained and dead assemblages. *Marine Micropaleontology* **46**(1-2), 83-110.

Gooding, R. A., Harley, C. D. G. & Tang, E. (2009) Elevated water temperature and carbon dioxide concentration increase the growth of a keystone echinoderm. *Proceedings of the National Academy of Sciences of the United States of America* **106**(23), 9316-9321.

Gordon, J. D. M. (2001) Deep-water fisheries at the Atlantic Frontier. *Continental Shelf Research* **21**(8-10), 987-1003.

Goreau, T. F. (1959) The physiology of skeleton formation in corals. I. A method for measuring the rate of calcium deposition by corals under different conditions. *The Biological Bulletin* **116**(1), 59-75.

Goreau, T. F., Goreau, N. I. & Yonge, C. M. (1971) Reef corals: autotrophs or heterotrophs? *The Biological Bulletin* **141**, 247-260.

Guinotte, J. M., Orr, J. C., Cairns, S., Freiwald, A., Morgan, L. & George, R. (2006) Will human-induced changes in seawater chemistry alter the distribution of deep-sea scleractinian corals? *Frontiers in Ecology and the Environment* **4**(3), 141-146.

Gutperlet, R. (2008) *Ökophysiologische Studien an der Kaltwasserkoralle Lophelia pertusa (Scleractinia)*. Diploma Thesis, IFM-GEOMAR, Kiel: Christian-Albrechts-University, 92 pp.

Halfar, J. & Fujita, R. M. (2007) Danger of deep-sea mining. *Science* **316**(5827), 987-987.

Hall-Spencer, J., Allain, V. & Fosså, J. H. (2002) Trawling damage to Northeast Atlantic ancient coral reefs. *Proceedings of the Royal Society B: Biological Sciences* **269**, 507-511.

Hansen, H. P. & Koroleff, F. (1999) Determination of nutrients. In *Methods of Seawater Analysis* (eds. K. Grasshof, K. Kremling & M. Ehrhardt) Weilheim: Wiley-VCH.

Hawkins, S. J., Southward, A. J. & Genner, M. J. (2003) Detection of environmental change in a marine ecosystem – evidence from the western English Channel. *Science of the Total Environment* **310**, 245-256.

Heinrich, R. & Freiwald, A. (1997) Shipboard Party 1997. The *Lophelia* reef on Sula ridge, mid-Norwegian shelf, Cruise report No 228/97. Bremerhaven, 12 pp.

Helle, K. (2000) Distribution of the copepodite stages of *Calanus finmarchicus* from Lofoten to the Barents Sea in July 1989. *ICES Journal of Marine Science* **57**(6), 1636-1644.

Hentschel, E. (1968) Die postembryonalen Entwicklungsstadien von *Artemia salina* Leach bei verschiedenen Temperaturen (Anostraca, Crustacea). *Zoologischer Anzeiger* **180**, 372-384.

Hii, Y.-S., Soo, C.-L. & Liew, H.-C. (2008) Feeding of scleractinian coral, *Galaxea fascicularis*, on *Artemia salina* nauplii in captivity. *Aquaculture International* **17**(4), 363-376.

Hirche, H.-J. (1991) Distribution of dominant calanoid copepod species in the Greenland sea during late fall. *Polar Biology* **11**(6), 351-362.

Hoegh-Guldberg, O. (1999) Climate change, coral bleaching and the future of the world's coral reefs. *Marine and Freshwater Research* **50**(8), 839-866.

Hoegh-Guldberg, O., Fine, M., Skirving, W., Johnstone, R., Dove, S. & Strong, A. (2005) Coral bleaching following wintry weather. *Limnology and Oceanography* **50**(1), 265-271.

Hoegh-Guldberg, O., Mumby, P. J., Hooten, A. J., Steneck, R. S., Greenfield, P., Gomez, E., Harvell, C. D., Sale, P. F., Edwards, A. J., Caldeira, K., Knowlton, N., Eakin, C. M., Iglesias-Prieto, R., Muthiga, N., Bradbury, R. H., Dubi, A. & Hatziolos, M. E. (2007) Coral reefs under rapid climate change and ocean acidification. *Science* **318**(5857), 1737-1742.

Holmes, R. M., Aminot, A., Kerouel, R., Hooker, B. A., Peterson, B. J. (1999) A simple and precise method for measuring ammonium in marine and freshwater ecosystems. *Canadian Journal of Fisheries and Aquatic Sciences* **56**, 1801-1808.

Holtmann, W. C. (2006) *Effects on behaviour of the cold-water coral Lophelia pertusa caused by increasing ammonium and a first try to define a maximal sustainable concentration of ammonium to Lophelia pertusa*. Student Thesis (Semesterarbeit), IFM-GEOMAR, Kiel: Christian-Albrechts-University, 17 pp.

Hostens, K. & Mees, J. (1999) The mysid-feeding guild of demersal fishes in the brackish zone of the Westerschelde estuary. *Journal of Fish Biology* **55**, 704-719.

Hough, A. R. & Naylor, E. (1992) Distribution and position maintenance behaviour of the estuarine mysid *Neomysis integer*. *Journal of the Marine Biological Association of the United Kingdom* **72**(4), 869-876.

Houlbrèque, F. & Ferrier-Pagès, C. (2009) Heterotrophy in tropical scleractinian corals. *Biological Reviews* **84**(1), 1-17.

Hovland, M. (2008) *Deep Water Coral Reefs: Unique Biodiversity Hot-spots*. Chichester: Springer-Praxis.

Hovland, M., Mortensen, P. B., Brattegard, T., Strass, P. & Rokoengen, K. (1998) Ahermatypic coral banks off Mid-Norway: Evidence for a link with seepage of light hydrocarbons. *Palaios* **13**(2), 189-200.

Hovland, M. & Risk, M. (2003) Do Norwegian deep-water coral reefs rely on seeping fluids? *Marine Geology* **198**(1-2), 83-96.

Hudson, J. H., Shinn, E. A. & Robbin, D. M. (1982) Effects of offshore oil drilling on Philippine reef corals. *Bulletin of Marine Science* **32**, 890-908.

Hurlbert, S. H. (1984) Pseudoreplication and the design of ecological field experiments. *Ecological Monographs* **54**(2), 187-211.

Husebo, A., Nottestad, L., Fosså, J. H., Furevik, D. M. & Jorgensen, S. B. (2002) Distribution and abundance of fish in deep-sea coral habitats. *Hydrobiologia* **471**, 91-99.

Huston, M. (1985) Variation in coral growth-rates with depth at Discovery Bay, Jamaica. *Coral Reefs* **4**(1), 19-25.

Hutchins, D. A., Fu, F. X., Zhang, Y., Warner, M. E., Feng, Y., Portune, K., Bernhardt, P. W. & Mulholland, M. R. (2007) CO_2 control of *Trichodesmium* N_2 fixation, photosynthesis, growth rates, and elemental ratios: Implications for past, present, and future ocean biogeochemistry. *Limnology and Oceanography* **52**(4), 1293-1304.

Hydes, D. J., Hartman, M. C., Hartman, S. E. & Bargeron, C. P. (2007) Evaluation of the Aanderaa oxygen optode in continuous use in the NOC Portsmouth Bilbao FerryBox system 2005, 2006, with an assessment of the likely errors in the estimation of oxygen concentration anomalies. In *Internal Document No. 7*, Southampton: National Oceanography Center, pp. 74.

Iglesias-Rodríguez, M. D., Halloran, P. R., Rickaby, R. E. M., Hall, I. R., Colmenero-Hidalgo, E., Gittins, J. R., Green, D. R. H., Tyrrell, T., Gibbs, S. J., von Dassow, P., Rehm, E., Armbrust, E. V. & Boessenkool, K. P. (2008) Phytoplankton calcification in a high-CO_2 world. *Science* **320**(5874), 336-340.

IPCC. (2007) Summary for Policymakers. In *Climate Change 2007: The physical science basis. Contribution of working group I to the fourth assessment report of the Intergovernmental Panel on Climate Change* (eds. S. Solomon, D. Qin, M. Manning, Z. Chen, M. Marquis, K. B. Averyt, M. Tignor & H. L. Miller) Cambridge, United Kingdom; New York, USA, 18 pp.

Jacques, T. G. & Pilson, E. Q. (1980) Experimental ecology of the temperate scleractinian coral *Astrangia danae* I. Partition of respiration, photosynthesis and calcification between host and symbionts. *Marine Biology* **60**(2-3), 167-178.

Johannes, R. E. & Wiebe, W. J. (1970) Method for determination of coral tissue biomass and composition. *Limnology and Oceanography* **15**, 822-824.

Jokiel, P. L., Maragos, J. E. & Franzisket, L. (1978) Coral growth: buoyant weight technique. In *Coral Reefs: Research Methods* (eds. D. R. Stoddard & R. E. Johannes) Paris: UNESCO, pp. 529-541.

Jokiel, P. L., Rodgers, K. S., Kuffner, I. B., Andersson, A. J., Cox, E. F. & Mackenzie, F. T. (2008) Ocean acidification and calcifying reef organisms: a mesocosm investigation. *Coral Reefs* **27**(3), 473-483.

Joly, N. (1873) Water turned to blood *The Popular Science Monthly* **4**, 202-208.

Jones, C. G., Lawton, J. H. & Shachak, M. (1994) Organisms as ecosystem engineers. *Oikos* **69**, 373-386.

Jury, C. P., Whitehead, R. F. & Szmant, A. M. (2009) Effects of variations in carbonate chemistry on the calcification rates of *Madracis auretenra* (= *Madracis mirabilis* sensu Wells, 1973): bicarbonate concentrations best predict calcification rates. *Global Change Biology* **16**(5), 1632-1644.

Kawaguti, S. (1954) Effects of light and ammonium on the expansion of polyps in the reef corals. *Biological journal of Okayama University* **2**, 45-50.

Kawakami, Y., Mochioka, N., Kimura, R. & Nakazono, A. (1999) Seasonal changes of the RNA/DNA ratio, size and lipid contents and immigration adaptability of Japanese

glass-eels, *Anguilla japonica*, collected in northern Kyushu, Japan. *Journal of Experimental Marine Biology and Ecology* **238**(1), 1-19.

Kemp, A. G. & Stephen, L. (2005) Optimizing oil and gas depletion in the maturing North Sea with growing import dependence. *Oxford Review of Economic Policy* **21**, 43-66.

Kerkhof, L. & Kemp, P. (1999) Small ribosomal RNA content in marine Proteobacteria during non-steady-state growth. *FEMS Microbiology Ecology* **30**(3), 253-260.

Kinsey, D. W. (1978) Alkalinity changes and coral-reef calcification. *Limnology and Oceanography* **23**(5), 989-991.

Kiriakoulakis, K., Fisher, E., Wolff, G. A., Freiwald, A., Grehan, A. & Roberts, J. M. (2005) Lipids and nitrogen isotopes of two deep-water corals from the North-East Atlantic: initial results and implications for their nutrition. In *Cold-Water Corals and Ecosystems* (eds. A. Freiwald & J. M. Roberts) Berlin, Heidelberg: Springer, pp. 715-729.

Kleypas, J. A., Feely, R. A., Fabry, V. J., Langdon, C., Sabine, C. L. & Robbins, L. L. (2006) Impacts of ocean acidification on coral reefs and other marine calcifiers: A guide for future research, report of a workshop held 18–20 April 2005, St. Petersburg, FL, sponsored by NSF, NOAA, and the U.S. Geological Survey. 88 pp.

Kleypas, J. A. & Yates, K. K. (2009) Coral reefs and ocean acidification. *Oceanography* **22**(4), 108-117.

Koop, K., Booth, D., Broadbent, A., Brodie, J., Bucher, D., Capone, D., Coll, J., Dennison, W., Erdmann, M., Harrison, P., Hoegh-Guldberg, O., Hutchings, P., Jones, G. B., Larkum, A. W. D., O'Neil, J., Steven, A., Tentori, E., Ward, S., Williamson, J. & Yellowlees, D. (2001) ENCORE: The effect of nutrient enrichment on coral reefs. Synthesis of results and conclusions. *Marine Pollution Bulletin* **42**(2), 91-120.

Koslow, J. A., Gowlett-Holmes, K., Lowry, J. K., O'Hara, T., Poore, G. C. B. & Williams, A. (2001) Seamount benthic macrofauna off southern Tasmania: community structure and impacts of trawling. *Marine Ecology Progress Series* **213**, 111-125.

Kuffner, I. B., Andersson, A. J., Jokiel, P. L., Rodgers, K. S. & Mackenzie, F. T. (2008) Decreased abundance of crustose coralline algae due to ocean acidification. *Nature Geoscience* **1**(2), 114-117.

Kuhlmann, D. (1984) Effects of temperature, salinity, oxygen and ammonia on the mortality and growth of *Neomysis integer* Leach. *Limnologica* **15**(2), 479-485.

Langdon, C. & Atkinson, M. J. (2005) Effect of elevated pCO_2 on photosynthesis and calcification of corals and interactions with seasonal change in temperature/irradiance and nutrient enrichment. *Journal of Geophysical Research - Oceans* **110**(C9), 1-54.

Langdon, C., Broecker, W. S., Hammond, D. E., Glenn, E., Fitzsimmons, K., Nelson, S. G., Peng, T. H., Hajdas, I. & Bonani, G. (2003) Effect of elevated CO_2 on the community metabolism of an experimental coral reef. *Global Biogeochemical Cycles* **17**(1), 1-14.

Langdon, C., Takahashi, T., Sweeney, C., Chipman, D., Goddard, J., Marubini, F., Aceves, H., Barnett, H. & Atkinson, M. J. (2000) Effect of calcium carbonate saturation state on the calcification rate of an experimental coral reef. *Global Biogeochemical Cycles* **14**(2), 639-654.

Lapid, E. D. & Chadwick, N. E. (2006) Long-term effects of competition on coral growth and sweeper tentacle development. *Marine Ecology Progress Series* **313**, 115-123.

Lasker, H. R. (1979) Light dependent activity patterns among reef corals: *Montastrea cavernosa*. *The Biological Bulletin* **156**(2), 196-211.

Lasker, H. R., Syron, J. A. & Clayton, W. S. (1982) The feeding response of *Hydra viridis*: Effects of prey density on capture rates. *The Biological Bulletin* **162**(3), 290-298.

Lavigne, H. & Gattuso, J. P. (2009) seacarb: seawater carbonate chemistry with R. Ver.: 2.0.

Le Pecq, J.-B. & Paoletti, C. (1966) A new fluorometric method for RNA and DNA determination. *Analytical Biochemistry* **17**(1), 100-107.

Leclercq, N., Gattuso, J. P. & Jaubert, J. (2002) Primary production, respiration, and calcification of a coral reef mesocosm under increased CO_2 partial pressure. *Limnology and Oceanography* **47**(2), 558-564.

Lee, C. S., O'Bryen, P. J. & Marcus, N. H. (2005) *Copepods in Aquaculture*. New York: Wiley-Blackwell.

Léger, P., Bengston, D. A., Sorgeloos, P., Simpson, K. L. & Beck, A. D. (1987) The nutritional value of *Artemia*: a review. In *Artemia Research and its Applications*, vol. 3 (eds. P. Sorgeloos, D. A. Bengston, W. Declair & E. Jaspers) Wetteren, Belgium: Universa Press, pp. 357-372.

Levitus, S., Antonov, J. & Boyer, T. (2005) Warming of the world ocean, 1955-2003. *Geophysical Research Letters* **32**(L02604), 1-4.

Levy, O., Dubinsky, Z., Achituv, Y. & Erez, J. (2006) Diurnal polyp expansion behavior in stony corals may enhance carbon availability for symbionts photosynthesis. *Journal of Experimental Marine Biology and Ecology* **333**(1), 1-11.

Levy, O., Mizrahi, L., Chadwick-Furman, N. E. & Achituv, Y. (2001) Factors controlling the expansion behavior of *Favia favus* (Cnidaria: Scleractinia): Effects of light, flow, and planktonic prey. *The Biological Bulletin* **200**(2), 118-126.

Lewis, E. & Wallace, D. W. R. (1998) Program developed for CO_2 system calculations. ORNL/CDIAC-105. Carbon Dioxide Information Analysis Center, Oak Ridge National Laboratory, U.S. Department of Energy.

Lewis, J. B. & Price, W. S. (1975) Feeding strategies of Atlantic reef corals. *Journal of Zoology* **176**, 527-544.

Lindén, E., Lehtiniemi, M. & Viitasalo, M. (2003) Predator avoidance behaviour of Baltic littoral mysids *Neomysis integer* and *Praunus flexuosus*. *Marine Biology* **143**(5), 845-850.

Lorenzon, S., Francese, M. & Ferrero, E. A. (2000) Heavy metal toxicity and differential effects on the hyperglycemic stress response in the shrimp *Palaemon elegans*. *Archives of Environmental Contamination and Toxicology* **39**(2), 167-176.

Losordo, T. M., Masser, M. P. & Rakocy, J. (1998) Recirculating aquaculture tank production systems: An overview of critical considerations. *Southern Regional Aquaculture Center Fact Sheets* **451**, 1-38.

Lough, J. M. & Barnes, D. J. (2000) Environmental controls on growth of the massive coral *Porites*. *Journal of Experimental Marine Biology and Ecology* **245**(2), 225-243.

Lucas, J. M. & Knapp, L. W. (1997) A physiological evaluation of carbon sources for calcification in the octocoral *Leptogorgia virgulata* (Lamarck). *Journal of Experimental Biology* **200**(20), 2653-2662.

Lüthi, D., Le Floch, M., Bereiter, B., Blunier, T., Barnola, J. M., Siegenthaler, U., Raynaud, D., Jouzel, J., Fischer, H., Kawamura, K. & Stocker, T. F. (2008) High-resolution carbon dioxide concentration record 650,000-800,000 years before present. *Nature* **453**(7193), 379-382.

Maier, C., Hegeman, J., Weinbauer, M. G. & Gattuso, J. P. (2009) Calcification of the cold-water coral *Lophelia pertusa* under ambient and reduced pH. *Biogeosciences* **6**(8), 1671-1680.

Mann, G. S. (1994) *Distribution, abundance and life history of the reef coral Favia fragum (Esper) in Barbados: Effects of eutrophication and of the black sea urchin Diadema antillarum (Philippi).* M.Sc. Thesis, Department of Biology, Montreal: McGill University.

Marcus, N. H. & Wilcox, J. A. (2007) A Guide to the Meso-scale Production of the Copepod *Acartia tonsa*. Gainesville: Florida State University, 29 pp.

Marshall, A. T. & Clode, P. L. (2003) Light-regulated Ca^{2+} uptake and O_2 secretion at the surface of a scleractinian coral *Galaxea fascicularis*. *Comparative Biochemistry and Physiology A - Molecular & Integrative Physiology* **136**(2), 417-426.

Martin, S. & Gattuso, J. P. (2009) Response of Mediterranean coralline algae to ocean acidification and elevated temperature. *Global Change Biology* **15**(8), 2089-2100.

Marubini, F. & Atkinson, M. J. (1999) *Effects of lowered pH and elevated nitrate on coral calcification*. Oldendorf: Inter-Research.

Marubini, F., Barnett, H., Langdon, C. & Atkinson, M. J. (2001) Dependence of calcification on light and carbonate ion concentration for the hermatypic coral *Porites compressa*. *Marine Ecology Progress Series* **220**, 153-162.

Marubini, F. & Davies, P. S. (1996) Nitrate increases zooxanthellae population density and reduces skeletogenesis in corals. *Marine Biology* **127**(2), 319-328.

Marubini, F., Ferrier-Pagès, C. & Cuif, J. P. (2003) Suppression of skeletal growth in scleractinian corals by decreasing ambient carbonate-ion concentration: a cross-family

comparison. *Proceedings of the Royal Society B: Biological Sciences* **270**(1511), 179-184.

Marubini, F., Ferrier-Pagès, C., Furla, P. & Allemand, D. (2008) Coral calcification responds to seawater acidification: a working hypothesis towards a physiological mechanism. *Coral Reefs* **27**(3), 491-499.

Mauchline, J. (1980) The biology of mysids and euphausiids. In *Advances in Marine Biology*, vol. 18 (eds. J. H. S. Blaxter, F. S. Russell & M. Yonge) New York: Academic Press, pp. 1-681.

Mauchline, J. (1998) The Biology of Calanoid Copepods. In *Advances in Marine Biology*, vol. 33 (eds. J. H. S. Blaxter, A. J. Southward & P. A. Tyler) San Diego: Academic Press, pp. 1-710.

McConnaughey, T. A., Adey, W. H. & Small, A. M. (2000) Community and environmental influences on reef coral calcification. *Limnology and Oceanography* **45**(7), 1667-1671.

McNamara, P. T., Caldarone, E. M. & Buckley, L. J. (1999) RNA/DNA ratio and expression of 18S ribosomal RNA, actin and myosin heavy chain messenger RNAs in starved and fed larval Atlantic cod (*Gadus morhua*). *Marine Biology* **135**(1), 123-132.

Medeiros, S. K., Albuquerque, E. L., Maia Jr., F. F., Caetano, E. W. S. & Freire, V. N. (2006) Structural, electronic, and optical properties of $CaCO_3$ aragonite. *Chemical Physics Letters* **430**(4-6), 293-296.

Meesters, E. H., Nieuwland, G., Duineveld, G. C. A., Kok, A. & Bak, R. P. M. (2002) RNA/DNA ratios of scleractinian corals suggest acclimatisation/adaptation in relation to light gradients and turbidity regimes. *Marine Ecology Progress Series* **227**, 233-239.

Mehrbach, C., Culberson, C. H., Hawley, J. E. & Pytkowicz, R. N. (1973) Measurement of the apparent dissociation constants of carbonic acid in seawater at atmospheric pressure. *Limnology and Oceanography* **18**, 897-907.

Menzies, R. J. (1965) Conditions for the existence of life on the abyssal sea floor. *Oceanography and Marine Biology Annual Review* **3**, 195-210.

Meyerhöfer, M., Form, A., Rüggeberg, A., Hissmann, K., Schauer, J., Holtmann, W. C., Margreth, S. & Riebesell, U. (2008) Geobiological investigations and sampling of Norwegian aphotic coral reef ecosystems. RV ALKOR Cruise Report AL316. Kiel: IFM-GEOMAR, 31 pp.

Mikkelsen, N., Erlenkeuser, H., Killingley, J. S. & Berger, W. H. (1982) Norwegian corals radiocarbon and stable isotopes in *Lophelia pertusa*. *Boreas* **11**(2), 163-171.

Miller, A. W., Reynolds, A. C., Sobrino, C. & Riedel, G. F. (2009) Shellfish face uncertain future in high CO_2 world: Influence of acidification on oyster larvae calcification and growth in estuaries. *Plos One* **4**(5), e5661.

Millero, F. J. (2007) The marine inorganic carbon cycle. *Chemical Reviews* **107**, 308-341.

Milliman, J. D., Manheim, F. T., Pratt, R. M. & Zarudzki, E. F. K. (1967) ALVIN dives on the continental margin off the southeastern United States, July 2-13, 1967. Woods Hole Oceanographic Institution, 70 pp.

Moen, T. L. (2006) A translation of Bishop Gunnerus' description of the species *Hydroides norvegicus* with comments on his *Serpula triqvetra*. *Scientia Marina* **70**(S3), 115-123.

Moldzio, S. (2008) *Einfluß verschiedener Futterqualitäten auf Freßverhalten und Kalzifizierung von Lophelia pertusa (Scleractinia)*. Diploma Thesis, IFM-GEOMAR, Kiel: Christian-Albrechts-University Kiel, 111 pp.

Mortensen, P. B. (2001) Aquarium observations on the deep-water coral *Lophelia pertusa* (L., 1758) (Scleractinia) and selected associated invertebrates. *Ophelia* **54**(2), 83-104.

Mortensen, P. B. (2005) Effects of fisheries on deepwater gorgonian corals in the Northeast Channel, Nova Scotia. *American Fisheries Society Symposium*, 369-382.

Mortensen, P. B., Hovland, M., Brattegard, T. & Farestveit, R. (1995) Deep water bioherms of the scleractinian coral *Lophelia pertusa* (L.) at 64°N on the Norwegian shelf: structure and associated megafauna. *Sarsia* **80**, 145-158.

Mortensen, P. B. & Rapp, H. T. (1998) Oxygen and carbon isotope ratios related to growth line patterns in skeletons of *Lophelia pertusa* (L) (Anthozoa, Scleractinia): implications for determination of linear extension rates. *Sarsia* **83**, 433-446.

Mortensen, P. B., Roberts, J. M. & Sundt, R. C. (2000) Video-assisted grabbing: a minimally destructive method of sampling azooxanthellate coral banks. *Journal of the Marine Biological Association of the United Kingdom* **80**(2), 365-366.

Mucci, A. (1983) The solubility of calcite and aragonite in seawater at various salinities, temperatures, and one atmosphere total pressure. *American Journal of Science* **283**, 780-799.

Muller-Parker, G., McCloskey, L. R., Hoegh-Guldberg, O. & McAuley, P. J. (1994) Effect of ammonium enrichment on animal and algal biomass of the coral *Pocillopora damicornis*. *Pacific Science* **48**(3), 273-283.

Muscatine, L. (1973) Nutrition of corals. In *Biology and Geology of Coral Reefs* (eds. O. A. Jones & R. Endean) New York: Academic Press, pp. 79-115.

Nagelkerken, I., van der Velde, G. & van Avesaath, P. H. (1997) A description of the skeletal development pattern of the temperate coral *Caryophyllia smithi* based on internal growth lines. *Journal of the Marine Biological Association of the United Kingdom* **77**(02), 375-387.

Nakata, K., Nakano, H. & Kikuchi, H. (1994) Relationship between egg productivity and RNA/DNA Ratio in *Paracalanus* sp. in the frontal waters of the Kurshio. *Marine Biology* **119**(4), 591-596.

Naumann, M., Niggl, W., Laforsch, C., Glaser, C. & Wild, C. (2009) Coral surface area quantification – evaluation of established techniques by comparison with computer tomography. *Coral Reefs* **28**(1), 109-117.

Nautilus Minerals Inc. (2011) Solwara 1 Project – High Grade Copper and Gold. http://www.nautilusminerals.com/s/Projects-Solwara.asp.

Newton, C. R., Mullins, H. T., Gardulski, A. F., Hine, A. C. & Dix, G. R. (1987) Coral mounds on the West Florida slope: unanswered questions regarding the development of deep-water banks. *Palaios* **2**(4), 359-367.

Nie, B., Chen, T., Liang, M., Wang, Y., Zhong, J. & Zhu, Y. (1997) Relationship between coral growth rate and sea surface temperature in the northern part of South China Sea during the past 100 a. *Science in China Series D: Earth Sciences* **40**(2), 173-182.

Noé, S., Titschack, J., Freiwald, A. & Dullo, W. C. (2006) From sediment to rock: diagenetic processes of hardground formation in deep-water carbonate mounds of the NE Atlantic. *Facies* **52**(2), 183-208.

Ohde, S. & Hossain, M. M. M. (2004) Effect of $CaCO_3$ (aragonite) saturation state of seawater on calcification of *Porites* coral. *Geochemical Journal* **38**, 613-621.

Ohde, S. & van Woesik, R. (1999) Carbon dioxide flux and metabolic processes of a coral reef, Okinawa. *Bulletin of Marine Science* **65**(2), 559-576.

Orejas, C., Gori, A. & Gili, J. M. (2008) Growth rates of live *Lophelia pertusa* and *Madrepora oculata* from the Mediterranean Sea maintained in aquaria. *Coral Reefs* **27**(2), 255.

Orr, J. C., Fabry, V. J., Aumont, O., Bopp, L., Doney, S. C., Feely, R. A., Gnanadesikan, A., Gruber, N., Ishida, A., Joos, F., Key, R. M., Lindsay, K., Maier-Reimer, E., Matear, R., Monfray, P., Mouchet, A., Najjar, R. G., Plattner, G. K., Rodgers, K. B., Sabine, C. L., Sarmiento, J. L., Schlitzer, R., Slater, R. D., Totterdell, I. J., Weirig, M. F., Yamanaka, Y. & Yool, A. (2005) Anthropogenic ocean acidification over the twenty-first century and its impact on calcifying organisms. *Nature* **437**(7059), 681-686.

Østvedt, O. J. (1955) Zooplankton investigations from weather ship M in the Norwegian Sea. 1948–1949. In *Hvalrådets Skrifter. Scientific Results of Marine Biological Research*, vol. 40, 1-93 pp.

Palardy, J. E., Grottoli, A. G. & Matthews, K. A. (2006) Effect of naturally changing zooplankton concentrations on feeding rates of two coral species in the Eastern Pacific. *Journal of Experimental Marine Biology and Ecology* **331**(1), 99-107.

Pearse, V. B. & Muscatine, L. (1971) Role of symbiotic algae (Zooxanthellae) in coral calcification. *The Biological Bulletin* **141**(2), 350-363.

Peck, L. S. & Uglow, R. F. (1990) Two methods for the assessment of the oxygen content of small volumes of seawater. *Journal of Experimental Marine Biology and Ecology* **141**(1), 53-62.

Picciano, M. & Ferrier-Pagès, C. (2007) Ingestion of pico- and nanoplankton by the Mediterranean red coral *Corallium rubrum*. *Marine Biology* **150**(5), 773-782.

Pierce, G. J., Key, L. N., Boyle, P. R., Siegert, K. J., Goncalves, J. M., Porteiro, F. M. & Martins, H. R. (1999) RNA concentration and the RNA to protein ratio in cephalopod

tissues: sources of variation and relationship with growth rate. *Journal of Experimental Marine Biology and Ecology* **237**(2), 185-201.

Pinho, G. L. L., Pedroso, M. S., Rodrigues, S. C., de Souzac, S. S. & Bianchini, A. (2007) Physiological effects of copper in the euryhaline copepod *Acartia tonsa*: Waterborne versus waterborne plus dietborne exposure. *Aquatic Toxicology* **84**(1), 62-70.

Pitois, S. G. & Fox, C. J. (2006) Long-term changes in zooplankton biomass concentration and mean size over the Northwest European shelf inferred from Continuous Plankton Recorder data. *ICES Journal of Marine Science* **63**, 785-798.

Porter, J. W. (1976) Autotrophy, heterotrophy and resource partitioning in Carribbean reef building corals. *American Naturalist* **110**, 731-742.

PreSens GmbH. (2005) *Instruction Manual OXY-10 10-Channel Fiber-Optic Oxygen Meter*. Regensburg: PreSens Precision Sensing GmbH.

PreSens GmbH. (2007) *Instruction Manual pH-10 mini 10-Channel Minisensor pH-Meter*. Regensburg: PreSens Precision Sensing GmbH.

Puverel, S., Tambutte, E., Pererra-Mouries, L., Zoccola, D., Allemand, D. & Tambutte, S. (2005) Soluble organic matrix of two Scleractinian corals: Partial and comparative analysis. *Comparative Biochemistry and Physiology B - Biochemistry & Molecular Biology* **141**(4), 480-487.

Quirt, J. & Lasenby, D. (2002) Cannibalism and ontogenetic changes in the response of the freshwater shrimp *Mysis relicta* to chemical cues from conspecific predators. *Canadian Journal of Zoology* **80**(6), 1022-1025.

Ralph, J. & Chau, I. (2010) Aragonite. mindat.org - the mineral and locality database, http://www.mindat.org/min-307.html.

Rapp, H. T. & Sneli, J. A. (1999) *Lophelia pertusa* – myths and reality. *Second Nordic Marine Sciences Meeting*, Hirthals, Denmark.

Rasband, W. S. (2004) ImageJ. National Institutes of Health, Ver.: 1.4.0g.

Raven, J., Caldeira, K., Elderfield, H., Hoegh-Guldberg, O., Liss, P., Riebesell, U., Shepherd, J., Turley, C. M. & Watson, A. (2005) Ocean acidification due to increasing atmospheric carbon dioxide. London: The Royal Society, 68 pp.

Rex, M. A. (1981) Community structure in the deep-sea benthos. *Annual Review of Ecology and Systematics* **12**(1), 331-353.

Reynaud, S., Leclercq, N., Romaine-Lioud, S., Ferrier-Pagès, C., Jaubert, J. & Gattuso, J. P. (2003) Interacting effects of CO_2 partial pressure and temperature on photosynthesis and calcification in a scleractinian coral. *Global Change Biology* **9**(11), 1660-1668.

Ricketts, E. R., Kennett, J. P., Hill, T. M. & Barry, J. P. (2009) Effects of carbon dioxide sequestration on California margin deep-sea foraminiferal assemblages. *Marine Micropaleontology* **72**(3-4), 165-175.

Ridgwell, A. & Schmidt, D. N. (2010) Past constraints on the vulnerability of marine calcifiers to massive carbon dioxide release. *Nature Geoscience* **3**(3), 196-200.

Riebesell, U., Bellerby, R. G. J., Engel, A., Fabry, V. J., Hutchins, D. A., Reusch, T. B. H., Schulz, K. G. & Morel, F. M. M. (2008) Comment on "Phytoplankton calcification in a high-CO_2 world". *Science* **322**(5907), 1466.

Riebesell, U., Schulz, K. G., Bellerby, R. G. J., Botros, M., Fritsche, P., Meyerhöfer, M., Neill, C., Nondal, G., Oschlies, A., Wohlers, J. & Zöllner, E. (2007) Enhanced biological carbon consumption in a high CO_2 ocean. *Nature* **450**(7169), 545-548.

Riebesell, U., Zondervan, I., Rost, B., Tortell, P. D., Zeebe, R. E. & Morel, F. M. M. (2000) Reduced calcification of marine plankton in response to increased atmospheric CO_2. *Nature* **407**(6802), 364-367.

Ries, J. B., Cohen, A. L. & McCorkle, D. C. (2009) Marine calcifiers exhibit mixed responses to CO_2-induced ocean acidification. *Geology* **37**(12), 1131-1134.

River, G. & Edmunds, P. J. (2001) Mechanisms of interaction between macroalgae and scleractinians on a coral reef in Jamaica. *Journal Experimental Marine Biology and Ecology* **261**, 159-172.

Roast, S. D., Thompson, R. S., Donkin, P., Widdows, J. & Jones, M. B. (1999) Toxicity of the organophosphate pesticides chlorpyrifos and dimethoate to *Neomysis integer* (Crustacea: Mysidacea). *Water Research* **33**(2), 319-326.

Roast, S. D., Widdows, J. & Jones, M. B. (2001) Effects of salinity and chemical speciation on cadmium accumulation and toxicity to two mysid species. *Environmental Toxicology and Chemistry* **20**(5), 1078-1084.

Roberts, J. M. (2002) The occurrence of the coral *Lophelia pertusa* and other conspicuous epifauna around an oil platform in the North Sea *Underwater Technology* **25**(2), 83-92.

Roberts, J. M. & Anderson, R. M. (2002) A new laboratory method for monitoring deep-water coral polyp behaviour. *Hydrobiologia* **471**, 143-148.

Roberts, J. M., Brown, C. J., Long, D. & Bates, C. R. (2005) Acoustic mapping using a multibeam echosounder reveals cold-water coral reefs and surrounding habitats. *Coral Reefs* **24**(4), 654-669.

Roberts, J. M., Long, D., Wilson, J. B., Mortensen, P. B. & Gage, J. D. (2003) The cold-water coral *Lophelia pertusa* (Scleractinia) and enigmatic seabed mounds along the north-east Atlantic margin: are they related? *Marine Pollution Bulletin* **46**(1), 7-20.

Roberts, J. M., Wheeler, A. J., Freiwald, A. & Cairns, S. D. (2009) *Cold-Water Corals: The Biology and Geology of Deep-Sea Coral Habitats*. Cambridge: University Press.

Rodolfo-Metalpa, R., Martin, S., Ferrier-Pagès, C. & Gattuso, J. P. (2010) Response of the temperate coral *Cladocora caespitosa* to mid- and long-term exposure to pCO_2 and temperature levels projected for the year 2100 AD. *Biogeosciences* **7**(1), 289-300.

Rodolfo-Metalpa, R., Richard, C., Allemand, D. & Ferrier-Pagès, C. (2006) Growth and photosynthesis of two Mediterranean corals, *Cladocora caespitosa* and *Oculina patagonica*, under normal and elevated temperatures. *Journal of Experimental Biology* **209**, 4546-4556.

Rogers, A. D. (1999) The biology of *Lophelia pertusa* (Linnaeus 1758) and other deep-water reef-forming corals and impacts from human activities. *International Review of Hydrobiology* **84**(4), 315-406.

Rüggeberg, A. & Form, A. (2007) Geobiological investigations and sampling of aphotic coral reef ecosystems in the NE-Skagerrak. RV ALKOR Cruise report AL275. In *IFM-GEOMAR-Report*, vol. 10, Kiel: IFM-GEOMAR, 36 pp.

Sabine, C. L. & Feely, R. A. (2007) The oceanic sink for carbon dioxide. In *Greenhouse Gas Sinks* (eds. D. Reay, N. Hewitt, J. Grace & K. Smith) Oxfordshire: CABI Publishing, pp. 31–49.

Sander, M. (1998) *Aquarientechnik in Süß- und Seewasser*. DATZ-Aquarienbücher. Stuttgart: Eugen Ulmer.

Schippers, P., Lürling, M. & Scheffer, M. (2004) Increase of atmospheric CO_2 promotes phytoplankton productivity. *Ecology Letters* **7**, 446-451.

Schneider, K. & Erez, J. (2006) The effect of carbonate chemistry on calcification and photosynthesis in the hermatypic coral *Acropora eurystoma*. *Limnology and Oceanography* **51**(3), 1284-1293.

Schrehardt, A. (1987) Scanning electron microscope study of the post-embryonic development of *Artemia*. In *Artemia Research and its Applications* (eds. P. Sorgeloos, D. A. Bengston, W. Decleir & E. Jaspers) Wetteren: Universa Press, pp. 5-32.

Schroeder, W. W. (2002) Observations of *Lophelia pertusa* and the surficial geology at a deep-water site in the northeastern Gulf of Mexico. *Hydrobiologia* **471**, 29-33.

Sciandra, A., Harlay, J., Lefevre, D., Lemee, R., Rimmelin, P., Denis, M. & Gattuso, J. P. (2003) Response of coccolithophorid *Emiliania huxleyi* to elevated partial pressure of CO_2 under nitrogen limitation. *Marine Ecology Progress Series* **261**, 111-122.

Sebens, K. P. (1987) Coelenterata. In *Animal energetics* (eds. F. J. Vernberg & T. J. Pandian) New York: Academic Press, pp. 55-120.

Sebens, K. P. (1991) Effects of water movement on prey capture and distribution of reef corals. *Hydrobiologia* **216-217**(1), 247-248.

Sebens, K. P. & Deriemer, K. (1977) Diel cycles of expansion and contraction in coral reef anthozoans. *Marine Biology* **43**, 247-256.

Sebens, K. P., Vandersall, K. S., Savina, L. A. & Graham, K. R. (1996) Zooplankton capture by two scleractinian corals, *Madracis mirabilis* and *Montastrea cavernosa*, in a field enclosure. *Marine Biology* **127**(2), 303-317.

Sebens, K. P., Witting, J. & Helmuth, B. (1997) Effects of water flow and branch spacing on particle capture by the reef coral *Madracis mirabilis* (Duchassaing and Michelotti). *Journal of Experimental Marine Biology and Ecology* **211**(1), 1-28.

Shelton, G. (1980) *Lophelia pertusa* (L.): electrical conduction and behaviour in a deep-water coral. *Journal of the Marine Biological Association of the United Kingdom* **60**(2), 517-528.

Shirayama, Y. & Thornton, H. (2005) Effect of increased atmospheric CO_2 on shallow water marine benthos. *Journal of Geophysical Research - Oceans* **110**(C09S08), 1-7.

Silverman, J., Lazar, B., Cao, L., Caldeira, K. & Erez, J. (2009) Coral reefs may start dissolving when atmospheric CO_2 doubles. *Geophysical Research Letters* **36**(L05606), 1-5.

Silverman, J., Lazar, B. & Erez, J. (2007) Effect of aragonite saturation, temperature, and nutrients on the community calcification rate of a coral reef. *Journal of Geophysical Research - Oceans* **112**(C5), 1-14.

Smith, S. V. & Key, G. S. (1975) Carbon-dioxide and metabolism in marine environments. *Limnology and Oceanography* **20**(3), 493-495.

Smith, S. V. & Pesret, F. (1974) Processes of carbon dioxide flux in the Fanning Island lagoon. *Pacific Science* **28**, 225-245.

Solomon, S., Qin, D., Manning, M., Chen, Z., Marquis, M., Averyt, K. B., Tignor, M. & Miller, H. L. (eds.) (2007) *Climate change 2007: The physical science basis: Contribution of working group I to the fourth assessment report of the Intergovernmental Panel on Climate Change*. New York: Cambridge University Press.

Spero, H. J., Bijma, J., Lea, D. W. & Bemis, B. E. (1997) Effect of seawater carbonate concentration on foraminiferal carbon and oxygen isotopes. *Nature* **390**(6659), 497-500.

Spinaze, K. A., Smith, S. D. A. & Simpson, R. D. (1996) The effect of depth and wave exposure on the density and porosity of *Pocillopora damicornis* in the Solitary Islands Marine Reserve, New South Wales. *Proceedings of The Great Barrier Reef, Science, Use and Management Conference*, Townsville, 72–76.

Spiro, B., Roberts, M., Gage, J. D. & Chenery, S. (2000) $^{18}O/^{16}O$ and $^{13}C/^{12}C$ in an ahermatypic deep-water coral *Lophelia pertusa* from the North Atlantic: a case of disequilibrium isotope fractionation. *Rapid Communications in Mass Spectrometry* **14**(15), 1332-1336.

Stambler, N., Popper, N., Dubinsky, Z. & Stimson, J. (1991) Effects of nutrient enrichment and water motion on the coral *Pocillopora damicornis*. *Pacific Science* **45**(3), 299-307.

Stanley, G. D. (2003) The evolution of modern corals and their early history. *Earth-Science Reviews* **60**(3-4), 195-225.

Stanley, G. D. & Fautin, D. G. (2001) Paleontology and evolution - The origins of modern corals. *Science* **291**(5510), 1913-1914.

Stoll, M. H. C., Bakker, K., Nobbe, G. H. & Haese, R. R. (2001) Continuous-flow analysis of dissolved inorganic carbon content in seawater. *Analytical Chemistry* **73**(17), 4111-4116.

Stratil, S. (2006) *Experimente zum Fraßverhalten der Kaltwasserkoralle Lophelia pertusa (L. 1758)*. Student Thesis (Semesterarbeit), IFM-GEOMAR, Kiel: Christian-Albrechts-University, 17 pp.

Strømgren, T. (1971) Vertical and horizontal distribution of *Lophelia pertusa* (LINNÉ) in Trondheimsfjorden on the west coast of Norway. *Det Kongelige Norske Videnskabers Selskabs Skrifter* **6**, 1-9.

Suchman, C. L. (2000) Escape behavior of *Acartia hudsonica* copepods during interactions with scyphomedusae. *Journal of Plankton Research* **22**(12), 2307-2323.

Suzuki, A. & Kawahata, H. (2003) Carbon budget of coral reef systems: an overview of observations in fringing reefs, barrier reefs and atolls in the Indo-Pacific regions. *Tellus Series B - Chemical and Physical Meteorology* **55**(2), 428-444.

Tambutte, E., Allemand, D., Mueller, E. & Jaubert, J. (1996) A compartmental approach to the mechanism of calcification in hermatypic corals. *Journal of Experimental Biology* **199**(5), 1029-1041.

Tambutte, S., Tambutte, E., Zoccola, D., Caminiti, N., Lotto, S., Moya, A., Allemand, D. & Adkins, J. (2007) Characterization and role of carbonic anhydrase in the calcification process of the azooxanthellate coral *Tubastrea aurea*. *Marine Biology* **151**(1), 71-83.

Tanaka, Y., Miyajima, T., Koike, I., Hayashibara, T. & Ogawa, H. (2007) Imbalanced coral growth between organic tissue and carbonate skeleton caused by nutrient enrichment. *Limnology and Oceanography* **52**(3), 1139-1146.

Tanaka, Y., Satoh, K., Yamada, H., Takebe, T., Nikaido, H. & Shiozawa, S. (2008) Assessment of the nutritional status of field-caught larval Pacific bluefin tuna by RNA/DNA ratio based on a starvation experiment of hatchery-reared fish. *Journal of Experimental Marine Biology and Ecology* **354**(1), 56-64.

Tanhua, T., Körtzinger, A., Friis, K., Waugh, D. W. & Wallace, D. W. R. (2007) An estimate of anthropogenic CO_2 inventory from decadal changes in oceanic carbon content. *Proceedings of the National Academy of Sciences of the United States of America* **104**(9), 3037-3042.

Tatersall, W. M. & Tatersall, O. S. (1951) *The British Mysidacea*. London: The Ray Society.

Taviani, M., Remia, A., Corselli, C., Freiwald, A., Malinverno, E., Mastrototaro, F., Savini, A. & Tursi, A. (2005) First geo-marine survey of living cold-water *Lophelia* reefs in the Ionian Sea (Mediterranean basin). *Facies* **50**(3-4), 409-417.

Thiel, H. (1979) Structural aspects of the deep-sea benthos. In *Ambio Special Report; The Deep Sea: Ecology and Exploitation*, vol. 6, pp. 25-31.

Thiem, Ø., Ravagnan, E., Fosså, J. H. & Berntsen, J. (2006) Food supply mechanisms for cold-water corals along a continental shelf edge. *Journal of Marine Systems* **60**(3-4), 207-219.

Thistle, D., Carman, K. R., Sedlacek, L., Brewer, P. G., Fleeger, J. W. & Barry, J. P. (2005) Deep-ocean, sediment-dwelling animals are sensitive to sequestered carbon dioxide. *Marine Ecology Progress Series* **289**, 1-4.

Thomson, C. W. (1873) *The Depths of the Sea: an account of the general results of the dredging cruises of H.M.SS. 'Porcupine' and 'Lightning' during the summers of 1868, 1869, and 1870, under the scientific direction of Dr. Carpenter, F.R.S., J. Gwyn Jeffreys, F.R.S., and Dr. Wyville Thomson, F.R.S.* London: Macmillan & Co.

Tittensor, D. P., Baco, A. R., Brewin, P. E., Clark, M. R., Consalvey, M., Hall-Spencer, J., Rowden, A. A., Schlacher, T., Stocks, K. I. & Rogers, A. D. (2009) Predicting global habitat suitability for stony corals on seamounts. *Journal of Biogeography* **36**(6), 1111-1128.

Treece, G. D. (2000) *Artemia* production for marine larval fish culture. *Southern Regional Aquaculture Center Fact Sheets* **702**, 1-7.

Tsounis, G., Orejas, C., Reynaud, S., Gili, J. M., Allemand, D. & Ferrier-Pagès, C. (2010) Prey-capture rates in four Mediterranean cold water corals. *Marine Ecology Progress Series* **398**, 149-155.

Turley, C., Eby, M., Ridgwell, A. J., Schmidt, D. N., Findlay, H. S., Brownlee, C., Riebesell, U., Fabry, V. J., Feely, R. A. & Gattuso, J. P. (2010) The societal challenge of ocean acidification. *Marine Pollution Bulletin* **60**(6), 787-792.

Turley, C. M., Roberts, J. M. & Guinotte, J. M. (2007) Corals in deep-water: will the unseen hand of ocean acidification destroy cold-water ecosystems? *Coral Reefs* **26**(3), 445-448.

UNEP-WCMC. (2009) Cold-water coral. *United Nations Environment Programme - World Conservation Monitoring Centre*, http://bure.unep-wcmc.org/marine/coldcoral/viewer.htm.

Vanhaecke, P., Lavens, P. & Sorgeloos, P. (1983) International study on *Artemia*. XVII. Energy consumption in cysts and early larval stages of various geographical strains of *Artemia*. *Annales de la Societe Royale Zoologique de Belgique* **113**, 155-164.

Vaughan, T. W. & Wells, J. W. (1943) Revision of the suborders, families, and genera of the scleractinian. *Geological Society of America* **44**, 1-363.

Veron, J. E. N. (2008) Mass extinctions and ocean acidification: biological constraints on geological dilemmas. *Coral Reefs* **27**(3), 459-472.

Verslycke, T., Vangheluwe, M., Heijerick, D., De Schamphelaere, K., Van Sprang, P. & Janssen, C. R. (2003) The toxicity of metal mixtures to the estuarine mysid *Neomysis integer* (Crustacea: Mysidacea) under changing salinity. *Aquatic Toxicology* **64**(3), 307-315.

Vlasblom, A. G. & Elgershuizen, J. H. B. W. (1977) Survival and oxygen consumption of *Praunus flexuosus* and *Neomysis integer*, and embryonic development of the latter species, in different temperature and chlorinity combinations. *Netherlands Journal of Sea Research* **11**(3-4), 305-315.

Wagner, M., Durbin, E. & Buckley, L. (1998) RNA:DNA ratios as indicators of nutritional condition in the copepod *Calanus finmarchicus*. *Marine Ecology Progress Series* **162**, 173-181.

Watanabe, T., Fukuda, I., China, K. & Isa, Y. (2003) Molecular analyses of protein components of the organic matrix in the exoskeleton of two scleractinian coral species. *Comparative Biochemistry and Physiology B - Biochemistry & Molecular Biology* **136**(4), 767-774.

Weast, R. C. (1979) *CRC Handbook of Chemistry and Physics. A ready-reference book of chemical and physical data*. Boca Raton: Chemical Rubber Company.

Weber, J. N., White, E. W. & Weber, P. H. (1975) Correlation of density banding in reef coral skeletons with environmental parameters; the basis for interpretation of chronological records preserved in the coralla of corals. *Paleobiology* **1**(2), 137-149.

Wiborg, K. F. (1976) Fishery and commercial exploitation of *Calanus finmarchicus* in Norway. *ICES Journal of Marine Science* **36**(3), 251-258.

Wilson, G. D. F. & Hessler, R. R. (1987) Speciation in the deep sea. *Annual Review of Ecology and Systematics* **18**(1), 185-207.

Wilson, J. B. (1979) Patch' development of the deep-water coral *Lophelia pertusa* (L.) on Rockall Bank. *Journal of the Marine Biological Association of the United Kingdom* **59**, 165-177.

Wilson, J. B. (2001) *Lophelia* 1700 to 2000 and beyond. *First International Symposium on Deep-Sea Corals*, Halifax.

Winkler, L. W. (1888) The determination of dissolved oxygen in water. *Berichte der Deutschen Chemischen Gesellschaft* **21**, 2834-2846.

Witherell, D. & Coon, C. (2001) Protecting gorgonian corals off Alaska from fishing impacts. *First International Symposium on Deep-Sea Corals*, Halifax.

Withers, P. C. (1992) *Comparative Animal Physiology*. New York: Saunders College Publishing.

Wo, K. T., Lam, P. K. S. & Wu, R. S. S. (1999) A comparison of growth biomarkers for assessing sublethal effects of cadmium on a marine gastropod, *Nassarius festivus*. *Marine Pollution Bulletin* **39**(1-12), 165-173.

Wolf-Gladrow, D. A., Zeebe, R. E., Klaas, C., Körtzinger, A. & Dickson, A. G. (2007) Total alkalinity: The explicit conservative expression and its application to biogeochemical processes. *Marine Chemistry* **106**(1-2), 287-300.

Wood, H. L., Spicer, J. I. & Widdicombe, S. (2008) Ocean acidification may increase calcification rates, but at a cost. *Proceedings of the Royal Society B: Biological Sciences* **275**(1644), 1767-1773.

Wright, D. A. & Hetzel, E. W. (1985) Use of RNA:DNA ratios as an indicator of nutritional stress in the American oyster *Crassostrea virginica*. *Marine Ecology Progress Series* **25**(2), 199-206.

Yu, Z. T. & Mohn, W. W. (1999) Killing two birds with one stone: simultaneous extraction of DNA and RNA from activated sludge biomass. *Canadian Journal of Microbiology* **45**(3), 269-272.

Zachos, J. C., Rohl, U., Schellenberg, S. A., Sluijs, A., Hodell, D. A., Kelly, D. C., Thomas, E., Nicolo, M., Raffi, I., Lourens, L. J., McCarren, H. & Kroon, D. (2005) Rapid acidification of the ocean during the Paleocene-Eocene thermal maximum. *Science* **308**(5728), 1611-1615.

Zeebe, R. E. & Wolf-Gladrow, D. A. (2001) *CO_2 in Seawater: Equilibrium, Kinetics, Isotopes*. Amsterdam: Elsevier Oceanography Series.

Zhu, B. H., Wang, G. C., Huang, B. & Tseng, C. K. (2004) Effects of temperature, hypoxia, ammonia and nitrate on the bleaching among three coral species. *Chinese Science Bulletin* **49**(18), 1923-1928.

Zibrowius, H. (1973) Scléractiniaries des Iles Saint Paul et Amsterdam (sud de l'Océan Indien). *Tethys* **5**, 747-778.

Zibrowius, H. (1980) Les Scléractiniaries de la Mediteranée et de l'Atlantique nord-oriental. In *Memoires Institute Oceanographique*, vol. 11, Monaco, 284 pp.

Zibrowius, H. (1984) Taxonomy in ahermatypic scleractinian corals. *Palaeontographica Americana* **56**, 80-85.

Zoccola, D., Tambutte, E., Kulhanek, E., Puverel, S., Scimeca, J. C., Allemand, D. & Tambutte, S. (2004) Molecular cloning and localization of a PMCA P-type calcium ATPase from the coral *Stylophora pistillata*. *Biochimica Et Biophysica Acta - Biomembranes* **1663**(1-2), 117-126.

Zondervan, I., Rost, B. & Riebesell, U. (2002) Effect of CO_2 concentration on the PIC/POC ratio in the coccolithophore *Emiliania huxleyi* grown under light-limiting conditions and different daylengths. *Journal of Experimental Marine Biology and Ecology* **272**(1), 55-70.

Zondervan, I., Zeebe, R. E., Rost, B. & Riebesell, U. (2001) Decreasing marine biogenic calcification: A negative feedback on rising atmospheric pCO_2. *Global Biogeochemical Cycles* **15**(2), 507-516.

Appendices

A. Experimental data and statistics

A1 Ammonium sensitivity experiment (2.1.3.3)

Tab. A1-1 Descriptive statistics of the polyp extension stages of the six time intervals during the ammonium sensitivity bioassay. See text for details.

Interval	Group	n	Missing	Median	25 %	75 %
I	control	114	0	2.4	1.6	2.6
	NH_4^+	114	0	2.2	2.0	2.4
II	control	114	0	2.4	1.4	2.6
	NH_4^+	114	0	1.8	1.0	2.2
III	control	114	3	1.8	1.4	2.0
	NH_4^+	114	7	1.5	1.0	1.8
IV	control	114	0	1.6	1.2	2.2
	NH_4^+	114	0	1.6	1.2	1.8
V	control	114	0	1.6	1.2	2.0
	NH_4^+	114	0	1.4	1.2	1.6
VI	control	114	0	1.6	1.4	1.8
	NH_4^+	114	0	1.2	1.4	1.4

Tab. A1-2 Results from the Mann-Whitney Rank Sum Test (differences between control and NH_4^+ treatment).

Interval	U Statistic	n (small)	n (big)	T	P
I	6052.0	114	114	13499.0	0.365
II	3585.0	114	114	15966.0	< 0.001
III	4113.0	107	111	9891.0	< 0.001
IV	5047.0	114	114	14503.5	0.003
V	4672.0	114	114	14879.0	< 0.001
VI	2295.5	114	114	17255.5	< 0.001

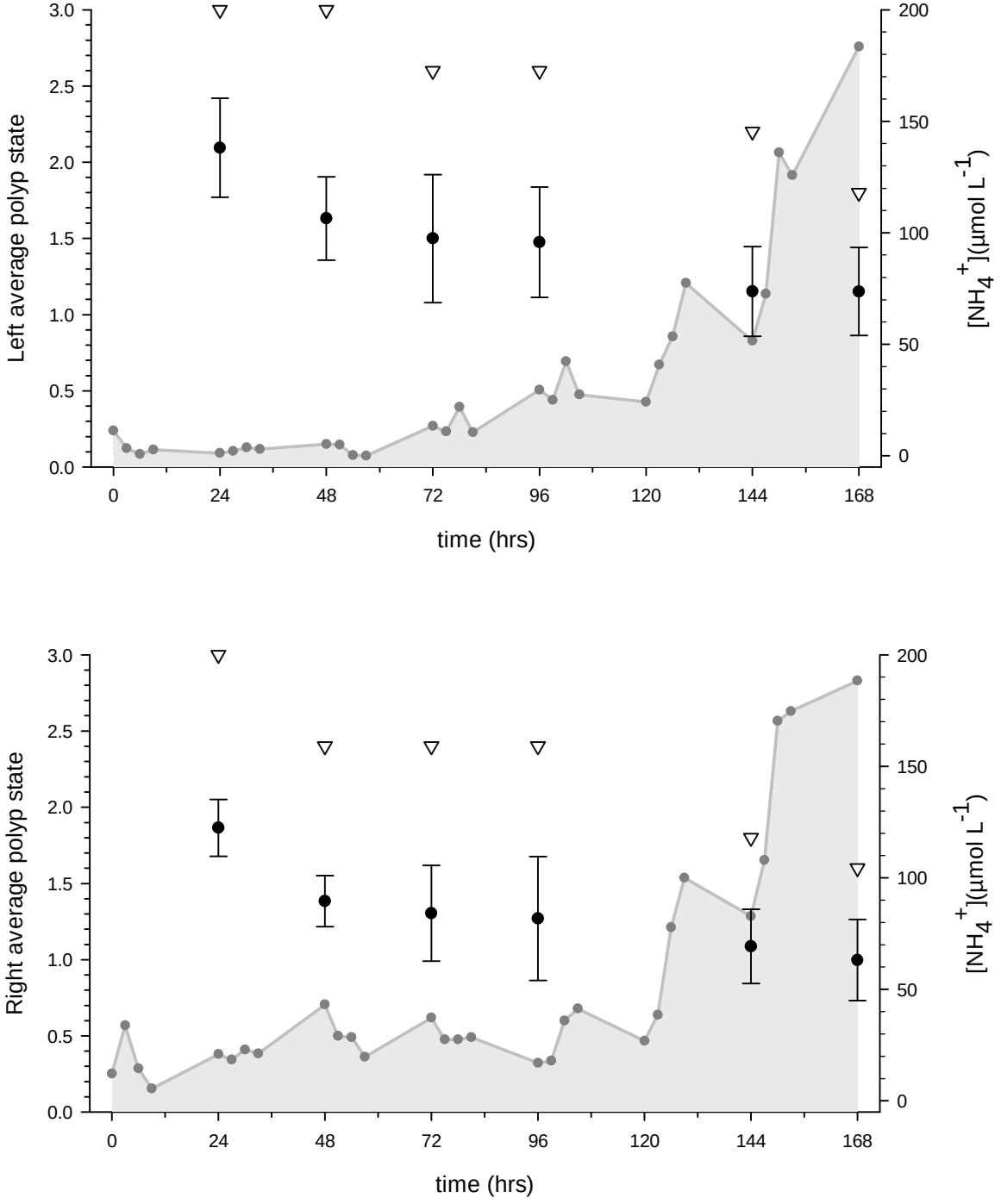

Fig. A1-1 Average coral polyp states in left (above) and right (below) compartiment in the ammonia tolerance bioassay. Black dots indicate mean polyp states of five selected polyps from one coral branch. Error bars: standard deviation. The white triangles representate the maximum recorded state for the 5 non-independent replicates during the 24 hrs interval. Grey dots and area: ammonia concentration development.

A2 Growth rates during food uptake experiments (3.1.2.3)

a) Paired t-test, normalisation: µg $CaCO_3$ $polyp^{-1}$ day^{-1}

Tab. A2-1 Descriptive statistics of calcification rates measured during feeding period 1 and 3. SD: standard deviation, SEM: standard error of the mean.

Treatment	n	Missing	Mean	SD	SEM
feeding period 1	9	0	140.878	129.457	43.152
feeding period 3	9	0	87.056	79.638	26.546
Difference	9	0	53.822	89.056	29.685

t = 1.813 with 8 degrees of freedom. (P = 0.107)

95 percent confidence interval for difference of means: -14.633 to 122.277

Tab. A2-2 Descriptive statistics of calcification rates measured during feeding period 1 and 2. SD: standard deviation, SEM: standard error of the mean.

Treatment	n	Missing	Mean	SD	SEM
feeding period 1	9	0	140.878	129.457	43.152
feeding period 2	9	0	82.544	159.049	53.016
Difference	9	0	58.333	274.896	91.632

t = 0.637 with 8 degrees of freedom. (P = 0.542)

95 percent confidence interval for difference of means: -152.970 to 269.637

b) Paired t-test, normalisation: µg $CaCO_3$ mm^{-2} day^{-1}

Tab. A2-3 Descriptive statistics of calcification rates measured during feeding period 1 and 3. SD: standard deviation, SEM: standard error of the mean.

Treatment	n	Missing	Mean	SD	SEM
feeding period 1	9	0	3.374	2.452	0.817
feeding period 3	9	0	2.021	1.170	0.390
Difference	9	0	1.353	2.413	0.804

t = 1.683 with 8 degrees of freedom. (P = 0.131)

95 percent confidence interval for difference of means: -0.501 to 3.208

Tab. A2-4 Descriptive statistics of calcification rates measured during feeding period 1 and 2. SD: standard deviation, SEM: standard error of the mean.

Treatment	n	Missing	Mean	SD	SEM
feeding period 1	9	0	3.374	2.452	0.817
feeding period 2	9	0	2.619	3.726	1.242
Difference	9	0	0.756	5.665	1.888

t = 0.400 with 8 degrees of freedom. (P = 0.700)

95 percent confidence interval for difference of means: -3.599 to 5.110

A3 Growth rates from the CWC-MS during long-term incubation (3.1.3.3)

a) Kruskal-Wallis One Way Analysis of Variance on Ranks, normalisation: µg $CaCO_3$ $polyp^{-1}$ day^{-1}

Tab. A3-1 Median, 25% and 75% percentiles of growth rates measured during unmanipulated long-term incubation of cold-water coral *L. pertusa*.

Day	n	Missing	Median	25%	75%
85	10	0	10.835	4.451	31.975
168	10	0	28.806	18.695	40.976
297	10	0	10.919	2.646	21.247
441	10	0	20.502	18.869	36.052

H = 6.932 with 3 degrees of freedom (P = 0.074).

b) Kruskal-Wallis One Way Analysis of Variance on Ranks, normalisation: % day^{-1}

Tab. A3-2 Median, 25% and 75% percentiles of growth rates measured during unmanipulated long-term incubation of cold-water coral *L. pertusa*.

Day	n	Missing	Median	25%	75%
85	10	0	0.00305	0.00067	0.00533
168	10	0	0.00703	0.00476	0.00814
297	10	0	0.00224	0.00059	0.00657
441	10	0	0.00444	0.00356	0.00614

H = 6.244 with 3 degrees of freedom (P = 0.100).

A4 Temperature stress response experiment (RNA/DNA ratios) (3.2.1.1)

Kruskal-Wallis One Way Analysis of Variance on Ranks

Tab. A4-1 Median, 25% and 75% percentiles of RNA/DNA ratios measured under various conditions. CG: control group, SG: stress group, starv: starvation.

Group	n	Missing	Median	25%	75%
CG 8°C	207	0	2.918	2.105	3.650
SG 11°C	40	0	2.254	1.909	2.583
SG 18°C	44	0	1.372	0.882	2.180
SG starv.	17	0	1.955	1.668	2.087

H = 68.217 with 3 degrees of freedom ($P \leq 0.001$).

Multiple comparisons versus control group (Dunn's method):

Tab. A4-2 Analysis results from Dunn's post-hoc multiple comparisons. CG: control group, SG: stress group, starv: starvation.

Comparison	Diff. of Ranks	Q	P < 0.05
SG 18°C vs. CG 8°C	110.657	7.485	Yes
SG starv. vs. CG 8°C	90.035	4.007	Yes
SG 11°C vs. CG 8°C	46.146	3.000	Yes

A5 Short-term ocean acidification experiment (3.2.2.1)

a) Growth rates

One Way Analysis of Variance

Tab. A5-1 Descriptive statistics of calcification rates measured after short-term incubation of *L. pertusa* under four different pCO_2 concentrations. SD: standard deviation, SEM: standard error of the mean.

Group	n	Missing	Mean	SD	SEM
509	4	0	57.34774	25.05241	12.52621
605	4	0	8.64701	13.50185	6.75093
856	4	0	-0.31405	18.69256	9.34628
981	4	0	3.41093	14.03804	7.01902

Tab. A5-2 ANOVA analysis results. DF: degrees of freedom, SS: sum of squares, MS: mean sum of squares.

Source of Variation	DF	SS	MS	F	P
Between Groups	3	8727.41445	2909.13815	8.57899	0.00259
Residual	12	4069.20518	339.10043		
Total	15	12796.61963			

All pairwise multiple comparison procedures (Tukey test):

Tab. A5-3 Results from the Tukey post-hoc test (P values). Statistically significant differences in bold.

	509 ppm	605 ppm	856 ppm	981 ppm
509 ppm	-	**0.01311**	**0.00408**	**0.00659**
605 ppm	**0.01311**	-	0.89969	0.97707
856 ppm	**0.00408**	0.89969	-	0.99148
981 ppm	**0.00659**	0.97707	0.99148	-

b) Fitness (RNA/DNA ratios)

Kruskal-Wallis One Way Analysis of Variance on Ranks

Tab. A5-4 Median, 25% and 75% percentiles of RNA/DNA ratios measured after short-term incubation of *L. pertusa* under four different pCO_2 concentrations.

Group (pCO_2)	n	Missing	Median	25%	75%
380	102	0	3.260	2.579	4.064
526	81	0	3.322	2.757	4.004
651	48	0	2.925	2.384	3.340
867	76	0	3.271	2.863	4.319

H = 15.092 with 3 degrees of freedom (P = 0.002).

Multiple comparisons versus control group (Dunn's method):

Tab. A5-6 Analysis results from Dunn's post-hoc multiple comparisons.

Comparison (pCO_2)	Diff. of Ranks	Q	P < 0.05
651 vs. 380	43.837	2.821	Yes
867 vs. 380	16.997	1.264	No
526 vs. 380	7.725	0.585	-

A6 Long-term ocean acidification experiment (3.2.2.2.2)

Growth rates vs. pCO_2 - regression analysis

Equation: f = y0+a×x

R	**R^2**	**Adj. R^2**	**Standard Error of Estimate**
0.47039	0.22127	0.16137	0.00842

Tab. A6-1 Regression analysis results applying linear equation. SE: standard error.

Coefficient	SE	t	P	Coefficient value
y0	-0.00784	0.01105	-0.70923	0.49071
a	0.00003	0.00001	1.92194	0.07681

Analysis of Variance:

Tab. A6-2 ANOVA analysis results. DF: degrees of freedom, SS: sum of squares, MS: mean sum of squares.

	DF	SS	MS
Regression	2	0.00279	0.00140
Residual	13	0.00092	0.00007
Total	15	0.00371	0.00025

Corrected for the mean of the observations:

Tab. A6-3 ANOVA analysis results. DF: degrees of freedom, SS: sum of squares, MS: mean sum of squares.

	DF	SS	MS	F	P
Regression	1	0.00026	0.00026	3.69387	0.07681
Residual	13	0.00092	0.00007		
Total	14	0.00118	0.00008		

B. RV ALKOR cruises, JAGO sampling positions

RV ALKOR cruise AL275

Tab. B-1 Submersible JAGO dive tracks during RV ALKOR cruise AL275 in March 2006.

Time (LT)	Depth (m)	Latitude (N)	Longitude (E)	Comments
dive 922 (1) 20060326				
09:39	0	59°05.699'	10°47.894'	Submerged, freshwater layer, thermocline with high density of plankton at 10 and 25 m
09:56	107	59°05.730'	10°47.880'	at bottom, current from south 160°
10:02	105	59°05.750'	10°47.910'	first coral rubble
10:05	95	59°05.750'	10°47.880'	first living corals
10:10		59°05.760'	10°47.895'	
10:14	90	59°05.758'	10°47.896'	small pieces of broken living corals, growth pattern of coral colonies similar to Stjernsund: short branches, relatively strong current from south pushing JAGO towards slope
10:20	90	59°05.778'	10°47.906'	strong bottom current, good corals, first trial to sample corals
10:36		59°05.780'	10°47.927'	
10:58	85	59°05.770'	10°47.940'	sampling corals
11:01	85	59°05.770'	10°47.936'	took three coral samples at same position
11:19	85	59°05.770'	10°47.910'	water samples with N iskin bottles
11:45	87	59°05.790'	10°47.916'	start ascent
12:13	0			surfaced
dive 923 (2) 20060326				
17:26	0	59°05.710'	10°47.860'	submerged
17:36	107	59°05.681'	10°47.880'	at bottom, low curr ent, first coral rubble
17:43	98	59°05.661'	10°47.897'	first living *Lophelia* corals
17:49	93	59°05.650'	10°47.890'	very nice *Lophelia* reef
17:53	87			at top of small seamount, nice reef, exclusively white *Lophelia* corals, sponges
18:01	91	59°05.670'	10°47.900'	

Time (LT)	Depth (m)	Latitude (N)	Longitude (E)	Comments
18:10		59°05.665'	10°47.898'	
18:25	95	59°05.600'	10°47.918'	took very nice *Lophelia* coral sample
18:40	94	59°05.654'	10°47.911'	took second coral samples, continue sampling
18:58	93	59°05.652'	10°47.920'	sampling basket full with pieces of corals, start ascent soon
19:03	93			lift off bottom
19:13	0			surfaced
dive 924 (3) 20060327				
8:26	0	59°05.520'	10°47.816'	submerged
9:14	147	59°05.548'	10°47.839'	at bottom
9:23		59°05.595'	10°47.827'	
9:28	120	59°05.633'	10°47.818'	
9:35	100	59°05.642'	10°47.838'	
9:41	91	59°05.648'	10°47.869'	
9:58		59°05.650'	10°47.936'	
10:06		59°05.643'	10°47.920'	
10:28	102	59°05.645'	10°47.939'	
10:49		59°05.660'	10°47.935'	still at same position, sampling basket full, filming
10:54		59°05.660'	10°47.947'	start ascent
11:20	0			surfaced
dive 925 (4) 20060327				
14:20	0	59°05.620'	10°47.820'	submerged
14:30	118	59°05.660'	10°47.770'	at bottom south of coral mound, on gravel field with lots of ascidians
14:54	100	59°05.650'	10°47.850'	
14:58	108	59°05.640'	10°47.880'	coral rubble, single small *Lophelia* colonies
15:12		59°05.630'	10°47.890'	
15:25	100	59°05.630'	10°47.880'	in the centre of reef, current experiment with coloured water
15:35		59°05.630'	10°47.880'	

Time (LT)	Depth (m)	Latitude (N)	Longitude (E)	Comments
15:57		59°05.650’	10°47.850’	
16:10		59°05.640’	10°47.860’	
16:36	94	59°05.660’	10°47.890’	
16:56		59°05.650’	10°47.860’	
17:27		59°05.650’	10°47.830’	
17:42		59°05.660’	10°47.880’	
18:03	80	59°05.660’	10°47.860’	start ascent
dive 927a (6a) 20060328				
13:11	0	59°05.830’	10°47.820’	submerged
13:26	122	59°05.811’	10°47.818’	at bottom
13:35	105	59°05.780’	10°47.870’	below coral reef
13:39	90	59°05.770’	10°47.890’	until now only coral rubble, no living corals yet
13:51		59°05.809’	10°47.909’	only dead corals
13:56	85	59°05.770’	10°47.910’	living corals
14:18	85	59°05.767’	10°47.907’	collected corals, st art ascent
14:26	0			surfaced
dive 929 (8) 20060329				
13:43	0	59°04.510’	10°44.088’	submerged
13:55	120	59°04.558’	10°44.126’	at bottom
14:01	110	59°04.540’	10°44.130’	strong bottom current, very nice coral reef
15:01	110	59°04.540’	10°44.120’	still strong current, stationary in middle of coral reef
15:09	110	59°04.540’	10°44.120’	still strong current, stationary, collecting corals (beautiful pieces)
15:17	100	59°04.538’	10°44.165’	start ascent with f ull sampling basket
15:43	0			surfaced

RV ALKOR cruise AL316

Tab. B-2 Submersible JAGO dive tracks during RV ALKOR cruise AL316 in March 2008.

Time (LT)	Depth (m)	Latitude (N)	Longitude (E)	Comments
dive 1050 (9) 20080315				
08:31	0	64°06.045'	08°05.493'	submerged
08:54	298	64°05.998'	08°05.406'	at bottom, coral rubble + first single corals
08:59		64°05.972'	08°05.436'	
09:09		64°05.962'	08°05.381'	
09:15		64°05.967'	08°05.325'	
09:23		64°05.982'	08°05.410'	collecting corals
09:58	275	64°05.960'	08°05.391'	
10:03	275	64°05.964'	08°05.392'	sampling busket full, start ascent
10:27	0			surfaced
dive 1051 (10) 20080315				
12:46	0	64°05.879'	08°05.423'	submerged
13:05	290	64°05.871'	08°05.407'	at bottom, gravel and sponges
13:10		64°05.879'	08°05.419'	at base of coral reef
13:14	285	64°05.893'	08°05.419'	
13:17		64°05.899'	08°05.438'	
13:26		64°05.907'	08°05.447'	
13:29	285	64°05.893'	08°05.419'	collecting corals, *Lophelia* white + red, *Madrepora*
13:40	285	64°05.882'	08°05.479'	moved a short distance
13:53		64°05.896'	08°05.467'	
14:03		64°05.900'	08°05.461'	
14:10	285	64°05.907'	08°05.463'	sampling busket full of corals
14:13	280	64°05.898'	08°05.467'	2 m above ground, start ascent
14:32	0			surfaced

Declaration of Academic Integrity

With this statement I declare that I have independently completed the above thesis, except for scientific consulting by my supervisor Prof. Dr. Ulf Riebesell.

The thoughts taken directly or indirectly from external sources are properly marked as such. This thesis was not previously submitted to another academic institution.

Selbstständigkeitserklärung

Hiermit erkläre ich, dass die vorliegende Dissertation - abgesehen von der Beratung durch meinen Betreuer Prof. Ulf Riebesell - nach Inhalt und Form mein eigenes Werk ist. Bei ihrer Anfertigung habe ich keine anderen als die angegebenen Quellen und Hilfsmittel verwendet.

Des Weiteren erkläre ich, dass die vorliegende Arbeit unter Einhaltung der Regeln guter wissenschaftlicher Praxis der Deutschen Forschungsgemeinschaft entstanden ist.

Ferner erkläre ich, das ich zuvor noch keinen Promotionsversuch unternommen habe und dass diese Arbeit weder vollständig noch in Teilen an anderer Stelle im Rahmen eines Prüfungsverfahrens vorgelegt, veröffentlicht oder zur Veröffentlichung eingereicht worden ist.

Kiel, ...

Armin U. Form